Proceedings of the 3. International Conference on Luminescence Dosimetry

Research Establishment Risø, Roskilde

Publication date:
1971

Document Version
Publisher's PDF, also known as Version of record

Risö Report No. 249
Part I (pp. 1-443)

Risö Report No. 249
Part I (pp. 1-443)

Danisn Atomic Energy Commission

Research Establishment Risö

Proceedings of The Third International Conference on Luminescence Dosimetry, held at the Danish AEC Research Establishment Risö 11-14 October 1971

Sponsored by The Danish Atomic Energy Commission and
The International Atomic Energy Agency

December 1971

Sales distributors: Jul. Gjellerup, 87, Sölvgade, DK-1307 Copenhagen K. Denmark
Available on exchange from: Library, Danish Atomic Energy Commission, Risö, DK-4000 Roskilde, Denmark

U. D. C.
535.37:539.12.08

December 1971

Risø Report No. 249
Part I (pp. 1-443)

Proceedings of the Third International Conference on Luminescence Dosimetry

Held at

The Danish Atomic Energy Commission
Research Establishment Risø

October 11-14 1971

Sponsored by

The Danish Atomic Energy Commission

and

International Atomic Energy Agency

Editor

V. Mejdahl

Abstract

Seventy-eight papers are presented from the 3rd International Conference on Luminescence Dosimetry. The papers are arranged according to the following topics: Mechaniams of Thermoluminescence (TL), TL Instrumentation, Improved TL Materials, Properties of TL Materials, Thermally Stimulated Exoelectron Emission, Radiophotoluminescence, TL in Clinical and Personnel Dosimetry, Dating and Background Radiation Monitoring, Charged Particle, Neutron and UV Response, Miscellaneous Properties, Effects and Applications.

ISBN 87 550 0120 3
ISBN 87 550 0121 1

FOREWORD

This publication presents the papers given at the third International Conference on Luminescence Dosimetry. The papers reflect the extensive research and development that have been accomplished since the second International Conference on Luminescence Dosimetry, held at Gatlinburg, Tennessee, in 1968. The great number of papers, seventy-eight, clearly indicates the continuing interest in this field. There were 144 registered attendees representing twenty-seven countries and three international organizations: Austria, Belgium, Brazil, Bulgaria, Canada, Czechoslovakia, Denmark, Finland, France, Germany (DDR and the Federal Republic), Greece, Hungary, India, Israel, Italy, Japan, Mexico, The Netherlands, Norway, Poland, Portugal, Sweden, Switzerland, United Kingdom, U.S.A., Yugoslavia, CERN, IAEA, and WHO.

In connection with the conference a commercial exhibition was arranged which showed the latest developments of measuring equipment. Eight companies representing six countries participated in the exhibition.

To enable rapid publication the papers have been reproduced directly from the manuscripts handed over by the authors. A few papers were withdrawn by the authors, and in such cases only abstracts are given. Discussion on a paper is inserted at the end of the paper. The publication is in three parts: Part I contains sessions I-V, part II sessions VI-IX, and part III sessions X-XII. The grouping of papers into sessions appears from the list of contents which is included in each volume.

The assistance of Miss L. Kristiansen, Miss B. Ramgill, and the printing office staff in the publication of the proceedings is gratefully acknowledged by the Arrangements Committee.

V. Mejdahl

CONFERENCE OFFICERS

Co-Chairmen:

J. F. Fowler
Research Unit in Radiobiology
Mount Vernon Hospital, Northwood, United Kingdom

A. Scharmann
University of Giessen,
Federal Republic of Germany

Programme Committee:

K. Becker, Chairman
Oak Ridge National Laboratory, U. S. A.

F. H. Attix
U. S. Naval Research Laboratory, U. S. A.

J. R. Cameron
University of Wisconsin, U. S. A.

J. H. Schulman, Special Advisor
U. S. Naval Research Laboratory, U. S. A.

Local Arrangements and Publications Committee:

V. Mejdahl, Chairman
Danish AEC, Risö, Denmark

C. A. Carlsson, Vice-Chairman
University of Linköping, Sweden

L. Bøtter-Jensen
Danish AEC, Risö, Denmark

E. Pedersen
Danish AEC, Risö, Denmark

CONTENTS

PART I

Page

Interpretation of Resolved Glow Curve Shapes in LiF(TLD-100) from 100° to 500°K.

by

E. B. Podgorsak, P. R. Moran, and J. R. Cameron

Laboratory of Medical Physics

Physics Department and Radiology Department

University of Wisconsin, Madison, Wis.

Abstract

We note that each glow peak of LiF(TLD-100) in the temperature range from 100° to 500°K displays a shape, peaking temperature dependence on heating rate, and lack of peaking temperature dependence upon total light output which are in detail as predicted by the most simple thermally activated kinetics in the first order Randall-Wilkins limit. We also note, however, that the glow curve breadth is anomalously large at low temperatures and anomalously small at high temperatures. While physically reasonable, although improbable, mechanisms might explain the larger breadths, there seem to exist no physically reasonable direct mechanisms to explain the narrower breadths. We propose an indirect explanation in which the activation energy is itself slightly temperature dependent. We discuss how this effect explains the observed results and speculate on other implications.

Introduction

Since our abstract was submitted, a detailed description of our experiments relating to correlations in glow peak behavior from 100° to 500°K has been published.[1] We therefore wish to discuss here primarily an interpretation of resolvable glow curve shapes and apply these results to the TLD-100 observations. Figure 1 shows the ten glow peaks we have studied; glow peaks (-1) and (-4) are not optically repopulated with uv irradiation, and this allows us to resolve the details of peaks (0) and (-3). These glow curve shapes each exhibit a 50% half-breadth asymmetry on the low temperature side and, at a given heating rate, neither the peaking temperature, T_m, nor temperature breadth, Δ, depend upon the peak TL intensity. This behavior characterizes first order kinetics and, consequently, we discuss here only the Randall-Wilkins description although our results can also easily be applied to the Garlick-Gibson limit. A particularly interesting feature is that all glow peaks in this temperature range have essentially the same temperature breadth, $\Delta = 20 \pm 2°C$.

Glow Curve Behavior

It is not appropriate to pursue all mathematical details here, but a brief review of the first order kinetics of thermally activated mechanisms is useful. The concentration of trapped charge carriers, n, corresponding to a single resolved glow peak obeys the relation

$$\partial_t n = -Wn \ , \tag{1}$$

where w is an activated rate function

$$W = se^{-E/kT} \ , \tag{2}$$

and the TL intensity, in the simplest case, is some fraction of the release rate,

$$I(t) = -\varepsilon \partial_t n \ . \tag{3}$$

The above equations can easily be integrated formally; one can obtain from them an implicit expression for the peak temperature

$$(E/kT_m) + \log(E/kT_m) = \log\{s(\partial_t T/T_m)^{-1}\}. \tag{4}$$

When the glow curve is narrow, $\Delta << T_m$, it is not difficult to show[2] that

$$(E/kT_m) >> 1 \ , \tag{5}$$

and Eq. 4 can be validly approximated as

$$(E/kT_m) = \log\{s(\partial_t T/T_m)^{-1}\} \ . \tag{6}$$

We shall return to the expression in Eq. 6 later.

For narrow glow curves one can also show[2] that analytic expressions can validly be used to approximate the integration of Eqs. (1) - (3). The result is

$$I(\delta T) = I_m \exp\{1 + (\delta T/T_m)(E/kT_m) - \exp[(\delta T/T_m)(E/kT_m)]\} \ , \tag{7}$$

where δT is the departure from T_m,

$$\delta T = T - T_m \quad . \tag{8}$$

Figure 2 shows the predictions of Eq. 7 compared to the experimental glow curve for peak (-3); peak (-3) is chosen because it is the fractionally broadest glow peak and therefore tests our approximations most severely. We note the characteristic ~50% low temperature asymmetry, and that the numerical result for the glow peak breadth at half-maximum is

$$\Delta \simeq (2.44)(kT_m/E)\ T_m \quad . \tag{9}$$

One can now use Eqs. (9) and (6) together with the experimentally observed T_m and Δ to determine E and s. There are, of course, other methods as well, but they give similar results, and Eqs. (9) and (6) most directly illustrate the effects we wish to point out.

If we examine glow peak (-1), which has $T_m = 267°K$ at our heating rate of 35°K/min, we find

$$E(-1) = .76 \text{ eV}, \tag{10a}$$

$$s(-1) = 5 \times 10^{12} \text{ sec}^{-1}. \tag{10b}$$

This value for s is to be expected; if the trapped carrier interacts as strongly with neighboring ions in the solid as the ions do with one another, the s is the limiting attempt frequency and must be approximately equal to the typical DeBye lattice vibration frequencies. These frequencies are indeed about 5×10^{12} sec^{-1} for LiF. If, on the other hand, we examine glow peak (-3), we find

$$E(-3) = 0.28 \text{ eV}, \tag{11a}$$

$$s(-3) = 10^{7} \text{ sec}^{-1}. \tag{11b}$$

Expressed another way, if we assumed $s(-3) = 10^{12}$ sec^{-1}, then the breadth of peak (-3) is about a factor of two broader than predicted. Many explanations have been put forward to explain such anomalously large breadth of glow peaks. For example, there might exist a spread in activation energies E, or the trapped carrier might somehow be effectively insulated from the lattice vibrations, or there might be overwhelming retrapping effects to effectively reduce the net attempt rate.

Finally let us examine glow peak (5), which has been extensively studied because of its use as the primary dosimetry glow peak. Here we find not an anomalously large breadth, but an anomalously narrow breadth. While it is not difficult to give plausible mechanisms to broaden a line, it is very difficult to propose narrowing mechanisms. The parameters determined are

$$E(5) = 2.2 \text{ eV}, \tag{12a}$$

$$s(5) = 10^{23} \text{ sec}^{-1}. \tag{12b}$$

Similar results are also obtained by measuring the logarithmic change of T_m as $\partial_t T$ is varied with an analysis according to Eq. 4.

The point we wish to emphasize is that while reasonable, although

perhaps unlikely, explanations can be made for $s = 10^7$ in glow peak (-3), there exists no simple physically reasonable mechanism for an actual $s = 10^{23}$ in peak (5) because this is a factor of at least 10^{10} larger than the limiting lattice interaction frequencies in the solid.

We have found that we can resolve these difficulties simply by assuming that the activation energy, E, is very slightly temperature dependent. We will not present the detailed mathematics here, but the following results are obtained.

1. When an observed glow peak is narrow, $\Delta << T_m$, then a simple analytic approximation is always valid in integrating the kinetic equations, Eqs. (1)-(3); this includes the possibility of a temperature dependent activation energy. The most important relation is

$$\int_0^t W(T)dt = W(\partial_t T)^{-1} [\partial_T \log W]^{-1} . \qquad (13)$$

2. The resulting glow curve descriptions have exactly the same form as Eqs. (4) through (9) except that E and s are replaced by the parameters E^* and s^*, where

$$E^* = \partial\beta(\beta E(\beta))|_{\beta_m}; \quad (\beta = 1/kT), \qquad (14a)$$

and

$$s^* = \exp\{(E^* - E(T_m)]/kT_m\}s. \qquad (14b)$$

3. *In Eq. 6, the difference between E^* and $E(T)$ is exactly balanced by the* difference between s^* and s. Thus Eq. 6 remains valid independent of whether one uses E and s or E^* and s^*.

4. For glow peak (5), a slight increase in E with temperature amounting to a fractional effect of less than 10^{-3} ($^\circ K^{-1}$) easily accounts for the anomalously narrow breadth and gives an $s^* = 10^{23}$ resulting from an actual interaction rate of $s = 10^{12}$.

5. All other aspects of shape, breadth, peak height behavior, etc. are preserved according to the basic Randall-Wilkins results.

As a final speculation we propose that other slight temperature dependences account for all anomalous breadths. For example, one need not invoke the somewhat unlikely existence of dominating retrapping terms to explain the large breadth of peak (-3), since only a small temperature dependence of E provides the same resulting behavior.

We can also speculate further on the E^* vs E behavior. Let us suppose, as a very crude model, that all glow peak traps are roughly the same character, for example, basically a weak coulomb-like binding stabilized by the surrounding ions. As the temperature increases from 0°K the lattice undergoes thermal expansion. We might expect that the trap depth will first increase due to the reduction of the neighboring ion repulsive potentials and, with continuing temperature increase, the binding will eventually begin to decrease due to reduction of the Coulomb attraction. Thus the fractional temperature dependence of E for each glow peak would show leading terms of the form

$$E = E_A(1 + \alpha T - \beta T^2), \tag{15}$$

which can be rewritten

$$E = E_o(1 - b(T-T_o)^2). \tag{16}$$

We think it is interesting that by choosing $b = 10^{-7}(°K)^{-2}$ and $T_o = 300°K$ we can fit all the observed glow curve shapes while retaining a single activation frequency, $s = 10^{12}$ sec^{-1}, characteristic of lattice vibration interactions and negligible retrapping.

References

(1) E. B. Podgorsak, P. R. Moran, and J. R. Cameron, J.A.P. 42, 2761 (1971).

(2) P. R. Moran, E. B. Podgorsak, USAEC Report, COO-1105-164, August 1971.

This work was supported by the United States Atomic Energy Agency and by the U.S. Air Force Office of Scientific Research.

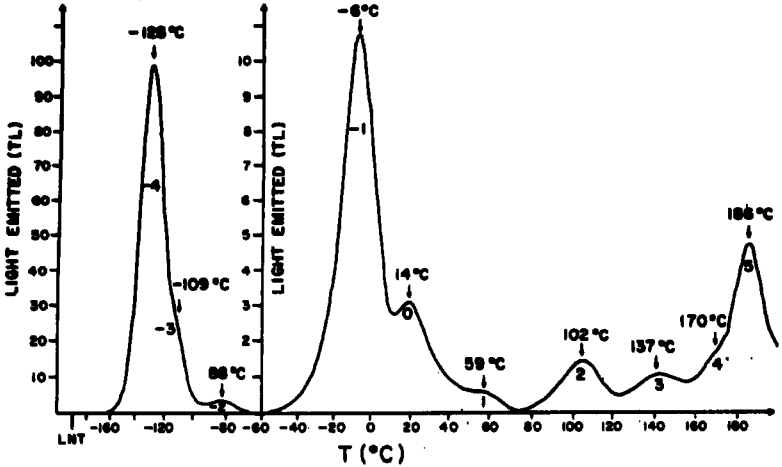

Figure 1 A typical glow curve of LiF (TLD-100) single crystal exposed to x-rays (∿ 16,000 R) at LNT and heated to 200°C (note change of scale at -60°C).

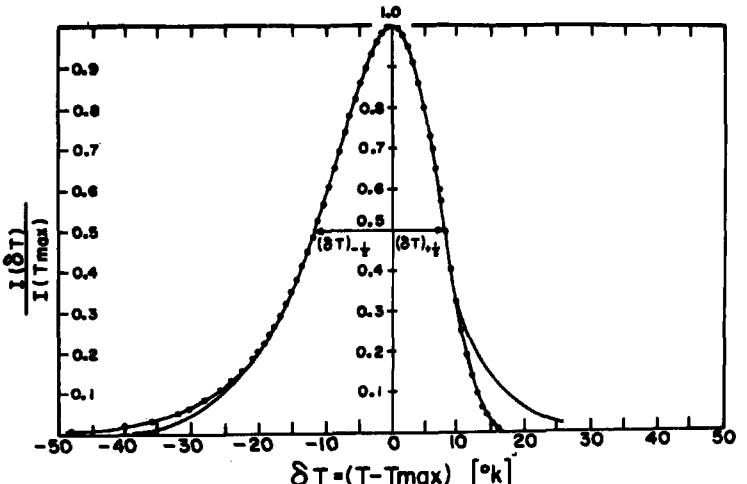

Figure 2 Glow peak (-3) of LiF(TLD-100). The dotted curve is calculated from Eq. 7 and the undotted line is the experimentally measured glow curve.

Fowler

Your explanation of a too narrow peak in terms of a dependence of activation energy on temperature is interesting. How did you come to this conclusion? What physical processes could lead to such a dependence, and are the orders of magnitude involved reasonable?

Moran

First, we looked for a single explanation which could give low-temperature peaks a "too large" breadth and high temperature peaks a "too small" breadth. At least for low irradiation levels in LiF (TLD-100), a reasonable single explanation was $E_{Act} = E(T)$. A possible physical process is suggested in the written version of this paper; we suggest that thermal lattice expansion can give a fractional variation of the form

$$E(T) = E_o(1 - b(T-T_o)^2)$$

By choosing $b \simeq 10^{-7}$ $(^oK)^{-2}$ and $T_o \simeq 290^oK$ we can fit the T_M and δ of all LiF (TLD-100) strong resolvable glow peaks using only a strong-coupling lattice vibration interaction frequency $s = 5 \times 10^{12}$ sec^{-1}.

Analysis of Thermoluminescence Kinetics of CaF_2:Mn Dosimeters.

G. Adam
and
J. Katriel

Nuclear Research Centre - Negev, P.O.B. 9001, Beer - Sheva, Israel.

Abstract

A new approach to the analysis of glow curves is used to study the kinetics of the thermoluminescence of CaF_2:Mn dosimeters. Activation energies, frequency factors and related parameters are obtained. The measurements were carried out on the M.B.L.E. thermoluminescence dosimeters using a PNH 801 reader in the temperature ranges 300 - 700 ^{0}K. The computational aspects of the analysis are discussed and the computer program performing the entire analysis using as an input the glow curve data is described in the appendix.

Introduction

The analysis of thermoluminescence glow curves is a conventional and powerful method for the determination of activation energies, frequency factors and related kinetic parameters for the processes involved. A new method of analysis has recently been suggested by Maxia et. al.[1], who also applied it to the thermoluminescence of ZnS and NaBr. The glow curves involved consist of single peaks. It is interesting to apply the method to a more complicated glow curve. The widespread use of the M.B.L.E. CaF_2:Mn dosimeters, which have three peaks in their glow curves, as well as the ease with which their glow curves are obtained by use of the commercial reader, made them a suitable example for the present study.

Description of the Method

The kinetic equation governing the light emission during a thermo-luminescence transition is assumed to be

$$-dm_i/dt = sexp(-E/kT)(B_i n m_i)/[A(N-n)+B_i m_i] \quad (1)$$

where

$m_i (cm^{-3})$ is the concentration of holes lying in the ith type luminescent center

$s(sec^{-1})$ is the frequency factor

E(eV) is the thermal activation energy

A and B_i $(cm^{-3}sec^{-1})$ are the probability factors, respectively, for retrapping and recombination with the ith type center

$N(cm^{-3})$ electronic trap concentration

$n(cm^{-3})$ is the trapped electron concentration

k is the Boltzman factor and T the absolute temprature.

From this equation the following equation for the line shape of the glow curve was developed in ref. (1).

$$\log[I(T)(\cos\theta + \sin\theta S(T))/(S^2(T) + \Delta S(T))] = -E/kT + \mu \quad (2)$$

I(T) being the intensity of the emitted light at temperature T,

$\Delta = \int_{Tfinal}^{\infty} I(T)dT$ and $S(T) = \int_{T}^{Tfinal} I(T)dT$. θ and μ are constants related to the kinetic parameters. For the correct value of θ, eq.(2) expresses a linear dependance of

$y = \log[I(T)(\cos\theta + \sin\theta S(T))/(S^2(T) + \Delta S(T))]$ on $x = 1/T$.

The numerical analysis involved in obtaining the proper value of θ is described in ref. (1)*.

---

* A typographical error was noted in eq. 23 of ref. 1. This equation should read: $E = -kcov(x,y)/v(x) = -kv(y)/cov(x,y)$

After the right value of θ has been obtained, the activation energy and the constant μ are determined from the slope and the intercept respectively, of the linear curve. The ratio A/B and the frequency factor are expressed in ref. (1) in terms of these parameters.

Measurements and Results.

As was noted above the investigated sample was CaF_2:Mn in the form of a thermoluminescent dosimeter type PNP 292 produced by M.B.L.E.. The dosimeters were irradiated by an X - ray machine with a maximum energy of 45 KeV to a dose of about 1000 R. The dosimeters were then heated using the M.B.L.E. thermoluminescence dosimeter reader type PNR 801 from room temperature to about 700 ^{0}K. The heating rate is 45^0 per second. The glow curves were recorded during the heating period using a special output provided in the reader. The points on the glow curve were then used as an input to the computer program described in the appendix, the intensity being measured in arbitrary units and the temprature in degrees centigrade. The rectified data is represented in figs. 2,3 4. The obtained results are summerized in the following table:

	activation energy eV	peaks temp. ^{0}K	frequency factor s	A/B
peak I	1.20	382	$3.98 \cdot 10^{15}$	2.37
peak II	1.65	447	$6.17 \cdot 10^{18}$	5.99
peak III	1.69	536	$4.14 \cdot 10^{18}$	7.03

The first peak has a particularly low activatio energy which is compensated with a low frequency factor. The roles of the activation energy and the frequency factor in defining the peaks' temprature can be judged from

the relation

$E\exp(-E/kT) = C$

where C is a constant depending on some general characteristics of the peak and T is the temperature at the peak's maximum. This relation is derived from eq. 11 of ref. 1.

Appendix: Description of the Computer Program

The glow curve data is introduced as a set of values of the emission intensity versus the corresponding temperatures. These are represented as a linear combination of a few Gaussians in the form

$$I(T) = \sum_{i=1}^{N} C_i \exp[-\alpha_i (T-t_i)^2] \equiv C^{\dagger} \underline{f} \qquad (3)$$

The non - linear parameters $[\alpha_i, t_i]$ are varied in order to optimize the representation. The vector of linear parameters is obtained as $\underline{C} = S^{-1}\underline{V}$ where $S_{ij} = \sum_{k=1}^{M} f_i(T_k) f_j(T_k)$ and $v_j = \sum_{i=1}^{M} I(T_i) f_j(T_i)$.

The analytic representation is compared with the experimental data in fig. 1. The analytic representation is used in order to determine the rectifying value of θ by minimizing $R = (1-\rho)^2$, ρ being defined in eq. 22 of ref. 1. The appropriate value of θ is used to determine the activation energy, frequency factor and related kinetic parameters.

References

1) V. Maxia, S. Onnis and A. Rucci, Journal of Luminescence 3, 378 - 388 (1971).

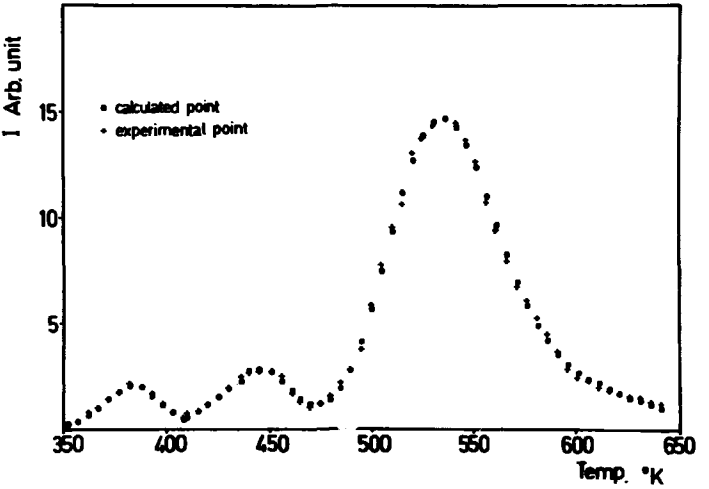

Fig. 1. Comparison of analytic versus experimental glow curve.

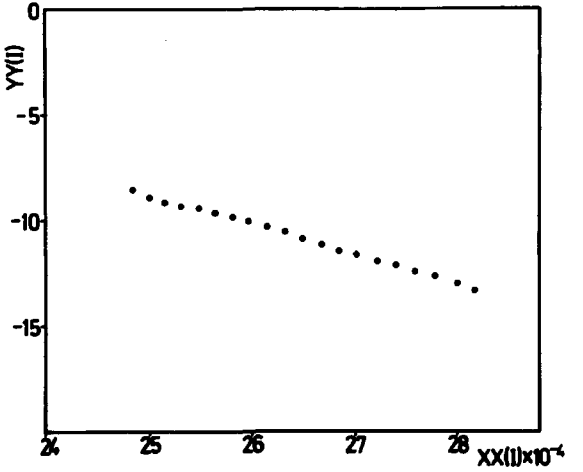

Fig. 2. Rectified data for peak I of CaF_2:Mn.

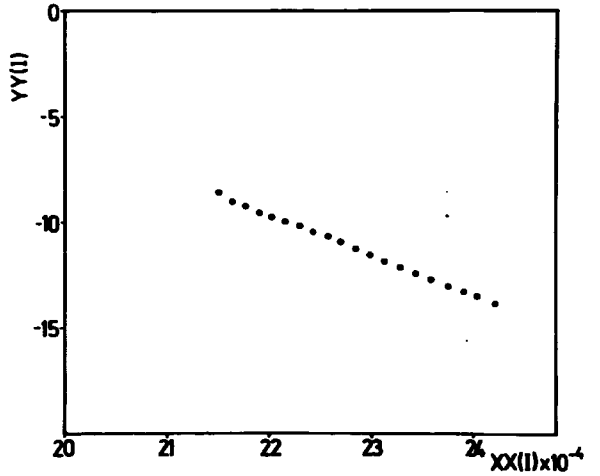

Fig. 3. Rectified data for peak II of CaF_2:Mn

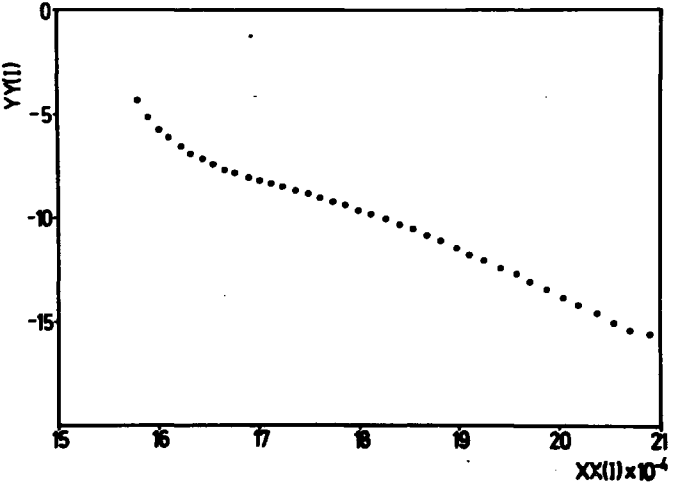

Fig. 4. Rectified data for peak III of CaF_2:Mn

Fowler

Would the attempt-to-escape frequency really be spuriously increased if the heating rate were so high that several true peaks only appeared as one? Is this in the right direction? Surely, Dr. Moran said that he obtained $s = 10^{23}$ (which is too high to be reasonable) when his peaks were narrower than expected from simple theory?

Adam

I do not think that there is a direct connection between the peak width and the frequency factor so that one could not say offhand what will be the effect of widening the peaks on the frequency factor.

Mason

In the second slide you determined E and s from a central portion of the curve. Did you try to determine E and s from the extreme parts of the curve?

Adam

Yes, we did some hand calculations, but the results were nonsensical.

Attix

Did you study natural fluorite, or CaF_2:Mn? I believe it must have been the fluorite, but your title erroneously specifies CaF_2:Mn.

Adam

MRLE gave us the dosimeters saying that the powder within was CaF_2:Mn. If, however, Dr. Attix says this is their natural fluorite, he is probably right.

Investigation of Thermoluminescent Lithium Borate Glasses using Electron Spin Resonance

by

Douglas R. Shearer

Physics Department

St. Bartholomews Medical College

London

Abstract

The trapping centres involved in the thermoluminescence of lithium borate glasses have been identified as holes trapped on bridging and non-bridging oxygens in the glas matrix. The results of isothermal annealing experiments indicate that the untrapping process occurs over a continuous spectrum of activation energies. The radiation induced E.S.R. signal from the glasses with a high alkali content decays fastest except for the anomalous behaviour of the pure borate glass in which the signal disappears rapidly at room temperature. The addition of manganese chlorides increases the decay rate and reduces the number of trapped holes. Manganese occurs in two sites in the glass lattice and their is evidence of this in the thermoluminescent spectrum. This spectrum can be altered by the addition of other activators. Heavily manganese doped glasses exhibit an additional glow peak at a higher temperature. This has been assigned to the transition

$$Mn^{+++} + e \longrightarrow Mn^{++} + h\nu$$

which occurs on post irradiation heating.

A model has been proposed for the thermoluminescent process in these glasses and some suggestions for the improvement of crystalline lithium borate phosphors have been advanced.

Present address: Physics Department, St. William's Hospital, Rochester, Kent

INTRODUCTION

There are well defined problems to solve in the investigation of any thermoluminescent substance. The nature and number of the trapping and luminescence centres (which may be synonymous) must be determined. The kinetics leading to the emission are also important. Electron spin resonance is a useful tool for investigating these parameters. In the case of the lithium borate group, irradiation induces a signal which can be easily followed. The customary activator - divalent manganese - is a paramagnetic element which gives a characteristic signal. Lithium borate itself is studied most easily over a wide range of composition in the vitreous state.

PREPARATION

All the experimental glasses were prepared from Analar and Purisa grade reagents in a platinum crucible. The firing temperature was 1000°C. Manganese and other impurities were added as chlorides. Nitrogen was passed through the furnace to minimise the quantity of trivalent manganese present in the glass. All glasses were quenched in water after 30 minutes in the furnace.

For E.S.R. work the glasses were left as small chunks, but for thermoluminescence studies the glass was ground and sieved to a grain size of 80 - 160 mesh. 15 MeV electrons from the linear accelerator at St. Bartholomew's Hospital were used for all the experimental irradiations. The secondary emission monitor described by Rotblat[1] was used for the dose calibrations.

For a valid comparison of signal heights from different glasses all signal heights were normalised to that of a ruby standard mounted on the compensating tube. This is essential for the range of glasses studied here as dielectric loss in the high alkali oxide glasses can reduce signal height by over 50%. The sensitivity of the spectrometer was assessed using a known quantity of DPPH in benzene and employing the standard double integration methods summarised by Poole[2].

Thermoluminescent spectra were determined using the apparatus described by Harris & Jackson[3] which has a range of 200 - 800 nm. The apparatus described by Karzmark et al[4] was used for all quantitative thermoluminescence. Fits to the various kinetics expressions were done using a PDP-8 computer with a 4K ferrite core memory store.

TRAPPING CENTRES

The E.S.R. signals from irradiated lithium borate glasses are as shown in Fig. 1. The top eight signals are the original radiation induced spectra. The bottom signal is that remaining after careful annealing.

The overlying 5 and 4 peaked signals have been attributed by Griscom et al[6] to a centre consisting of a hole trapped on an oxygen bridging between three and four co-ordinated borons in the glass structure.

The Hamiltonian suggested by the above authors for the structured signal is

$$\mathcal{H} = \beta(g_1 S_1 H_1 + g_2 S_2 H_2 + g_3 S_3 H_3) + A_1 S_1 I_1 + A_2 S_2 I_2 + A_3 S_3 I_3$$

with g & A values which vary with composition.

The underlying signal has not been as thoroughly investigated but is believed by some workers to be due to holes trapped on non-bridging oxygens.

The number of trapped holes is a function of composition, dose, temperature and storage time. The signal is seen to decay at all temperatures down to 77°K - the lowest investigated. It seems likely that there is a continuous spectrum of activation energies for the untrapping process.

Growth curves for the signal are shown in Figs. 2 & 3. The effect of decay is seen in the difference between the relative positions of the curves at 77°K and room temperature.

The curves saturate at about 2×10^7 rad when the number of trapped holes is of the order of 5×10^{17}/cc after 24 hours at 77°K. The number of trapped holes is independent of pre-irradiation and annealing. (See Fig. 4.) This indicates that the traps are not radiation induced.

The rate of decay is composition, dose and temperature dependent. The decay rates of the low alkali oxide glasses (with the exception of the pure borate glass) are least (Fig. 5). The pure glass decays rapidly at room temperature. The high dose signals decay relatively faster (see Fig. 6). Decay curves cannot be fitted by simple 1st or 2nd order expressions. However, an expression equivalent to that proposed by Medlin[7] for thermoluminescent decay from levels with a distribution of activation energies gave reasonable fits (Figs. 7 & 8.)

LUMINESCENCE CENTRES

The usual activator - divalent manganese - gives an E.S.R. signal which varies with base glass composition and manganese concentration. The manganous ion is more stable in the lower alkali-oxide glasses. (Table I).

TABLE I

	1:1	1:2	1:3	1:4	1:5	0:1
Intensity/unit sample mass	1±0.1	0.98±0.01	0.97±0.02	1.7±0.7	1.5±0.1	3.48±0.11
Intensity/ manganese atom	1±0.01	1.56±0.02	2.31±0.05	5.3±2.1	5.78±0.35	2.47±0.08

There are two signals, one at g = 2 and the other at g = 4.3. The g = 2 signals for 10^{-4} gm mole are shown in Fig. 9. The change in the g = 2

signal for increasing manganese concentration is shown in Fig. 10. The loss in resolution of the hyperfine structure at higher concentrations is due to dipolar broadening. The $g = 4.3$ signals are shown in Fig. 11. A Hamiltonian for the $g = 2$ signal has been proposed by Bleaney & Rubins[8] i.e.

$$\mathcal{H} = g\beta \underset{\sim}{H}.\underset{\sim}{S} + D\left[S_z^2 - \tfrac{1}{3}S(S+1)\right] + A\,\underset{\sim}{I}.\underset{\sim}{S} - g_I\beta_I\,\underset{\sim}{H}.\underset{\sim}{I} \qquad \text{for } S=\tfrac{5}{2}, I=\tfrac{5}{2}$$

Kedzie et al[9] have given a Hamiltonian for the $g = 4.3$ signal produced by isoelectronic Fe^{3+} in lithium silicate glasses. This has been applied by Lunter et al[10] to manganese in some glassy matrices, i.e.

$$\mathcal{H} = g^1\beta \underset{\sim}{H}.\underset{\sim}{S} + A^1\underset{\sim}{I}.\underset{\sim}{S}^1 \qquad \text{for } I=\tfrac{5}{2}, S^1=\tfrac{1}{2}, g^1=4{\cdot}3, A = \frac{g}{g^1}A^1$$

These signals have been attributed to manganese in two different sites in the glass lattice. The dominant $g = 2$ signal corresponds to manganese in an axially symmetric site. The signal at $g = 4.3$ is associated with rhombic symmetry. The two sites concerned can be tentatively identified as manganese in network modifying and network forming positions.

Cerium, copper and iron have also been added as chlorides. The only E.S.R. signal was seen at $g = 4.3$ from iron. This has been attributed to ferric iron in an orthorhombic electrostatic crystal field (Castner et al[11]).

THE EFFECT OF RADIATION ON THE E.S.R. SIGNAL FROM DOPED GLASSES.

It is found in these glasses that the number of trapped holes after irradiation is less than in the undoped glasses - the greatest decrease being seen in the glasses with the most added impurity (Figs. 12 & 13).

These results are compatible with those obtained by Griscom et al[12] which show that halogen Vk centres compete for liberated holes with the boron oxygen centres thus reducing the characteristic alkali borate radiation induced signal. The rate of decay of the signal is also increased in the doped glasses (Fig. 14). This will also decrease the effective number of trapped holes.

THERMOLUMINESCENT SPECTRA

Thermoluminescent spectra have been obtained from pure and doped glasses. The nonactivated glass spectra are similar to those of the more lightly manganese doped glasses. This implies that luminescence in undoped glasses is due to traces of manganese. These spectra peak at approximately 620 nm. The spectra were substantially the same for the two hole traps which indicates that the luminescence centre is the same in both cases. Within the limits of the experiment no dependence of the spectrum on dose was observed. The thermoluminescent spectrum moved towards longer wavelengths the greater the concentration of manganese. A subsidiary feature in the spectrum of the pure lithium borate glasses was a small peak at about 475 nm (Fig. 15), which was more obvious in the lower alkali oxide glasses. In addition the pure 0:1 glass activated with 10^{-4} gm. mole manganese showed

a peak at 530 mu. In the 1:5 glass doped with 10^{-4} gm. mole manganese another small peak was observed at 220 mu. This was only visible on the log scale (Fig. 16). These spectra are slightly temperature dependent - the emission shifting towards the shorter wavelengths on increase of temperature (Table II).

TABLE II

Temp. Range \ Glass Composition	1:1 10^{-4}	1:2 10^{-4}	1:3 10^{-4}	1:4 10^{-4}	1:5 10^{-4}	0:1 10^{-4}
77°K⇒Room Temp. Peak(mu)	615±15	620±10	640±10	640±10	610±10 (545 - 700 Peaks (A B C	610±5 (500-675 Peaks A B
77°K⇒Room Temp. Width (mu)	550-710	560-700	570-710	535-720	530-450-270	530-425
Room Temp.⇒200°C Peak(mu)	610±10	615±10	630±5	630±5	615± 10	610± 5
Room Temp.⇒200°C Width(mu)	540-700	560-690	570-695	575-710	555-710	560-675
200°C⇒400°C Peak(mu)	610±10	630±20		625± 5	610± 5	610± 5
200°C⇒400°C Width(mu)	535-700	520-690		570-700	545-695	560-680

It has been shown (Bingham & Parke[13], Lunter et al[10]) that the emission peaking at ~620 mu is associated with manganese in octahedral coordination while manganese in tetrahedrally symmetric surroundings gives rise to a green emission (approximately 530 mu). It has also been noted (Wagl[14]) that the orange emission is quenched at higher temperatures while the green is relatively unaffected. This may explain the temperature effect seen in the spectrum of most glasses.

The predominant emission at about 620 mu and the 530 mu emission have been explained (Medlin[12], Bingham & Parke[12]) as due to the $^4T_{1g} \rightarrow {}^6S\ (A_{1g})$ transition - the difference in wavelength being due to the symmetry change. There is a probability of the $^4T_{2g} \rightarrow {}^6S\ (A_{1g})$ transition which could give rise to the observed emission at about 450 mu - the higher levels giving rise to the shorter wavelength emissions.

When doped with cerium and copper the spectrum is altered as shown (Fig. 17). The blue luminescence for cerium at 385 mu has been attributed (Curie[16]) to a transition between the doublet levels

$$^2D_{\frac{1}{2}} \quad ^2D_{\frac{5}{2}} \longrightarrow {}^2F_{\frac{5}{2}} \quad {}^2F_{\frac{7}{2}}$$

Monovalent copper is reported (Karapetyan[17]) to give an emission peaking at about 500 mu and the absence of any E.S.R. spectrum reinforces this conclusion. The copper spectrum is extremely temperature dependent.

THERMOLUMINESCENT EMISSION

The thermoluminescent emission can be examined as a function of E.S.R. signal height by step annealing individual glass samples. The resultant plot is not completely linear in all cases. This is not surprising, in view of the two contributory traps and the spectral shift with temperature. Plots for two glasses are shown in Figs. 18 & 19. The relationship is significant enough, however, to assign the glow peak in these glasses to the hole traps observed by E.S.R.

The glow curves are shown in Fig. 20. Data are given in Table III.

TABLE III

Composition \ Dose	10^7 rads	10^6 rads	10^5 rads	10^3 rads
L_{1_2} 0.2 B_2O_3	190 ± 8	168 ± 8	168 ± 8	150 ± 8
L_{1_2} 0.2 B_2O_3 10^{-4} gm Mole Mn	200 ± 8	163 ± 8	155 ± 8	150 ± 8
" 10^{-3} "	141 ± 8	147 ± 8	155 ± 8	157 ± 8
" 10^{-2} "	Low temp. 150 ± 8 High temp. 278 ± 8		138 ± 8	
" 10^{-1} "	Low temp. 138 ± 8 High Temp. 265 ± 8			

It can be seen that increasing manganese concentration gives rise to a higher temperature glow peak. After irradiation these glasses have a purple tint due to Mn^{+++}. This disappears at the higher glow peak temperature. The peak may therefore be correlated with the transition:

$$e + Mn^{+++} \rightarrow Mn^{++} + h\nu$$

The actual glow peak temperatures are dependent on composition, dose, time and temperature of storage.

Thermoluminescent response curves are shown in Fig. 21. These are for undoped glasses. The low responses for the B_2O_3 and $La_2O.B_2O_3$ glasses are due mainly to the lack of trapped holes. With the addition of 10^{-4} gm mole manganese in each glass the results are as shown in Fig. 22. These results can partially be explained by better activator efficiency and trap stability in the low alkali oxide glasses. The response curves for the manganese activated 1:2 glasses are shown in Fig. 23. The peak for the 10^{-3} gm mole activated glass can be explained as the best compromise between number of effective activator atoms and number of trapped holes. The response curves due to the other activators are as shown (Fig. 24). The

increased responses due to copper and cerium are primarily due to the change in emission spectra. That the above considerations are not the whole story is shown by Fig. 25, i.e. the number of observable trapped holes and luminescent centres do not entirely determine the thermoluminescent output. Concentration quenching mechanisms are almost certainly involved in the more heavily doped glasses and differences in energy transfer properties of the base glasses may be important.

MODEL FOR THERMOLUMINESCENCE

The above experimental data lead to a model with at least two hole traps. These traps have a distribution of activation energies. The traps are not dependent on radiation formation. Added impurities provide additional trapping centres. The luminescent centre is independent of the trap and the emission spectrum can be altered by changing activators. So far it has not been possible to determine whether electrons or holes are untrapped but a simple model assuming electron untrapping is shown in Fig. 26.

The high temperature peak in the heavily manganese doped samples can be pictured as a result of the process shown in Fig. 27.

CONCLUSIONS

From the above data it would seem that the most efficient manganese activated phosphors are those in which the alkali oxide content is as low as possible and which are prepared under reducing conditions. As halogens appear to be responsible for decreasing the number of useful trapped holes the manganese should not be introduced as the chloride. Manganese acetate would serve the purpose of eliminating the competitive traps. It would also help to reduce the manganese to the divalent state.

Preliminary preparations of crystalline lithium borate phosphors have been carried out along these lines with good results.

An alternative method of increasing the effective efficiency is to shift the emission spectrum. This can be achieved by doping with activators giving emission spectra in the shorter wavelength region.

As the E.S.R. signals from crystals appear substantially the same, work is being carried out to extend these ideas to the range of crystalline phosphors.

REFERENCES

1. J. Rotblat, Nature (London), 175, 745 (1955).
2. C.P. Poole, Electron Spin Resonance (Interscience). (1967).
3. A.M. Harris & J.H. Jackson, C.E.G.B. Report RD/B/N111 (1968).
4. C.S. Karsmark, J. White and J.F. Fowler, Phys. Med. Biol. 2, 273 (1964).
5. P. Beekenkamp, Philips Research Report Supplements No. 4 (1966).
6. D.L. Griscom, P.S. Taylor & P.F. Ware & P.J. Bray, J. Chem. Phys. 48, 5158 (1968).
7. W.L. Medlin, Phys. Rev. 123, 502,(1961).
8. B. Bleaney & R.S. Rubins Proc. Phys. Soc. 77, 103, (1961).
9. R.W. Kedzie, D.H. Lyons & Kestigian M. Phys. Rev. 138, A(918) (1965).
10. S.G. Lunter, G.O. Karapetyan, N.M. Bokin & D.M. Yudin, Soviet Physics - Solid State 9, 2259 (1968).
11. T. Castner, G. Newell, N. Holton & C. Slichter, J. Chem. Phys. 32, 668 (1960).
12. D.L. Griscom, P.S. Taylor & P.J. Bray. J. Chem. Phys. 50, 977 (1969).
13. K. Bingham & S. Parks, Physics & Chem. of Glass 6, 224 (1965).
14. W.A. Weyl, Coloured Glasses (The Society of Glass Technology) (1951).
15. W.L. Medlin, J. Opt. Soc. Amer. 53, 1276, (1963).
16. D. Curie, Luminescence in Crystals, Methuen & Co. Ltd. (1963).
17. G.O. Karapetyan, IZV. AKAD. NAUK. SSSR. SER. FIZ 25, 539 (1961).

RADIATION-INDUCED E.S.R. SPECTRA
OF LITHIUM BORATE GLASSES

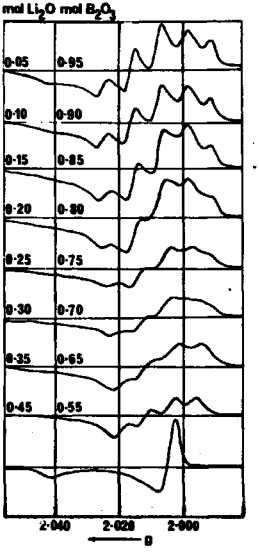

Fig. 1.

DOSE RESPONSE CURVES OF PURE LITHIUM BORATE GLASSES AT 77° K

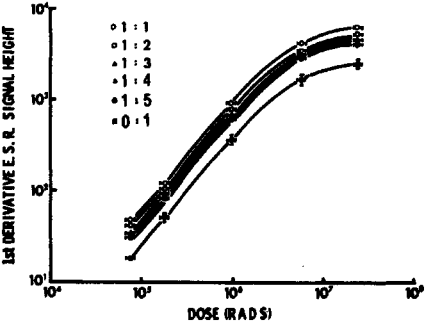

Fig. 2.

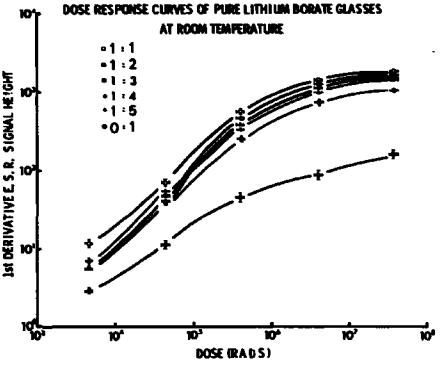
DOSE RESPONSE CURVES OF PURE LITHIUM BORATE GLASSES
AT ROOM TEMPERATURE
1 : 1
1 : 2
1 : 3
1 : 4
1 : 5
0 · 1
1st DERIVATIVE E.S.R. SIGNAL HEIGHT
DOSE (RADS)

Fig. 3.

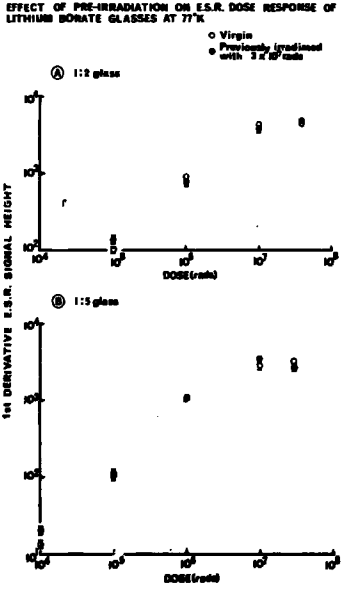
EFFECT OF PRE-IRRADIATION ON E.S.R. DOSE RESPONSE OF
LITHIUM BORATE GLASSES AT 77°K
Virgin
Previously irradiated
(A) 1:2 glass
(B) 1:5 glass
1st DERIVATIVE E.S.R. SIGNAL HEIGHT
DOSE(rads)

Fig. 4.

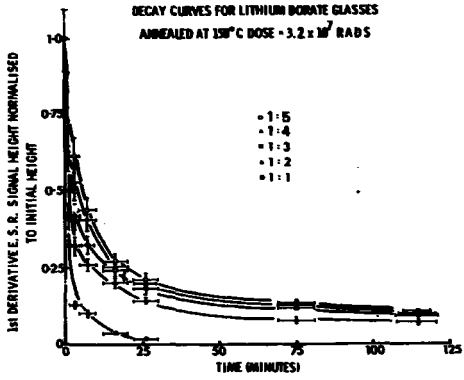
DECAY CURVES FOR LITHIUM BORATE GLASSES
ANNEALED AT 150°C DOSE = 3.2 x 10⁷ RADS
1st DERIVATIVE E.S.R. SIGNAL HEIGHT NORMALISED TO INITIAL HEIGHT
1·0
0·75
0·5
0·25
0
1:5
1:4
1:3
1:2
1:1
0
25
50
75
100
125
TIME (MINUTES)

Fig. 5

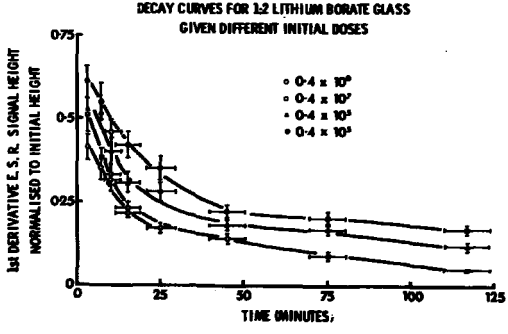
DECAY CURVES FOR 1:2 LITHIUM BORATE GLASS
GIVEN DIFFERENT INITIAL DOSES
1st DERIVATIVE E.S.R. SIGNAL HEIGHT NORMALISED TO INITIAL HEIGHT
0·75
0·5
0·25
0
0·4 x 10⁶
0·4 x 10⁷
0·4 x 10⁸
0·4 x 10⁹
0
25
50
75
100
125
TIME (MINUTES)

Fig. 6.

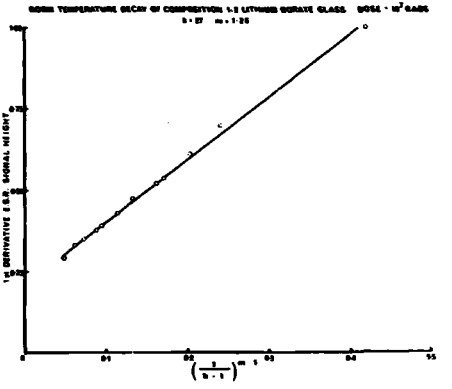
1st DERIVATIVE E.S.R. SIGNAL HEIGHT
0.25
0.5
0.75
1.0
0
0.1
0.2
0.3
0.4
0.5
$\left(\frac{1}{b+1}\right)^{m-1}$

Fig. 7.

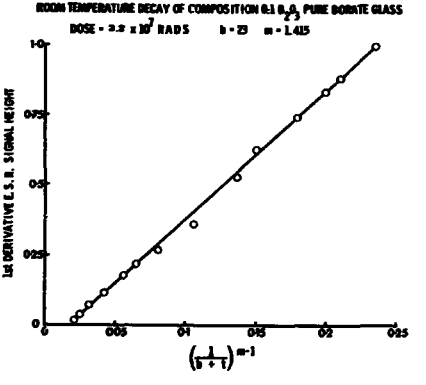
ROOM TEMPERATURE DECAY OF COMPOSITION 0.1 B_2O_3 PURE BORATE GLASS
DOSE - 2.2 x 10^7 RADS b - 23 m - 1.415
1st DERIVATIVE E.S.R. SIGNAL HEIGHT
0
0.25
0.5
0.75
1.0
0
0.05
0.1
0.15
0.2
0.25
$\left(\frac{1}{b+1}\right)^{m-1}$

Fig. 8.

E.S.R. SIGNALS AT g ~ 2 FOR DIFFERING BASE-GLASS COMPOSITIONS WITH 10^{-4} GM. MOLE MANGANESE

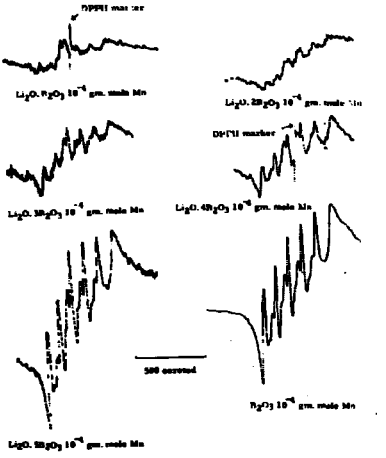

Fig. 9.

E.S.R. SIGNALS AT g ~ 2 FOR 1:2 GLASS WITH DIFFERENT PROPORTIONS OF MANGANESE

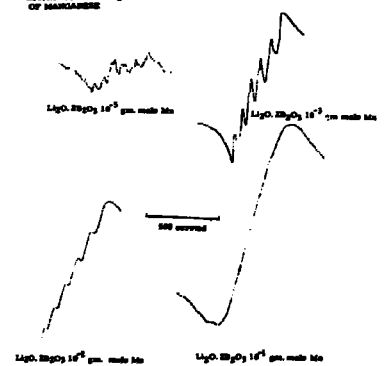

Fig. 10.

E.S.R. SIGNALS AT g= 4.3 FOR 1:2 GLASS ACTIVATED WITH DIFFERENT PROPORTIONS OF MANGANESE

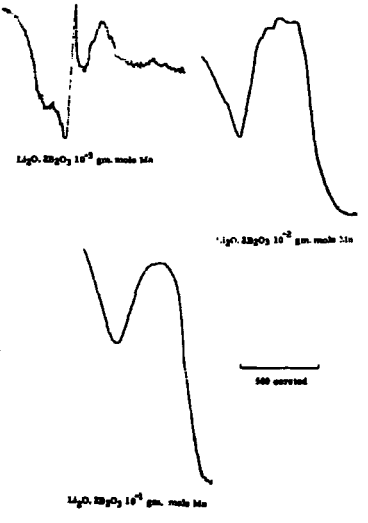

Fig. 11.

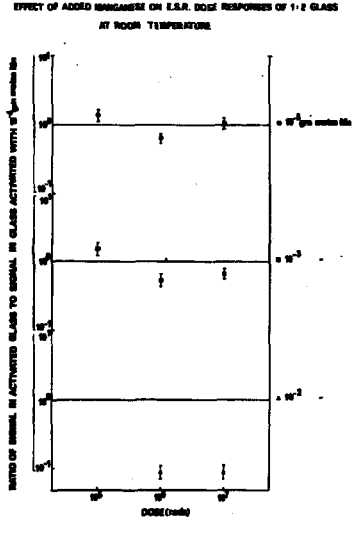
EFFECT OF ADDED MANGANESE ON E.S.R. DOSE RESPONSES OF 1·2 GLASS
AT ROOM TEMPERATURE
DOSE (rads)

Fig. 12.

EFFECT OF 0·1% BY WEIGHT ADDED ACTIVATOR ON ESR DOSE RESPONSES OF 1:2 GLASS AT ROOM TEMPERATURE

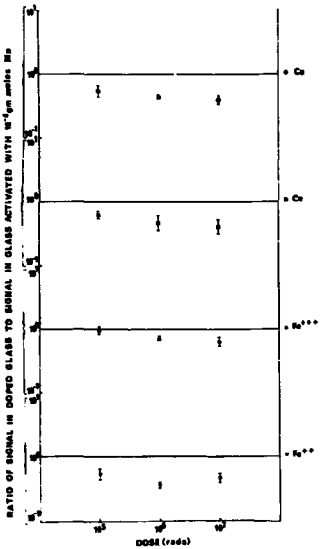

Fig. 13.

DECAY RATES OF IRRADIATED MANGANESE ACTIVATED 1:2 GLASS AT ROOM TEMPERATURE

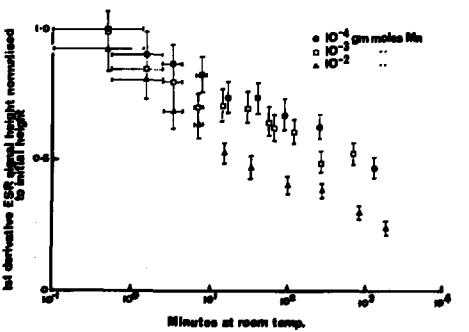

Fig. 14.

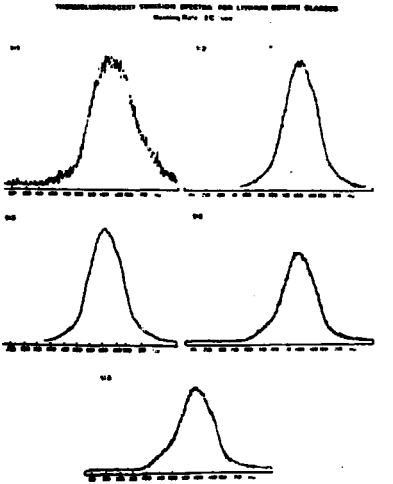

Fig. 15.

THERMOLUMINESCENT EMISSION SPECTRA FOR GLASSES DOPED WITH 10^{-4} GRAM MOLES MANGANESE.

Natural warming from 77°K to room temp.

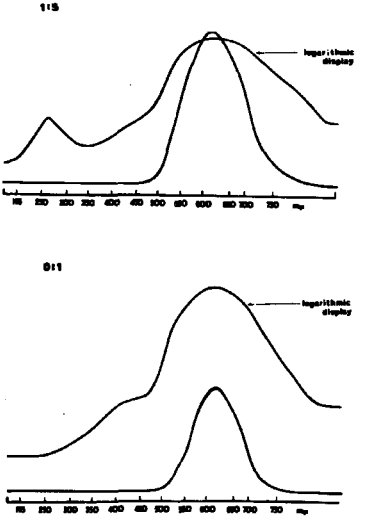

Fig. 16.

THERMOLUMINESCENT EMISSION SPECTRA FOR
Co AND Cu ACTIVATED 1:2 GLASS

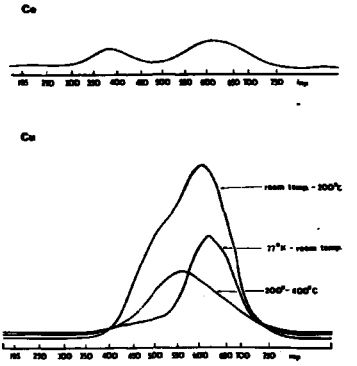

Fig. 17.

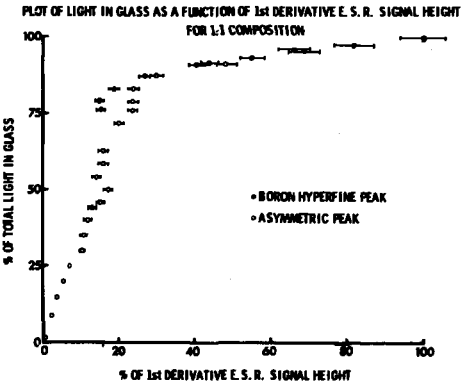

Fig. 18.

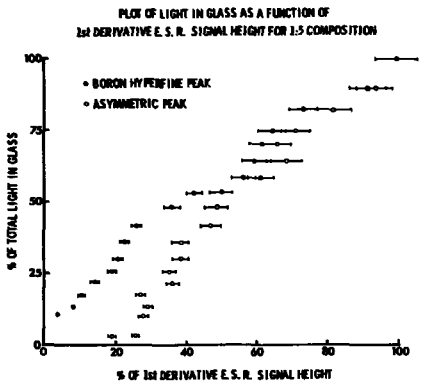
PLOT OF LIGHT IN GLASS AS A FUNCTION OF
1st DERIVATIVE E. S. R. SIGNAL HEIGHT FOR 1:5 COMPOSITION
• BORON HYPERFINE PEAK
◦ ASYMMETRIC PEAK
% OF TOTAL LIGHT IN GLASS
% OF 1st DERIVATIVE E. S. R. SIGNAL HEIGHT
0
25
50
75
100
0
20
40
60
80
100

Fig. 19.

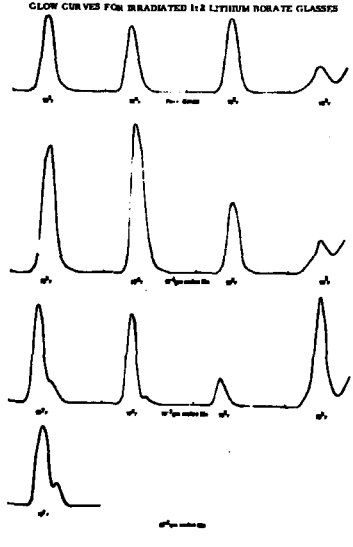
GLOW CURVES FOR IRRADIATED 1:2 LITHIUM BORATE GLASSES

Fig. 20.

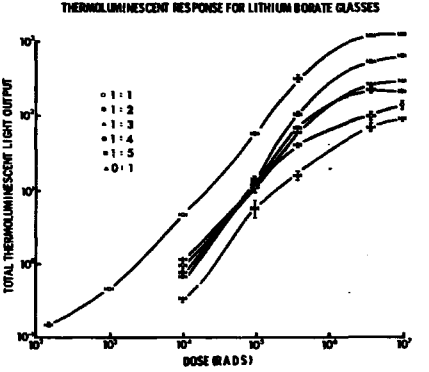
THERMOLUMINESCENT RESPONSE FOR LITHIUM BORATE GLASSES
TOTAL THERMOLUMINESCENT LIGHT OUTPUT
DOSE (RADS)
1 : 1
1 : 2
1 : 3
1 : 4
1 : 5
0 : 1

Fig. 21.

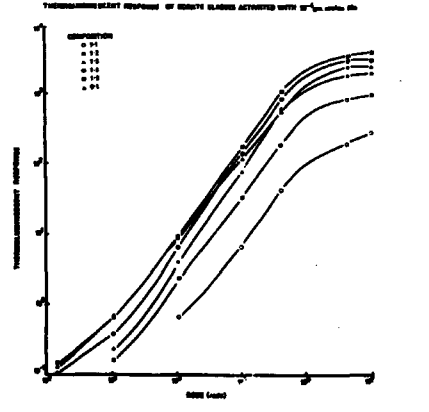

Fig. 22.

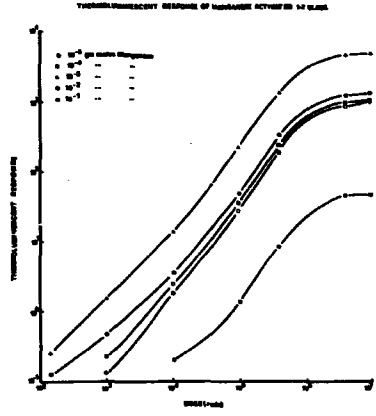

Fig. 23.

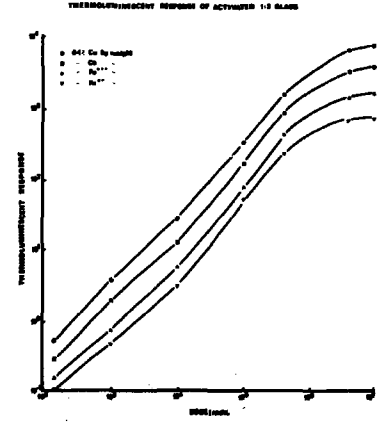

Fig. 24.

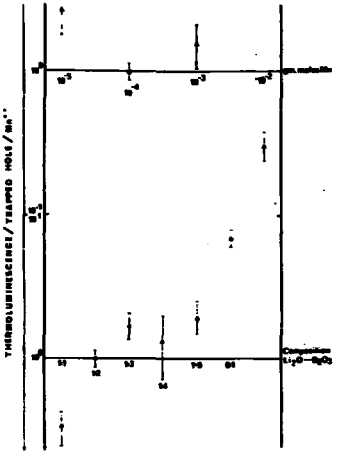

Fig. 25.

MODEL FOR THERMOLUMINESCENT PROCESS IN LITHIUM BORATE GLASSES ACTIVATED BY MANGANESE

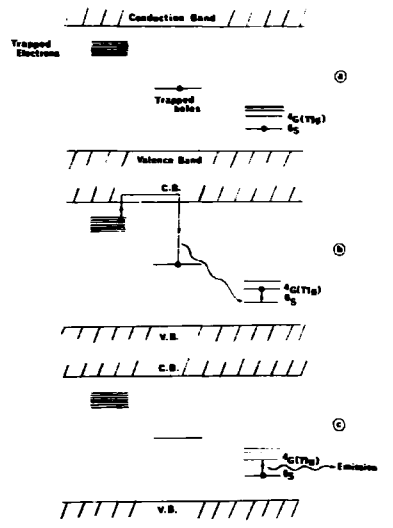

Fig. 26.

MODEL FOR HIGH TEMPERATURE PEAK EMISSION

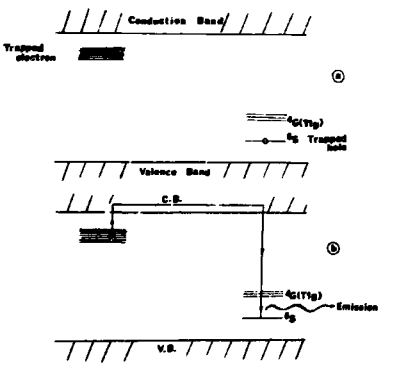

Fig. 27.

Becker

Some years ago, we did similar experiments with lithium borate glasses at GKNL. Despite stabilizing additives such as BeO these glasses had, however, the serious disadvantage of being rather hygroscopic in a humid climate, making protective coatings or similar measures necessary.

A Simple Thermoluminescence Model and its Application in Thermoluminescent Dosimetry

by

P.Abedin-Zadeh

International Atomic Energy Agency, Vienna, Austria.

Abstract

A simple thermoluminescence model based on the concept of energy levels is presented. The number of traps and holes is assumed to be the same as the number of peaks of the glow curve. All relevant parameters of the model as transition probabilities and the energy depth of traps can be obtained from experiment. Furthermore, for LiF (TLD-100) phosphor the calculated glow curve and integrated light output as a function of post irradiation annealing temperature and time is presented.

Introduction

All previous theories on the phenomenon of thermoluminescence make use of the band model. However, the qualitative energy level scheme for possible states of crystal electrons has a limited scope of applicability because of its approximative character. Therefore, many model parameters must be obtained from experiment for comparison with theory [1,2].

This paper presents a simple model of thermoluminescence using simplified general balance equation (Schön [3,4]). The corresponding parameters are given which allow to calculate the glow curve and integrated light output of LiF (TLD-100).

Model

Figure 1 shows a hypothetical energy diagram of an insulating crystal exhibiting thermoluminescence due to ionising radiation.

Ionising radiation releases an electron from the valence band to the conduction band, leaving a hole in the valence band. The electron and the hole move through the crystal until they recombine or until they are trapped in the metastable states. There are some possible ways by which a thermoluminescence photon is emitted. Here it is assumed that, as the

crystal is heated, sufficient energy may be given to the electrons and holes to raise them to the conduction and valence band. Thermoluminescent photons are emitted by recombining of conduction electron with valence holes (Exo-electrons are neglected). The number of traps and holes are assumed to be the same as the number of peaks of the experimentally known glow curve. With these assumptions one can write the following simplified Schön differential equation system [4] for the density of electrons in trap i and their density in the conduction band.

$$\begin{aligned} \frac{dh_i}{dt} &= -\gamma_i \, h_i \\ \frac{dC_i}{dt} &= \gamma_i \, h_i - \mu_i \, C_i \end{aligned} \qquad (1)$$

where γ_i is the probability per unit time for ejection of the electron in trap i to the conduction band, h_i is the concentration of electrons in trap i, C_i is the concentration of electrons in the conduction band coming from trap i and μ_i is the transition probability per unit time to the valence band of the electrons C_i.

Since the intensity I(t) of thermoluminescence (light output) is proportional to the number of radiative transitions per unit time and volume during the heating cycle, one can write

$$I(t) = \sum_i I_i(t) \approx \sum_i \mu_i \, C_i \qquad (2)$$

If we assume that the concentration of electrons in the conduction band is constant, the solution of equation (1) is as follows:

$$\begin{aligned} h_i(t) &= h_i(0) \cdot \mathrm{Exp}\left[- \int_0^t \gamma_i(t)dt \right] \\ I_i(t) &\approx \mu_i C_i = h_i(0) \cdot \gamma_i(t) \cdot \mathrm{Exp}\left[- \int_0^t \gamma_i(t)dt \right] \end{aligned} \qquad (3)$$

The temperature dependency of γ_i is given by:

$$\gamma_i(t) = S_i \, e^{-E_i/kT(t)} \qquad (4)$$

where T is the absolute temperature, k the Boltzmann's constant, and S_i are factors having the dimensions of a frequency.

A major problem is to determine the trap parameters S_i and E_i from the experimentally determined parameters of the glow curve. The S_i are related to the half-lifes τ_i of the peaks and the E_i are related to the times t_i determining the location of the maxima of the glow curve. This implies:

$$\left.\frac{dI_i}{dt}\right|_{t_i} = 0$$

Therefore we have

$$S_i = \frac{\ln 2}{\tau_i} \cdot \mathrm{Exp}\left[\frac{E_i}{k.T(0)}\right]$$

$$\frac{E_i}{k.T^2(t_i)} \cdot \left.\frac{dT}{dt}\right|_{t_i} \cdot \tau_i \cdot \mathrm{Exp}\left[\frac{E_i}{k}\left(\frac{1}{T(t_i)} - \frac{1}{T(0)}\right)\right] - \ln 2 = 0 \quad (5)$$

These equations with known quantities τ_i, t_i and $T(t_i)$ allow us to calculate the desired parameters S_i and E_i.

The application of this model shall be demonstrated by a simple example. We take a LiF (TLD-100) sample which was annealed 1 hr at 400°C and exposed to 100 R. For T(t) we assume the following linear relationship between T and t:

$$T(t) = 295 + 7.456 \cdot t$$

For the values τ_i[5] and $T(t_i)$ we found

τ_1 = 5 min	$T(t_1)$ = 351.66	[K]
τ_2 = 10 hr	$T(t_2)$ = 383.0	[K]
τ_3 = .5y	$T(t_3)$ = 414.3	[K]
τ_4 = 7 y	$T(t_4)$ = 444.1	[K]
τ_5 = 80 y	$T(t_5)$ = 465.0	[K]

If we insert this data in equation (5) we obtain:

E_1 = .88 eV	S_1 = 281.64 . 10^{10} [sec^{-1}]
E_2 = 1.16 eV	S_2 = 129.54 . 10^{13} [sec^{-1}]
E_3 = 1.68 eV	S_3 = 278.31 . 10^{18} [sec^{-1}]
E_4 = 1.45 eV	S_4 = 179.23 . 10^{14} [sec^{-1}]
E_5 = 1.50 eV	S_5 = 997.65 . 10^{13} [sec^{-1}]

Furthermore, we have to adjust the peak heights of the measure glow curve to the calculated one.

Figure 2 shows the measured [5] and the calculated glow curves for 3 post irradiation annealing temperature functions. The corresponding integrated thermoluminescent light output is shown in figure 3 as a function of storing time.

Conclusions

The accuracy of thermoluminescent dosimetry can be improved if the correction coefficients are taken into account. For various reasons the storage temperature or the heating cycle can vary during a series of measurements. Under these circumstances it is important to know which coefficients have to be applied in order to correct for the change in the heating curve. Such considerations are important, for instance, for the IAEA dose intercomparison program, where such series of measurements are conducted.

With the existing computer programmes one can calculate, in the frame of the model presented, all parameters and factors needed for the corrections.

Acknowledgements:

The author wishes to thank Dr. H. Eisenlohr for helpful discussions in the course of this work.

References:

1. J.R. Cameron, N. Suntharalingam, G.N. Kenny: Thermoluminescent dosimetry, the University of Wisconsin press 1968.
2. J.H. Schulman: AEC symposium series 8, 3-33 (1967)
3. M. Schön, in Schottky Halbleiterprobleme, vol. IV, p. 282 (1968)
4. P. Bräunlich, D. Schäfer and A. Scharmann: AEC symposium series 8, 57 - 73 (1967)
5. D.W. Zimmerman, C.R. Rhyner and J.R. Cameron: AEC symposium series 8, 86 - 100 (1967).

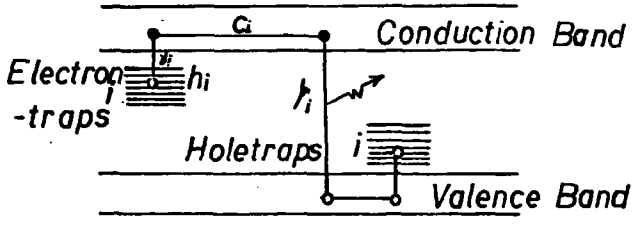

Fig. 1 - Energy-level scheme

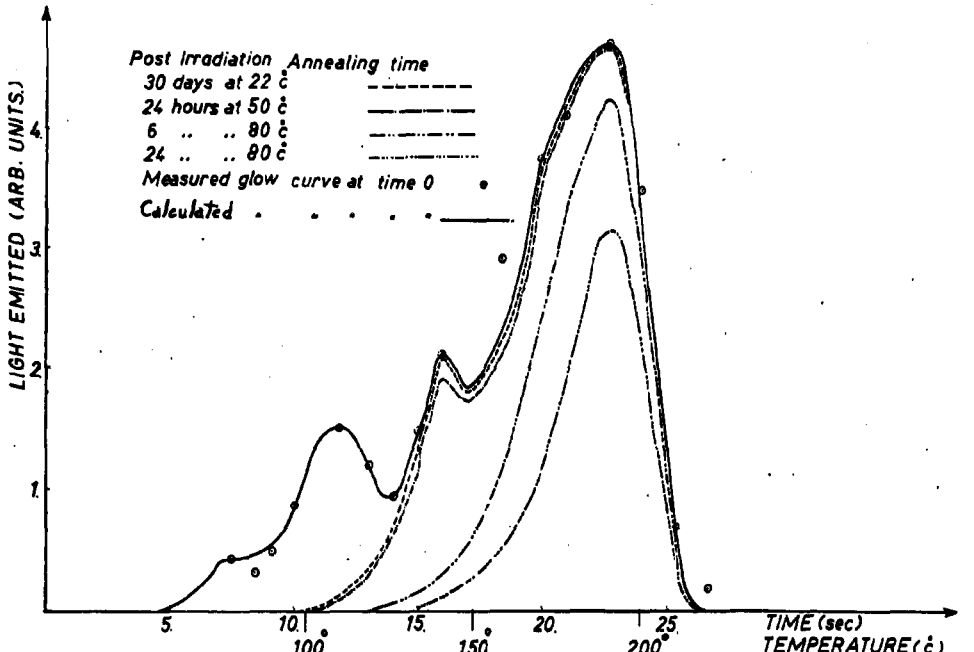

Fig. 2 - Calculated glow curve of LiF(TLD-100) as a function of post irradiation annealing times at various temperatures. The referred measured glow curve is indicated by circles.

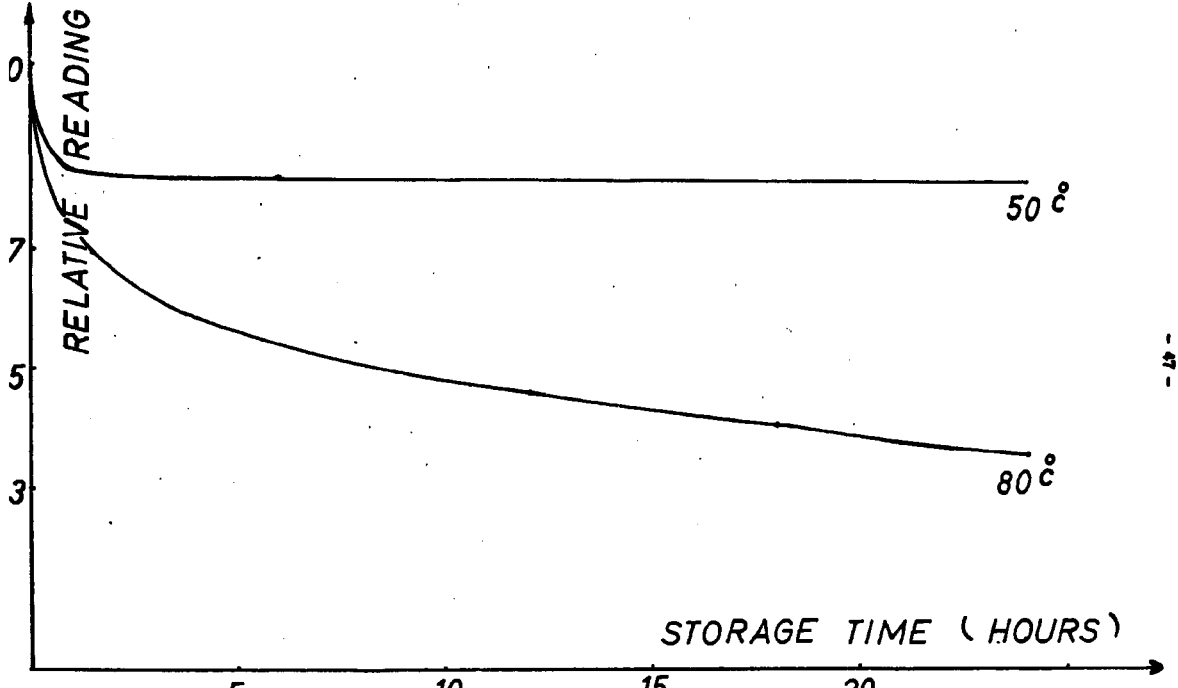

Fig. 3 - Fading characteristic of LiF(TLD-100) as a function of storage time and temperature.

Efficiency Variations of Thermoluminescent LiF Caused by Radiation and Thermal Treatments

by

Per Spanne and Carl A. Carlsson

Radiation Physics Department,
Linköping University
S-581 85 Linköping, Sweden

Abstract

Some preliminary results of an investigation concerning the efficiency of thermoluminescent LiF are reported. The TL-efficiency is tested following various radiation and thermal treatments. It is found that both radiation sensitation and radiation damage increase with increasing predose, and with decreasing LET of the predose radiation. Furthermore, both effects can be repaired by thermal treatment. Radiation damage is also found to increase if the predose followed by a thermal treatment is fractionated. It is easier to introduce and repair the sensitizing effect than the damaging effect of the radiation.

Introduction

Thermoluminescent (TL) LiF may be sensitized or damaged as a result of previous irradiation. Sensitation means that the efficiency (signal per unit energy imparted) of TL-LiF increases with previously given absorbed doses. Radiation damage means the opposite, that is, the efficiency decreases in repeated use.

The sensitation effect is more marked the lower the LET of the radiation (Naylor[1] 1965, Cameron[2] et coll. 1966, Carlsson and Alm Carlsson[3] 1968). The LET-dependence of radiation damage is

not as well investigated.

The sensitation seems to be relatively simple to avoid by suitable thermal treatments before re-use of the dosemeter (Cameron[2] et coll. 1966). The effects of radiation damage seem on the other hand to be difficult to repair (Marrone and Attix[4] 1964, Cameron[2] et coll. 1966).

The efficiency of TL-LiF also varies with its thermal history, that is, with temperature, time in a certain temperature and cooling rate (Zimmerman[5] et coll. 1966, Carlsson[6] 1969). Efficiency variations of TL-LiF in repeated use may then be a result of the combined effects of radiation sensitation, radiation damage and thermal history. An experiment designed to study one of these effects may easily be misunderstood as due to the two other effects. We have started an investigation to study these combined effects and have some preliminary results to report.

Thermal treatment

All the dosemeters (extruded LiF) used in the experiment were initially treated thermally for 1 hour at 410° C, cooled in room temperature and then individually calibrated. The TL-efficiency was then tested with 10 rad ^{60}Co-gamma radiation after thermal treatments at different temperatures for 1 and 20 hours.

The results of the thermal treatments are shown in Figs 1, 2 and 3. It should be noted that the results in the glow-peak case (Figs 2 and 3) are more qualitative than quantitative, because the glow-peaks were not very well resolved (Fig. 4).

The TL-efficiency as a function of pre-irradiation annealing temperature differs if the light sum of all the peaks in the glowcurve or the heights of single peaks are measured (Figs 1, 2 and 3). The total light sum is less dependent on thermal history than is the peak height. This is partly due to a rearrangement of electron traps from one glow peak to another at certain temperatures. This effect is observed whether the thermal treatment takes place before or after the irradiation (Pohlit[7] 1969, Booth[8] et coll. 1971). By standardizing the storing temperature after preannealing, and standardizing the time intervals between irradiation and readout, the rearrangement of traps during these periods will have negligible effect on the interpretation of effects of the thermal treatment. This standardizing also eliminates the influence of fading.

The variation of light sum-efficiency for pre-annealing temperatures below 300° C is in accordance with the results of Carlsson[6] (1969). At 300-410° C, it seems as if the TL-efficiency is independent of whether the annealing time is 1 hour or 20 hours. At 495° C, however, a decrease in TL-efficiency is observed as the annealing time is increased. This is,

according to Nakajima[9] (1970), partly due to a decrease in the optical transmission of LiF-crystals caused by OH -ions.

It was not possible to restore or increase the efficiency of the dosemeters annealed at 495° C as was the case for the dosemeters annealed below 400° C. Irreversible high temperature damage seems then to be the result of annealing in temperatures of 500° C or higher.

Radiation treatment

Marrone and Attix[4] (1964) as well as Cameron[2] et coll. (1966) have investigated the TL-efficiency of LiF as a function of previously absorbed dose. They observed a decreasing efficiency with increasing predose (radiation damage). The efficiency was less if the predose was given in multiple irradiations and thermal treatments than if it was given in one single irradiation and thermal treatment. (These thermal treatments are applied in order to empty all traps before the efficiency control with a test dose.) Marrone and Attix[4] interpreted this difference as a "fixing" of radiation damage during the thermal treatment (400° C for 15 minutes) between the irradiations. Cameron's[2] explanation was that the radiation damage to traps in LiF-crystals takes place at different rates depending on whether the traps have captured electrons or not.

In these experiments the dosemeters receiving the predose in fractions were thermally treated at about 400° C between the irradiations, that is, they were treated thermally for a longer period than those predosed in one single irradiation. Since treatment at 400° C decreases the radiation-induced sensitation, it might be possible to ascribe the difference in TL-efficiency after single and multiple predose to a difference in the reduction of the sensitation due to different thermal treatments.

The following experiments were made to find eventual combined effects of sensitation and damage.

The dosemeters were initially given a thermal treatment for 1 hour at 410° C and thereafter individually calibrated. They were then exposed (predosed) to ^{60}Co γ-radiation with doses ranging from 10 rad to 1 Mrad. After that they were again thermally treated at 410° C for different times (15 min, 2 h and 19 h). The TL light-sum after a test dose of 10 rad ^{60}Co γ-radiation was then used as a measure of the efficiency.

The efficiency after multiple (double) predoses was determined by repeating the predose irradiation, thermal treatment, and test dose. The dosemeters predosed twice had then been annealed twice as much as those predosed once. The results are shown in Fig. 5.

15 minutes annealing

With 15 minutes annealing at 410° C the efficiency increases with increasing predose up to 10^4-10^5 rad (Fig. 5). It is evident that this annealing is not enough to eliminate the radia-

tion induced sensitation of the dosemeters.

2 hours annealing

After an annealing for 2 hours the TL-efficiency is monotonically decreasing with increeasing predose (Fig. 5). The efficiency seems to be independent on whether the predose is given in one or two irradiations for predoses lower than $2 \cdot 10^4$ rad and the efficiency difference is constant to its absolute value above 10^5 rad. The difference in efficiencies is then due to different annealing methods.

19 hours annealing

Even after 19 h post-irradiation annealing the TL-efficiency is monotonically decreasing with increasing predose. The TL-efficiency is, however, higher relative to that after 2 h annealing. The efficiency difference between single and multiple doses and annealing remains (Fig. 5).

Discussion

The efficiency of TL-LiF to a small test dose (here 10 rad) varies with both thermal and radiation history of the dosemeter. The variation of light sum efficiency for different thermal treatments is shown in Fig. 1. What is remarkable here is the short time for receiving thermal equilibrium in the region 300° C - 400° C (Carlsson 1968). No difference in efficiency is seen with pre-irradiation annealing of 1 or 19 hours in this temperature interval.

The efficiency to a small test dose as a function of previously given radiation doses as shown in Fig. 5, is a result of both radiation and thermal treatments. The efficiency is lower when the predose is given in two sessions each followed by a thermal treatment at 410° C, independent of the length (15 min, 2 h, 19 h) of the thermal treatment. This decreased efficiency may at least partly be explained as a desensitizing effect of the longer thermal treatment. In the 15 min-case this is evidently true. 2 h at 410° C should be enough to desensitize TL-LiF after a predose of $3 \cdot 10^5$ rad (Cameron et coll. 1966). After 19 h no sensitizing effects should be present. The increased efficiency with increased annealing time from 2 h to 19 h indicates that thermal treatment at 410° C can repair radiation damage. The reason why the efficiency is lower with multiple irradiation and thermal treatment sessions is not as satisfactorily understood.

Fig. 6 shows our few experimental data presented as fractional radiation damage. The fractional radiation damage is defined

$$\frac{(TL)_0 - (TL)_D}{(TL)_0}$$

where (TL) means the thermoluminescent light sum for a test dose and index 0 and D are previously absorbed doses in the dosemeters.

Results obtained by Cameron[2] et coll. (1966) are included for comparison in Fig. 6. They irradiated TL-LiF at 290° C. Their results may be interpreted as obtained with infinitesimal irradiation periods immediately followed by infinitesimal thermal treatments at 290° C. The latter results indicate that the radiation damage increases with increasing fractionation of irradiations and thermal treatments. The effect of fractionating the predose and thermal treatment on radiation sensitation is not yet investigated, but the results of Cameron[2] et coll.(1966) indicate that even the radiation sensitation increases with increasing fractionation. They observed an increasing sensitation at doses lower than $2 \cdot 10^4$ rad when the irradiations were performed at 290° C, rather than at lower temperatures.

The following comparison of radiation sensitation, radiation damage and thermal damage summarizes some parallels in these effects.

Both radiation sensitation and radiation damage
a) increase with increasing predose
b) increase with decreasing LET of the radiation,
c) can be repaired by thermal treatment at about 400° C, and
d) seem to increase with increasing fractionation of irradiation and thermal treatment.

The radiation sensitation is easier to introduce and easier to repair than radiation damage.

The radiation damage and the damage caused by thermal treatment at 500° C seem to both affect all the glow-peaks equally (Figs 2 and 3). The radiation damage can be interpreted as a result of heating small volumes within the crystal to high temperatures (Point heat theory, Dessauer[10] 1923, Chadderton[11] 1965). Using the point heat theory in comparing thermal and radiation damage is, however, a very complex task. Temperatures, heating times, temperature gradients and cooling rates in the small volumes, traversed by charged particles are, however, difficult to estimate and even to define.

Acknowledgments

This work has been supported by Riksföreningen mot cancer. The authors express their sincere gratitude to Drs L. Bøtter-Jensen, P. Christensen and K. Sehested for generous help with the experiments.

References

1. G.P. Naylor
   Thermoluminescent phosphors: variation of quality response with dose
   Phys. Med. Biol. 10, 564-565 (1965)

2. J.R. Cameron, L. De Werd, J. Wagner, C. Wilson, K. Doppke, and D. Zimmerman
   Non-Linearity of thermoluminescence as a function of dose for LiF (TLD-100)
   In Proc. Symp. Solid State Chem. Radiat. Dosimetry, IAEA, Vienna (1966)

3. C.A. Carlsson and G. Alm Carlsson
   Induced LET-dependence in thermoluminescent LiF and its application as LET-meter
   Sec. Int. Conf. Lum. Dosimetry, Gatlinburg, Tenn., USA. September 1968. USAEC Rept. CONF-68 09 20 (1969)

4. M.J. Marrone and F.H. Attix
   Damage effects in CaF_2: Mn and LiF thermoluminescent dosimeters
   Health Physics 10, 431-436 (1964)

5. D.W. Zimmerman, C.R. Rhyner and J.R. Cameron
   Thermal annealing effects on the thermoluminescence of LiF
   Health Physics 12, 525-531 (1966)

6. C.A. Carlsson
   Thermoluminescence of LiF: Dependence of thermal history
   Phys. Med. Biol. 14, 1, 107-118 (1969)

7. W. Pohlit
   Zur Thermolumineszenz in Lithium fluorid
   Biophysik 5, 341-356 (1969)

8. L.F. Booth, T.L. Johnson and F.H. Attix
   Use of Miniature glass-needle-type TL dosimeters in finger-ring applications
   Naval Research Laboratory Report 7276 (1971)

9. T. Nakajima
   Effects of atmosphere and grain size on thermoluminescence sensitivity of annealed LiF crystals
   J. Phys. D: Appl. phys. 3, 300-306 (1970)

10. F. Dessauer
    Über einige Wirkungen von Strahlen IV
    Zeitschrift für Physik, 20, 288-298 (1920)

11. L.T. Chadderton
    Spike phenomena and the displacement cascade
    In Radiation damage in crystals, Methuen & Co Ltd, London (1965)

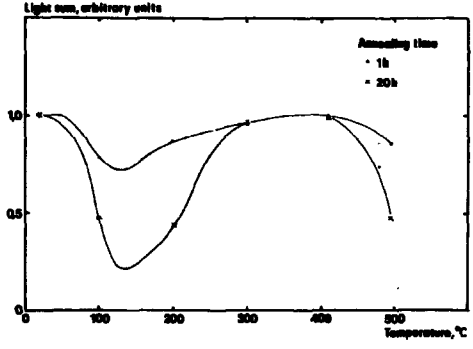

Fig 1 The TL light-sum after preirradiation annealing at different temperatures for 1 and 20 hours.

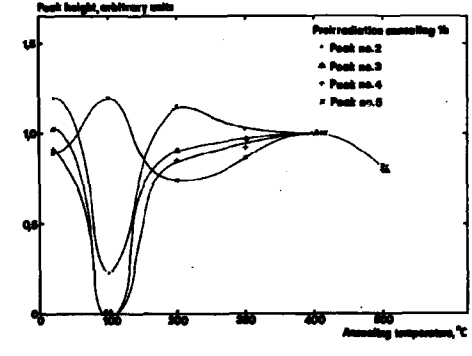

Fig 2 The TL-efficiency measured by glow peaks heights after preirradiation annealing at different temperatures for 1 hour.

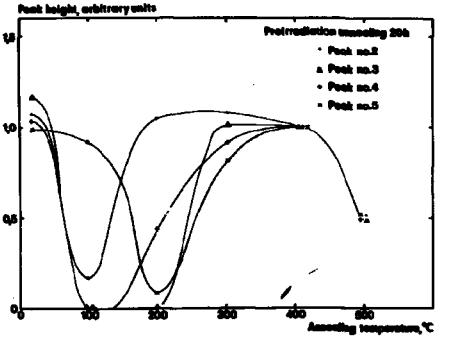

Fig 3 The TL-efficiency measured by glow peak heights after preirradiation annealing at different temperatures for 20 hours.

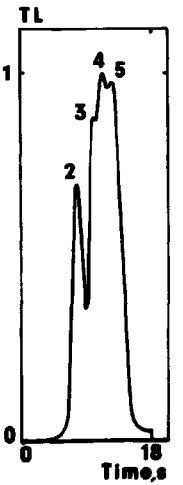

Fig 4 Glow curve obtained after preirradiation annealing at 410° C for 1 h and a testdoseirradiation of 10 rad.

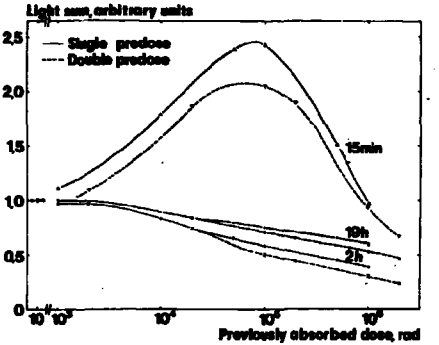

Fig 5 The TL-efficiency to a test dose of 10 rad of ^{60}Co-gamma radiation after different predoses followed by thermal treatments at 410° C for 15 min, 2 h and 19 h.

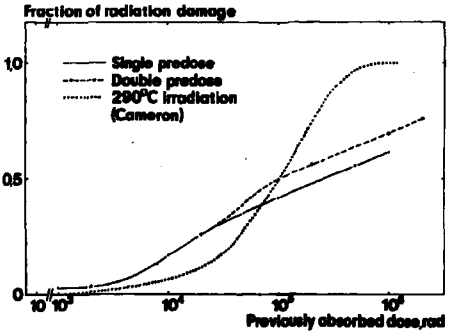

Fig 6 Fraction of radiation damage after different predoses followed by a thermal treatment for 2 h at 410° C. The dotted curve is obtained from Cameron[2] (1966).

Suntharalingam

The glow curve you showed appears different from the glow curve we are normally used to see in LiF (TLD-100) powder. Could you please tell us whether the curve you obtained was for a fabricated dosimeter or for loose powder. Also could you please indicate the heating rate used.

Spanne

We used TLD-100 extruded ribbons. The dosimeters were read out with an approximately linear heating rate (15°C/s) to about 280°C.

Becker.

Having watched for many years the constant struggle with the many mysterious and confusing properties of lithium fluoride, some of which have been the subject of this paper, I keep wondering why people are still so fascinated by this rather unpleasant substance. Why not use equally energy-independant, but much better behaving, materials such as the BeO:Na described by Yasuno and Yamashita (see paper No. 20 of this conference).

Suntharalingam

I would like to respond to Klaus Becker's remarks. Research studies on lithium fluoride certainly show many interesting and confusing phenomena. However, what is important is to find out how these effects influence the routine use of LiF for certain applications. Later at this meeting I will show how we are successfully using LiF dosimeters.

CONTINUOUS MODEL FOR TL TRAPS (*)

Shigueo Watanabe and Spero Penha Morato
Instituto de Energia Atômica and Instituto de Física da Universidade de São Paulo. - São Paulo - Brasil.

ABSTRACT

Analysis of glow curves in CaF_2:natural demonstrated that some glow peaks in this material do not obey the simple model of thermoluminescence proposed by Randall and Wilkins. In particular these peaks do not decay exponentially during isothermal heating; and, moreover, the peak positions change during such treatment. A model based on the superposition of two peaks was first proposed, wherein two closely spaced, unresolved peaks assumed to add to give the observed behavior. The calculations revealed that this model can reasonably well explain the isothermal decay curves, but not the isothermal change in the peak position. As a result, a second model was developed based on a narrow, continuous distribution of trap depth, thus modifying the model of Randall and Wilkins which is based on only one distinct trap depth. This second model, which supposes a Gaussian distribution for the trap depths, was used to explain the behavior of two glow peaks in natural CaF_2, giving satisfactory fits for the glow curve, for the isothermal decay, and for the isothermal change in the peak position. The application of this model also enables calculation of the trap parameters, which had not been previously accomplished. Analysis based on this continuous model was also extended to similar behavior of 280°C and 370°C peaks in the glow curve of dosimetric LiF:Mg. Isothermal decay, and isothermal change in the position of these peaks were measured for this material.

(*) Based in part upon portions of a thesis submitted by Spero Penha Morato to the Institute of Physics, University of São Paulo, in partial fulfillment of the requirements

INTRODUCTION

Randall and Wilkins proposed a model which has been widely used to fit observed glow curves of thermoluminescent crystals. This model assumes a well defined depth for traps giving rise to a glow peak.

If we denote by E the trap depth, the probability per unit time at absolute temperature T for a trapped electron to escape can be written as

$$p = \tau^{-1} = s \exp(-E/kT) \tag{1}$$

where k is the Boltzmann constant, τ is the mean lifetime, and s is the frequency factor. If, further, we denote by β the heating rate of the TL reader, and by $n(E,T_o)$ the number of trapped electrons at temperature T_o, then after heating the sample to temperature T, the number of remaining electrons is given by:

$$n(E,T) = n(E,T_o) \exp\left[-\int_{T_o}^{T} \frac{s}{\beta\ (T)} \exp(-E/kT)dT\right] \tag{2}$$

Emitted light at temperature T is given by

$$I(T) = s \exp(-E/kT)n(E,T) \tag{3}$$

Let us now consider an irradiated sample subjected to an isothermal annealing at temperature T_a during a time t_a. The number of electrons left in the traps is given by

$$n(E,T_a,t_a) = n(E,T_a,0) \exp\left[-st_a \exp(-E/kT_a)\right] \tag{4}$$

In the subsequent reading cycle this number acts as the initial number of trapped electrons in Eq.(3). It is, therefore, easy to recognize that at peak temperature T_p,

$$\log I(T_p) = \text{const.} - st_a \exp(-E/kT_a) \tag{5}$$

This linear dependence of $\log I(T_p)$ on t_a is a typical result of the Randall and Wilkins model.

Furthermore, the peak temperature T_p is a constant for each peak.

Measurements on fading or other isothermal decay carried out by several investigators [1,2,3] indicate, however, that $\log I(T_p)$ does not always follow a linear law. Hence, the glow curve does not obey the Randall and Wilkins equation.

We extended post-annealing decay measurements to Brazilian fluorite (peaks I, II and III) and to the 280°C and 370°C peaks in LiF:Mg, again finding a behavior not predicted by the Randall and Wilkins model.

EXPERIMENTAL METHODS

a) Natural Calcium Fluorids

Green colored samples of natural calcium fluoride extracted from a mine located in Criciuma, Santa Catarina State, Brazil, were pulverized and sieved through 80 or to 200 mesh Tyler screens to be used in this experiment. To eliminate TL induced in the fluoride by natural surrounding radioactivity, the samples were heated for 10 minutes at 580°C and then at 400°C for 2 hours. Subsequently they were irradiated to 100R with Cs-137 gamma-rays, to be annealed isothermally at temperatures listed in Table I for times varying between 15 and 180 minutes. Then the TL was read on a CON-RAD model 5100 reader.

TABLE I

PEAK	POST-ANNEALING TEMPERATURE T_a (°C)				
I	18	26	38		
II	87	113	123	131	138
III	177	200	214	233	240

The error in oven temperature during post-annealings was estimated to be $\pm$ 1°C.

Figures 1 to 3 and Figures 6 to 9 show isothermal decay curves and peak displacements for peaks II and III, as functions of annealing time t_a.

b) The 280°C and 370°C peaks in LiF:Mg

Peaks occurring at 280°C and 370°C in the glow curve of dosimetric LiF:Mg, known as TLD-100 and produced by Harshaw Chemical Company, were considered in this experiment. Samples annealed for one hour at 400°C were exposed to 30,000 R of Cobalto-60 gamma-rays (*), and subsequently divided into several groups for isothermal post-annealing at temperature listed in Table II, for times t_a varying between 5 and 120 minutes.

TABLE II

PEAK	POST-ANNEALING TEMPERATURES T_a (°C)			
280 °C	210	223	235	249
370 °C	290	298	305	320

The results for log $I(T_a)$ vs. t_a are presented in Fig.11 for the 280°C peak and in Fig.13 for the 370°C peak. Figures 12 and 14 show the displacement of the peak position as a function of t_a for the 280°C and 370°C peaks, respectively.

(*) The cobalt source we used belongs to Instituto Central de Câncer and Hospital A.C.Camargo - São Paulo.

Two peaks model

Let us assume that there are two sets of traps giving rise to two closely spaced, unresolved peaks, which add to give the observed glow peak. Let us denote by E_1 and E_2 their depths and by s their common frequency factor. The probability of liberating an electron being given by Eq. (1), and assuming that the rate of empting each trap is not affected by the presence of other one, we can write the following expression for the emitted light intensity:

$$I(T) = n'_o s \exp(-A_1) + n''_o s \exp(-A_2) \tag{6}$$

where

$$A_i = s t_a \exp(-E_i/kT_a) + E_i/kT + s \int_{T_o}^{T} \frac{\exp(-E_i/kT)}{\beta} dT \tag{7}$$

$$i = 1,2$$

Schulman et al.[4] considered a superposition of several closely spaced components to explain anomalous fading of CaF_2:Mn. No quantitative discussion was reported though.

Continuous Model

Saddy[5], Curie[6], and Medlin[7] have discussed a model that assumes a Gaussian distribution of trap depths around a value E_o to explain decay curves in the phosphorescence of ZnS and calcite.

Let $n(E,t_a)$ denote the number of trapped electrons per unit interval of trap depth after time t_a of isothermal post-annealing at temperature T_a:

$$n(E, t_a) = \frac{dN(E,t_a)}{dE} \tag{8}$$

We now assume that

$$\frac{d}{dt}(dN) = -dN\, s \exp(-E/kT) \tag{9}$$

such that

$$dN = dN_o \exp\left[-st_a \exp(-E/kT_a)\right] \tag{10}$$

Integrating over trap depth E we obtain

$$N(E,t_a) = \int n(E,0) \exp\left[-st_a \exp(-E/kT_a)\right] dE \tag{11}$$

for the actual number of unemptied traps after time t_a, where $n(E,0)$ is the distribution function of trap energies at $t_a = 0$.

Let us take a Gaussian form for $n(E,0)$ with half-width σ :

$$n(E,0) = \frac{N_o}{\sqrt{2\pi}\,\sigma} \exp\left[-\frac{(E-E_o)^2}{2\sigma^2}\right] \tag{12}$$

where N is the initial density of filled traps. Thus the glow curve can be expressed as

$$I(T) = \frac{N_o s}{\sqrt{2\pi}\sigma} \int_{E_1}^{E_2} \exp\left[-\frac{(E-E_o)^2}{2\sigma^2} - s t_a \exp(-E/kT_a) - \frac{E}{kT} - s \int_{T_o}^{T} \frac{\exp(-E/kT)}{\beta(T)} dT \right] dE \quad , \quad (13)$$

where E_1 and E_2 are values of E for which the integrand becomes negligible.

If we denote by $F(E, t_a, T_a, T)$ the integrand of Eq.(13) and let

$$G(E, t_a, T_a, T_p) = \left[\frac{E}{k T_p^2} - \frac{s}{\beta(T_p)} \exp(-E/kT_p) \right] F(E, t_a, T_a, T_p), \quad (14)$$

where T_p is the peak temperature, the condition that $I(T)$ is maximum at $T=T_p$ can be expressed as

$$\int_{E_1}^{E_2} G(E, t_a, T_a, T_p) \, dE = 0 \quad (15)$$

The slope of $\log I(T_p)$ at $t_a = 0$, which will be denoted by m, is obtained expanding $\log I(T_p)$ in a power series of t_a; m is the coefficient of the linear term. So m can be expressed as

$$m = -\int_{E_1}^{E_2} H(E,0,T_a,T_p) \, dE \Big/ \int_{E_1}^{E_2} F(E,0,T_a,T_p) \, dE \quad (16)$$

where $$H(E,0,T_a,T_p) = s \exp(-E/kT_a) \, F(E,0,T_a,T_p). \quad (17)$$

NUMERICAL CALCULATIONS

a) Two peaks model for natural CaF_2

We set $n'_o = n''_o$ in Eq.(6) to simplify the computation. Initial values of s, E_1 and E_2 were obtained solving Eq.(5) for s and E using decay data. E_1 and E_2 were then varied, and for each pair of E_1 and E_2, s was varied. Once a set of parameters which produces a glow curve and decay curve close to the observed ones was found, the numerical calculations were carried out in finer steps around that set of parameters. Starting with peak III and $T_a = 200^\circ C$ the best result obtained was for $E_1 = 1.53$ eV, $E_2 = 1.71$ eV and $s = 2 \times 10^{11}$ sec^{-1}. These values were used to obtain decay curves for $T_a = 214, 233, 244^\circ C$. The results of these calculations are plotted in Figures 6 to 10. Practically no displacement of peak position resulted.

A similar procedure of computation was applied to peak II. The results are shown in Figures 1 to 4. Best fits were found for E_1 = 0.94 eV, E_2 = 0.96 eV and $s = 2 \times 10^8$ sec^{-1}. No displacement of peak position was obtained.

b) Continuous model for natural CaF_2

Again the analysis was carried out for peak III and T_a = 200°C, varying E_0 between 1.50 and 1.60 eV in a step of 0.02 eV. For each value of E_0, s was varied from 10^{11} sec^{-1} to 10^{12} sec^{-1} in steps of 2×10^{11} sec^{-1} while σ was kept at 0.1 eV. This analysis lead to E_0 = 1.58 eV and $s = 5 \times 10^{11}$ sec^{-1} as best parameters. These values were then held fixed and σ varied, resulting in σ = 0.09 eV as the best value. This set of parameters was subsequently used to fit experimental data for different values of T_a. Similar calculations were carried out for peak II, and the results are represented in Figures 1 to 11 (except Figs. 4 and 10). For this model there was a clearcut displacement of peak position.

c) Continuous model for 280 and 370°C peak of LiF:Mg

Follwing the same procedure as described in Section b, we searched for a set of parameters to fit glow curves and decay curve for the 280°C peak starting with T_a = 223°C : E_0 = 1.50 eV, $s = 5 \times 10^{11}$ sec^{-1}, and σ = 0.09 eV. These values were used to compute decay data and displacement of peak position for T_a = 210°, 235 , and 249°C. The results are plotted in Figures 12 and 13.

For the 370°C peak the search for parameters was carried out for T_a = 290°C data, obtaining E_0 = 1.66 eV, $s = 8 \times 10^{11}$ sec and σ = 0.09 eV. The results of calculation for T_a = 298, 305, and 320°C are shown in Figures 14 and 15.

Since there is a slight possibility that the variation of oven temperature during the operation of inserting the sample for annealing might influence short-time decay data, we performed isothermal post-annealing measurements at 118, 132, and 140°C for peak 5 of LiF:Mg. This peak was chosen because it has σ very close to zero, so that its log $I(T_a)$ is linear in t_a, as shown in Fig.16. The experimental result agrees with this statement. Since the same oven was used in all the experiments of the present work, the curvatures in decay data are crystal's properties.

CONCLUSIONS

Although extensive calculations were performed, a more complete numerical analysis can and will be carried out, especially for the 280°C and 370°C peaks in TLD-100. Nonetheless, the following conclusions can be drawn:

1. The two peaks model predicts too small a displacement of peak position found in isothermal decay data in fluorite and in LiF:Mg, although decay curves and glow curves can be fitted reasonably well.

2. The continuous model predicts the displacement observed experimentally in the TL peaks of fluorite. In TLD-100, it predicts well enough the displacement of the 280°C peak, but in the case of the 370°C peak, the model gives only qualitative agreement.

In the two peaks modal one might try $n'_0 \neq n''_0$, but then we will be introducing one more parameter to be adjustad. The situations would be similiarly complicated if we assume three or more peaks model. Furthermore, it is hard to understand why two peaks would explain every case that does not follow the Randall and Wilkins model.

The detailed study of the behavior of functions, F, G, H and n will be discussed elsewhere.

ACKNOWLEDGEMENT

We would like to acknowledge Dr. Emico Okuno for taking data on natural calcium fluoride; Miss Rejane A.Nogueira for taking data on TLD-100; Miss Wanda C.Lee for numerical calculations on TLD-100 data. Thanks are due to personnel at the computation section of the physics institute of the University of São Paulo, and also to Dr.Michael R.Mayhugh for discussions.

REFERENCES

1. W.Binder, S.Disterhoft and J.R.Cameron, Proc. of Second Int. Conf. on Luminescence Dosimetry, CONF - 680920 - USAEC, p.43 (1968).

2. P. Christesensen, Proc.of Second Int.Conf.on Luminescence Dosimetry , CONF-680920, USAEC, p.90 (1968).

3. C.R. Wilson and J.R.Cameron, Proc.of Second Int.Conf. on Luminescence Dosimetry, CONF-680920, USAEC, p.161 (1968).

4. J.H.Schulman, R.J.Ginther, S.G.Gorbics, A.E.Nash, E.J. West, and F.H. Attix, Int.Jour.of Applied Radiation and Isotopes, 20 , 523 (1969).

5. M.J.Saddy, Compt.Rend. 228, 2022 (1949)

6. M.D.Curie, Compt.Rend.229 , 193 (1949).

7. W.L.Medlin, Phys.Rev. 122, 837 (1961), Idem, Phys.Rev. 123 , 502(1961).

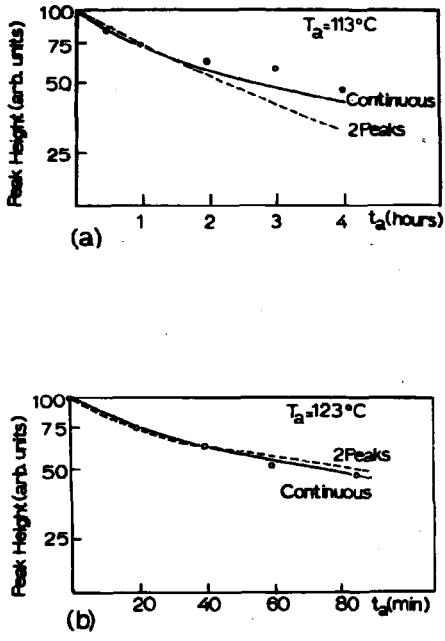

Fig. 1. Decay data for peak II in fluorite. (a) for T_a = 113°C. (b) for T_a = 123°C. E_1 = 0.94 eV, E_2 = 0.96 eV, $s \doteq 2 \times 10^8$ sec^{-1} ; E_o^a = 0.96 eV, $s' = 2 \times 10^8$ sec^{-1} , σ = 0.05 eV.

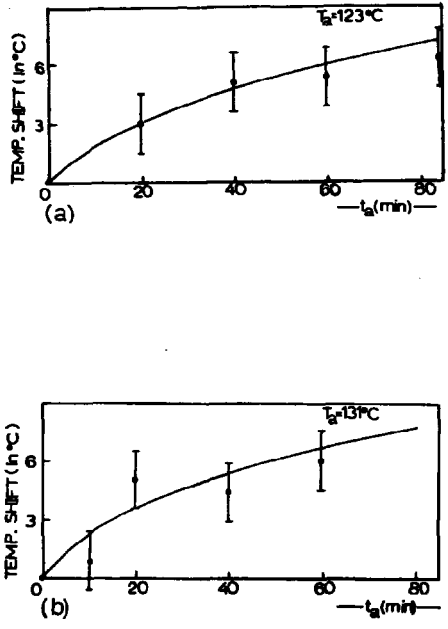

Fig. 2. (a) Decay data for peak II in fluorite for T_a = 131°C. Same parameters as in Fig.1 were used. (b) Displacement of peak II in fluorite for T_a = 113°C. Solid line: Continuous model calculation.

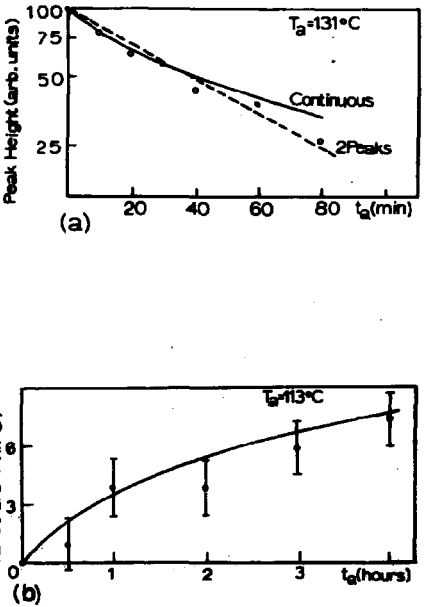

Fig. 3. Displacement of peak II in fluorite. (a) for T_a = 123°C. (b) for T_a = 131°C. Solid line: Continuous model calculation.

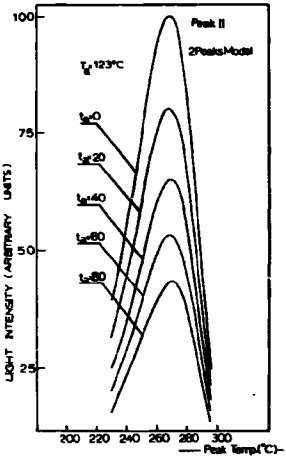

Fig. 4. Theoretical glow curves for peak II using 2 peaks model. E_1 = 0.84 eV, E_2 = 0.96 eV, s = 2 x 10^8 sec^{-1}.

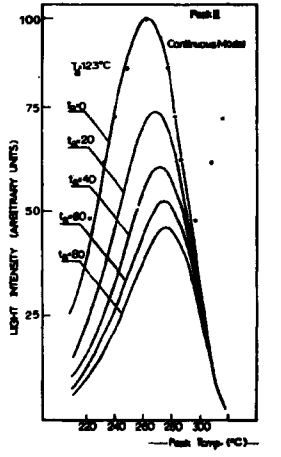

Fig. 5. Solid lines: Theoretical glow curves for peak II using continuous model. E_o = 0.96 eV, s= 2 x 10^8 sec^{-1}, σ = 0.05 eV.Circles : Experimental points.

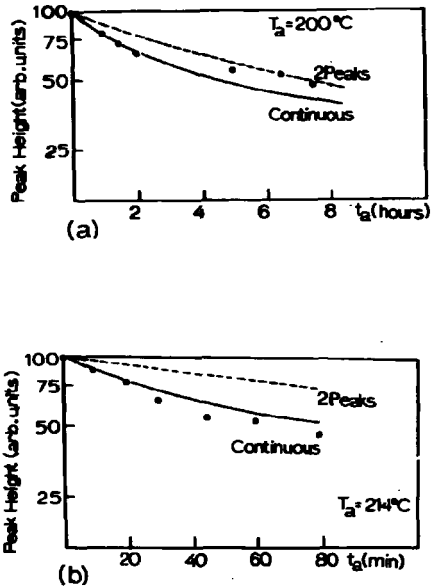

Fig. 6. Decay data for peak III in fluorite. (a) for T_a = 200°C. (b) for T_a = 214°C. E_o = 1.58 eV, s = 5×10^{11} sec^{-1}, σ = 0.09 eV; E_1 = 1.53 eV, E_2 = 1.71 eV, s = 5×10^{11} sec^{-1}.

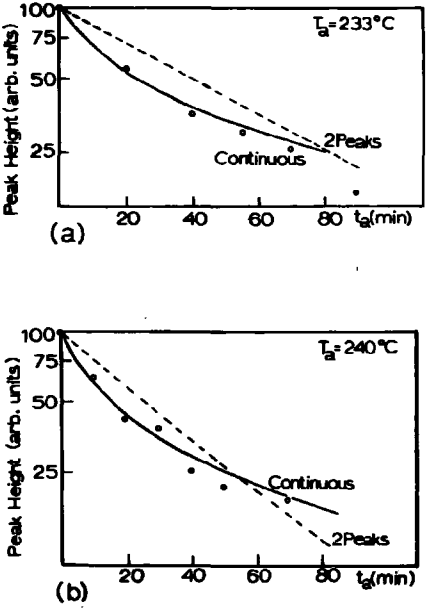

Fig. 7. Decay data for peak III in fluorite. (a) for T_a = 233°C. (b) for T_a = 240°C. Same parameters as in Fig. 6 were used.

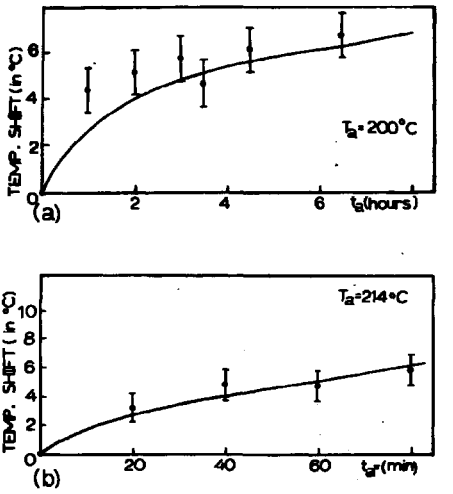

Fig. 8. Displacement of peak III in fluorite. (a) for T_a = 200°C. (b) for T_a = 213°C.

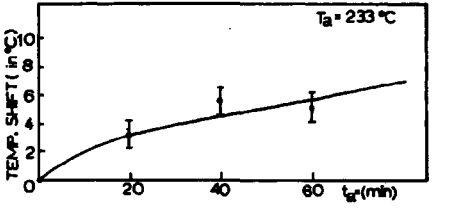

Fig. 9. Displacement of peak III in fluorite for T_a = 233°C.

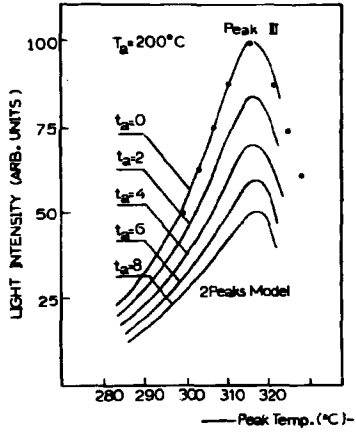

Fig.10. Theoretical glow curves for peak III using 2 peaks model E_1 = 1.53 eV, E_2 = eV and s = 2 x 10^{11} sec^{-1}.

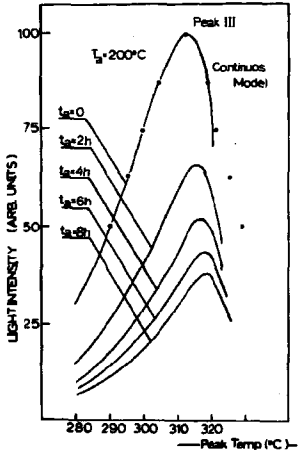

Fig.11. Solid lines: Theoretical glow curves for peak III using Continuous model. E_a = 1.58 eV, s= 5 x 10^{11} sec^{-1}, σ = 0.09 eV.Circles:Experimental points.

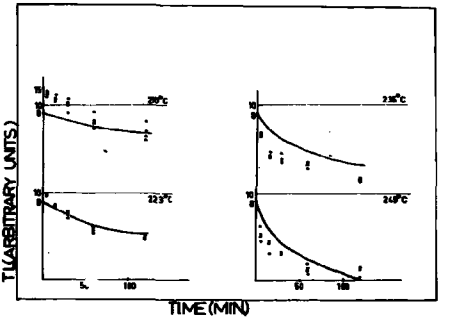

Fig.12. Decay data for 280°C peak in TLD-100. Solid lines: Continuous model calculation for E_o = 1.50 eV, s = 5 x 10^{11} sec^{-1}, σ = 0.09 eV.

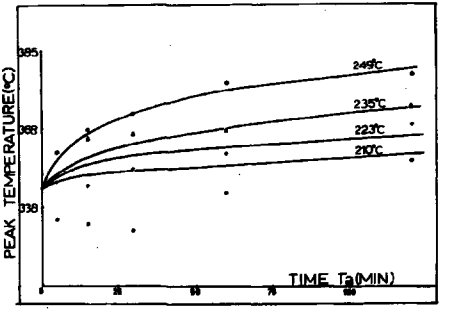

Fig.13. Displacement of 280°C peak in TLD-100. Solid lines: Continuous model calculation for same parameters listed in Fig.12.

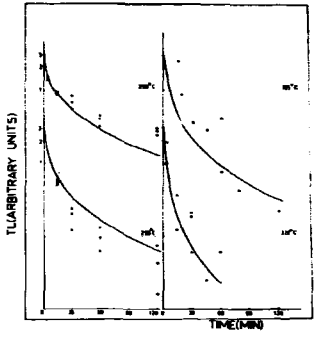

Fig.14. Decay data for 370°C in TLD-100. Solid lines: Continuous model calculation for E_o = 1.66 eV, s = 8 x 10^{11} sec^{-1}, σ = 0.09 eV.

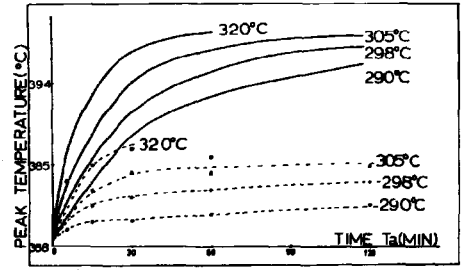

Fig.15. Displacement of 370°C peak in TLD-100. Solid Lines: Continuous model calculation for same parameters as in Fig.14.

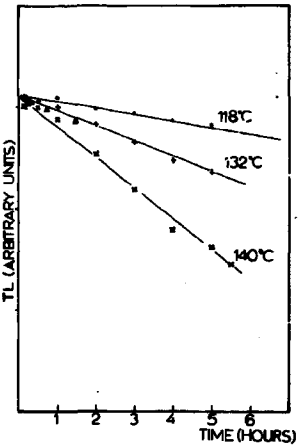

Fig.16. Experimental decay data for peak 5 in TLD-100.

Aitken

I am surprised that you say that on the two-peak model you expect no shift in peak position of the composite peak, following annealing. Surely if one of the peaks is at a lower temperature than the other, it will fade more quickly and therefore give rise to a shift in the position of the maximum in the composite peak.

The Influence of Hydroxide Impurities on Thermoluminescence in Lithium Fluroide

by

L. A. DeWerd and T. G. Stoebe

University of Washington
Division of Metallurgical Engineering
Seattle, Washington 98195

Abstract

Crystals diffused with OH ions show variations in thermoluminescent (TL) output with the concentration of OH ion complexes present in the crystal. The results show a decrease in TL intensity with an increase in the concentration of hydroxide ions, a change in the TL glow curve, and an absence of supralinearity in the presence of a large amount of OH ion complexes. From infrared absorption studies, the OH ion is found to complex with Mg^{2+} -cation vacancy dipoles. The decrease in TL sensitivity is caused by these OH ion complexes, which eliminate the Mg^{2+} -cation vacancy dipoles and dipole complexes from participating as traps in the luminescent process. The observed glow curve shapes are dependent upon the concentration of dipoles and dipole complexes, as modified by interactions with hydroxide ions. OH ion complexes can act as deep electron traps having a large capture cross section; the supralinearity decreases depending on the number of these complexes present. These results are consistent with the non-luminescent trap model of supralinearity.

Introduction

Thermoluminescence (TL) in LiF (TLD 100), as used in dosimetry, suffers from variations in sensitivity and from a non-linear TL vs. dose response. The variations in sensitivity are probably the result of varying impurity concentrations and distributions. The processes responsible for the non-linear TL vs dose response, called supralinearity, are not entirely understood.

The first models proposed to explain supralinearity were based on the creation of additional traps or recombination centers[1]. These models have been rejected because the temperatures of the TL peaks do not change and because the emission spectrum for the supralinear regions at high exposure is the same as for the linear regions at low exposure[2,3]. Utilizing various energies of radiation, Suntharalingam[4] found that the magnitude of the supralinearity is dependent on the amount of linear energy transfer(LET). This led him to postulate the existence of non-luminescent traps which are fewer in number, but have a higher capture cross-section for electrons, than the luminescent traps. Consequently, as the non-luminescent traps fill up, there are more electrons available for the luminescent traps resulting in an increased thermoluminescent response and supralinearity.

TL in LiF (TLD 100) is a result of lattice defects, including impurities, vacancies, and impurity-vacancy complexes. The major impurity, magnesium, is thought to be involved in the electron trap responsible for thermoluminescence[5,6], while titanium is thought to be involved in the recombination process[6,7]. Grant[8] has shown that peak 2 of the TL spectrum correlates well with the concentration of Mg^{2+} -cation vacancy dipoles. Harris and Jackson[9] have shown that impurity-vacancy dipoles are related to both peaks 2 and 3. It has also been shown that a separate lattice defect is responsible for both peaks 4 and 5[9,10]. Using annealing and quenching studies in conjunction with ionic conductivity experiments, Dhar[11] has confirmed that dipoles are closely associated with peak 2 of the LiF (TLD 100) glow curve. Dhar[11] has also been able

to associate peak 5 with the presence of higher order dipole complexes, such as trimers, using this same method.

The influence of impurities other than magnesium and titanium on TL has not been studied extensively. One important impurity is the hydroxide ion, which is generally present in varying concentrations in all Harshaw LiF crystals including LiF (TLD 100). It has been suggested tentatively that this impurity may be important in the TL sensitivity in LiF[12]. The types of lattice defect configurations present in LiF containing OH ions in addition to divalent cation impurities has been discussed[13]; the various hydroxide ion configurations in the LiF lattice can be observed experimentally using infrared absorption techniques. The purpose of the present investigation is to study the influence of the concentration and distribution of hydroxide ions on TL sensitivity and supralinearity in LiF (TLD 100).

Experimental

Single crystals of LiF (TLD 100) were doped with OH ions using controlled diffusion experiments at 700°C. The source of OH ions was distilled water or LiOH, and diffusion proceeded by vapor transport of H_2O or LiOH to the LiF surface. For each set of crystals, the source of OH ions is designated in parentheses. Diffusion times ranged from 54 to 297 hours. Three crystals were diffused for each set of data obtained. When further diffusion in crystals LiF(H_2O) failed to give significantly larger concentrations of OH ions in the crystals, additional diffusion with LiOH was undertaken. These latter crystals are designated LiF(LiOH). Other crystals, denoted as W1 and W2, contained OH ions as-grown, in addition to about 100 ppm Mg^{2+}. Infrared absorption results, performed using a Perkin-Elmer 225 infrared spectrometer, indicate that crystals W2 contain a greater concentration of OH ions than the LiF (LiOH) crystal, and that crystal W1 contains even greater amount of OH ions than W2.

The TL results were obtained after annealing for 1 hour at 400°C,

followed by irradiation with 250 kVp Thoraeus III filtered X-rays (135 keV effective). Readout was performed using a Harshaw 2000 reader. TL results for the sensitivity change after diffusion on each set of crystals were always determined relative to a set of crystals which were subject to the same heating cycle at the same time, but without diffusion.

TL Sensitivity

The influence of OH ions on the TL glow curve in LiF (TLD 100), diffused from a distilled water source, is shown in Figure 1. In general, the TL sensitivity is seen to be decreased by this treatment. Peaks 2 and 3 show a decreased TL sensitivity, followed by a slight increase at longer diffusion times, while peaks 4 and 5 are greatly decreased for all diffusion times. Crystals W2 and the LiF (LiOH) crystals show glow curves similar to Figure 1(c) or (d) with slightly lower sensitivities. The TL sensitivity of crystal W1 is two orders of magnitude less than crystals W2 at 100 R exposure.

The difference between crystals W1 and W2 may be demonstrated by the use of infrared absorption studies, as shown in Figure 2. It has been determined previously[14] that the sharp line spectrum near 2.8 μ, shown in Figure 2, is caused by Mg^{2+} -cation vacancy-OH ion complexes, while the broad band near 2.68 μ is caused by free OH ions in the crystal lattice. Since the available impurities will associate with hydroxide ions to as great an extent as possible[14], a sample indicating a broad absorption band has more hydroxide ions than are necessary to form complexes with all of the available impurities. Thus crystal W1 contains more than enough OH ions to combine with the available divalent impurities in the form of OH ion complexes. In contrast to crystals W1 and W2, LiF (TLD 100) shows no detectable infrared absorption, in agreement with the results of Claffy[15]. This is true in LiF (TLD 100) crystals up to 1 cm^3 in size. This does not mean that there are no OH ion impurities in LiF (TLD 100), however, since a more sensitive

technique should be used for such a determination.

Ionic conductivity is one technique that can provide information regarding impurities, such as OH ions, which can associate with divalent cations. Ionic conductivity measurements in LiF (TLD 100) show a conductivity curve nearly identical to that of a LiF crystal containing 320 mole ppm of Mg^{2+} and a small amount of OH ions, labeled H5 in earlier work[14,16]. In the low temperature association region, the conductivity of regrown Harshaw crystals, including H5 and LiF (TLD 100), is quite similar, whereas the conductivities of samples from other sources differ considerably in the same region[16]. The latter samples include crystals containing greater OH ion concentrations than crystal H5, as well as crystals containing fewer OH ions and fewer divalent impurities.[14] This indicates the presence of a background impurity, present in small concentrations in all Harshaw LiF, which can associate with divalent impurity complexes and cause a common low temperature conductivity region. This background impurity is probably the OH ion.

The present results show that if the OH ion concentration increases, the TL sensitivity in the water diffused LiF (H_2O) crystals decreases, as observed in Figure 1. Furthermore, crystals LiF (LiOH) and W2, which contain increasing amounts of OH ion complexes as determined using infrared absorption, show a further decreased sensitivity. Therefore, the TL sensitivity is seen to decrease with increasing OH ion complex concentration.

Since peaks 2 and 3 are closely related to Mg^{2+} -cation vacancy dipoles, and peaks 4 and 5 are related to trimers or similar dipole complexes, the decrease in sensitivity with the increase in OH ion complex concentration, observed above, is caused by a decrease in these trapping centers. The more rapid decrease in peaks 4 and 5 in comparison with peaks 2 and 3, as demonstrated in Figure 1, may be caused by the dissociation of the dipole complexes into OH ion complexes and Mg^{2+} -cation vacancy dipoles. This would also explain the observed increase in peaks 2 and 3 at longer diffusion times shown in Figure 1.

Supralinearity

LiF (TLD 100) normally shows a supralinear response as shown in Figure 3. The supralinearity curves for crystals LiF (H_2O) diffused for 55 hours, LiF (LiOH), diffused in the presence of water for 217 hours and of LiOH for 80 hours, and W2 are also shown in Figure 3. Here the decreasing sensitivity with increasing OH ion-complex concentration may also be noted. The relative supralinearity for crystal LiF (H_2O) is very similar to that of LiF (TLD 100). However, greater concentrations of OH present in the crystals apparently remove all supralinearity, as shown for crystals LiF (LiOH) and W2 in Figure 3.

These results indicate the importance of OH ion complexes in the process responsible for supralinearity. The large numbers of OH ion complexes present in crystals LiF (LiOH) and W2 reduce the sensitivity since their presence results in a reduction of the concentration of Mg^{2+} -cation vacancy dipoles. They also apparently supply non-luminescent traps as in Suntharalingam's model of supralinearity[4]. In this model, the OH ion complexes would act as deep, non-luminescent electron traps having a large capture cross section; depending on the number of these complexes present in the crystal, the supralinearity decreases, as is observed in Figure 3.

When the available (OH ion complex) traps are finally filled at higher exposures, one would expect a new region of supralinearity. Beyond 10^5R, however, this may be compensated for by damage effects. Such compensation may be present at high exposures in Figure 3.

Based on these results, another way of eliminating supralinearity would be to remove all OH ion complexes from the crystals. This has been attempted by annealing LiF (TLD 100) crystals in argon and vacuum atmospheres. Such treatments increase the sensitivity of peak 5 and decrease supralinearity as would be expected from the model discussed above.

These results are consistent with the non-luminescent trap model of supralinearity[4]. This model is also consistent with data previously reported

for the variation of supralinearity with temperature of irradiation[17]. As the irradiation temperature of LiF (TLD 100) is increased from -196°C to 280°C, less supralinearity is observed. Irradiations at a higher temperature would be expected to allow the excited electrons to wander through the conduction band for a longer period of time, possibly participating in a number of retrapping processes before finally being trapped. This would allow more electrons to be trapped preferentially by the non-luminescent traps which are deeper and have a larger capture cross section than the luminescent traps. This will decrease the amount of supralinearity as the temperature of irradiation increases. A consequence of this is that supralinearity should begin at a lower exposure for higher temperatures, as has also been observed[17].

These results regarding the importance of OH ion complexes in LiF (TLD 100) in determining the sensitivity and the supralinearity of the TL response, and the temperature dependence of supralinearity, are difficult to explain by any other proposed model of TL than that of Suntharalingam[4]. Further work is needed, however, before supralinearity in LiF (TLD 100) will be completely understood.

Acknowledgments

The authors wish to thank Dr. J. H. Jones, Mr. A. Dhar and Mr. C. Unume for experimental assistance. Crystals W were supplied by Dr. K. A. Wickersheim. This work is supported by USPHS, Food and Drug Administration, Bureau of Radiological Health, under research grant RL00125-03.

REFERENCES

1. J. R. Cameron, N. Suntharalingam, and G. N. Kenney, Thermoluminescent Dosimetry, University of Wisconsin Press, Madison, Wisconsin, 1968.

2. D. W. Pearson, USAEC progress report COO-1105-123 (1966).

3. L. A. DeWerd and T. G. Stoebe, Phys. Med. Biol. (in press).

4. N. Suntharalingam, Ph.D. Thesis, University of Wisconsin, 1967; J. R. Cameron, N. Suntharalingam, C. R. Wilson, and S. Watanabe, Proc. 2nd Int'l. Conf. Luminescence Dosimetry, p. 332, (1968).

5. E. W. Claffy, Proc. Int'l. Conf. Luminescence Dosimetry, p. 74 (1967).

6. M. J. Rossiter, D. B. Rees-Evans and S. C. Ellis, J. Phys. D 3, 1816 (1970): M. J. Rossiter, D. B. Rees-Evans, S. C. Ellis, J. M. Griffiths, J. Phys. D. 4, 1245 (1971).

7. D. W. Zimmerman and D. E. Jones, Appl. Phys. Lett. 10, 82 (1967).

8. R. M. Grant, Ph.D. Thesis, University of Wisconsin, Madison, 1965; R. M. Grant and J. R. Cameron, J. Appl. Phys. 37, 3791 (1966).

9. A. M. Harris and J. H. Jackson, Brit. J. Appl. Phys. (J. Phys. D.) 2, 1667 (1969); J. H. Jackson and A. M. Harris, J. Phys. C.: Solid St. Phys. 3, 1967 (1970).

10. M. R. Mayhugh, R. W. Christy, and N. M. Johnson, J. Appl. Phys. 41, 2968 (1970).

11. A. Dhar, M.S. Thesis, University of Washington, Seattle, 1971, to be published.

12. T. Nakajima, J. Appl. Phys. 39, 4811 (1968).

13. T. G. Stoebe, J. Phys. Chem. Solids 31, 1291 (1970).

14. T. G. Stoebe, J. Phys. Chem. Solids 28, 1375 (1967).

15. E. W. Claffy, Phys. Stat. Sol. 22, 71 (1967).

16. T. G. Stoebe and P. L. Pratt, Proc. Brit. Ceram. Soc. 9, 181 (1967).

17. L. A. DeWerd and J. R. Cameron, USAEC progress report COO-1105-118 (1966); also in reference 1, p. 167.

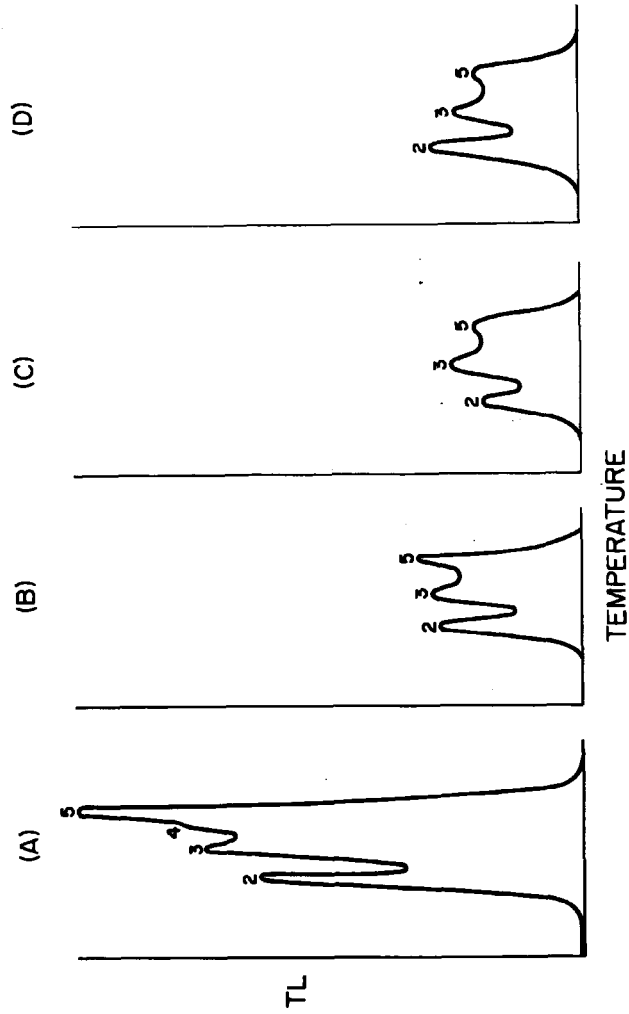

Fig. 1. TL glow curves of LiF (TLD-100) with normal peak designations, as indicated, after an exposure of 100 R.

A) As received. B) After 81 hours of H_2O diffusion at 700°C.

C) After 136 hours of H_2O diffusion at 700°C.

D) After 217 hours of H_2O diffusion at 700°C.

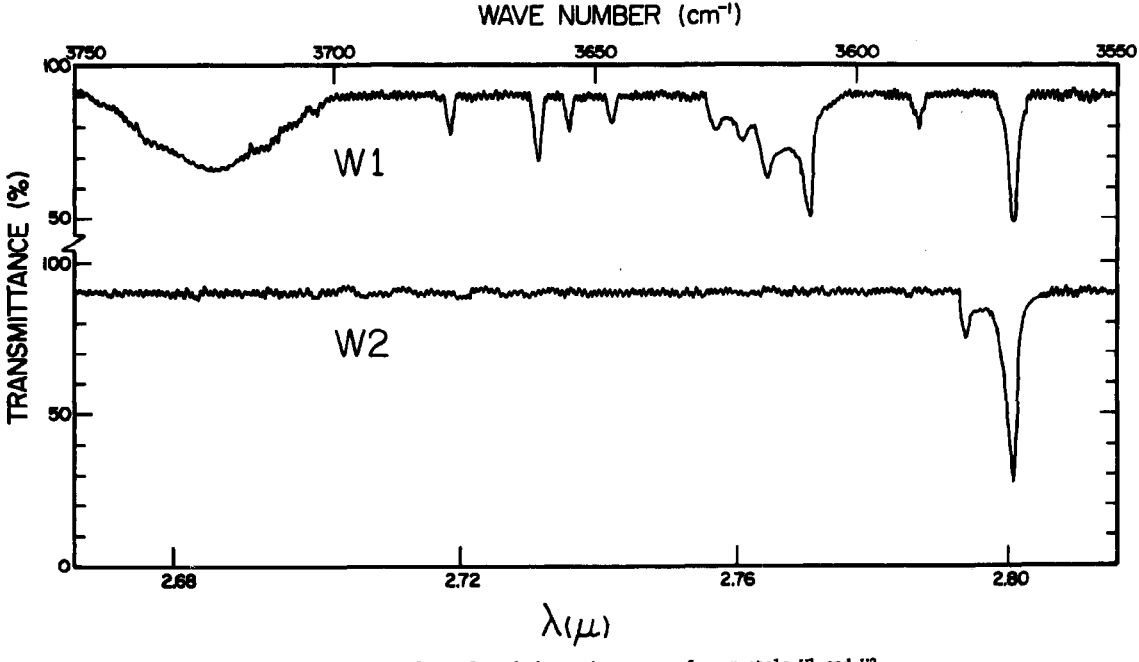

Fig. 2. Infrared absorption curves for crystals W1 and W2.

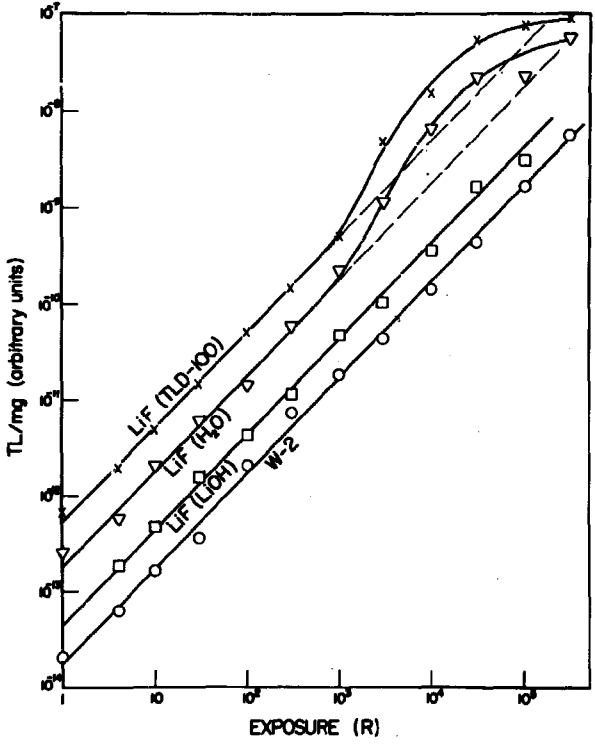

Fig. 3. TL/mg versus Exposure for peak 5 in LiF (TLD 100) as recieved; LiF (TLD 100) after 55 hours of H_2O diffusion: LiF (H_2O); LiF (TLD 100) after 217 hours of water diffusion and 80 hours of LiOH diffusion: LiF (LiOH); and for crystal W2.

Mason

Could the removal of supralinearity with increasing hydroxyl concentration be explained by a removal of deep traps? Would the simultaneous destruction or partial destruction of recombination centres account for the decrease in sensitivity which accompanies the removal of supralinearity?

Stoebe

This is an interesting possibility.

Moran

In commenting on the Oxford thesis proposal, you said that the supralinearity effect might be due to changes in recombination efficiency rather than changes in luminescence efficiency. Can you say what the distinction is between these two?

Stoebe

The Oxford work (Joan Thompson, Thesis, 1971) indicates that supralinearity is due to a change in the probability of a thermally released electron causing luminescence rather than changes in the trapping process.

Aitken

The work that Joan Thompson did at Oxford on LiF showed that the pre-dose effect was in the probability of a thermally released electron producing light rather than in the trapping process. Her results do not exclude a competition process affecting this probability; therefore it would seem that Dr. Stoebe's results are quite consistent with her observations. Her work will appear shortly in the journal Solid-State Physics.

The Influence of OH Anion on the Thermoluminescence Yields of Some Phosphors

Toshiyuki Nakajima

Division of Physics, National Institute of Radiological Sciences,
9-1, 4-chome, Anagawa, Chiba-shi, Japan

Abstract

Effects of OH anion on thermoluminescence sensitivity of LiF, CaF_2, BeO, Mg_2SiO_4(Tb) and $CaSO_4$(Tm) crystals have been studied. When OH anion were doped in the crystals through thermal treatment in atmosphere of water vapor, the sensitivity of the oxide crystals such as BeO and Mg_2SiO_4 was scarcely affected by doping, but that of the non-oxide crystals was considerably decreased with doping the OH anion.

The effect of illumination on the radio-thermoluminescence of the irradiated $CaSO_4$(Tm) is a slight but it is evidently observable on that of the irradiated Mg_2SiO_4(Tb). Influence of irradiating temperature on the response is scarcely detectable in temperature range from 0°C to 40°C.

Introduction

Because re-usibility of phosphor is the important factor of a thermoluminescence dosimeter phosphor, in general, the phosphor is annealed under the suitable thermal conditions for re-use. However, when the phosphor of LiF crystal is annealed at high temperature in air, a sensitivity of the phosphor has been reported to decrease with annealing temperature, and the causes of the decrease of the sensitivity are considered to be mainly due to OH anion.[1] But the influences of OH anion on both sensitivity and trapping levels in many thermoluminescenc phosphors have not been yet investigated.

On the other hand, recently, the high sensitive phosphor has been developed for measurement of low dose, and then the effects of light illuminating and of irradiating temperature on the sensitivity of phosphor must be studied for the measurement of low dose.

In this paper, the influence of OH anion on both the sensitivity and trapping levels of phosphors, illuminating effect on thermoluminescence yields and mechanism of annealing effects on LiF-TL sensitivity are treated.

Experiments

The crystals of Mg_2SiO_4(Tb), $CaSO_4$(Tm), BeO(Na) and LiF used for thermoluminescence measurement were prepared from the powdered crystals supplied by Dai Nippon Toryo Co., Matsushita Electric Co., and Institute of Applied Optics, respectively.

The thermal treatment for these phosphors was carried in water vapor with argon gas in order to dope the OH anion. And these crystals were thermally treated at either 600 °C or 800 °C for several periods. Immediately after removal from the electric furnace, the crystals were rapidly cooled in air to freeze the imperfections.

In order to compare the thermoluminescence yields between un-treated and

treated samples, these crystals were enclosed with lucite plates to ensure uniform electron build up over the entire volume of the sample and were irradiated at room temperature with γ-rays of a ^{60}Co source to a constant exposure which was measured using a Victoteen condencer R-meter with a calibrated chamber. Thermoluminescence yields were measured at least 24 hrs or over after the end of exposure in order to allow all samples to reach an equilibrium in fading of thermoluminescence yields. In case of observation of the glow curve, the crystal was irradiated at room temperature with exposure of about 10000 R and was heated from room temperature to about 450 °C with a constant heating rate of 10 °C/min.

Optical absorption of a tablet of each sample in the infra-red region was measured at room temperature using a Koken DS-301 infra-red spectrometer.

Results

Identification of the OH anion, which was doped in the crystals by thermal treatment, might be carried out in measurements of the infra-red absorption.

Figures 1 and 2 show the absorption curves of either the untreated (curve A) or treated sample (curve B) at 600 °C in water vapor. As can be seen in Fig. 1, the absorption trough of 3500 cm^{-1} corresponding to OH anion is observed from either the un-treated or treated BeO crystals. Being stored in air, BeO is known to be strongly affected by water vapor and be doped with OH anion. Therefore, the difference of OH anion density between the un-treated and treated crystals could be scarcely obtained. Such tendency is also found in Mg_2SiO_4 crystals. On the other hand, as shown in Fig. 2, the difference of the absorption trough at 3500 cm^{-1} between the non-oxide crystals such as LiF and CaF_2 is evidently observed.

In Fig. 3 are presented the changes in the relative dosimetric thermoluminescence yields of LiF, CaF_2, Mg_2SiO_4(Tb), BeO and $CaSO_4$(Tm) crystals treated in water vapor at either 600 °C or 800 °C against the annealing time. The vertical axis is represented as a relative thermoluminescence yields between the un-treated and treated crystals. As shown in Fig. 3, a large difference in the yields is obtained due to depend on the kinds of crystal. When the crystals were thermally treated in water vapor at high temperature, the thermoluminescence yields of the oxide crystals such as Mg_2SiO_4 and BeO are scarcely affected with OH anion, but that of the non-oxide crystals such as LiF and CaF_2(Dy) is strongly influenced with the OH anion. In case of the non-oxide crystals, TL yields due to annealing in water vapor decreases with annealing time. It may be inferred that the difference in the effects of thermal treatment in the oxide and the non-oxide crystals is caused by both different fabrication and activity of each phosphor with OH anion.

Figures 4 and 5 show record-registered traces of glow curves from (A) untreated and (B) treated crystals of $CaSO_4$ and LiF. Furthermore, Fig. 6 shows glow curves of both treated(B) and un-treated (A) Mg_2SiO_4(Tb) phosphor.

In comparison with the glow curve of the un-treated and the treated crystals, the relative intensities of individual glow peak heights for the oxide crystals scarcely vary, but that for the non-oxide crystal is markedly attenuated. Especially, the height of the dosimetric glow peak decreases due to dope of OH anion. Therefore, it is concluded that OH anion in the non-oxide crystals mainly affects on the deep traps to diminish its trap action.

In Fig. 7 are presented the changes of the total TL yields in LiF crystal treated at 600 °C in dry argon gas, and irradiated with exposure of 110 R against the annealing time.

In Fig. 7, curves A and B are obtained from the Harshaw TLD-100 LiF and optical grade crystal of LiF, respectively. In case of optical grade crystal, the sensitivity, in general, increases with annealing time and saturates at 3000 min but the sensitivity of TLD-100 LiF crystal slowly and gradually

decreases after its sudden enhancement for very short annealing time. But the difference in the enhancement of sensitivity may be inferred to be caused by different fabrication or preparation for LiF crystals.

It has been reported that the enhancement of the sensitivity for TLD-100 LiF scarcely varies with each annealing temperature from 300 °C to 600 °C and on the other hand, when the optical grade crystal is treated in argon gas or vacuum, its total intensity linearly increases with reciprocal of annealing temperature.[2] Therefore, the difference of the enhancement of sensitivity may be inferred to be caused by different preparation of the crystal. Mechanism for the enhancement of sensitivity due to annealing is as follows:

There are three kinds of mechanism for the enhancement of sensitivity. The first is an increase of a density of lattice defects. In this case, the sensitivity due to annealing increases linearly with reciprocal of annealing temperature and with annealing time, and the glow curve scarcely changes after and before annealing. The second is a new trap creation caused by changing the valance of impurities with annealing. In this case, the glow curve must be changed in order to created new traps. The last one is the release of the sleeping activator in the crystal to activator. In this case, if the crystal is thermally treated under the suitable condition for the release of the sleeping activator, the sensitivity will easily increase in short annealing period with reproducing the sleeping activator, and new glow peaks may be considered to scarcely appear. It may be inferred from the previous and present experimental results[2] that the enhancement in optical grade crystal is mainly due to the first mechanism and in the case of Harshaw TLD-100 LiF crystal, is mainly caused by the third mechanism, respectively.

Thermoluminescence yields of the un-irradiated sample with illumination are given by table 1. In order to eliminate the pre-dose, these samples are thermally annealed. After annealing, samples are illuminated with energy of 6 cal/cm^2/min from white light of a tungsten lamp. A background of these phosphors after thermal treatment, corresponds to signal of about 0.3 mR. From table 1, these phosphors may be sensitive on light, but a net thermoluminescence yields of $CaSO_4$(Tm) phosphor illuminated for 9 min is about 0.8 mR. This phosphor has a little sensitivity on light illumination. On the other hand, Mg_2SiO_4(Tb) phosphor illuminated for 9 min has light yields of about 600 times the background.

Optical fading of the illuminated phosphor after irradiation at room temperature is shown in Fig. 8.

As can be seen in Fig. 8, $CaSO_4$(Tm) phosphor is a little sensitive to white light as well as the un-irradiated one. However, the optical fading of Mg_2SiO_4(Tb) phosphor rapidly decreases with illumination. This optical fading ratio between the un-illuminated and the illuminated phosphors depends on the irradiated dose. Namely, the fading ratio of the phosphor with low dose is saturated within a short period but the time for equilibrium of the fading ratio increases with the dose as shown in Fig. 8. It may be concluded that the fading equilibrium within a short period in the one R-irradiated phosphor is caused from balance between the optical fading of thermoluminescence and the abovementioned thermoluminescence emission due to illuminating with light.

Next, influence of the temperature at which the irradiated phosphor was stored, on the response is shown in Fig.9. These sample was irradiated at various temperature with the dose rate of about 100 mR/min. Each response was normalized with that of the irradiated phosphor at 20 °C.

The thermal fading of Mg_2SiO_4(Tb) phosphor stored at various temperature is shown in Fig.10, in which the vertical axis is a ratio between the response of the phosphor immediately measured after irradiation and one of the measured phosphor stored for several period after irradiation. Each ratio is normalized with the response of the phosphor immediately measured after irradiation at 18 °C.

In case of thermal fading at 18 °C, the response gradually increases with

stored interval and reach to the maximum response of 1.14 at 240 hrs after irradiation. But the fading of the 40°C-stored phosphor reaches to the maximum response within 10 minutes after irradiation. It is found that the maximum response of the 22°C-stored phosphor appears at an intermediate interval between 10 minutes and 240 hrs.

As can be seen Figs. 9 and 10, the response is scarcely dependent on the temperature at which the phosphor is irradiated and is stored. These results reveal that these phosphors are used for the radiation dosimetry in the field of the temperature such as human body and driftway in mine.

Conclusion

When the thermoluminescence phosphors are annealed in water vapor, OH anion is doped in these phosphors. In this case, the sensitivity of the non-oxide crystal such as LiF, $CaSO_4$(Tm) and CaF_2(Dy) decreases , but that of the oxide crystals such as BeO and Mg_2SiO_4(Tb) is scarcely affected with OH anion.

The OH anion in the non-oxide crystals acts as a killer for thermoluminescence emission and is especially influenced on the deeper trapping levels.

Then, being annealing for the purpose of the re-use of the phosphor, the non-oxide crystal has to be annealed in dry atmosphere and in non-active gas such as vacuum or inert gas.

Acknowledgments

The author thanks Miss. I. Taneichi, and Mrs. K. Fujimoto and M. San for experimental assistance.

References

1. T. Nakajima, J. Appl. Phys., 39, 4811 - 4816 (1968)
2. T. Nakajima, J. Physics, D(Applied Physics) 3, 300 - 306 (1970)

Table 1.

Thermoluminescence yields of the un-irradiated phosphors illuminated with light(6 cal/ cm^2 min)

Time	6	7	8	9 (min)
$CaSO_4$(Tm)	0.43± 0.171	0.47± 0.08	0.46± 0.11	1.13±0.56 (mR)
Mg_2SiO_4(Tb)		65 ±46.7	78 ± 36.2	183± 40 (mR)

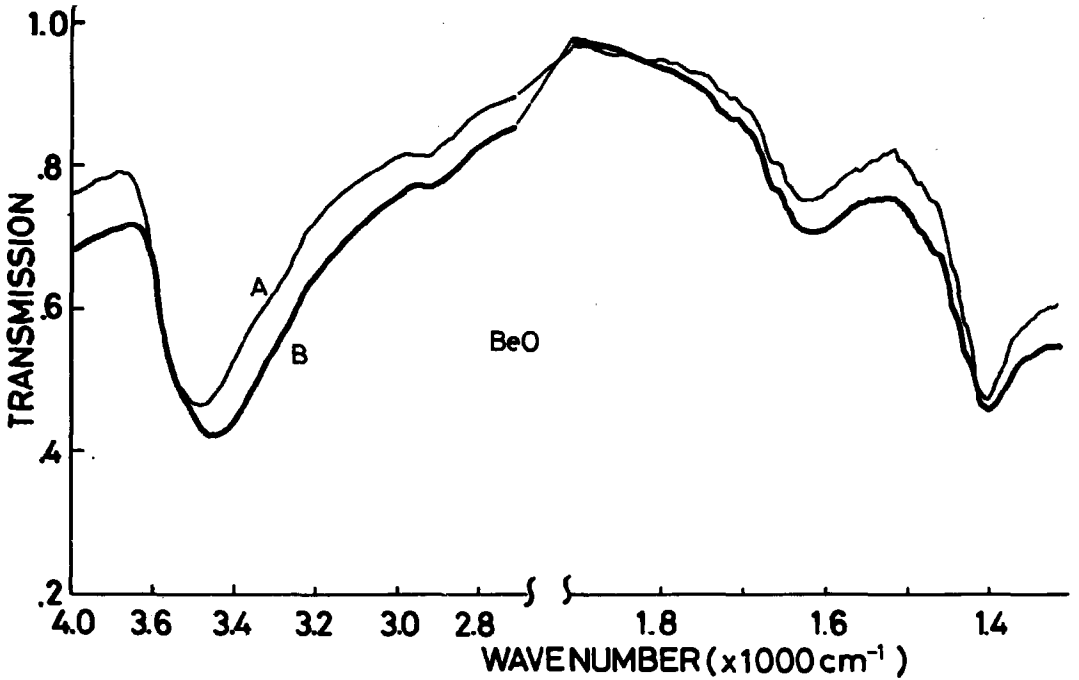

Fig. 1. Infra-red absorption spectra of BeO(A: un-treated crystal, B: treated crystal at 800 °C for 15 hrs in water vapor)

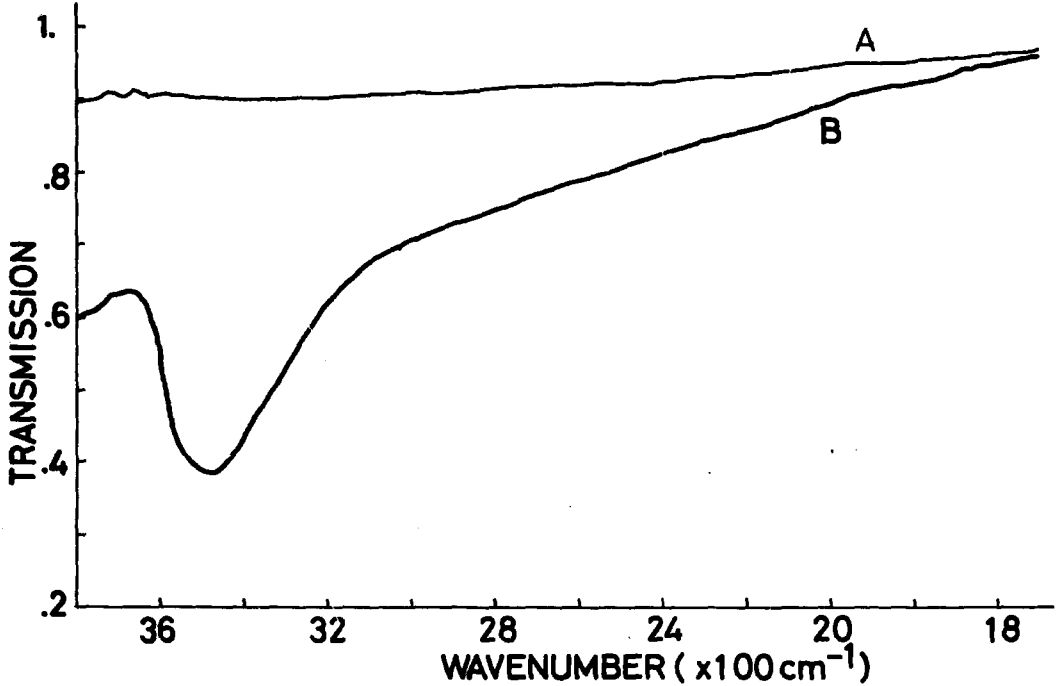

Fig. 2. Infra-red absorption spectra of CaF_2(A: un-treated crystal, B: treated crystal at 800 °C for 36 hrs in water vapor)

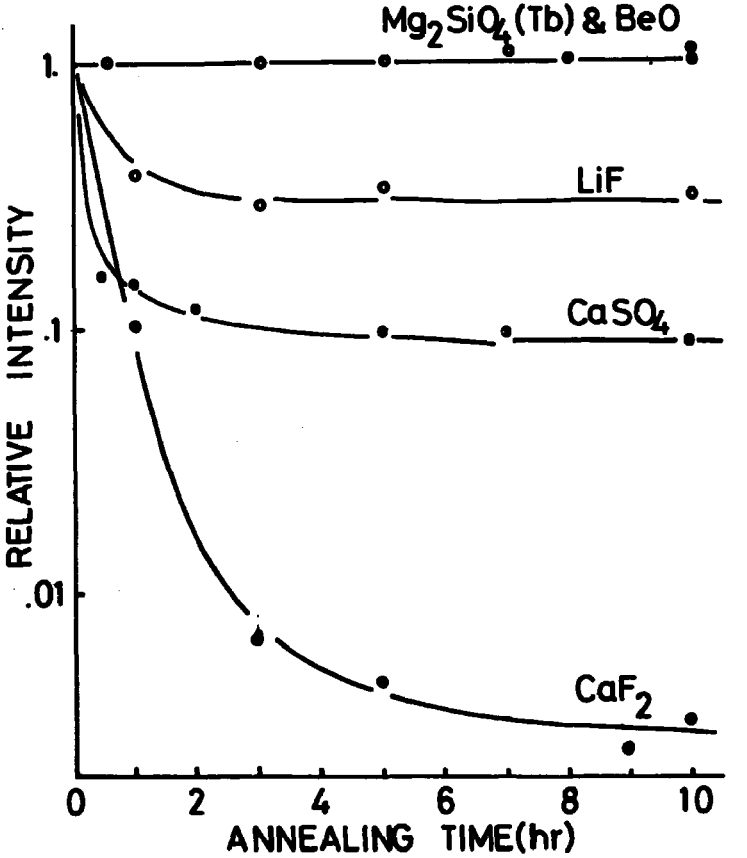

Fig. 3. The changes in the thermoluminescence yields of some phosphors thermally treated in water vapor at either 600 °C (LiF, $CaSO_4$) or 800 °C (other crystals) as a function of annealing time

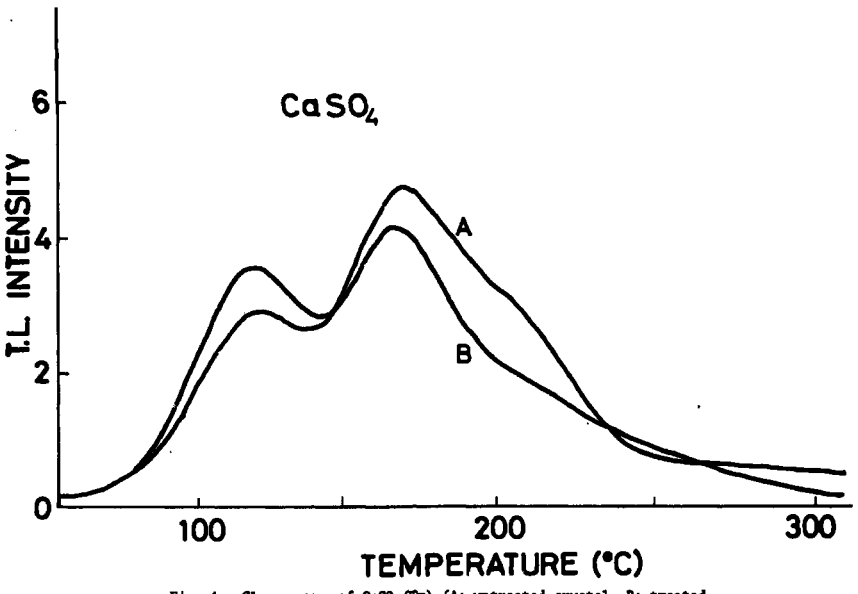

Fig. 4. Glow curves of $CaSO_4$(Tm) (A: untreated crystal, B: treated one)

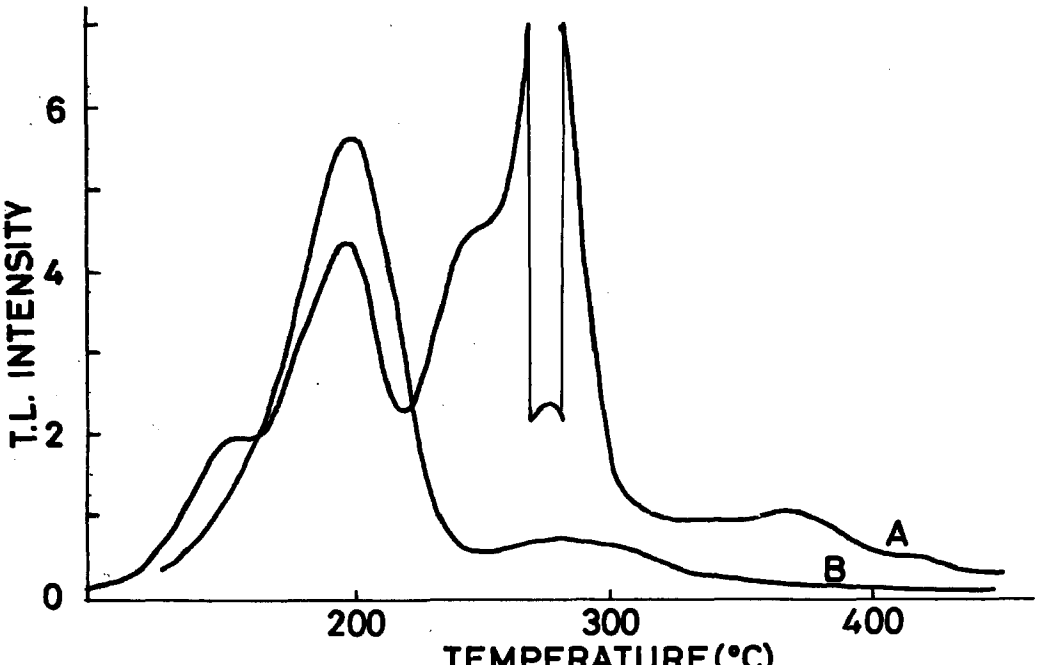

Fig. 5. Glow curves of optical grade LiF (A: un-treated crystal, B: treated one at 600 °C for 24 hrs in water vapor)

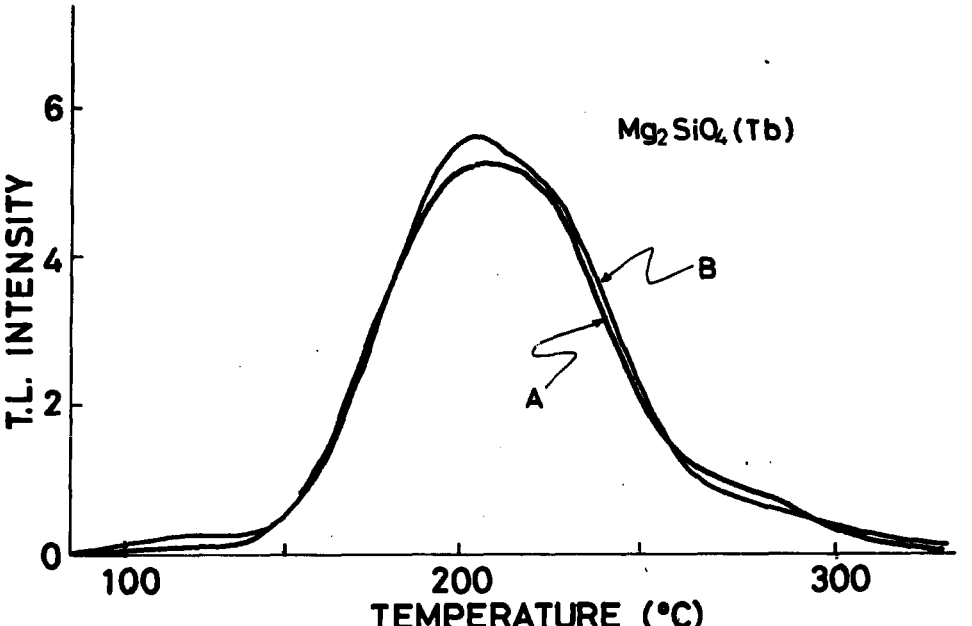

Fig. 6. Glow curves of both treated and un-treated Mg_2SiO_4(Tb) phosphor(curve B: treated at 800 °C for 10 hrs)

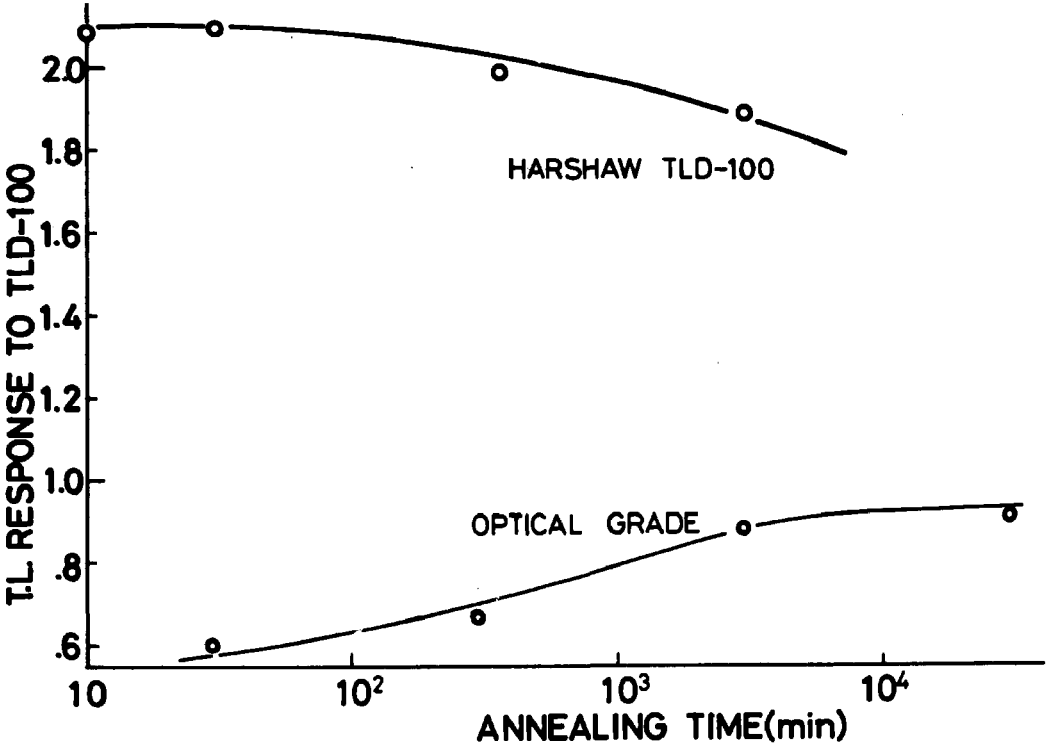

Fig. 7. Changes in the thermoluminescence yields of LiF crystals as a function of annealing time (These crystals were treated at 600°C in argon gas)

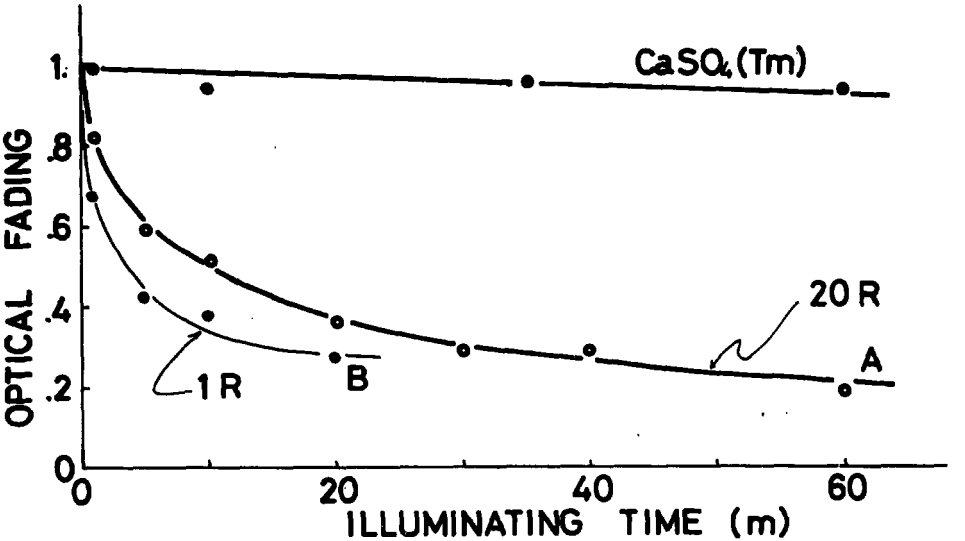

Fig. 8. Optical fading of irradiated $CaSO_4$(Tm) and Mg_2SiO_4(Tb) phosphors illuminated with 6 cal/cm^2/min white light (A: Mg_2SiO_4(Tb) irradiated with 20 R, B: with 1 R)

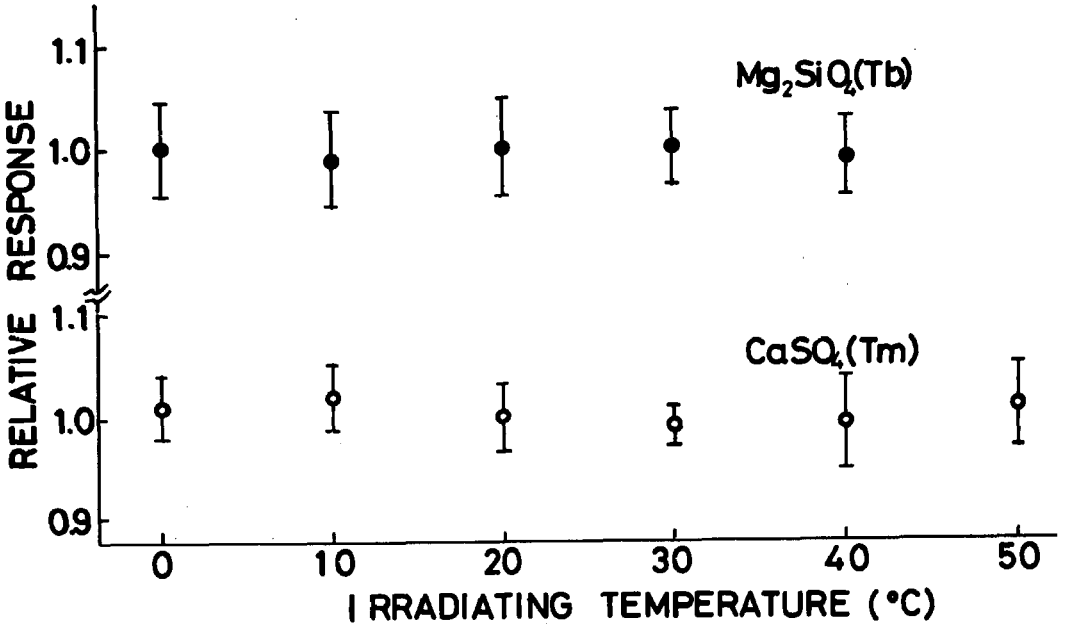

Fig. 9. Influence of irradiating temperature on the response of TLD phosphor which is normalized with the response of the 20°C-irradiated phosphor

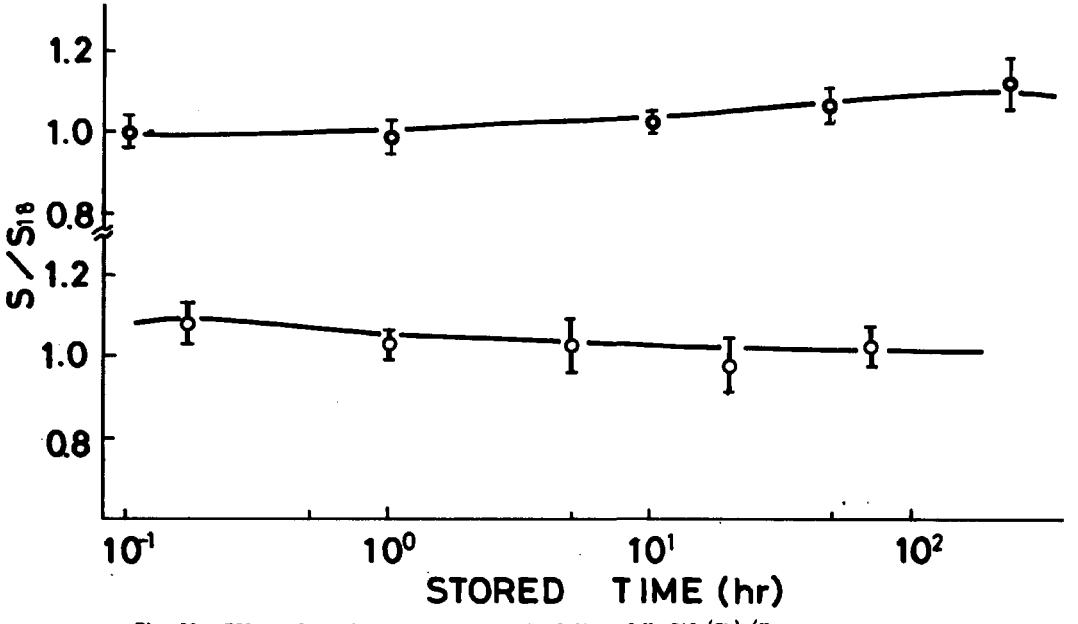

Fig. 10. Effect of storing temperature on the fading of Mg_2SiO_4(Tb) (Upper curve shows the fading of the 18°C-irradiated phosphor stored at 18°C and the other curve is of the 40°C-one stored at 40°C. All responses of the irradiation ones stored for various periods are normalised with that of the 18°C-irradiated one within a few minutes after irradiation)

Abnormal Thermoluminescence Fading Characteristics

by

A.G. Wintle, M.J. Aitken, J. Huxtable

Research Laboratory for Archaeology
and the History of Art,
Oxford University,
Oxford, England.

ABSTRACT

In some minerals and some samples of archaeological pottery there is significant fading of the TL even in the 400°C - 500°C region of the glow-curve; this is for overnight storage at room temperature, following artificial irradiation. The minerals studied include orthoclase, labradorite, microcline, andesine and mullite. In some cases the fading is not markedly reduced even if the storage temperature is -18°C, suggesting that the effect is due to a'non-thermal' mechanism. The fading in mullite and in the dosimetry phosphor CaF_2:Mn is in this category.

INTRODUCTION

In archaeological and geological dating studies it is commonly assumed that the TL observed in the temperature region of the glow-curve above about 350° C is associated with traps that are deep enough to retain their electrons (or holes) without significant leakage over tens of thousands of years or more. However, it has now been observed in some minerals and some samples of pottery that even in the 400° C - 500° C region of the glow-curve there is a component (typically about 10% of the total TL) that fades significantly during overnight storage between irradiation and measurement. A similar effect has been observed in lunar samples and terrestrial plagioclases by Garlick et al[1] who suggest that the mechanism involved is not the usual thermal activation but is a 'non-thermal' process associated with overlap of wave functions. In the present study there is evidence in some cases that the mechanism is 'thermal' and in the other cases that it is 'non-thermal'; sometimes both mechanisms are operative in the same substance.

A typical example of abnormal fading is shown in figure 1. This shows glow-curves for artificial irradiation (beta radiation from ^{90}Sr as throughout this work unless otherwise stated) of a sample of modern brick; in one case the TL has been measured within a few minutes of irradiation whereas in the other there has been a delay of 15 hours. It is to be expected theoretically from thermal activation considerations that in the delayed case there will be some fading until a temperature of around 200° C is reached. What is unexpected is the significant difference between the glow-curves from 200° C upwards, a difference amounting to about 20% even above 350° C and not sharply dependent on the glow-curve temperature. This difference is hereafter referred to as the 'Abnormal Fading Component' - AFC. It has been checked, by repeat experiments at different heating rates (between 1° C and 20° C per sec.) that the effect is not associated with thermal lag in the sample. In regard to age determination there are three immediate comments:-

i) Since the AFC will be absent from the natural TL, if the sensitivity of the sample is measured by means of a glow-curve taken immediately after artificial irradiation, the age obtained will be too low. The obvious solution would seem to be to delay this measurement until the AFC has disappeared. However the difficulty is that even with a delay of a week there is no guarantee that additional to the observed AFC there is not some longer term AFC that would manifest itself only in experiments lasting over tens

or even hundreds of years. This may well be a remote possibility, but since it strikes at the confidence that can be placed in TL dating it is a possibility that must be faced. Consequently a study of abnormal fading is very pertinent to TL dating even if it does no more than identify the minerals with which it is associated and allow exclusion of all samples containing such minerals from dating application.

ii) From the satisfactory agreement between absolute TL ages for archaeological pottery and the ages according to archaeological chronology (for a summary of some such 'test programmes' see Aitken and Alldred[2]) it is clear that abnormal fading is not too generally significant and that exclusion of affected samples will not extinguish the field.

iii) In pottery dating the 'plateau test' is usually used as evidence of each sample's good TL stability (see for example, Aitken[3]). In this the ratio of natural TL/(natural + artificial)TL is plotted as a function of glow-curve temperature and the onset of a plateau is taken to indicate the glow-curve temperature above which the associated traps are deep enough to have retained their electrons without leakage since the pottery was fired. However, since the APC is not very dependent on glow-curve temperature, the presence of APC in the artificial TL may not be detected by the plateau test.

In addition to the type of APC just described there is a more subtle form in some pottery. This is only observed in the first irradiation of a sample following preparation by crushing; irradiations given after the sample has been heated do not induce this type of APC. It appears that quite a mild heating (e.g. 'thermal washing': 10 minutes at 150° C) may be sufficient to remove a sample's potentiality for exhibiting this effect and so it can be eliminated without drainage of the natural TL. Consequently it represents a much less serious hazard for TL dating than the former type.

Abnormal fading characteristics have already been noted for the artificially-prepared dosimetry phosphor CaF_2:Mn (Schulman[4]). Because of its higher light level and because of its very much simpler glow-curve shape this was included in the present investigations on the assumption that conclusions reached for this phosphor might be relevant to abnormal fading in pottery and minerals. Study of the phosphorescence from CaF_2:Mn has been made and it appears that at room temperature there is a component which is associated with the APC. Such associated phosphorescence has also been observed in mullite.

2. STUDIES ON GEOLOGICAL SAMPLES AND MINERALS

The occurrence of abnormal fading was brought to the authors' attention when anomalously low TL ages were obtained both for some 35,000 year old basaltic lava (from Prenal in the Massif Central, France) and for the pottery from a Neolithic site in South-East Europe (see section 3). Further study of the lava sample was made using gamma irradiation (from ^{60}Co) of a lump from which natural TL had been drained. After crushing, the material was separated into mineral components and the individual TL studied. The remarkable observation was made that although quartz grains carried a TL equivalent to 5,000 rads (the administered gamma dose), some coarse grains (~ 0.7 mm) of andesine showed no significant TL whatsoever (the limit of detection corresponding to a dose of 500 rads).

Glow-curves for the andesine are shown in fig. 2, both for measurement immediately following irradiation and when there is a delay of 80 hours. Estimates of E(0.6 eV) and s (2×10^6 sec^{-1}) for the peak gave a half-life of about 3 hours for storage at 20° C, agreeing reasonably with the observed fading of the peak of 50% in 4 hours. Above the peak temperature the TL decays with a half-life of about 120 hours, this being independent of glow-curve ordinate. Although this gives an adequate explanation of the absence of TL in the gamma-irradiated lump below the peak (the delay between gamma irradiation and measurement being about 20 hours) it does not immediately explain the absence of TL at higher temperatures. However it is to be expected that in the crushing process there will be localized generation of heat and as is shown in fig. 3 the TL (450° C ordinate) of the andesine decays much more rapidly when the temperature is raised than does that of the quartz. This suggests that at any rate for part of the AFC the mechanism is of the thermal activation type.

It was also found that when crushed down into fine grains (1 to 5 microns) the andesine had a quite different glow-curve shape (see fig. 4) and a stability similar to that of quartz. It is evidently dangerous to characterize TL behaviour without reference to grain size.

Table I summarizes the fading characteristics of other minerals included in this study. Loss on washing at 150° C is indicative of a thermal process as also is a dependence of fading rate on storage temperature. Comparison was also made for samples that had been washed at 150° C, between one measured immediately and one measured after a delay. A difference here is suggestive of a non-thermal process as is also indicated by

independence of fading on storage temperature. It is of course quite reasonable for both types of process to be exhibited by the same substance.

For labradorite the fading measurements were repeated using a photomultiplier EMI type 9558 (having a response extending from 0.3 microns to 0.7 microns), whereas the measurements of table I were all carried out using an EMI type 9635Q with a Corning 7-59 filter interposed (thereby restricting the response to a 0.12 micron-wide window centred on 0.38 microns). No significant difference in fading behaviour were observed, suggesting that the colour of the TL that fades is not dramatically different from the stable TL. In addition to beta radiation, some fading studies have been made using alpha radiation (from ^{244}Cm). With the latter the rate of fading was sometimes as much as 2 or 3 times as rapid as with beta irradiation but the results were not entirely conclusive.

Phosphorescence studies on CaF_2:Mn and mullite are reported in section 4. TL glow-curves for these substances are shown in figs.5 and 6 both for measurement immediately after irradiation and for measurement after a delay. Mullite ($3Al_2O_3.2siO_2$) is of particular interest because at about 1200° C kaolinite, illite and montmorillonite and other clay minerals start to decompose and form mullite, the process being accelerated by the presence of feldspars. Thus mullite is to be expected in highly-fired pottery and also in modern brick; this presumably accounts for the observed fading in the latter. Fig. 7 shows plots against glow-curve temperature of the TL remaining after 20 hours both for storage at -18° C and -25° C. The fading is the same above 200° C, suggesting a 'non-thermal' process. This is in agreement with the observation that fading occurs even in a sample that has been thermally washed at 150° C (see figs. 8 and 9).

Stability tests were also carried out on natural CaF_2 (MBLE type S). Kinetic studies by Fleming[5] give the following data:

Peak II (200°): $E = 1.4$ eV, $s = 7 \times 10^{14}$ sec.$^{-1}$

τ (20°) = 39 years

τ (54°) = 0.12 years

Peak III (300°): $E = 1.8$ eV, $s = 6 \times 10^{15}$ sec.$^{-1}$,

τ (20°) = 44×10^6 years

τ (54°) = 24×10^3 years

Long term storage at room temperature (over 2 years) showed a decay of about 8% in peak II (compared with a predicted 3.6%) but no significant (< 3%) decay in peak III. Storage over 3 months at 54° C indicated a fading rate of 0.25% per day for peak II (compared with a predicted 1.6% per day) and an overall decay of about 3% for peak III (compared with a predicted 0.001%). Thus there is some indication of abnormal fading in this phosphor too although, as far as the use of peak III in long-term dosimetry at ordinary temperatures is concerned, it is not significant.

3. STUDIED ON ARCHAEOLOGICAL POTTERY SAMPLES

Abnormal fading of the types described in the previous section (i.e. both 'thermal' and 'non-thermal') has also been observed in some types of pottery. This is not surprising since most of the minerals chosen for study were in fact clay-forming minerals. In addition with some pottery there is a more subtle form of abnormal fading that appears to be associated with the process of crushing the pottery (by squeezing in a vice) in order to obtain fine-grain samples according to the method of Zimmerman[5]. The fine-grains are deposited on a thin 1 cm. diameter aluminium disc and from each fragment of pottery about a dozen such discs are obtained, equivalent in TL to within about ±5%. The equivalent dose which the pottery has accumulated during antiquity is evaluated by comparing N, the natural TL, with (N+β), the TL carried by a disc which has been given an additional known dose of beta particles. Comparison with the TL from a beta dose given to a disc which has been drained of its natural TL is avoided, because in the latter case the sensitivity is likely to have been changed by heating (for discussion see Zimmerman[6]). The 'plateau-test' (see section 1) is made by plotting N/(N+β) as a function of glow-curve temperature and the level of the plateau determines the equivalent dose.

A study was made of samples from the archaeological site mentioned at the beginning of section 2 which gave an anomalously low age (by about 10%). Figs. 10 and 11 show the effect on the natural TL and on the (N+β) of 'thermal washing' of the sample for 10 minutes at 150° C before measurement. As is to be expected there is considerable drainage of the TL up to about the 300° C region of the glow-curve. In the higher temperature region there is negligible effect on the natural TL , as might be expected from kinetic considerations, but for the (N+β) there is significant drainage. This is illustrated more clearly in fig. 12 which shows the plateau test both for 'no

washing' and '150° C washing'. Not only is the plateau flatter in the latter case but its level is higher by about 10%. Washing was also carried out at various higher temperatures up to 300° C; there was some irregularity in the results (possibly due to the onset of pre-dose effects) but the average level of the plateaux was close to that for the 150° C washing.

It might be thought that the above observations could be simply interpreted as due to the presence of an abnormal fading component in the (N+β) which had long since faded from N. However, it was found that the TL induced by beta radiation of discs that had been heated to 500° C (in the course of a glow-curve) exhibited the response to washing of the natural TL rather than (N+β). It was also found that somewhat over half of the loss due to washing of (N+β) occurred even if the washing was carried out before the additional beta dose had been administered. Another experiment carried out (see fig. 13 and 14) was to give a known gamma dose to a fragment of the pottery from which the natural TL had been drained and then to make disc samples from this fragment in the usual way, evaluating the gamma dose by comparing the gamma-induced TL with the TL from a disc which had been given an additional (known) beta dose. This was done both with unwashed discs and with discs washed at 150° C for 10 minutes. In this instance the loss due to washing of the (γ + β) TL was appreciable (see fig. 13). on the other hand the loss of the gamma induced TL was comparatively small. Also, the evaluation of the gamma dose using washed discs was within 6% of the known value whereas the unwashed evaluation was 30% low (see fig. 15).

The tentative interpretation is that the crushing of the fragment induces additional traps, and that these can be 'washed out' by heating to 150° C. The evidence is not entirely conclusive, probably owing to the irregular nature of the phenomenon. The effect seems to be enhanced if the fragment is deliberately ground up in an agate rather than crushed by the more gentle process of squeezing in a vice that is used routinely. So far it has not been conclusively established whether the effect occurs to a lesser or greater degree when alpha radiation is used.

It should be emphasized that the above results were obtained with pottery from one particular archaeological site. It has not yet been established to what extent the effect is shown by pottery from other sites.

4. PHOSPHORESCENCE

CaF_2:Mn

Assuming that the decay shown in fig. 5 represents the release of trapped electrons it is of interest to ask whether luminescence is produced in this process. With a dose of 5000 rads, a sample of 30 mg and using a photomultimplier type 6255 (with type S photocathode) the difference between the immediate glow-curve and the glow-curve taken after a delay of 18 hours is equivalent to 10^7 pulses from the photocathode. Assuming the decay to proceed uniformly over the period concerned this represents a rate of 200 pulses per sec. (henceforth abbreviated to p.p.s.); this should be easily detectable above the photomultiplier dark count of around 100 p.p.s. In fact the pulse rate observed during decay might be expected to be up to two or three times higher than the rate predicted because of the occurrence of thermal quenching when the TL is observed (Gorbics, Nash and Attix).[7]

Using the same conditions as for the TL the observed phosphorescence (at 17°C) about 10 minutes after completion of the dosage amounted to 5×10^5 p.p.s. However if the sample was thermally washed for 10 minutes at 100°C after irradiation the 17°C phosphorescence subsequently observed was reduced to 2.8×10^3 p.p.s., presumably because of the emptying of shallow traps during the washing (there is a subsidiary TL peak at about 100°C). With higher washing temperatures the phosphorescence was reduced still further, for 150°C: 700 p.p.s., for 200°C: 200 p.p.s., for 225°C: 60 p.p.s. After measuring the phosphorescence and following its decay for a few hours, the TL in the sample was measured. Figure 16 shows integrated phosphorescence (obtained by multiplying the initial pulse rate by the mean lifetime) expressed as a percentage of the TL. It is difficult to determine whether or not the release of an electron during storage at room temperature has the same probability of producing luminescence as when it is released in the course of a TL glow-curve; this is because of the relatively small amount of fading that occurs after washing.

Is there reason to believe that the small amount of phosphorescence observed is in fact associated with the abnormal fading of the TL? As noted in section 2, the rate

of fading is the same at -18° C and 25° C to within experimental error, and only a little enhanced at 65° C. It appears that the room temperature phosphorescence also is largely independent of temperature: fig. 17 shows a logarithmic plot of the phosphorescence versus the reciprocal of the absolute temperature for the range 17° C to 190° C. The higher temperature part of the graph shows strong temperature dependence, corresponding to the emptying of a trap of depth E ~ 1 eV. However, near to room temperature the dependence is slight, corresponding to a trap of depth only ~ 0.1 eV; this predicts that the rate of trap emptying at -18° C would be only 30% less than at 25° C, and that at 65° C the rate would be 30% more than at 25° C. This is not inconsistent with the observed fading of the TL and consequently it seems reasonable to assume that the phosphorescence is in fact associated with the fading. On this assumption characteristics of the fading can be determined by study of the phosphorescence and this is experimentally advantageous. One immediate question is whether the room temperature phosphorescence can in fact be justifiably ascribed to a 'non-thermal' process, the observed slight dependence on temperature being due to interference from thermal emptying of some other set of traps. This is the favoured interpretation since the other alternative gives a ludicrously low s value of $\sim 10^{-2}$ sec.$^{-1}$; this is deduced from E ~ 0.1 eV noted above and the observed half-life for decay of the phosphorescence of 52 minutes (see fig. 18). Another supporting observation is that more prolonged washing (50 minutes instead of 10 minutes) at 225°C did not alter the ratio of phosphorescence to TL remaining. If the trap depth and room temperature half-life quoted above are taken seriously, the half-life at 225° C should be 10 minutes indicating a reduction by a factor of 16 due to the additional washing time, whereas experimentally there was no emptying of the traps responsible for the phosphorescence other than that proportional to the loss of TL.

The phosphorescence and the TL were also observed using a photomultiplier type EMI 9635Q with a Corning filter type 7-59. The reduction in intensity was the same for both (by x 0.1), consistent with the two being of the same colour. Observations using a photomultiplier type EMI 9558 gave similar intensities to EMI type 6255.

The phosphorescence following alpha irradiation (using a 10 mCi 244-Cm source) was also observed. The irradiation was adjusted so that the TL remaining after a 225° C washing was the same as for the beta irradiations. The level of phosphorescence in the case of alpha irradiation was twice that for beta irradiation, although the phosphorescence decayed with the same half-life in both

cases (52 minutes after an initial more rapid decay: see fig. 18). It is surprising that the two cases are so similar since for alpha irradiation both the 'dose within a track' and the dose-rate are many orders of magnitude higher than in the beta case (the beta dose-rate used was 1000 rads per minute). Whatever detailed mechanism is postulated it might be expected that the effects would be enhanced by close proximity of trapped holes to the traps responsible for the TL.

Mullite

The phosphorescence was studied after a gamma dose (from ^{60}Co) of 1.75×10^6 rads followed by thermal washing for 10 minutes at 150°C. With this mineral the phosphorescence decayed with an initial half-life of about 14 hours.

Phosphorescence was also observed after washing at 225°C. Fig. 20 shows that after subtraction of a deep-trap contribution (~ 1.2 eV in this case), the residual phosphorescence shows a temperature dependence of less than 1.45 in 50° (corresponding to a trap depth of only .07 eV) and that the data is consistent with regarding the room temperature phosphorescence as independent of temperature. It will be recalled from section 2 that the observed decay of TL in mullite was the same at -18°C as it was at 25°C. The phosphorescence overnight in this case corresponds to a relatively small loss of photons and is within the experimental error of the thermoluminescent measurements.

Natural CaF_2

Phosphorescence was also observed from natural CaF_2 (MBLE) but at a comparatively slight level. This was for a sample dosed with 5000 rads and washed for 30 mins. at 200°C. The count-rate at room temperature was 10 p.p.s. which, relative to the TL remaining after washing (entirely peak III), was down by a factor of 10^3 on CaF_2 (Mn).

Acknowledgements

We are indebted to Dr. B. Stedeford and Mrs. A. Dickson-Brown for arranging the gamma irradiations at the Churchill Hospital Oxford (by kind permission of Dr. F. Ellis), to Mr. J.C. Alldred for advice and assistance in the phosphorescence studies and Dr. B. Butler for providing the mullite. A studentship for one of the authors (A.G.W.) from the National Environment Research Council is gratefully acknowledged as well as financial assistance from the Nuffield Foundation.

REFERENCES:

1. G.F.J. Garlick, W.E. Lamb, G.A. Steigmann and J.E. Geake, Proceedings Second Lunar Science Conference, Houston (1971), forthcoming.

2. M.J. Aitken and J.C. Alldred, Archaeometry 14 (2) forthcoming (1972).

3. M.J. Aitken, Reports on Progress in Physics 33, 963-974 (1970).

4. J.H. Schulman, First International Conference on Luminescence Dosimetry, 3-33 (1965).

5. S.J. Fleming, Unpublished D.Phil. thesis, Oxford University.

6. D.W. Zimmerman, Archaeometry 13 (1), 29-52 (1971).

7. S.G. Gorbics, A.E. Nash and F.H. Attix, Second International Conference on Luminescence Dosimetry, 568-586 (1967).

TABLE I

	GRAIN SIZE MICRONS	FADING AT 18° C	FADING At -18° C	THERMAL WASHING	WASHING AND STORAGE AT ROOM TEMP.	ALPHA DOSED
ORTHOCLASE	100-150	10% in 14 hours 25% in 4 days	25% in 4 days	at 175° C for 15 mins removes 25%	no further decay	25% in 4 days (same as for beta)
LABRADORITE	100-150	20% in 15 hours				30% in 15 hours
MICROCLINE	100-150	2% in 15 hours 3% in 4 days	2% in 10 days			10% in 6 days
ANDESINE	300	40% in 80 hours		at 200° C for 5 mins removes 8%		
	90-105			at 150° C for 5 mins removes 50%		
	90-105			at 50° C for 10 hrs. removes 65%		
	1-5			at 150° C for 5 mins removes < 3%		

TABLE I (continued)

	GRAIN SIZE MICRONS	FADING AT 18° C	FADING AT -18° C	THERMAL WASHING	WASHING AND STORAGE AT ROOM TEMP.	ALPHA DOSED
QUARTZ	90-105	less than 3% in 27 days		at 150° C for 5 mins removes <3%		
MULLITE	100-150	6% in 20 hours	6% in 20 hours	at 150° C for 5 mins removes 6%	6% further decay in 20 hours	8% in 6 days 16% in 40 days
MODERN BRICK	90-150	18% in 15 hours	3% in 15 hours	at 150° C for 15 mins removes 24%	13% further decay in 15 hours	
	90-150	35% in 83 hours	28% in 83 hours			
CaF_2:Mn	90-150	5% in 15 hours	5% in 15 hours	at 100° C for 20 mins removes 3%	5% further in ⩽5 hours	same as for beta
CaF_2(MBLE) type S	50-100	less than 3% in 2 years				

Note 1. The above data refers to the 350° C ordinate of the glow-curve (heating rate 6°C per second) except for CaF_2:Mn and CaF_2(MBLE) when the heights of main peak have been used (respectively 312° C and 280° C).

Note 2. The data is for beta irradiation except for the last column.

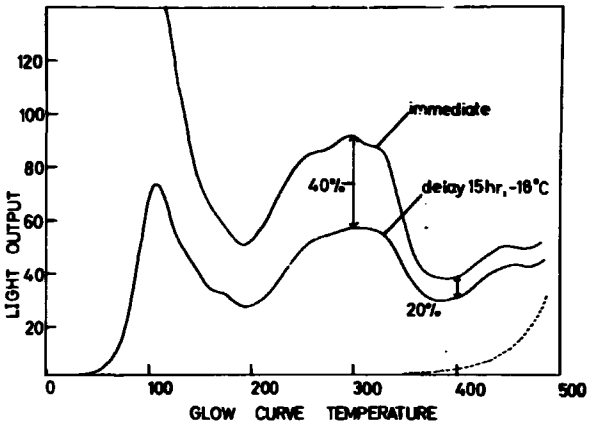

Fig. 1 Glow-curves for a fine-grain (1-5 microns) sample of modern brick, after 5000 rads of beta radiation. In one case the TL was measured immediately and in the other after 15 hours storage at -18° C.

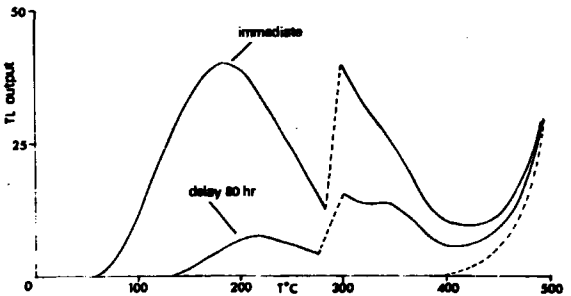

Fig. 2 Glow-curves for large grains (∿ 0.7 mm) of andesine, after 5000 rads of beta radiation. Storage in the case of the delayed measurement was at 17° C.

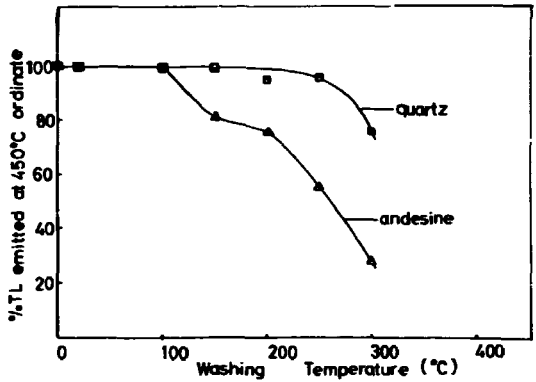

Fig. 3 Decay of 450° C ordinate of glow-curve due to 5 minutes 'thermal washing' of sample after irradiation; quartz and andesine.

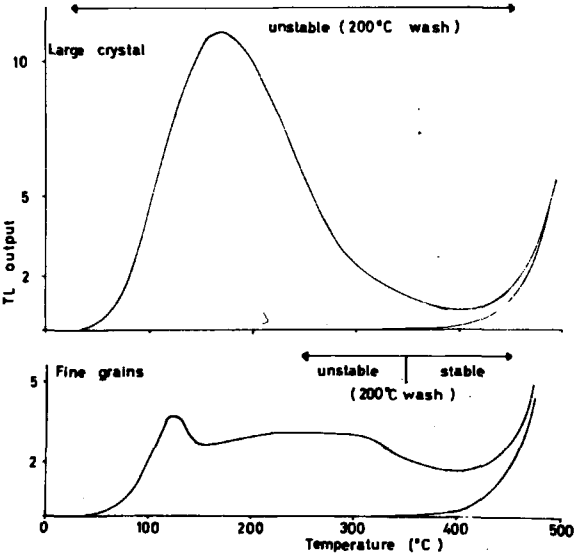

Fig. 4 Glow-curve from large grain (∿ 0.7 mm) of andesine (after beta dose of 5000 rads) and glow-curve from the same material after crushing down into fine-grains (1-5 microns). Whereas thermal washing for 5 minutes at 200° C causes appreciable decay for the large grain at all glow-curve ordinates, for the fine grains the TL is stable above the 350° ordinate.

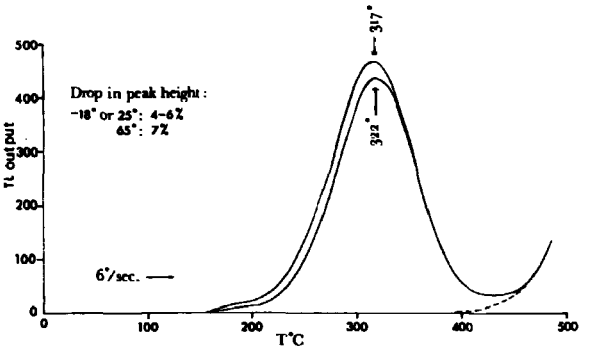

Fig. 5 Glow-curve for CaF_2:Mn, measured immediately after irradiation and measured after 18 hours storage at -18° C. Beta dose 100 rads.

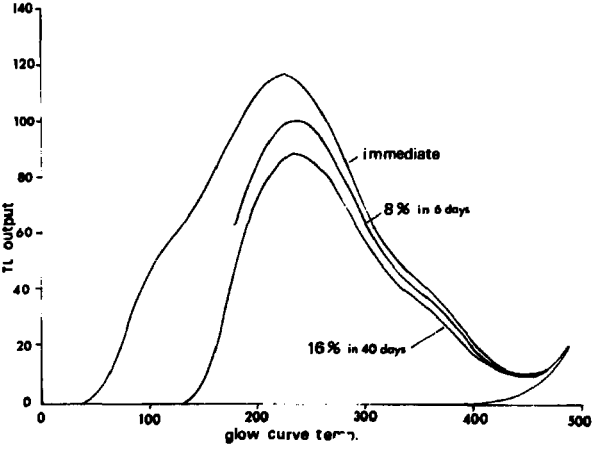

Fig. 6 Glow-curves for mullite, immediate and delayed, after alpha irradiation.

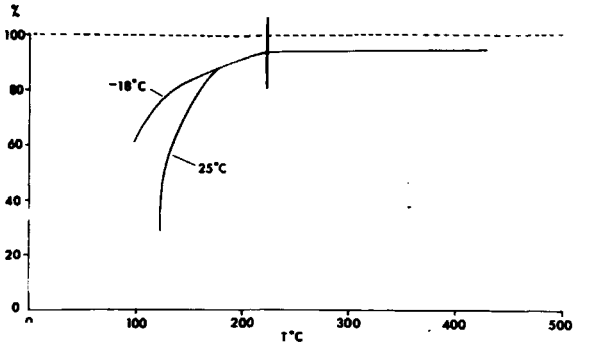

Fig. 7 Mullite: TL remaining after 20 hours storage (at -18° C and 25° C) expressed as percentage of TL if measured immediately (for beta dose of 100 rads in each case). Horizontal scale is glow-curve temperature.

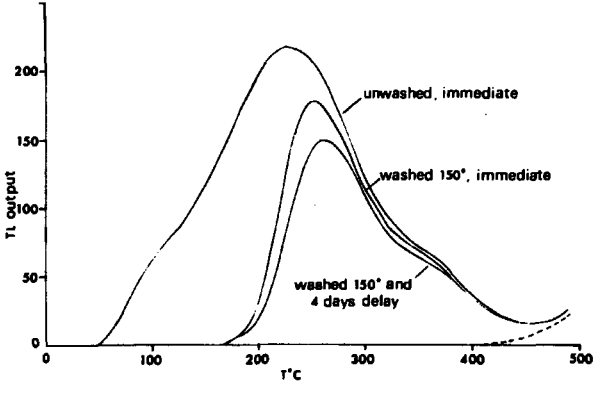

Fig. 8 Mullite: glow-curves after 100 rads beta dose:- (i) measured immediately, (ii) thermally washed for 5 minutes at 150° C and measured immediately, (iii) thermally washed for 5 minutes at 150° C and measured after 4 days delay.

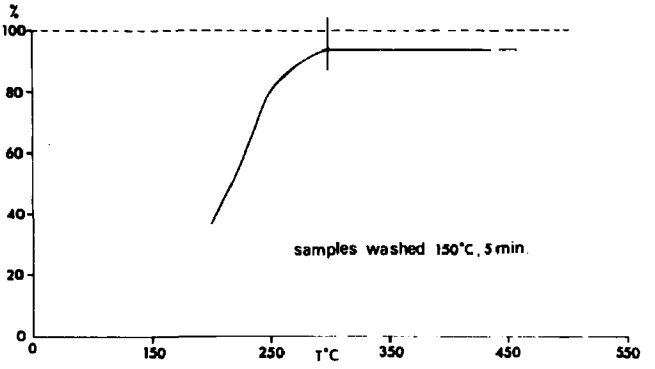

Fig. 9 Mullite, samples thermally washed at 150° C for 5 minutes: TL remaining after 4 days storage at 25° C expressed as percentage of TL if measured immediately (for beta dose of 100 rads in each case). Horizontal scale is glow-curve temperature.

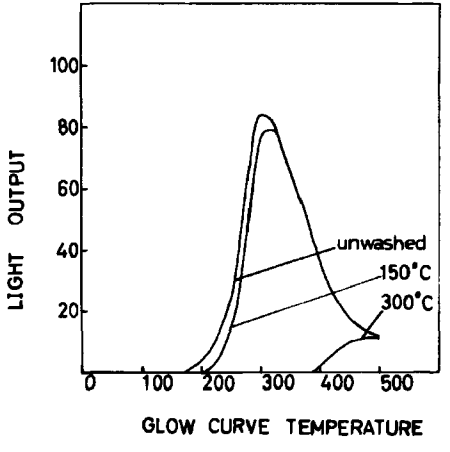

Fig. 10 Natural TL from pottery sample. Effect of 10 minutes thermal washing at 150° C and 300° C.

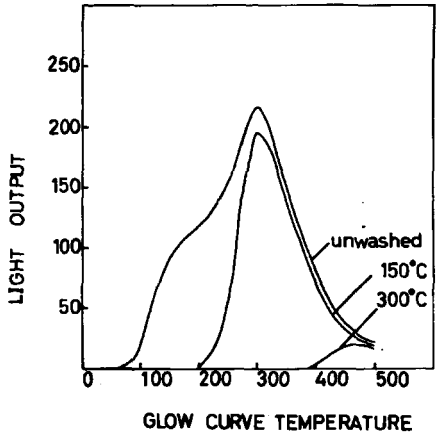

Fig. 11 TL from undrained pottery sample which has been given an artificial beta dose of 2300 rads. Effect of washing at 150° C and 300° C.

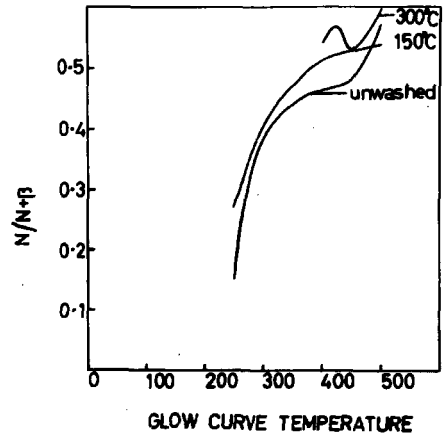

Fig. 12 Ratio of Natural TL to (natural + artificial) TL for unwashed samples and for samples washed at 150° C and 300° C.

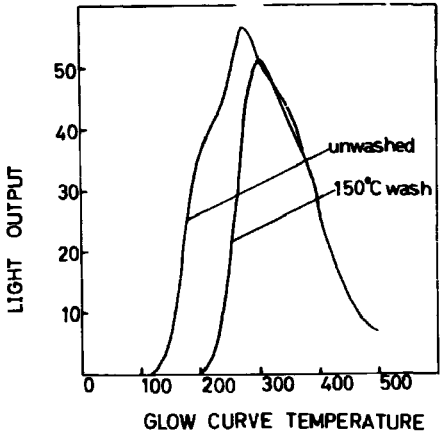

Fig. 13 TL from drained pottery fragment which has been given a gamma dose (2300 rads) before crushing, for unwashed sample and for sample thermally washed at 150° C after the beta dose.

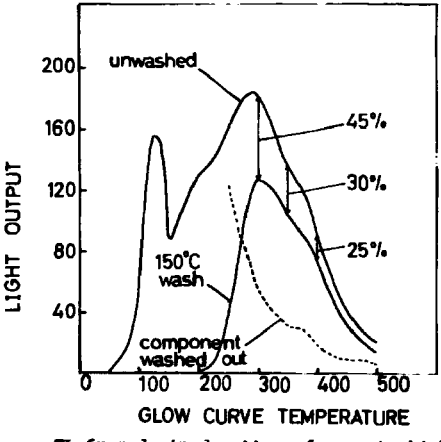

Fig. 14 TL from drained pottery fragment which has been given a gamma dose (2300 rads) before crushing and a beta dose after crushing, for unwashed sample and for sample thermally washed at 150° C after the beta dose.

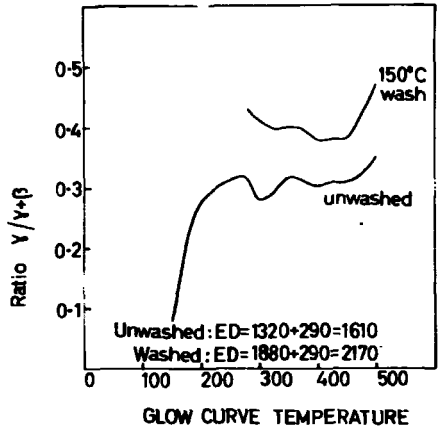

Fig. 15 Ratio of gamma TL to (gamma + beta) TL for unwashed sample and for samples washed at 150° C 300° C.

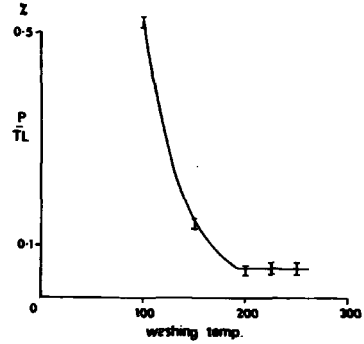

Fig. 16 CaF_2:Mn. Integrated phosphorescence (at room temperature) expressed as percentage of TL remaining, after thermal washing for 10 minutes at various temperatures. Beta dose 5000 rads.

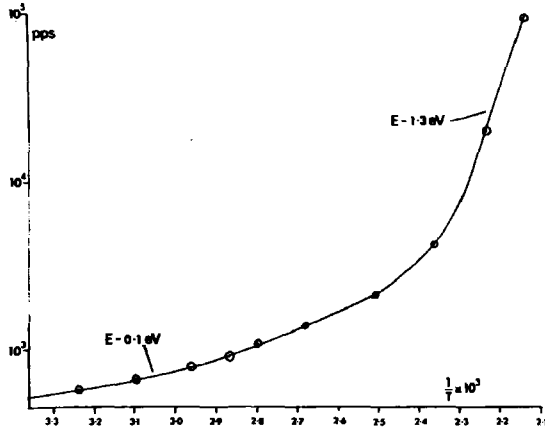

Fig. 17 CaF_2:Mn. Temperature dependence of phosphorescence after thermal washing at 225° C. The values of E are derived from the slope at the indicated point of the graph.

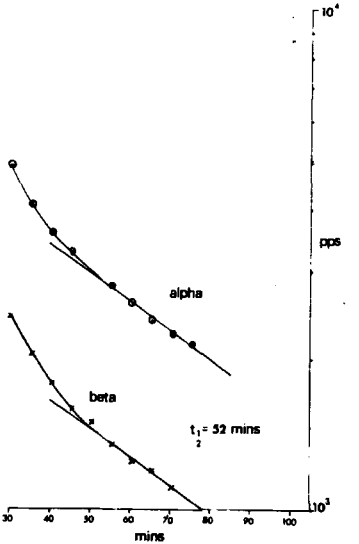

Fig. 18 CaF_2:Mn. Decay of phosphorescence after alpha irradiation, and after beta irradiation, for sample thermally washed at 225° C. The doses were adjusted so that the TL was the same in each case.

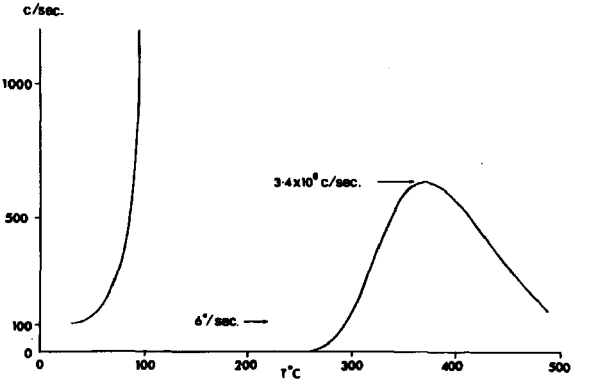

Fig. 19 Mullite. Residual TL after thermal washing at 225° C. The ordinate scale applies only to the TL curve up to 100° C.

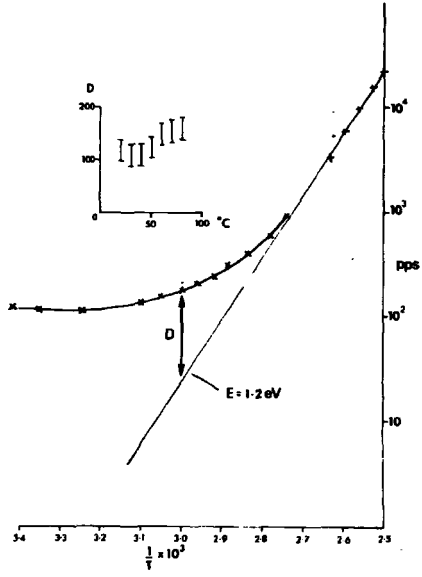

Fig. 20 Mullite. Temperature dependence of phosphorescence after thermal washing at 225° C. The inset plot of D represents the difference between the actual level and the level predicted by the straight line drawn through the data points around 120° C. This straight line has a slope corresponding to a trap depth of 1.2 eV.

Becker

Similar results have been reported by John Garlick for lunar materials. It seems possible that in some cases chemical processes such as hydration of surface regions, resulting in the destruction of traps, may also be involved in the frequently observed "abnormal" TL fading (we have demonstrated this to occur in particular in TSEE, as one would expect from the thin surface layer which is involved). Did you look into the possibility of chemically induced fading?

Wintle

Most of the work was done with 100 μ grains, therefore it is unlikely that surface effects played a significant part. It is also unlikely that chemically induced fading would be independent of temperature.

Attix

Jackson and Harris (Berkeley Laboratory, UK) and others have noted that the traps in LiF (TLD-100) can migrate and rearrange themselves into other more complex traps during annealing. This is not a "fading" process, inasmuch as it occurs while the traps are empty (although in some cases the traps can carry trapped charges along with them in migration). Perhaps some of the fading changes you observe in other materials are of this type and could be identified by studying the effect of administering annealing (or "washing") processes to samples before irradiation.

Wintle

It is unlikely that any change in sensitivity (presumably from changes in defects) would proceed at a rate that is independent of temperature.

Fading in Thermoluminescent Dosimetry

by

Zdenek S p u r n ý and Josef N o v o t n ý

Nuclear Research Institute and
Faculty of Nuclear Engineering, Prague

Abstract

Fading in thermoluminescent dosimetry is discussed in general and particularly in a glass, LiF, CaF_2, Al_2O_3 and $CaSO_4$ phosphors. Special attention and experimental investigation is paid to "anomalous fading", when TL signal of a certain phosphor haeving relatively high peak temperature (T_M) decays with storage time at room temperature. Based on thermoluminescence, absorption spectroscopy and delayed isothermal luminescence measurements a model of a trap has been suggested and fading explained.

I. Introduction

We know that the probability of electron escape (p) from a trap is a function of the depth of this trap (E) and of a frequency factor (s):

$$p = s \cdot \exp(-E/kT) \quad \ldots\ldots\ldots\ldots \quad (1)$$

The deeper the trap, the smaller the probability of electron escape at given temperature and frequency. The spontaneous electron escape from a trap, i.e. the escape at room temperature, is refferod to as "fading". Fading is strictly undesirable pheno-

menon as the signal of an integrating detector is time-dependent. Nevertheless only few actual dosimeters are not time-dependent; let us be reminded,for example, of the film dosimeter which is widely used in spite of its fading (it is dependent on humidity, temperature, sort of emulsion, etc. and keeps within 10-30% per month).

Also solid-state dosimeters show more or less fading. Theoretically, the probability of spontaneous escape of electron from 1 eV deep trap should be zero for all s and room temperature, but actualy we find fading also from a phosphor with deep traps.

Fading in TLD is a hard-measurable parameter. There is a great scattering of experimental points owing to many factors, and different groups of authors obtain different results for the same phosphor (see the situation of LiF: till now, it is not clear if there is fading or not). Certain common phosphors with relative deep traps show, undoubtedly, some losses of signal after irradiation; this is the well known case of NRL synthetic CaF_2(Mn) phosphor discussed recently by Gorbics et al. /1/. Commercial type of DT-284 dosimeter losses 10% of captured electrons in 3 weeks after irradiation in spite of its simple glow-curve with one maximum at 260°C /2/. This surprising effect has been explained by Gorbics as a simulated fading; in fact, there is a thermal quenching induced by unreasonable high heating rate. Calculating the frequency factors, the author demonstrated unsuitability of Randall-Wilkins' theory in such case. In spite of all efforts this undesirable parameter of CaF_2(Mn) has not been removed yet /3/.

Lately, this case turned out not to be rare in TLD. In our paper on 2nd International Conference on Luminescence Dosimetry we directed the attention to the fact that aluminophosphate glass shows fading, too /4/. After some months of difficulties with a bad reproducibility, we firmly established for given type of glass a loss of about 15% per month. At the same time or later also the other authors stated fading for this detector: Keirim-Marcus et al. 32% per year /5/, Schwartz about 30% per month /6/ and Békés et al. even 40% per 10 days /7/. These data differ greatly because of differences in glass samples, but certain loss of signal surely exists, while the phosphor has a simple glow-

-curve with 270°C peak.

As it is not eliminated that similar phenomenon may exist in some other materials, too (for samples with shallow traps, as $CaSO_4Mn$ such behaviour is evident) and can be used for the explanation of time-irregularities in radiation dosimetry or archeometry, we tried to study this antagonism.

II. Experimental

Many errors may influence the estimation of the fading curve, the experimental points may be enormously scattered and it is extremely difficult to draw some curve.

We have accepted the Webb method /8/ to eliminate as many random variables as possible. In particular to avoid the possibility of reader drift over a period of weeks a large number of samples was made up initially; sets of them were removed for irradiation every day and then returned to store. At the end of the period all samples were read out during a single session. Even then the reproducibility was around 4% because of slight differences in samples (from this point of view it will be better to estimate the whole curve using one sample only - on the other hand, this is very laborious and lengthy). Using the firm irradiation geometry there is another error of about 1%. During their storage samples must be temperred and kept in dark; the history of samples plays also a role: all of them should be used fresh only and subjected to the same annealling procedures. Exposures to ionizing radiation should be low enough to avoid the induction of new traps /9/, etc. All these procedures and treatments will not allow better reproducibility for the same experimental point then 5-6%, mostly more and because the fading could be within the same range, a statistical method must be applied. For example, Webb /8/ has this scattering within 6%, in our case this was 6-10%. Some differences in published data yielded from the peak-heights instead peak-area measurements. Sometimes an accelerating method for the fading measurements is used (maintaining the phosphor at a temperature somewhat above room temperature and reducing the necessary time); this may be further source of errors and we cast it off.

Glass samples were irradiated in a firm geometry with radium source. All TL measurements were carried out on laboratory reader of our own-made provided with low noice PM cooled by semiconductors, especially stabilized HV unit and linearized heater up to 10°C/sec. The long time stability of the ascent of this apparatus was controlled by radioactive luminescent standard.

Absorption spectra of glass samples were recorded by universal spectrophotometer SPECORD-ZEISS against untreated sample. Luminescence decay-curves were measured by special photographic method developed in our laboratory.

Composition and parameters of mentioned glass were described previously /4/.

III. Results and Discussion

The most important step was to conform the peak-temperature as one of the decisive factor for trap-depth calculation. The value T_M was established by various independent procedures (with regard to sample-thickness and heating rate) as $265 \pm 5^{\circ}C$. This value was proved also in some other laboratories+) but was not in agreement with some published data /6, 10/. Corresponding frequency factor $\underline{s}$ was calculated for heating rate $1^{\circ}C$/sec and trap depth $E = 1.1$ eV as 1.4×10^{10} sec^{-1}.

In Fig. 1. the fading of our glass-sample is entered in a diagram as log of reduced peak area against time in a decadic scale. This illustration is the only suitable one for a kinetic decision of the fading phenomenon (some authors diagrammed time in log-scale which is incorrect from kinetic point of view). In correct diagramme the fading ought to be a linear for monomolecular mechanism.

In the course of annealling studies certain relationship between luminescent and colour centra in given glass was proved and this enabled to establish the fading via colour centra. As may be seen from Fig. 1. a good agreement of both measurements is evident (see triangel points). Since the spectrophotometric technique is generally more reproducible the fading was firmly expres-

+) Thanks to Dr Jech from the Physical Chemistry Institute of Prague

sed as 20% per 1000 hrs with maximum error of $\pm$ 2%.

Also surface effects as cleanness or presence of inertial atmosphere were without considerable influence. Regarding a semicrystalic structure a systematic study of annealling procedures up to very high temperature or very fast cooling rate was done, but fading has improved in maximum of ~5%.

Carefull study of the fading curve from $CaSO_4$(Mn), which has a single peak at 110°C, gives the same character as the glass-curve (see Fig. 2.).

In Fig. 2. and 3. are summarized results of experimentally established decay-curves of isothermal luminescence; both curves were registered by a photographic method and in the same range of time as the fading. We can see that the agreement of both curves is very striking: all curves obtained in this work are similar, and by graphical analysis they may be divided into two linear lines. While the TL fading is proportional to the number of trapped electrons n, the isothermal luminescence decay to the rate of trapped electrons $-\frac{dn}{dt}$, i.e. the same character of both curves testify the monomolecular character of both processes.

Using the estimated frequency factor s and under the presumption that this factor is constant for given phosphor and using the values of mean lifetime (estimated from fading and decay curves), the trap-depths were calculated and results are in Table I.

The experiments with $CaSO_4$ show an excellent agreement among E_1 and E_2 values estimated both from fading and from luminescence decay measurements. The glass sample data for trap-depth E_1 and E_2 does not agree so well: the E_2 values are different because we evidently were not able to catch the decay from such a deep trap and the resultant decay curve belongs to the first trap only.

Agreement in trap depths is in favour with our idea that each TL peak presented in TL by "single trap" consists of two separate, or better to say, two level-traps. Similar situation as in case of $CaSO_4$ and aluminophosphate glasses has been noticed for CaF_2(nat.) and Al_2O_3(Cr) phosphors; each single peak on TL glow-curve consists of two components /11/. But not only these experimental data are in favour with our idea.

Using the spectrophotometric method we studied the changes in absorption spectra after the isothermal heating of glass samples. We detected here a very interesting blue-shift: after a certain period of time of isothermal heating, the extinction coefficient evidently drops (i.e. the number of colour centra has been reduced), but to our surprise, the absorption maximum shifted to the region of long wavelength. This shift has been evident also with the naked eye and testified the disappearance of red component. In more detail we intend to discuss this phenomenon elsewhere/12/ and here we shall summarize only: there is an analogy with glassy state of supercooled water solutions /13/; here also has been done a presumption of the existence of fine structure of single colour centra. Some "blue" and "red" centra preexist in the glass before its irradiation and give together one absorption band only. In our point of view the most likely environment for an electron is a structural cavity. The walls of this cavity we regard as entirely comprised of PO_3^- ions (in the case of aluminophosphate glasses) in specific orientations which are not precisely the same for all cavities. Consequently, a distribution of traps can be forseen. Blue and red traps are illustrated according to Dainton suggestion /13/ in Fig. 4. If the optical transition is from 1s to 2p state, the blue traps requiring more energy must have the smaller cavity size. If 2p electron level is not actually the part of the conduction band it must be very close to it because a weak thermal energy is required only to carry an electron from 2p level to the conduction band (see Fig. 4.).

It is evident from Fig. 4. that the release of electron from the blue-trap is attained at higher energy (temperature) than from the red one. In other words, the mean lifetime of electron in both traps will not be the same at constant temperature. Consequently, both values τ_1 and τ_2 can be adjudged to diffsrent structures; the same model may be applied to $CaSO_4$ phosphor. The global rate of fading will be the function of trap distribution and will be characterized by "mean trap-depth E_m". Glassy and polycrystalic material should have a broader distribution of traps in comparison with pure crystalic matter and hence higher fading.

Second parameter describing an electron trap is the frequency factor s . It seems reasonable that different distribu-

tion of electron levels should be accompanied also by different frequency factors. Usually calculated values are then necessarily a certain "mean frequency factors s_m", similarly as E_m. The high value of the frequency factor /1/ for the second-order decay of the electron may raise the question whether this is in fact a true frequency factor. Second-order kinetics of decay are readilly obtained if several groups of electrons decay simultaneously by first-order processes the rate constants of which are significantly different.

Using this model of electron traps and presuppozing a variability of s, we can easily understand that for certain condition product E_m and s_m yield into fading even when T_M of a "single peak" is at relatively high temperature. Furthermore, the rate of fading is the function of crystallinity of the matter; the more amorphous is the structure in a sample, the higher fading should be expected through the broader maxima of the glow curve.

In the last part of our work we studied the influence of an activator concentration on the rate of fading. For this experiment the $CaSO_4$ and Al_2O_3 phosphors systematically activated with different concentration of manganese and chromium were chosen respectively (more detail-description of their preparation and chemical analysis can be found in papers /14, 15/). For both kinds of crystals the decay and fading curves were measured analogous to those introduced in Fig. 1. - 3. From these experimental curves the mean lifetime values of trapped electrons were calculated and thus obtained average values were plotted vs concentration of activator (Fig. 5 and 6); in fact, there is the value τ_2 in both cases only. Assumed maximum deviation here is $\pm$ 15%). We can see that the optimal concentration of manganese atoms in $CaSO_4$ matrix for longer lifetime is around 0.3%. This value does agree well with the optimal concentration of the same activator and matrix for luminescence yield - this has been 0.24% /11/. As regarded to Al_2O_3 phosphor, the optimal concentration of chromium atoms for better lifetime is 0.175% and for higher luminescence yield 0.2% /12, 14/.

These experiments give a very interesting conclusion: if the TL phosphor is activated by optimal amount of activator then simultaneously the excited electrons will be captu-

red most firmly and given phosphor will have a smaller fading. The optimal concentration of impurity atoms in crystal lattice may probably influence the distribution of traps. We are not sure yet if this experimental fact may be enlarged generally onto all TL phosphors and for its theoretical appreciation we will need further data.

Conclusion

Fading in TLD may not be simply estimated according to glow-curve having high temperature maxima; the decisive factor is a structure of a trap itself. In some cases when glow maxima are in high temperature - range the product of trap-depth and frequency factor gives a certain probability for electron-escape even at room temperature. Consequently, the fading must be verified experimentally in every case.

Literature

/1/ S.G. Gorbics et al., Thermal quenching of luminescence in TLD phosphors, Part I, Int.J.Appl.Rad.Isotop. 20, 829 (1969)
Part II, -"- 20, 843 (1969)

/2/ J. Johnson et al., Proc. of the 1st Int.Conf. IRPA, Pergamon Press 1968, p. 466

/3/ L.F. Booth et al., Use of miniature glass needle type TLD in finger ring applications, NRL Rept. 7276, May 1971

/4/ Z. Spurný, A glass TLD, Proc. of the 2nd Int.Conf.on Lum. Dos. USAEC, Conf. 680920, 1968, p.18

/5/ Keirim-Marcus K.A. et al., Accidental dosimetry for n,gamma radiation, Panel IAEA PL-329, 1969

/6/ K.K. Schwartz et al., Thermoluminescence dosimetry, Zinatne Press, Riga 1968, p. 52

/7/ E.Békés et al., Thermoluminescent glass-dosimeter, KFKI Közlemények 17, 179 (1969)

/8/ G.A.M. Webb, Fading in thermoluminescent LiF after irradiation with low doses, Brit.J.Appl.Phys. 18, 7 (1967)

/9/ G.A.M. Webb, Fading in thermoluminescent LiF after irradia-

tion with doses up to 1000 rad, Brit.J.Appl.Phys. 18, 1567 (1967)

/10/ I.A. Botschvar et al., Dosimetry of ionizing radiation with thermoluminescent glass, At.Energy (USSR) 15, 48 (1963)

/11/ Pernička F., Diploma Thesis, ČVUT FJFI, Prague 1971

/12/ J.Novotný et al., Blue-shift in optical glasses, to be published

/13/ F.S. Dainton et al., Recent experiments on steady-state and puls radiolysis of alkaline aqueous systems, Int.Discussion on progress and problems in contemporary radiation chemistry, Mariánské Lázně 1970, vol. II., p. 295

/14/ J. Novotný et al., Exo-electron emission from activated $CaSO_4$ phosphors, J.Phys.Chem.Solids 31, 1412 (1970)

/15/ J. Novotný et al., Effect of ionizing radiation on Ruby, J.Czech.Phys. B16, 2 (1966).

TABLE I

Calculated values E for glass and $CaSO_4$ phosphors

Sample	Experimental method	Frequency factor (s^{-1})	τ_1 (s)	τ_2 (s)	E_1 (eV)	E_2 (eV)
$CaSO_4$	fading	1.2×10^{11}	2.1×10^{4}	3.7×10^{5}	0.88	0.96
	decay	1.2×10^{11}	2.8×10^{4}	5.6×10^{5}	0.89	0.97
Glass	fading	1.4×10^{10}	1.8×10^{5}	9.2×10^{7}	0.88	1.10
	decay	1.4×10^{10}	1.2×10^{4}	1.1×10^{5}	0.82	0.87

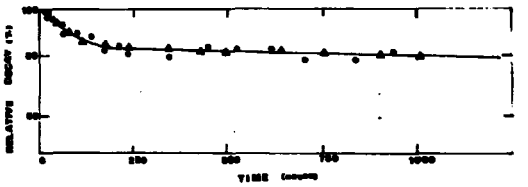

Fig. 1. Rate of fading in TL glass

o .... luminescent experimental points, average of 10 measurements
▲ .... photometer " " " "

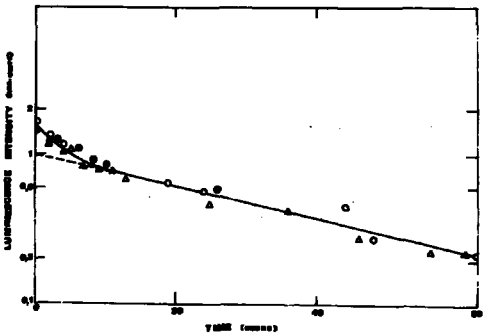

Fig. 2. Rate of fading in $CaSO_4$(Mn)
Three various samples, average of 5 measurements

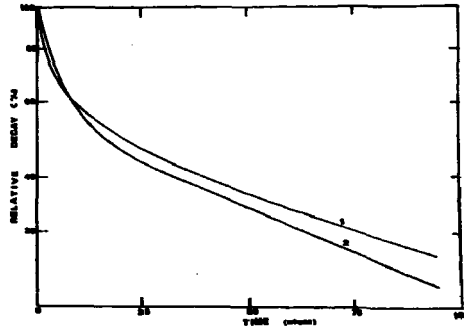

Fig. 3. Isothermal decay curve (1) and fading curve (2) in $CaSO_4(Mn)$

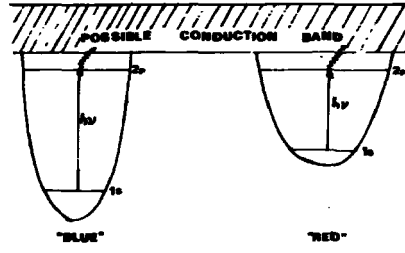

Fig. 4. "Blue" and "red" traps in glassy state

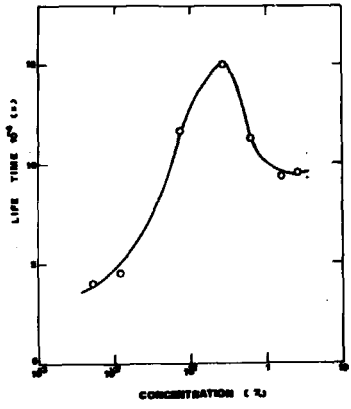

Fig. 5. Rate of fading in dependence on the concentration of an activator in $CaSO_4$(Mn) phosphor

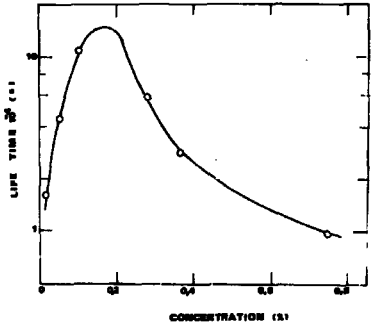

Fig. 6. Rate of fading in dependence on the concentration of an activator in Al_2O_3(Cr) phosphor

Scharmann

You spoke of two different kinds of traps, a "blue" and a "red" one. Did you make any ESR experiments to confirm this idea?

Spurny

No, we did not make any ESR measurements.

Watanabe

Did you obtain glow curves from the bimolecular theory?

Spurny

No, we did not calculate glow curves using bimolecular theory.

Fowler

The difference in shape of a fading curve as between bimolecular and two monomolecular processes can sometimes be distinguished by plotting the reciprocal of the residual reading instead of the logarithm. A true bimolecular process decays according to the equation

$$\frac{1}{n} = \frac{1}{n_0} + at$$

where n is the amount of signal remaining, n_0 is the initial signal remaining at t = 0, t is time, and a is a constant representing the probability of combination of the two components - e.g. the cross section of luminescent centres for electrons. This would in general be the likely process if electrons were released into the conduction band and then had to find a centre other than the one from which they came; so perhaps electrical conductivity measurements would be helpful here.

Effects of Deep Traps on Supralinearity, Sensitisation and Optical Thermoluminescence in LiF TLD

By

C.M.Sunta, V.N.Bapat and S.P.Kathuria
Health Physics Division
Bhabha Atomic Research Centre
Bombay-85, India

Abstract

A glow curve study of LiF samples from room temperature to 550°C using a linearly programmed heating system shows 10 glow peaks namely at about 75, 100, 135, 170, 190, 225, 250, 285, 310 and 395°C. The exposure response of LiF TLD is studied after annealing at 280, 350 and 400°C subsequent to a high gamma exposure. The observations obtained are used to examine the two models of supralinearity and sensitisation namely, (1) early saturating competing deep trap model of Suntharalingam and Cameron and (2) interacting track model of Claffy, Klick and Attix. Studies on photostimulated glow peaks lead to the conclusion that the observed glow peaks are due to untrapping of electrons.

1. Introduction

Earlier workers[1,2] have attributed the supralinearity and radiation sensitisation effects to the unannealed deep traps. However, thermoluminescence glow peaks corresponding to the postulated deep traps were not observed. In the present work such glow peaks are recorded using a reader system designed in the laboratory. The newly observed glow peaks which appear above the temperature of dosimetry peak (190°C) remain residual in the sample after readout if the sample is not heated sufficiently to bleach all of these. The paper presents some studies on the effects of the residual peaks.

2. Glow Peaks and Their Response

Glow curves were recorded using a specially designed heater system which consists of a small kanthal strip of size 30 x 5.5 x 0.25 mm having a 4 mm diameter circular depression of

0.5 mm depth at the centre to hold 5 mg of the sample. An iron-constantan thermocouple is spot-welded on the lower side of the strip underneath the sample position. The strip is directly heated at a linear rate of 20°C per minute from 25°C to 550°C. TL is read by a photomultiplier tube and recorded on a strip chart recorder. Fig.1 shows the glow curves of three samples of Harshaw's LiF TLD powder. Ten glow peaks are observed namely at about 75, 100, 135, 170, 190, 225, 250, 285, 310 and 395°C. These are numbered 1 to 10 in the figure.

Glow peak height vs radiation exposure curves are drawn in Fig.2 for the four prominent peaks namely those appearing at 100, 190, 250 and 395°C. It is observed that all of these show a supralinear response for exposures above about 1000 R.

Peak height vs radiation exposure relations are also obtained for the dosimetry peak (190°C peak) after pre-exposure annealing at 280, 350 and 400°C subsequent to a high gamma ray exposure (10^5R). The residual glow curves after 280 and 350°C treatments (1 hour each) are shown in Fig.3. 400°C treated sample does not show any residual TL. The response curves after the three treatments are given in Fig.4. It is observed from this figure that the enhancement of sensitivity and the linearity of response are almost same in 280 and 350°C treated samples whereas 400°C treated sample behaves like the original fresh sample. It thus means that the presence of 395°C peak alone is responsible for the sensitisation and the elimination of supralinearity. The competing deep trap hypothesis[1] would then require that the glow peak of 395°C must begin to approach towards saturation after 1000 R exposure i.e. near the exposure level where supralinearity begins in the 190°C peak. Experimental results of Fig.2 are however contrary to this, as it is seen that the response of 395°C peak continues to increase supralinearly even after 190°C peak has reached saturation. The competing deep trap hypothesis is therefore unsuccessful.

Chaffy, Klick and Attix[2] have proposed that the supralinear response and sensitisation are due to recombination of released holes from one track of ionisation with F centres of nearby tracks (in addition to recombinations within the same track) at higher doses of radiation. However, the assumption in this hypothesis that the thermoluminescence of 190°C glow peak is due to release of trapped holes and their recombination with F centres is contradicted by the present investigation (cf. Para 5) as well as by some recent papers[3,4]. Th fact that the glow peak of 190°C as well as other peaks appearing at lower temperatures (cf. Fig.5) are regenerated by exposure of a partially annealed (heated at temperature 350°C)

LiF sample to F band light (250 nm), leads to the conclusion that the released carriers at these glow peaks are electrons and not holes. At the same time the interacting track model seems to gain support from the observation that the supralinearity of response increases with the temperature of the glow peak (cf. Fig.2), since the greater mobility of the released carriers at higher temperatures may result in greater probability of track to track recombination giving rise to increased response. The model may therefore hold good with the simple modification that the released carriers at the glow peaks are electrons instead of holes.

3. Annealing Temperature

Zimmerman, Rhyner and Cameron[5] found that for reproducible results LiF TLD should be heated at 400°C for one hour before irradiation. The reason for the specificity of this temperature has not been given. It may now be said that the most appropriate annealing temperature is that at which all the traps including those corresponding to the glow peak of highest temperature are completely emptied without any damage to the sensitivity of the phosphor. Such a temperature would obviously be near the peak of highest temperature. For LiF it is at 395°C. It was observed that heating for a duration of 30 minutes at this temperature completely bleaches the residual glow peaks and brings the sensitivity of the phosphor to the pre-irradiation value.

4. Photo Stimulated Thermoluminescence (PSTL)

If an LiF sample is heated at 350°C subsequent to a high gamma exposure and is then exposed to 254 nm wave length Hg lamp light, all the glow peaks previously bleached during heating at 350°C are regenerated (except the one appearing at 170°C). Fig.5 shows the residual glow peak and the optically generated glow curve along with the glow curve after γ exposure. It is seen that if UV exposure (254 nm) is continued for longer time, the residual peak decays in intensity and the newly generated peaks first strengthen rapidly and later these also start decaying (Fig.6). The decay rate of all the peaks becomes quite slow in due course. This behaviour indicates a to and fro movement of trapped charge carriers between the residual and optically generated peaks under the UV exposure. Such a behaviour has actually been observed earlier[6] in case of natural CaF_2 glow peaks.

5. Nature of the Liberated Charge Carrier During Thermoluminescence

It is well known in LiF crystals that the 250 nm absorption band which develops after X and γ exposure is due to F centres. We have observed in our laboratory that 26% of

the absorption band around 250 nm still remains to be bleached after heating of the irradiated sample at 350°C. Exposure of such a crystal to F band light (λ ~ 250 nm) destroys the F centres by ejecting out the electrons from these. Since almost all of lower temperature glow peaks are regenerated by F band light exposure when the F band and residual peak of 395°C are present, it is logical to assume that the traps corresponding to the regenerated peaks are repopulated during light exposure. These peaks should therefore be due to the untrapping of electrons. The 395°C peak may either be due to the thermal ionisation of F centres or due to some kind of hole centres which recombine with F centres, since the 395°C peak and the F band both vanish simultaneously on heating the sample at 400°C.

References

1. Suntharalingam,N. and Cameron,J.R., Phys. Med. Biol. 14, 397 (1969).
2. Claffy,E.W., Klick,C.C. and Attix,F.H., "Proc.Int.Conf. Luminescence Dosimetry", Gatlinberg, Tennessee (USAEC Division of Technical Information CONF-680920, 1968) P.302.
3. Mayhugh,M.R., Christy,R.W. and Johnson,N.M., J.Appl.Phys. 41, 2968 (1970).
4. Podgorsak,E.B., Moran,P.R. and Cameron,J.R., J.Appl. Phys. 42, 2761 (1971).
5. Zimmerman,D.W., Rhyner,C.R. and Cameron,J.R., Health Physics 12, 525 (1966).
6. Sunta,C.M., Phys. Stat. Sol. 37, KB1 (1970).

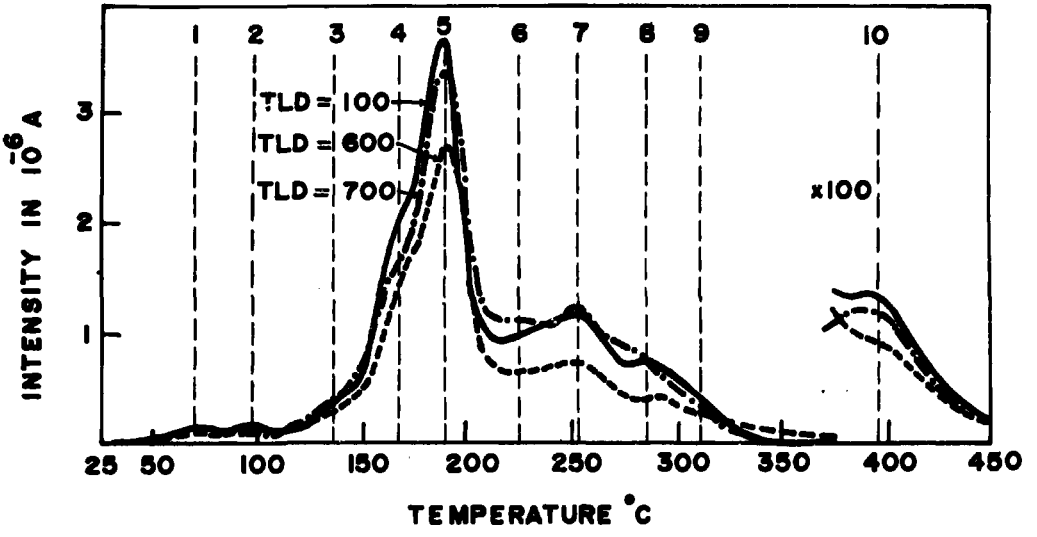

Fig.1 - TL glow curves of different LiF samples

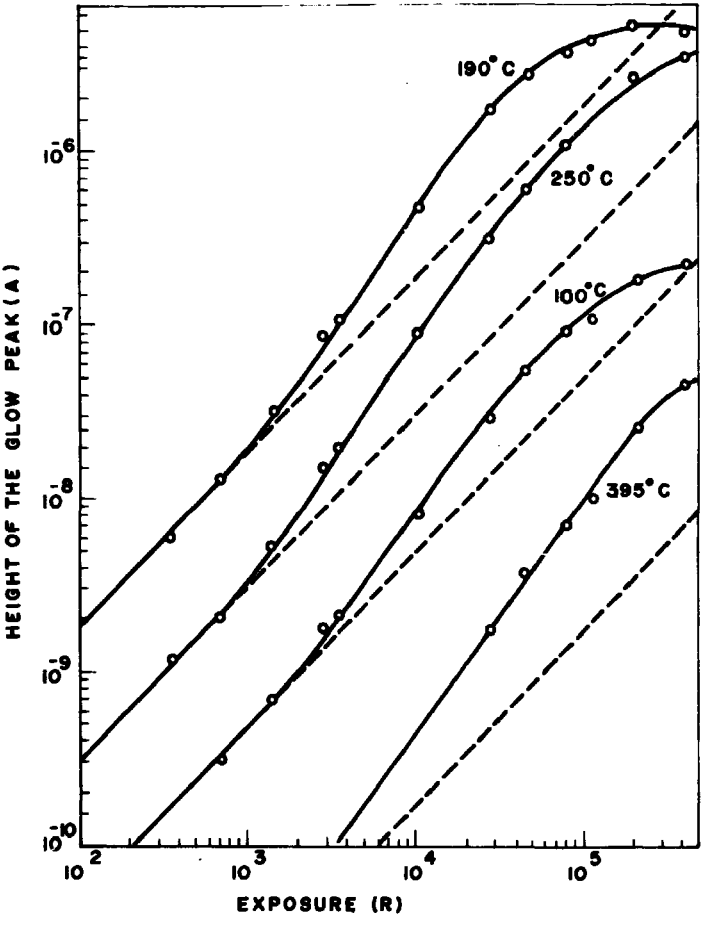

Fig.2 - Exposure vs TL peak height for different glow peaks

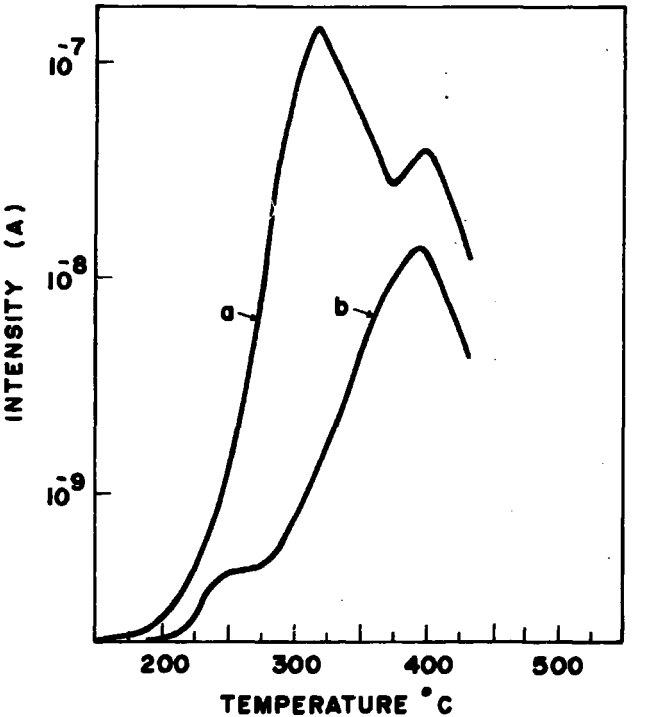

Fig.3 - Residual TL peaks after heating an irradiated LiF sample upto (a) 280°C and (b) 350°C.

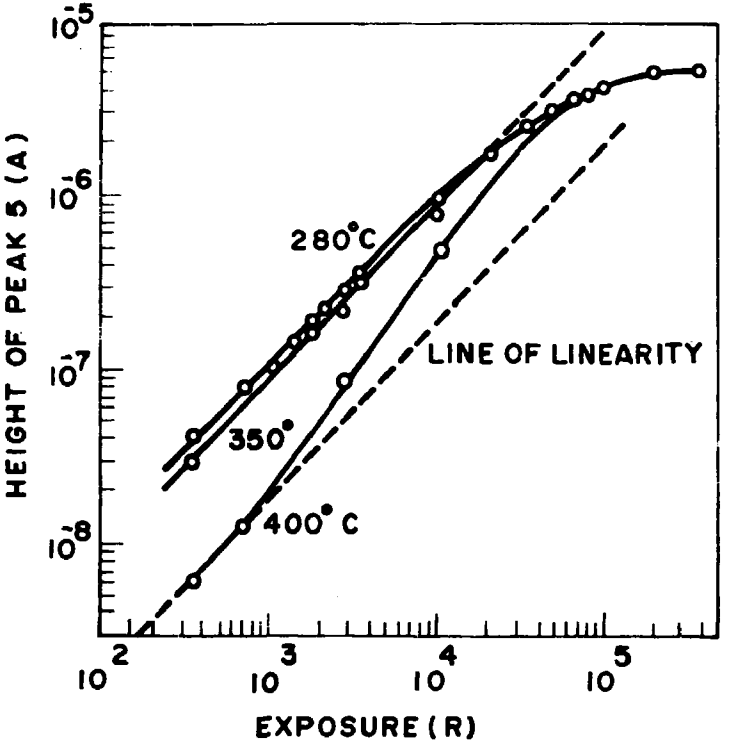

Fig.4 - Exposure vs TL peak height of 190°C glow peak of LiF samples given different annealing treatments after gamma exposure.

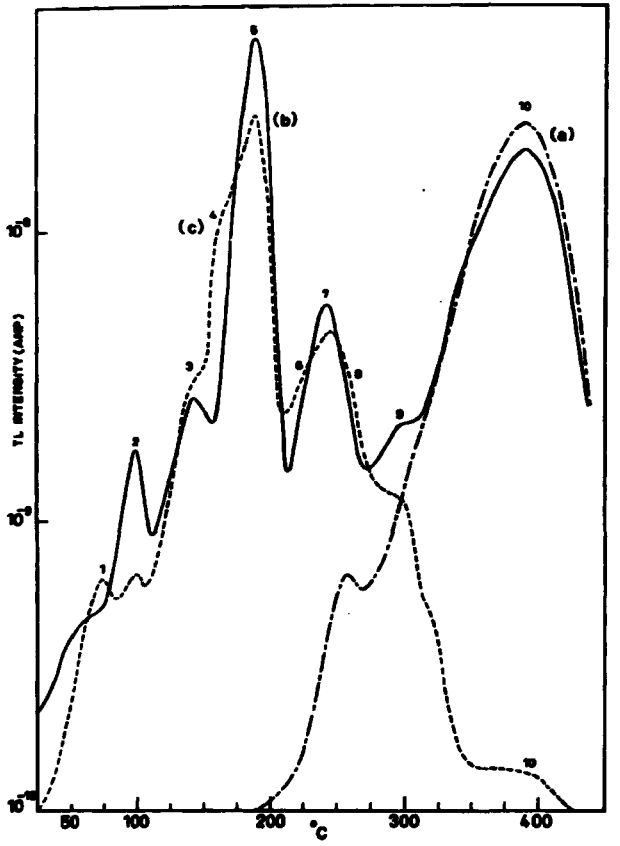

Fig.5 - (a) Residual TL glow curve after heating an irradiated LiF sample at 350°C.

(b) PSTL glow curve after exposing sample of (a) above 254 nm light.

(c) TL glow curve after 1400 R of γ exposure.

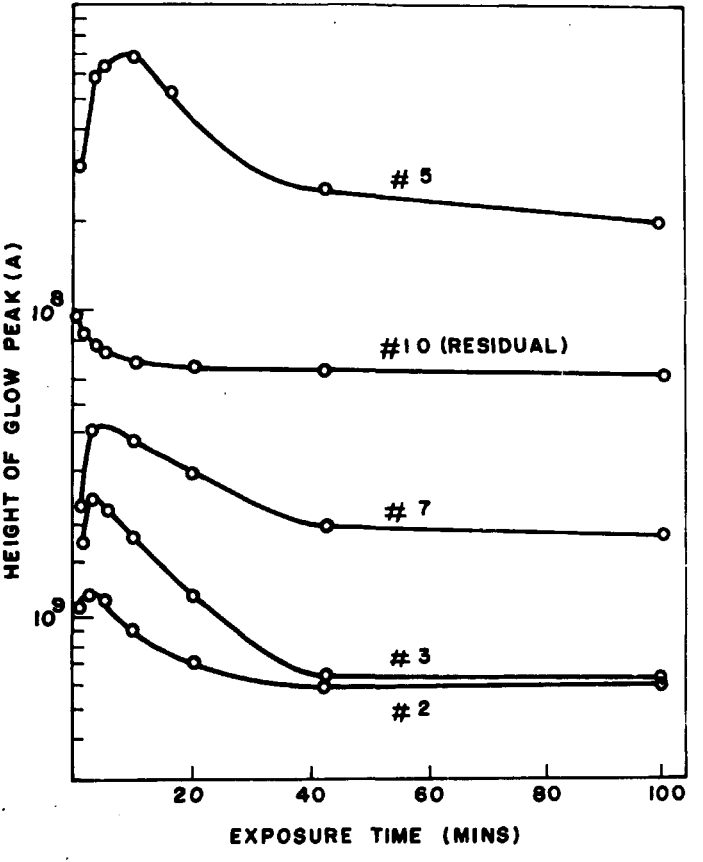

Fig.6 - Growth and decay of NETL peaks

Supralinearity and Sensitization

V. K. Jain and J. B. Sasane
DRP, BARC,
Trombay, Bombay-85
India

LiF (TLD-100) and $Li_2B_4O_7$ show supralinear response abcve exposures of about 1000 R and 200 R respectively. Further LiF (TLD-100) can be sensitized by giving high exposures and annealing at 280°C for one hour. No such sensitization is observed in $Li_2B_4O_7$.

The thermoluminescent phosphors available fall into two categories, namely low Z and high Z. LiF and $Li_2B_4O_7$ belong to the former and CaF_2, $CaSO_4$, etc. belong to the latter category. The high Z phosphors are in general an order of magnitude more sensitive than the low Z phosphors. It is, therefore, suggested that in the high Z phosphors track interactions take place even at low exposures. In the case of low Z phosphors, however, there is no track interaction at low exposures. As the exposure increases, the track interactions start taking place and the response bocomes supralinear. Further in LiF during the process of TL measurement or the 280°C annealing the filled peak 4 traps are emptied and converted to peak 5 traps. This conclusion is reached at by observing that peak 4 is absent in the glow curve of the sensitized LiF. In $Li_2B_4O_7$ no such phenomenon takes place and, therefore, no sensitization is observed. To explain the difference between the sensitization on the basis of total TL measurement and peak 5 height measurement, it is suggested that the luminosity of peak 5 centers is more than that of peak 4 centers.

Re-estimation of Dose in LiF

G. S. Linsley and E. W. Mason

National Radiological Protection Board,
Scottish Centre,
11 West Graham Street,
Glasgow, C.4.
U.K.

Abstract

A method for dose re-estimation with TLD-700 LiF is described using a series of unresolved thermoluminescent glow peaks centred around 300°C for a heating rate of 10°C/sec. The method involves a normal read-out cycle to 240°C followed by a second read-out to 370°C. The cut-off at 240°C is critical and an expression is developed relating the cut-off temperature Tc with the areas under each peak. In re-estimating dose, the supralinear dose versus intensity relationship of the "300°C" peak has to be taken into account. For virgin TLD-700 LiF doses as low as 5 rads can be re-estimated using the method. A method of enhancing the re-estimation sensitivity by using sensitized phosphors is discussed. This permits the re-estimation of doses of about 1 rad.

1. Introduction

In a previous paper[1] it was pointed out that personnel TL dosimetry with LiF had a number of drawbacks. In particular the difficulty of dose re-estimation with LiF after initial read-out was emphasised. It was suggested that the problem could be alleviated using a re-estimation technique involving optical bleaching. Doses of about 10 rads can be estimated by this technique. A similar method is successfully used for CaF2 TL dosimetry but requires special equipment.

In the present paper the feasibility of using the high temperature peaks discussed by Mason and Linsley[2] for re-estimation purposes is considered.

2. Experimental Methods

The measurement of the TL emitted from irradiated Harshaw TLD-700 lithium fluoride was carried out using a Dynatron Reader and the associated Harwell 2000 series electronics. Accurate control of heating rates and temperatures was obtained using the controller described by Gall and Mason[3].

In view of the relatively high temperatures encountered during the experiments the PM tube (EMI 6097S) was maintained at constant temperature in a thermoelectrically cooled enclosure.

All radiation doses refer to absorbed dose in tissue, measured in rads, and were delivered from a ^{60}Co sealed source.

3. Results

3.1 The "300°C" Glow Peak in LiF

Mason and Linsley[1] have described the glow peak which occurs at approximately 300°C in LiF. This single maximum is in fact composed of at least three separate peaks which are not normally resolved.

The behaviour of the individual glow peaks will not be considered here and observations will be restricted to the unresolved "300°C" peak as a whole.

For the purposes of dose re-estimation the "300°C" peak has been separated from the TLD peak at 210°C and the variation of the TL intensity of the peak with increasing absorbed dose has been determined.

3.2 Separation of the peaks

It can be shown that if the shape and position of two overlapping peaks remain constant with increasing dose then it is possible to measure the actual integrated intensity of the individual peaks by selecting a suitable temperature (T_1) at which heating is stopped during a first cycle. The integrated intensity of the peak at the lower temperature is measured during this cycle. A second cycle to a further suitable temperature T_2, where $T_2 > T_1$ gives the integrated intensity of the second peak.

Considering the situation in which the peak separation $(T_2 - T_1) > B_2$ and B_1 (figure 1), where B_1 and B_2 are the widths at half height of P_1 and P_2 the peaks may be roughly represented by two overlapping triangles. For convenience isosceles triangles are chosen. At T_c the heating is switched off and the temperature then falls rapidly to ambient.

Using the properties of similar triangles it can be shown that the integrated intensity measured during the first heating period is given by

$$A_1 = A_{P_1} - \frac{A_{P_1}}{2}\left(\frac{B_1 - T_c + T_1}{B_1}\right) + \frac{A_{P_2}}{2}\left(\frac{B_2 - T_2 + T_c}{B_2}\right) \qquad (1)$$

where A_{P_1}, A_{P_2} are the areas under the respective peaks.

Similarly the second heating period to Tp gives an integrated intensity

$$A_2 = A_{P_1} \left(\frac{B_1 - T_c + T_1}{2B_1}\right) + A_{P_2} \left(\frac{B_2 - T_c + T_2}{2B_2}\right) \qquad (2)$$

The requirement that the integrated intensity measured during the first heating period should be just equal to Ap_1 is expressed by putting $A_1 = Ap_1$ in equation (1) or $A_2 = Ap_2$ in equation (2). Consequently we obtain an expression for the number of degrees centigrade above T_1°C at which the temperature must be arrested to give this condition, viz:

$$T_c - T_1 = \frac{B_1B_2(R-1) + B_1(T_2 - T_1)}{B_1 + RB_2}$$

where $R = \frac{A_{P_1}}{A_{P_2}}$

This expression is not meant to provide an accurate means of determining $(T_c - T_1)$ but simply to emphasise the factors involved in peak separation.

In practice it is found that T_c = 240°C gives a clean separation between the 210°C and "300°C" peaks. The procedure for re-estimation is then as follows:-

1st cycle: 20°C-240°C Heating rate 10°C/sec - normal read-out
The 1st cycle is then repeated. - background read-out

2nd cycle: 20°C-370°C Heating rate 10°C/sec - re-estimation read-out
The 2nd cycle is then repeated. - background read-out

Glow curves produced during the repeat of the 1st cycle indicate whether or not the 210°C traps were cleaned during the previous cycle and also the extent to which the 1st cycle removes TL from the "300°C" peak. In practice there is a slight nett loss of intensity from the second peak to the first.

For doses between 10^4 and 10^5 rads the extra contribution to the 210°C peak amounted typically to about 1-2% but was less for lower doses.

3.3 Variation of TL with dose

The integrated TL intensity was determined for doses up to about 10^5 rads for both the 210°C and the "300°C" peaks. The TL versus dose curves are shown in figure 2 for virgin TLD-700 LiF which was annealed for one hour at 400°C followed by one hour at 100°C before irradiation. Insets 1 and 2 show examples of the unresolved and resolved peaks. At present there is insufficient data to calculate meaningful standard deviations at each dose level. However, it is clear that the "300°C" peak in LiF can be used to give a second estimate of dose if the normal first read-out cycle is terminated at 240°C.

3.4 Methods of increasing sensitivity

With Virgin ^{7}LiF annealed in the manner described above, dose re-estimation is possible for doses as low as 5 rads using about 30 mgm of phosphor. Possible methods of increasing the sensitivity of the "300°C" peak have been considered.

The sensitivity of the "300°C" glow peak may be enhanced if the number of associated trapping centres which are available at a given dose can be increased. Two methods of achieving this increase have been considered.

Method 1 - annealing

In a previous paper[2] it was shown that the "300°C" peak may be increased substantially by annealing for a suitable period at 100°C or 150°C prior to irradiation. The obvious disadvantage which arises from this procedure is that the 210°C peak is gradually destroyed as the anneal progresses. Attempts to restore the 210°C peak without similarly destroying the enhancement in the "300°C" peak have not proved successful.

Method 2 - pre-irradiation

According to the competition theory described by Cameron et al.[4] sensitisation, that is, an increase in the TL response per rad, occurs in LiF when the number of empty deep traps which normally compete strongly for the electrons freed by radiation becomes significantly reduced. Traps at other levels which are more numerous but have smaller cross-sections for trapping freed electrons are then able to compete more favourably for the available carriers. Sensitization occurs for doses above 10^{3} rads for LiF and is not removed except by adequate annealing. Unfortunately it is also for large doses that the "300°C" traps occur in really proficient numbers. A dilemma arises if one wishes to preserve the "300°C" traps in order to give increased sensitivity for re-estimation purposes, since the normal method of removing sensitisation is to anneal at 400°C for one hour which also destroys the "300°C" traps. It may be that at some optimum temperature below 400°C the destruction of the "300°C" traps proceeds much more slowly than the removal of sensitisation thus enabling a large proportion of "300°C" traps to be preserved during the selected annealing period whilst subetantially reducing the sensitization. A detailed investigation to determine a suitable annealing temperature and period would be quite involved.

It is therefore necessary at present to avoid sensitization effects if possible and Method 2 is designed to achieve this for doses up to about 500 rads.

Virgin ^{7}LiF was given a standard anneal at 400°C for one hour, and then pre-irradiated to 500 rads. This was sufficient to increase the number of "300°C" traps significantly yet avoid sensitisation. The phosphor was then annealed for 30 minutes at 300°C and cooled reproducibly to room temperature. This removed the stored TL from the traps associated with the 210°C and "300°C" peak. Subsequent post-irradiation fading was minimised by an anneal at 100°C for one hour. Samples were then irradiated to 10 rads and 1 rad and read-out. Table 1 compares these results with those obtained for virgin phosphor which had been given the standard anneal before irradiation. It is apparent from Table 1 that this method should allow doses of about 1 rad to be re-estimated.

Table 1

Dose rads	Virgin ^{7}LiF TL response (ARB.units)		Sensitized ^{7}LiF TL response (ARB.units)	
	210°C	"300°C" peak	210°C	"300°C" peak
1	1,857	-	2,105	137
10	19,000	372	20,050	1,094

Although the TL v Dose curve for pre-irradiated LiF will differ from that shown in Figure 2 no significant sensitization effects are to be expected until further doses of about 500 rads have been received.

It should be pointed out that although the number of deep traps filled by the pre-irradiation to 500 rads is not sufficient to produce significant sensitisation effects another effect has been observed at higher doses which may occur to a lesser extent near the 500 rad dose level.

At room temperature there is a finite probability that electrons will escape from even the deepest traps in lithium fluoride with the result that a proportion become retrapped in shallower traps such as those associated with the 210°C and "300°C" peak. The effect was observed with ^{7}LiF TLD-700 previously dosed to approximately 10^{4} rads which had not been correctly annealed and had been allowed to stand. The "300°C" trap accumulated electrons from the uncleaned deep traps and gave the apparent but false conclusion that a dose of 100 mrads could be detected using the "300°C" peak.

3.5 Comparison with the U.V. bleaching technique for re-estimation of dose

The present method of dose re-estimation using the "300°C" peak in ^{7}LiF may be used for doses as low as 5-10 rads in the situation where the standard anneal (400°C for one hour followed by 80°C for 24 hours) is being used to recycle the phosphor. The limits of detection may be further reduced by the pre-irradiation method described above to around the 1 rad level.

The technique offers somewhat greater sensitivity than re-estimation by U.V. bleaching[1] and requires no extra equipment or expertise. In addition to this there is no reason why a dose re-estimation with the "300°C" peak should not be followed by a second re-estimation using the U.V. bleaching technique if circumstances require it.

It should be emphasised that both the U.V. bleaching technique and the present method of dose re-estimation have only been investigated regarding their suitability for use with lithium fluoride in powdered form. The application of the techniques to LiF:teflon dosimeters poses some quite separate problems.

Re-estimation of doses with LiF:teflon discs might be expected to be at least an order of magnitude less sensitive than with powders. The absorption of 250 nm light in teflon must be considered if U.V. bleaching is to be used. The use of the "300°C" peak for re-estimation with LiF: teflon discs is complicated by the teflon which may not normally be heated above about 300°C.

This does not rule out the technique. If the disc was held at 300°C the resulting phosphorescence could be measured. Excessively long holding times would not be required since the decay half-live for the longest lived component of the peak is only a few minutes at 300°C.

Acknowledgements

The work reported here is part of the technical development programme of the National Radiological Protection Board. The authors are grateful to Mr. N. T. Harrison for continual encouragement and advice; to Miss Anne Wotherspoon for her patient help during the preparation of the manuscript; to Mr. A. Gall and Mr. A. F. McWhirter for their admirable technical assistance and to Miss Elizabeth Gardner and Mrs. Yung-Shiang Wang for experimental assistance.

References

1. E. W. Mason, Phys. Med. Biol. 16, 2, 303-310 (1971)

2. E. W. Mason and G. S. Linsley, 3rd Int. Conf. Luminescence Dosimetry, Riso, Denmark (1971)

3. A. Gall and E. W. Mason, Phys. Med. Biol. 14, 4, 661-664 (1969)

4. J. R. Cameron, N. Suntheralingam and G. N. Kenney, Thermoluminescent Dosimetry (Wisconsin: University Press 1968).

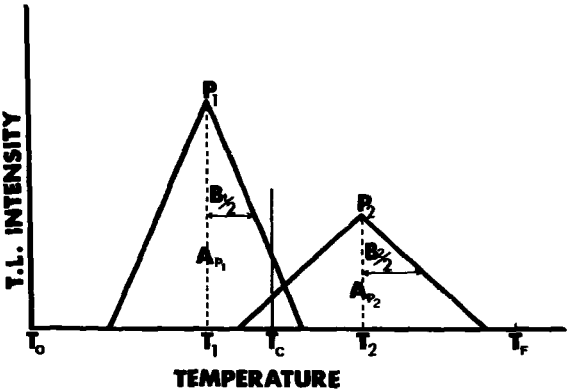

Figure 1. Overlapping thermoluminescent glow peaks represented by two isosceles triangles.

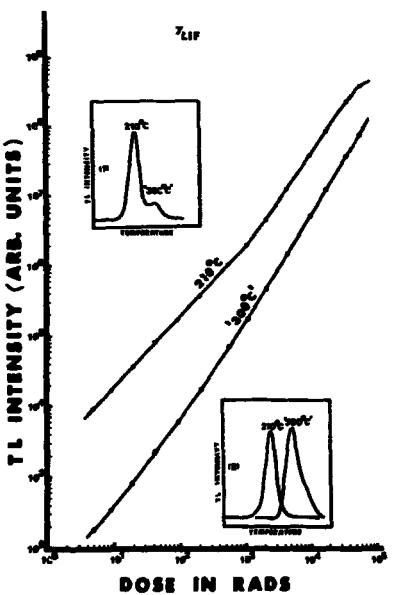

Figure 2. TL Intensity versus ^{60}Co gamma-ray doses for the "300°C" and 210°C peaks. Insets (1) and (2) dmonstrate the resolution of the peaks obtained by a double read-out

Properties of some deep traps in lithium fluoride

E. W. Mason and G. S. Linsley

National Radiological Protection Board,
Scottish Centre,
11 West Graham Street,
Glasgow, C.4.
U.K.

Abstract

A thermoluminescent glow peak has been observed in irradiated TLD-700 LiF at about 300°C for a heating rate of 10°C/sec. The peak consists of at least three components. For absorbed doses of the order of 10 rads the peak is typically about 1% of the intensity of the 210°C peak but becomes much more prominent at large doses. The dose versus TL intensity curve for the "300°C" peak is supralinear up to at least 10^5 rads. It is suggested that the trap concentration is actually increased by the radiation.

The results of thermal annealing experiments have been explained in terms of the formation of clusters of impurity atoms. This process is particularly prominent in the temperature range 100°C to 200°C. Annealing in this range results in a simultaneous increase in the "300°C" trap concentration and a decrease in the number of 210°C traps. It is postulated that the formation of clustered impurities results in the destruction of 210°C traps but gives rise to an increase in the density of the crystal defects associated with the "300°C" traps.

Observed departures from first order kinetics in isothermal decay experiments have been explained in terms of the temperature instability of the "300°C" traps and the possible effects of impurity atom agglomeration at temperatures close to 200°C.

Optical experiments reveal that the "300°C" traps are occupied by electrons. The "300°C" traps have been distinguished from another deep trap which also bleaches with F-band light. At this stage it is not possible to decided conclusively which of these is the F-centre.

1. Introduction

The more prominent peaks which appear in the thermoluminescent glow pattern of irradiated lithium fluoride have been studied by many groups of workers. Several unresolved, less prominent peaks, do occur in the approximate temperature range from 300°C to 400°C. This paper describes the initial stages of an investigation of the physical properties associated with these peaks.

2. Experimental Method

Thermoluminescence measurements were carried out using a Dynatron Reader head modified by the addition of an iris to reduce black body radiation to the PM tube (EMI 6097S). The reader was used in conjunction with Harwell 2000 Series electronics. Accurate temperature control was achieved by using the research heat controller described by Gall and Mason[1]. A fresh batch of Harshaw TLD-700 LiF has been used throughout the investigation. A standard pre-annealing procedure of one hour at 400°C followed by one hour at 100°C to minimise fading of the TL signal has been adopted.

Emission spectra were produced on a spectrometer using a Bellingham and Stanley monochromator with a controlled rotating prism.

A Bausch and Lomb High Intensity Monochromator in conjunction with either a High Pressure or a Super Pressure Mercury lamp was used for optical bleaching experiments.

Sample irradiations were carried out using a 2000 Ci ^{60}Co gamma-ray source. All radiation doses refer to absorbed dose in tissue, measured in rads.

3. Results and Discussion

3.1 Dose dependence of TL

Figure 1 shows a typical thermoluminescent glow curve for annealed LiF irradiated to 10^4 rads of ^{60}Co gamma-rays. The glow curve is dominated by the familiar peak which occurs at about 210°C for a heating rate of 10°C/sec. Careful examination shows that other glow peaks do exist at higher temperatures and can be observed more easily if the recording sensitivity is increased after the temperature of the 210°C peak has been exceeded. Throughout these investigations we have separated the high temperature peaks from the 210°C peak by means of a double read-out cycle. Using a linear heating rate of 10°C/sec the first cycle was terminated at 240°C. A second run through this cycle at a higher recording sensitivity does not give any TL at the position of the 210°C peak, although a small response due to phosphorescence of the high temperature peaks is observed. The second cycle uses the same linear heating rate but does not terminate until a temperature of 370°C is reached. The recorder sensitivity is maintained at a higher level during the second cycle and the glow curve reveals a group of unresolved high temperature peaks (figure 2), referred to collectively as the "300°C" peak. The cut-off temperatures used during this procedure were set very accurately using the heat controller.

The form of the glow curve produced for the second cycle depends on the radiation dose received by the LiF. Figure 3 shows the glow curves for doses ranging from 1 rad to about 10^5 rads. For virgin LiF which has had a standard anneal, the "300°C" peak can be detected for doses of 5 rads or more. At lower doses the rising background is a prominent feature. For all these doses only a single maximum at 290°C is observed. The shape of the glow curve however suggests the presence of other unresolved peaks. The data in figure 3 indicates that as the dose increases the relative prominence of the high temperature peaks also increases until at 10^5 rads the ratio of the integrated intensity of the "300°C" peak to the 210°C peak is about 20%. The peak height ratio is also about 20%. Over the dose range examined the 290°C peak is always dominant and contributes 80-90% of the intensity of the unresolved "300°C" peak. No gross changes in the shape of the glow peak have been observed. This suggests that although the observed behaviour of the "300°C" peak reflects strongly the properties of the 290°C component, the other components do not behave in a very different manner.

Figure 4 shows the TL versus Dose curve for the "300°C" peak for the dose range 10 to about 10^5 rads. The results are plotted in the form of log (TL)versus log (Dose) and a linear response with dose is therefore indicated by the straight line at 45° to the axes. For purposes of comparison the figure includes TL v Dose results for the 210°C peak also. For both peaks the TL response is expressed relative to the response at 10 rads.

The curve for the 210°C peak follows a linear TL v Dose relationship up to about 1000 rads before becoming supralinear. A maximum occurs in the relationship at about 10^5 rads.

In contrast the TL v Dose curve for the "300°C" peak is always supralinear and does not approach a linear relationship over this dose range. The same behaviour occurs whether one plots integrated intensity or peak height.

The fact that the TL response of the "300°C" peak is supralinear with dose down to the smallest dose at which it is detectable suggests that the traps associated with the glow peak are actually being created by the radiation. In contrast the supralinearity of the 210°C peak above 1000 rads has been associated with the preferential filling of a second trap which competes for the available electrons[2].

The general treatment of thermoluminescence by Shiragai[3] takes account of the creation of traps by the radiation. The qualitative data for the "300°C" peak has been compared with the behaviour predicted by this theory. Since the peak at 290°C dominates throughout the dose range it is considered unlikely that any major changes or effects predicted by theory would be masked by the contributions of the other peak components. Assuming that the initial density of "300°C" traps is negligible and that the probability that a filled trap is emptied per unit time at the temperature of irradiation is also negligible, it may be shown that

$$n = ft - \frac{f}{kR} (1 - e^{-kD}) \qquad (1)$$

where n is the density of filled traps (proportional to TL)
f is the density of traps created per unit time (as a function of dose rate)
t is irradiation time
k is the fraction of empty traps filled with unit dose
R is the dose rate
D is the dose

Where $f = mR^a$ Shiragai considered the two cases

(1) $f = mR$
(2) $f = mR^2$ where m is a constant.

In the former case the theory predicts that TL is independent of dose rate and no threshold dose exists. At high doses the TL versus Dose response should be linear. In case (2) dose rate dependence is predicted and at high doses a linear variation of TL with dose is to be expected for constant dose rate. No threshold dose is to be expected.

Experimentally it has been shown that the "300°C" peak does not significantly vary in intensity with R for dose rates up to 1.5×10^3 rads/min.

For doses of less than 5 rads the "300°C" glow peak is not observed. This probably indicates a very small response at these doses rather than a genuine threshold. However, the fact that a non-linear TL response with dose has been observed for doses up to almost 10^5 rads indicates that either the Shiragai theory with $f = mR$ does not describe the behaviour of the "300°C" traps or else k in expression (1) is very small and higher doses are required to produce a linear dose response.

3.2 Emission Spectrum

It is interesting to note that whilst the 210°C peak has a maximum in the TL v Dose relationship at approximately 10^5 rads the "300°C" peak shows no sign of a maximum. This is to be considered in conjunction with the emission spectrum of each peak measured at a dose level of 10^4 rads. Intensities of the "300°C" emission peak were small, but within the experimental accuracy the spectra were identical. This implies that the recombination centres associated with each peak are also identical. It is therefore unlikely that the maximum in the TL v Dose curve for the 210°C peak is directly attributable to an insufficient supply of recombination centres.

3.3 Effect of Pre-irradiation annealing on the "300°C" peak

A great deal of work has been done on annealing procedures[4, 5] and it has been necessary to duplicate some of this work during the examination of the "300°C" peak.

Virgin ^{7}LiF was annealed at 450°C for one hour and cooled rapidly to room temperature. The powder was then divided into portions and annealed for one hour at its pre-irradiation temperature prior to receiving a dose of 200 rads Ra^{226} gamma-rays. The glow curves for any pre-irradiation temperature could contain any of the usual six glow peaks[2] of ^{7}LiF and also

the "300°C" peak. The relative intensity of the peaks varied widely with annealing temperature. Read-out consisted of the double cycle described in section 3.1.

Figure 5 compares the change in peak height of the 210°C and "300°C" peaks over the range of annealing temperatures. Similar behaviour is observed for the "300°C" peak if integrated intensity is considered rather than peak height.

Between 250°C and 450°C the pre-irradiation anneal has little significant effect on the peaks. Between 100°C and 250°C substantial changes are observed. As the annealing temperature is increased there is an initial decline in the 210°C peak, followed by an increase in magnitude between 150°C and 250°C. Conversely, the "300°C" peak shows an initial increase as the pre-annealing temperature increases, followed by a decrease in magnitude between 150°C and 250°C. These effects are associated with changes in the impurity distribution of the LiF during the period of anneal. It is thought that the traps associated with some of the glow peaks in TLD-LiF consist of combinations of impurity centres and crystal defects[6].

The preliminary anneal at 450°C which all samples received produced the equilibrium impurity distribution for that temperature in the LiF. This distribution was preserved during the subsequent rapid cool so that although the phosphor was at room temperature the impurity distribution was that which one would normally find at about 450°C. This situation is thermodynamically unstable and if the annealed LiF is subsequently held at some temperature other than 450°C then the equilibrium impurity distribution for that temperature will be approached. The time required for thermodynamic equilibrium to be attained at the new temperature decreases with increasing temperature.

Above 250°C the impurities and defects responsible for thermoluminescence in LiF come into thermodynamic equilibrium within the one hour period of anneal. The equilibrium distribution does not vary much between about 250°C and 450°C so that rapid cooling to room temperature after annealing results in similar "frozen-in" distributions for samples annealed in this range.

In the temperature region 100°C to 200°C the equilibrium distribution of defects and impurities is markedly different from that observed at say 450°C. As the annealing temperature is decreased from 250°C the added impurity atoms such as magnesium, have an increasing tendency to form agglomerates rather than distribute themselves as individual ions[7]. Annealing at temperatures within this range results in an approach to a new equilibrium distribution characteristic of the annealing temperature. The rate at which this proceeds depends upon the temperature.

As a result, traps which are characteristically associated with, for example, single impurity ions, are destroyed as the single ions form clusters of two, three or more. Any traps which are associated with several impurity ions are possibly unaffected until the later stages of clustering. These processes reflect themselves in observable changes in the glow pattern and probably cause complications in the isothermal decay of TL.

Samples annealed at 200°C almost achieve their equilibrium impurity distribution in one hour and this is not vastly different from the distribution at 450°C. In contrast the equilibrium distributions at 100°C and 150°C are significantly different from that at 450°C.

At 100°C the "frozen-in" distribution changes only slightly in one hour so that the corresponding changes in the 210°C and "300°C" peaks after the anneal are small.

At 150°C the approach to equilibrium from the "frozen-in" situation is more rapid and after one hour the changes in the 210°C and "300°C" peaks are very apparent.

The reduction in the intensity of the 210°C peak produced by annealing in the range 100°C–200°C indicates that it is adversely affected by clustering. The increase observed in the "300°C" peak may well be a consequence of clustering in another sense. The effect of clustering is to "purify" the LiF lattice but crystal defects freed of the association with impurity centres may also result. The increase in density of freed crystal defects may well be associated with the growth of the "300°C" peak.

In view of the increase in the "300°C" peak at 100°C and 150°C it was decided to systematically observe the effect on the peak of pre-irradiation annealing over extended periods. The results are shown in figures 6 and 7. After the pre-irradiation anneal the ^{7}LiF was dosed to 100 rads before read-out.

Holding the LiF at either temperature increases the subsequent TL response of the "300°C" peak. The growth of the "300°C" peak is accompanied by the decline of the 210°C TLD peak and the peaks at 120°C and 170°C.

At 100°C, figure 6, the 210°C peak shows little decrease after about three hours, whereas the 120°C and 170°C, which are undesirable for dosimetry purposes, have been reduced to 25% and 40% of their original intensity in this time.

At 150°C, figure 7, the 170°C and 210°C peaks decline very rapidly and the latter is almost completely destroyed within four hours.

The peak at 120°C shows an initial increase which results in a maximum after four or five hours. The effect has also been observed by Zimmerman et al.[4]

This behaviour supports the proposition that clustering destroys the traps associated with the peaks at 210°C, 170°C and 120°C and results in a simultaneous increase in "300°C" traps which seem to be associated with crystal defects.

At this stage the effects of post-irradiation annealing at 100°C and 150°C have not been examined but it would undoubtedly be a profitable line of study.

3.4 Trap Depths and Frequency Factors

The observation of the isothermal decay of thermoluminescence of the unresolved "300°C" peak at several temperatures has been used to determine the trap depths and frequency factors associated with the individual glow peaks. This technique in conjunction with another method of trap depth and frequency factor determination has revealed the complexity of the glow curve of LiF in this region and has produced some interesting problems of interpretation.

Figure 8 shows the decay of the continuously monitored thermoluminescence observed for irradiated LiF at a temperature of 270°C. The decay is plotted as log (TL) versus Time and each point represents the intensity (counts) observed during a fixed interval. The time intervals were varied between 30 seconds and 10 minutes depending on the isothermal temperature and the rate of decay. The error involved in effectively integrating over a portion of the decay curve during each interval is small when the overall time taken for the decay is considered. In the lower temperature region, at temperatures less than about 250°C, due to the lack of intensity, it was found necessary to use an alternative isothermal technique. In this method, the irradiated ^{7}LiF is isothermally annealed in an oven and aliquots removed for reading at regular intervals[4].

The curve of figure 8 consists of at least three exponential components which decay with half lives of 6 mins, 31.5 mins and 520 mins.

If the TL processes involved in the production of the components of the "300°C" peak follow first order kinetics then the following relation should be obeyed:

$$t_{\frac{1}{2}} = \frac{0.693}{S} \exp\ (E/kT)$$

A plot of log $t_{\frac{1}{2}}$ versus $\frac{1}{T}$ should then yield a straight line of slope E/k. However, figure 9 shows that for each of the components A, B and C the relation is by no means linear and that a marked change of slope occurs for each component in the region 270°C to 280°C. On either side of this region it is possible to fit two distinct straight lines which would give two widely differing values of E and S as shown in Table 1.

Table 1

Trap Depths and Frequency Factors by the Decay Method

Component	Low Temperature Region		High Temperature Region	
	E (eV)	S (sec^{-1})	E (eV)	S (sec^{-1})
A	~0.2	1	~2.6	4×10^{22}
B	0.57±0.30	70	3.2±0.2	1×10^{26}
C	0.72±0.10	100	4.2±0.4	4×10^{33}

The values of E and S for T < 275°C are of the same order as those determined by Hwang[8] in similar experiments involving high temperature glow peaks in LiF.

In view of this anomaly it was decided to determine E and S values for the components of the "300°C" peak by other available methods which do not depend upon isothermal decay. Methods involving glow peak shape are not appropriate for the unresolved "300°C" peak. The Heating Rate method as used by Hoogenstraten[9] provides an accurate means of determining E and S by observing the change in glow peak position (T^*), as the heating rate (β) is varied. A plot of $\log \frac{\beta}{T^{*2}}$ versus $\frac{1}{T^*}$ gives a straight line for first order kinetics, of slope ($-E/k$). S can be determined by extrapolation when $\frac{1}{T^*} = 0$. Since the peak centred on 290°C accounts for about 80-90% of the intensity of the unresolved "300°C" peak, observation of the change in its position with heating rate should give reasonably accurate values of E and S, even in the presence of the other peaks. Experimentally, it has been found that a straight line relation exists between $\log \frac{\beta}{T^{*2}}$ and $\frac{1}{T^*}$ for the 290°C peak. The values of E and S determined for the 290°C and the TLD peak at 210°C are included in Table 2.

Table 2

Trap Depths and Frequency Factors by the Heating Rate Method

Peak	E (eV)	S (sec^{-1})
"210°C"	1.14±0.05	2×10^{11}
290°C	1.33±0.12	3×10^{11}
Component C	1.67±0.14	5×10^{12}

In addition an estimate of the trap depth and frequency factor associated with component C of the decay experiment has been made by annealing out the other components at 290°C and then using the heating rate method on the remaining peak. The E and S values for the 210°C peak compare favourably with those determined by other workers[4, 10].

However, comparing the values of E and S, in tables 1 and 2, it is apparent that widely differing values are obtained for the "300°C" peak by the two methods.

Discrepancies of this sort in the determination of E and S for TLD LiF are not unknown. Gorbics et al.[11] reported values of E and S of 2.4 eV and 5×10^{23} sec^{-1} using a heating rate method while Zimmerman et al.[6] using an isothermal decay method dstermined E and S to be 1.25 eV and 5×10^{10} sec^{-1}. Both measurements were on the 210°C peak in TLD-100 LiF. Gorbics et al. suggested that the discrepancy might be due to more than one trap being associated with the glow peak or to a change in the mount of thermal quenching with heating rate. However in the present situation it seems more likely that the poor correlation is related to changes in the traps with temperature.

The extreme values of E and S (Table 1) determined by the decay method at temperatures below and above about 270°C lead us to believe that first order decay is modified at both high and low temperatures by the action of other processes.

Experimentally we have observed that at 300°C the trapping centres associated with the "300°C" peak are destroyed over a period of time. The rapid decrease in $t_{\frac{1}{2}}$ with temperature, for temperatures greater than 270°C, may well be the result of a trap destroying process occurring in parallel with the normal thermal emptying of traps. This assumes that the destroying process operates on filled traps as well as empty ones and that it increases with increasing temperature.

In the lower temperature range the decay mechanism will probably be affected by the increasing tendency for impurity atoms to cluster as the temperature approaches 200°C. For example, if it were assumed that as a result of impurity atoms becoming grouped together the filled "300°C" traps were emptied or destroyed then this would alter the rate of decay at a particular temperature. It seems reasonable to suggest that in the region of temperature below 200°C processes of some kind related to impurity migration will alter the isothermal decay kinetics and that the decays observed by ourselves and Hwang[8] in this region are not representative of a simple thermal emptying process.

One difficulty with these models is in reconciling the apparently mono-exponential final decays which occur throughout the tempeature range with the existence of more than one competing mechanism for decay.

3.5 Optical Bleaching and Repopulation of the "300°C" Peak

Many of the changes occurring in the glow pattern of irradiated LiF due to thermal or optical bleaching have been related to corresponding changes in the optical absorption spectrum. Peaks, which are sometimes unresolved, have been reported at wavelengths of 196, 205, 225, 250, 270, 310, 340 and 380 nm in the absorption spectrum of irradiated LiF. Heating for a short time at 200°C removes, almost completely, those peaks of wavelength greater than about 250 nm.

A similar heat treatment removes all the dosimetry glow peaks in LiF but does not remove the "300°C" peak. In view of these changes we have examined the effect of optical bleaching at 220 nm and 250 nm in irradiated LiF. Results of bleaching at 220 nm with phosphor previously irradiated to 100 rads show no marked changes in either the 210°C peak or the "300°C" peak compared with unbleached phosphor. This may be the result of the relatively low intensity available at this wavelength.

In contrast both the 210°C and "300°C" peaks were reduced by about 30% and 60% respectively after a bleach at 250 nm for one hour. No change in the shape of either peak was detected. The optical bleaching of the 210°C peak with 250 nm as well as 310 nm light has been reported previously[12].

It has previously been shown that the dosimetry peaks in irradiated LiF can be induced to reappear after normal read-out by suitable bleaching at 250 nm[12, 13, 14]. This has been associated with a corresponding reduction in the F-absorption band. Bleaching at this wavelength is thought to release electrons from F-centres distributed throughout the LiF. Some of the freed electrons then become re-trapped at the dosimetry traps and give rise to the reappearance of the dosimetry glow peaks. We have observed a similar reappearance of the "300°C" peak due to bleaching with 250 nm light.

Virgin ^{7}LiF was given a standard anneal and irradiated to about 10^{4} rads with ^{60}Co gamma-rays. Subsequently the 210°C and "300°C" peaks were removed by suitable thermal treatment. At this stage no peaks appeared in the glow pattern. After bleaching the phosphor for 30 mins with 250 nm light it was again read-out. Both the dosimetry peaks and the "300°C" peak reappeared in the glow pattern. The shape of the "300°C" peak was slightly changed by this procedure with the 290°C peak less prominent than it is after gamma-irradiation. This could be due to different nett repopulation of the component traps.

These results are strong evidence that the charge carriers associated with the "300°C" peak are similar to those associated with the 210°C peak and that yet another deep trap which bleaches with 250 nm light is responsible for the repopulation of both peaks. This deep trap has previously been assumed to be the F-centre. Although the "300°C" traps bleach with 250 nm light the above experiment clearly distinguishes them from the deep trap. On the basis of the optical bleaching results above it is not possible to say unequivocally that the deep trap is actually the F-centre. It is equally possible for "300°C" traps to provide electrons for repopulation during 250 nm bleaching with a consequent reduction in the F-band absorption. However, the fact that the "300°C" traps are so easily dissociated by annealing at temperatures of even 300°C seems to suggest that they are more complex defects than the F-centre.

Conclusions

The "300°C" TL glow peak observed in ^{7}LiF is composed of at least three unresolved components. While it is recognised that the results for the "300°C" peak usually reflect the behaviour of the dominant peak at 290°C it has been possible to draw conclusions about the other components. The shape of the composite peak does not change substantially over the dose range 0-10^{5} rads suggesting that the component peaks all grow in a roughly similar manner with increasing dose. The TL v Dose curve for the "300°C" peak is supralinear over the whole range examined. It is postulated that the associated trapping centres are created by the radiation. The traps are visualised as being defects in the host (LiF) lattice caused by radiation damage. In an unirradiated phosphor some defects of this type will be present but most of them will be associated with impurity atoms. Centres of this sort are thought to be associated with other glow peaks in TLD-LiF.

However, if the phosphor is held at a temperature of about 100°C the dispersed impurity ions tend to form clusters. As a result of this process the traps which give rise to the dosimetry peaks at 120°C, 170°C and 210°C, dissociate and the impurity ions and crystal defects become segregated. Consequently, the density of "300°C" traps is increased resulting in an increase in TL response.

Although the "300°C" peak is not normally detectable for doses of less than 5 rads, it is unlikely that any real threshold dose exists. In contrast the high temperature peaks discussed by Hwang[8] in TLD-100 LiF seemed to have a threshold dose at about 10^3 rads. Hwang also reports that in the range 10^3-10^4 rads the TL response of the 370°C and 430°C peaks is linear with dose. The "300°C" peak has a supralinear TL variation with dose which is independent of dose rate over a wide range. Further observations at higher dose levels may show that the TL response of the "300°C" peak does become linear. In this case the behaviour of the peak would fit the general model of thermoluminescence proposed by Shiragai provided one assumed that the initial density of "300°C" traps was negligible and no significant loss of trapped electrons occurred at ambient temperature.

It has been established that the charge carriers associated with the "300°C" glow peak are similar to those associated with the 210°C dosimetry peak and another deeper trap which like the "300°C" traps is bleached by 250 nm light. It seems probable that either "300°C" traps or the deeper traps are F-centres. The carriers are therefore almost certainly electrons. The fact that the "300°C" peak is destroyed by annealing at temperatures as low as 300°C suggests that the associated traps are more complex than the F-centre. However it is desirable that more corroborative data from optical absorption and bleaching experiments is obtained.

The isothermal decay of the "300°C" peak has been closely fitted by three exponential curves. However a plot of $\log t_{\frac{1}{2}}$ v $\frac{1}{T}$ does not give the straight line expected for first order kinetics. It was found possible to fit <u>two</u> straight lines to the curve above and below the region 270°C-280°C for each component of the isothermal decay curve. Values of E and S calculated from the straight line fit in the low temperature region are of the same order of magnitude as those determined by Hwang[8] for the 370°C and 430°C peaks. The values calculated from the straight line fit to the high temperature region are quite different. However, both high and low temperature values seem to be unreasonable compared with accepted values for other peaks in TLD LiF. It is possible that these results could be explained using first order kinetics if it is assumed that the decays are modified by temperature instability of the associated trapping centres above about 270°C. Below this region it seems possible that the onset of impurity agglomeration could be indirectly responsible for a decrease in the observed values of $t_{\frac{1}{2}}$ particularly at the lower temperatures near to 200°C.

Acknowledgements

The work reported here is part of the technical development programme of the National Radiological Protection Board. The authors are grateful to Mr. N. T. Harrison for continual encouragement and advice; to Miss Anne Wotherspoon for her patient help during the preparation of the manuscript; to Mr. A. Gall and Mr. A. F. McWhirter for their admirable technical assistance and to Miss Elizabeth Gardner and Mrs. Yung-Shiang Wang for experimental assistance.

References

1. A. Gall and E. W. Mason, Phys. Med. Biol. 14, 4, 661-664 (1969)

2. J. R. Cameron, N. Suntheralingam and G. N. Kenney, Thermoluminescent Dosimetry (Wisconsin: University Press 1968)

3. A. Shiragai, Jap. J. Appl. Phys. 7, 9, 1101-1104 (1968)

4. D. W. Zimmerman, C. R. Rhyner and J. R. Cameron, Health Physics, 12, 525-531 (1966)

5. A. M. Harris and J. H. Jackson, Health Physics, 15, 457-461 (1968)

6. E. W. Claffy, Proc. Int. Conf. Luminescence Dosimetry (1965)

7. W. G. Johnston, J. Appl. Phys. 33, 2050 (1962)

8. F. S. W. Hwang, J. Phys. D. Appl. Phys. 4, 598-607 (1971)

9. W. Hoogenstraten, Phillips Res. Repts. 13, 515-693 (1958)

10. G. A. M. Webb, Brit. J. Appl. Phys. 18, 7-11 (1967)

11. S. G. Gorbics, A. E. Nash and F. H. Attix, Int. J. Appl. Rad. and Isotopes, 20, 843-852 (1969)

12. M. R. Mayhugh, R. W. Christy and N.W. Johnson, Submitted to J. Appl. Phys. (1970)

13. E. W. Mason, Phys. Med. Biol. 16, No. 2, 303-310 (1971)

14. E. B. Podjorsak and J. R. Cameron, TLD Progress Report for USAEC COO-1105-161 (1970)

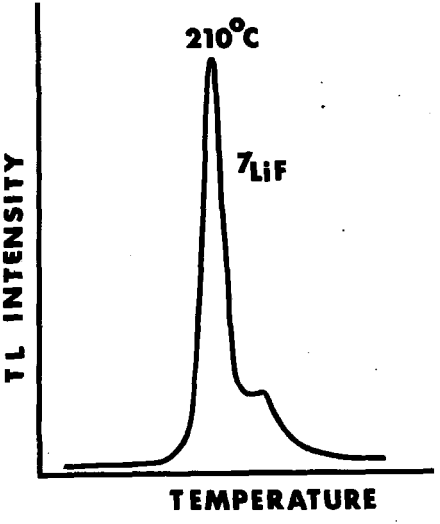

Figure 1. Thermoluminescent Glow Curve of TLD-700 LiF irradiated to 10^4 rads.

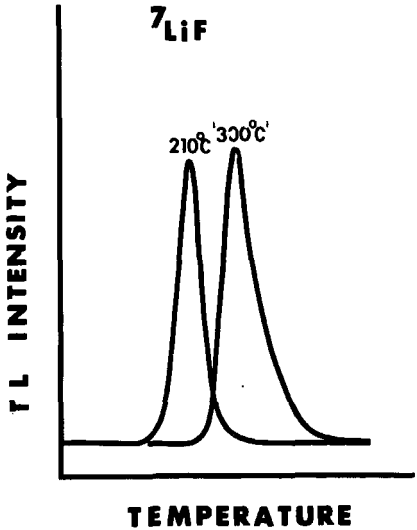

Figure 2. The 210°C and "300°C" glow peaks resolved by a double heating cycle. The scale sensitivity is increased by a factor of 10 for the "300°C" peak. Dose = 10^4 rads.

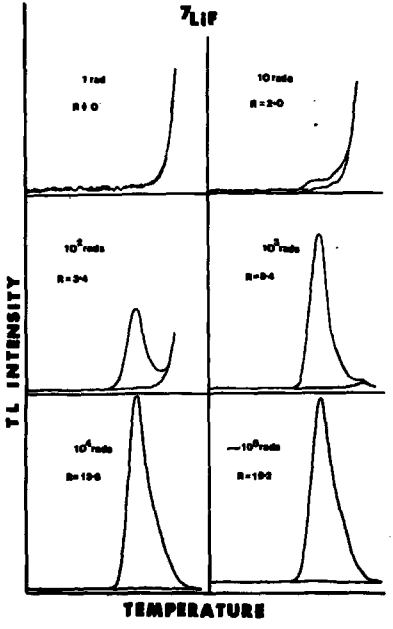

Figure 3. The appearance of the "300°C" glow peak at different dose levels.

$$R = \frac{\text{Intensity of "300°C" peak}}{\text{Intensity of 210°C peak}} \%$$

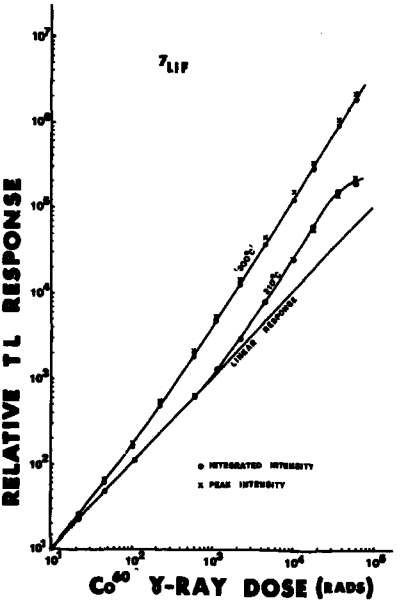

Figure 4. Variation of the normalised intensity of the 210°C and "300°C" peaks with dose.

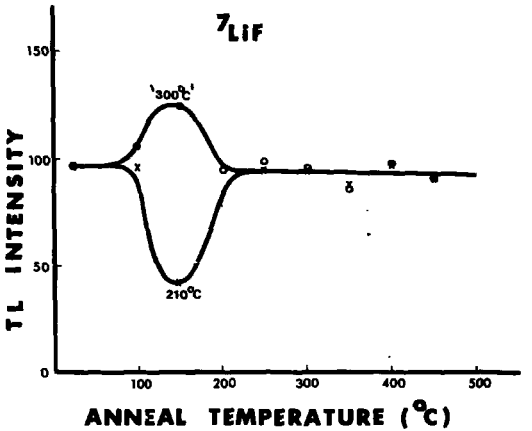

Figure 5. Variation in peak height of the 210°C and "300°C" peaks with pre-irradiation anneal temperature. Samples were annealed for one hour prior to receiving a dose of 200 rads.

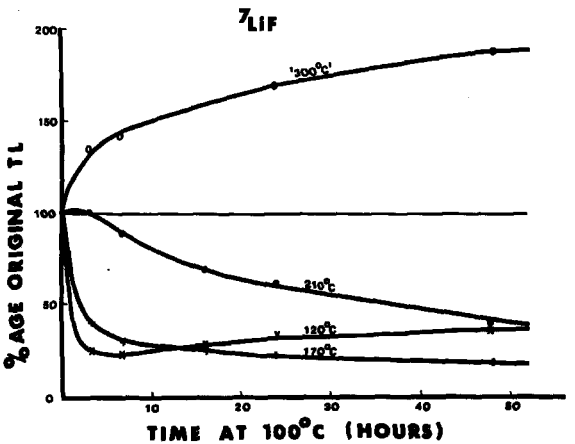

Figure 6. Changes in the peak heights of 120°C, 170°C, 210°C and "300°C" glow peaks after pre-irradiation annealing at 100°C for various times.

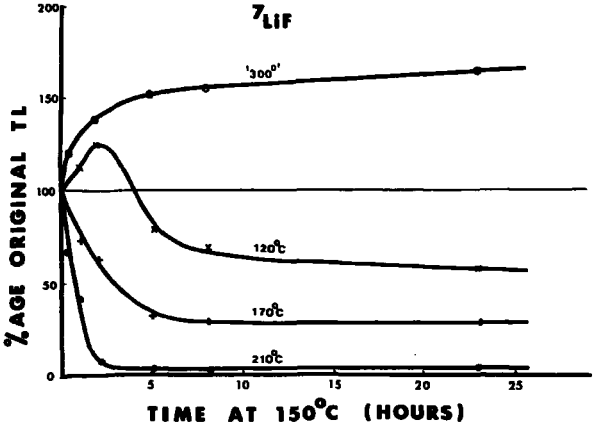

Figure 7. Changes in the peak heights of 120°C, 170°C, 210°C and "300°C" glow peaks after pre-irradiation annealing at 150°C for various times.

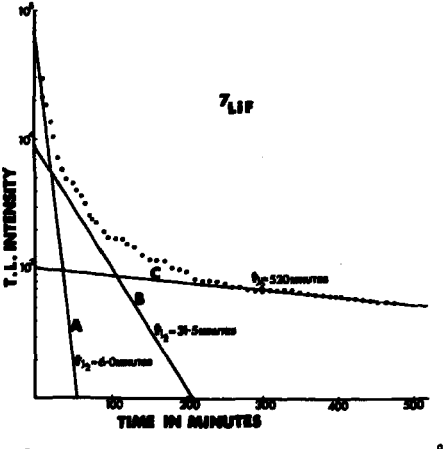

Figure 8. Isothermal Decay of TL Intensity "300°C" peak with time at 270°C.

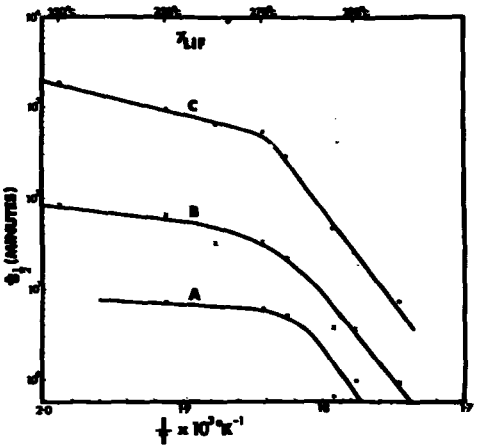

Figure 9. Variation of log $t_{\frac{1}{2}}$ with $\frac{1}{T}$ for components A, B and C of the "300°C" peak.

Stoebe

Could you clarify your annealing procedure?

Mason

Annealing in air; cooling on a block of metal.

Stoebe

Your results regarding the growth of the 300°C peak at the expense of the 210°C peak could certainly indicate a defect (trap) agglomeration process, such as dimers or trimers (for the 210°C peak) attracting more impurity-vacancy dipoles to produce a larger defect complex. Further experiments, such as annealing and quenching studies, could help to verify such a model. Our observation is that the determination of activation energies and frequency factors does not particularly help in determining the processes going on in the material.

Shearer

Perhaps some of the discrepancies could be removed from the whole area of kinetic studies if the possibility of a distribution in activation energies was taken more seriously instead of resolving all composite curves into enough exponentials to give a fit.

Mason

This may be, in general, a legitimate comment. In the present case we have been able to show, by suitable thermal bleaching, that peaks A and C do in fact exist. The exponential fit for the component B was found to be good in each case. The fit of three exponentials to the decay curve is therefore considered to be well justified.

Niewiadomski

Were your samples irradiated only with Co-60 gamma radiation? Did you measure the influence of radiation energy on the behaviour of the high-temperature peaks?

Mason

Yes, our samples were only irradiated with Co-60 gamma rays. It would obviously be instructive to examine the effect of radiation energy on the high temperature peaks, and it is our intention to do so. In particular it will be very interesting to compare the energy dependence of the 300°C thermoluminescence with any corresponding changes in the F-band absorption. Grant and Jones (2nd International Conference on Luminescence Dosimetry) reported that no significant difference in the growth of the F-band absorption with increasing dose (in the range $0-1.2\times10^{4}$ rads) was observed between 4 keV X-rays and Co-60 gamma rays.

Possible Elimination of the Annealing Cycle for Thermoluminescent LiF

by

Geoffrey A. M. Webb and Howard P. Phykitt
Teledyne Isotopes, Westwood, N.J.

Abstract

The standard annealing cycle in thermoluminescent Lithium Fluoride has three components. First is maintenance at a high temperature, followed by cooling to 80°C and maintenance for 24 hours. An attempt has been made to replace all these components by modifying the heating cycle during readout. The modified cycle has four stages. Pre-heat for 12 seconds; Readout at a fixed temperature for a further 12 seconds; Anneal at a high temperature for 18 seconds; Cool rapidly and reproducibly in a nitrogen gas stream. Integration of signal is carried out only during Readout, the other three stages are solely for annealing. The high temperature anneal zeroes the dosimeters, the cooling is more reproducible and the pre-heat bleaches out the low temperature peaks before integration commences.

A new readout instrument based on these principles is described. The high temperature anneal leaves less than 0.03% residual signal. The reproducible cool rate brings sensitivities of different batches of dosimeters within ± 5% by cycling once through the readout cycle. The performance of the pre-heat has been studied by glow curve analysis and by fading studies. The results of 100 re-use cycles on LiF dosimeters are given, together with results for other phosphors.

Introduction

The use and application of thermoluminescence dosimetry is now established. Although Lithium Fluoride is the most commonly used phosphor, it brings with it in addition to its basic simplicity a number of unusual problems and a troublesome annealing procedure before it can be re-used.

We have attempted to carry out two inter-related tasks. One to design a readout instrument which will minimize the problems involved in using TLD and the other to suggest procedures of use to assist in that goal. A stated objective of the design was the elimination of the long annealing procedure necessary for re-use of LiF.

This paper describes the design philosophy of the reader (Teledyne Isotopes Model TLD-7300) particularly involving the heating cycle; the problems it was intended to solve and evaluates its success in solving these problems.

2. The "Standard" Annealing Cycle for LiF

TLD was put into use as a dosimetry technique long before satisfactory theoretical explanations of the havior of various phosphors was available. As a result certain procedures which seemed necessary to obtain good results assumed an aura of "magic". A good example is the so-called "standard" anneal discovered by Cameron's group at the University of Wisconsin.[1] This procedure was followed for years before substantial justification for it was available and the significance of the various parameters explained. Even now a completely satisfactory theoretical explanation for all facets of the behavior of LiF is not agreed upon, however further work[2,3] has produced the phenomenological explanation given below for the effects of the different portions of the cycle.

2.1 High Temperature Anneal

Originally set by Cameron[1] as "1-1/2 hours at 400°C,"but generally reduced to 1 hour at 400°C in practice, this portion of the procedure serves the basic purpose of erasing the remaining signal due to prior irradiations. Since the main thermoluminescence glow peak in LiF is at about 200°C and the half life of trapped electrons giving rise to this peak is approximately 0.1 secs at 300°C it was obvious very early that the temperature time integral could be reduced for normal purposes. On the introduction of the phosphor-Teflon dosimeter[4] with its attendant convenience this procedure was reduced to "several hours at 300°C". For most purposes the 300°C anneal is quite adequate and it will remove signal from prior exposure in the Krad region with no trouble.

The 400°C anneal, however, also accomplishes another purpose in LiF which is to remove the retained sensitivity increase from prior irradiation into the superlinear region[5] above about 1000 R. The removal of this increased sensitivity is a function of the temperature and time of the anneal and is further complicated by radiation damage effects above 50,000 R[6]. This means in practice that dosimeters with large cumulative exposure histories may not always be restored to their original sensitivities even by

The "standard" high temperature anneal. It may be noted that the stability of the increased sensitivity is different in other phosphors, for example in $Li_2B_4O_7$:Mn the enhanced sensitivity is normally removed in the readout cycle.

A further purpose served by the high temperature anneal is to release the trap distribution in the crystal from that imposed by any previous diffusion process (low temperature anneal). For this 300°C seems as effective as 400°C.

An unexpected effect of the 400°C anneal was found by Martensson[7] who studied the effect of high temperature annealing on the precision of measurement. He found that annealing times and high annealing temperatures both increased the standard deviation of measurements. He recommended an optimum annealing procedure of a few seconds at 300°C. This conclusion is in direct contradiction to the recommendation of Harris and Jackson[3] who concluded that "60 minutes at 500°C" gave the best ratio of sensitivity of the main peak to background for LiF. However the latter authors did not work with dosimeters and any standard deviation increase is not detectable with loose powders. Furthermore these authors base this conclusion on the existence of a very much higher background level in unirradiated phosphor following 300°C anneal than following 400°C anneal. The present authors have been unable to reproduce this background increase in a number of batches of LiF phosphor, all of which gave effective net backgrounds of between 10 - 15 mR equivalent (with infrared, noise and other components subtracted) when readout on a commercial reader with Nitrogen flow.

2.2 Cooling from High Temperature to Low Temperature

It was not originally realized that the cooling rate from the high temperature anneal had a significant effect on the subsequent sensitivity of LiF phosphor. This has been studied by various groups[2,3] with substantial agreement that rapid cooling gives an increase in the overall sensitivity in all peaks (See Fig.1). Above a cooling rate of about 100°C/minute the heights of peaks 4 and 5 remain substantially constant but there is a continued increase in the relative heights of the low temperature peaks. The increase in sensitivity found between the cooling rate for a typical oven (5°C/minute) and a fast cool (greater than 100°C/minute) is about 30% for peak 5. The slope of the sensitivity versus cooling rate curve is greatest in the region where most ovens operate and partially accounts for the sensitivity differences generally observed when dosimeters are annealed in an oven.

2.3 Low Temperature Anneal

This portion of the standard anneal was originally prescribed as "24 hours at 80°C" and has stood the test of time and many investigations well. The best study[2] confirmed that 80°C is indeed a specific temperature and that for example a shorter time at a higher temperature does not produce the same effect. The effect produced by this low temperature anneal is a redistribution of the trapping centers in LiF to favour the high temperature traps used in dosimetry. It has been shown that the time of 24 hours is not critical and any convenient time between 10 and 50 hours is suitable[3]. This procedure again applies only to LiF, similar effects have not been found with other phosphors, for example an 80° anneal has no effect on the low temperature peak in Lithium Borate (Mn).

An alternate to the 80° pre-irradiation anneal has long been recognized in a post-irradiation but pre-readout anneal at 80°C or 100°C for 10-20 minutes. This has no effect on the trap distribution but merely empties the low temperature and more unstable traps before readout. Its principal disadvantage was that it could not be carried out in bulk for a large number of dosimeters but had to be given to a few at a time after their irradiation.

3. The New Anneal Cycle in the 7300 Reader

3.1 Description of the Temperature Control System

In order to provide very reliable long term control over temperature an infra-red detector was chosen as the temperature monitoring element. The sample carriers are removable nichrome elements similar to those used for many years in earlier commercial readout instruments (Teledyne Isotopes Model 7100; Con-Rad Model 5100) except that they are blackened on the underside to increase their infra-red emissivity. The detector is mounted under an Irtran filter and averages the temperature over about a 1 cm^2 area of the underside of the element immediately below the dosimeter. A second matched detector is mounted in the same enclosure to compensate for changes in ambient temperature and an electronic compensating circuit is also employed. The detector output is used in a feedback manner to control the element temperature. The major advantages of the infra-red system are increased reliability as there are no moving parts, elimination of contact and wear problems in thermocouples, faster response speed, no local cooling of the element at the point where the thermocouple touches and averageing of temperature over an area comparable with that of the dosimeter.

The system is controlled by a solid state sequencer which takes the temperature through three sequential "ramp and hold" cycles followed by a cooling period. The heating rate and times are fixed in production readers but the hold temperatures may all be varied between 25 - 350°C. Since control is by temperature directly, the same temperature is used for all physical forms of dosimeter including phosphor-Teflon discs, microrods, extrusions etc.

3.2 The New Anneal Cycle

The temperature cycle found to be optimum is shown in Fig. 2 This consists of:

1. Pre-Heat - Temperature raised to 135°C and held for a total of 12 seconds

2. Readout - Temperature is raised linearly to the predetermined readout temperature (270°C for LiF) and held for a total of 12 seconds.

3. Anneal - (Optional) Temperature is raised to 305°C and held for 20 seconds

4. Cool - Heating is ceased and element is allowed to cool for 18 seconds in Nitrogen flow to 120°C

Integration of signal is carried out only during stage 2, the other three stages are solely for annealing purposes in an attempt to replace the "standard" annealing

Stage 3. replaces the high temperature annealing (Section 2.1)

Stage 4. ensures a fast reproducible cooling rate (Section 2.2)

Stage 1. replaces the low temperature annealing (Section 2.3)

4. Ultra-Violet Light Effects

Before proceeding to describe the experimental justification for the new anneal cycle described above, one other contributing phenomenum needs to be examined. This is the response of LiF to Ultra-Violet light. There is considerable data already in the literature [8,9,10] and several other papers at the present meeting are concerned with the same subject.

Although there are some discrepancies which can possibly be explained by differences in phosphors, thermal and radiation histories, types of readout instruments etc. we will attempt to extract some general points.

In TLD Grade LiF which has had the "Standard" anneal and which has not been irradiated the sensitivity to U-V light is generally small (less than 20 mR equivalent).

In LiF which has been cooled from a high temperature reasonably fast and not given the 80° anneal there is a sensitivity to U-V light which may be as high as several hundred mR equivalent. Practically all of this sensitivity (called intrinsive sensitivity by Mason[9]) is in a low temperature peak at 80-90°C. The degree to which any given experiment would observe this peak would depend on the time between U-V irradiation and readout, U-V intensity and whether the reader has any "pre-heat" or lower temperature integration limit.

Mason[9] also observed an "induced" U-V response in the high temperature peaks following gamma irradiation when the U-V exposure is given after readout with no intervening annealing. He attributes this to transfer from a deeper trap to the normal dosimetry traps of electrons not released in readout. Using his particular readout technique, U-V source and U-V exposure time he found a response of the order of 1% of the previous gamma exposure. Observation of this would be critically dependent on the previous irradiation and annealing history, readout temperatures used and U-V intensity.

In attempting to duplicate the "standard" anneal the problem of minimizing the U-V sensitivity has been one of the most difficult to overcome.

5. Selection of Anneal Temperature

Based on the suggestion [7] that a 300°C anneal for the minimum time necessary to empty all filled traps is optimum and since phosphor-Teflon dosimeters will not withstand temperatures above 327°C without affecting sensitivity the anneal temperature was selected as a nominal 305°C. In practice this may vary between 300 - 310°C.

Table 1 shows the residual signal remaining after a 20 second anneal at different anneal temperatures. The choice of 20 seconds as the time is determined by practical considerations.

TABLE 1 Residual signal remaining after anneal for 20 seconds at different temperatures for LiF - Teflon discs 12.7 mm dia x 0.4 mm thick

Anneal Temperature °C	Exposure	500,000 mR	100,000 mR	50,000 mR
300		0.1%	0.05%	0.03%
310		0.05%	0.02%	<0.02%
320		0.03%	0.01%	<0.02%

It will be seen that after an exposure of 50,000 mR, the residual signal is less than 15 mR in the worst case.

Results for other dosimeters are similar, but loose powder is less efficiently annealed if a 45 mg aliquot is used.

It is of interest that the anneal becomes less efficient as the dose is increased. This is attributable to the growth of higher temperature glow peaks at these doses.

5.1 Re-useable or Disposable Dosimeters

As part of the design philosophy of the self-annealing reader we have attempted to formalise the use of "disposable" as opposed to "re-usable" dosimeters.

If measurements are predominantly in the "Health Physics" range (1-10,000 mR) with occasional excursions to 1,000,000 mR, then a high sensitivity dosimeter must be used such as our LiF-Teflon disc 12.7 mm dia x 0.4 mm thick loaded 30% weight LiF. This contains about 30 mg LiF and is correspondingly high in cost. When used with anneal this may be re-used indefinitely in this range provided dosimeters above 10,000 mR are discarded or re-read. Similar reasoning applies to other relatively expensive dosimeters containing the large quantities of phosphor needed for maximum sensitivity.

If measurements are in the "Clinical" range (1 - 100,000 R) then there is no need for the sensitivity obtainable with the high phosphor content dosimeter. Consequently a dosimeter such as our small LiF-Teflon disc 8 mm dia x 0.5 mm thick loaded 5% by weight LiF may be used. This contains only 3 mg LiF and is cheap enough to use once and throw away. This is even more the case with the extruded LiF-Teflon microrod containing only 0.4 mg phosphor.

The advantages of treating high level dosimeters as disposable are many. The cost of a high-temperature annealing oven is saved (one good oven costs the same as 10,000 microrods). The problem of retained superlinearity is eliminated. The problem of radiation damage is eliminated. The problem of re-calibration after an oven annealing is eliminated. The problem of induced U-V sensitivity is eliminated.

We are thus recommending as part of the design philosophy of the self-annealing reader that the following dosimeters be used with the anneal cycle and re-used.

Large Phosphor-Teflon discs loaded 30% by weight with phosphor

Extruded or Hot Pressed Dosimeters

Loose Powders

The following dosimeters should be used without the anneal cycle for high level measurements and treated as disposable

Small Phosphor-Teflon Discs loaded 5% by weight with phosphor

Phosphor-Teflon Micro-rods loaded 5% by weight with phosphor

5.2 The Cooling Period

The cooling is allowed to follow the natural curve shown in Fig. 2. Some of the heat is removed by the Nitrogen flow but the majority flows through the Berylluim Copper current contacts which have a very large thermal capacity. The cooling rate is unaffected by changes of the nitrogen flow rate of $\pm$ 3 C.F.H. from the nominal flow rate of 6 C.F.H. The final temperature after a 20 second cooling period is 110 $\pm$ 10°C. The mean cooling rate is about 10°C/second with a rate of 25°C/second from 300°C to 200°C.

The reproducibility and speed of cooling result in maximum sensitivity for re-use and no change in sensitivity among groups of dosimeters or in a single dosimeter over a number of re-use cycles. (See Section 9)

The glow curve obtained on a slow linear heating after anneal and cooling in the 7300 is as shown in Fig. 1.

6. Selection of Preset Readout Temperature for LiF

The basic principle given earlier[11] of minimizing the residual after readout still applies but in this case the long hold at the readout temperature makes possible very efficient release of trapped electrons at temperatures well below those giving incandescence. Table 2 shows the second reading from LiF-Teflon disc dosimeters given 100,000 mR, read once and allowed to cool before re-reading for different readout temperatures. Also shown are the readings from unirradiated dosimeters expressed in mR equivalent. These were taken with no background subtraction in the reader so they include dark current, noise, incandescence emission, background radiation and spurious luminescence. The pre-heat temperature used in these measurements was 135°C but the dosimeters had been given a standard anneal with 19 hours at 80°C before irradiation to minimize the contribution from low temperature peaks. This is necessary in this procedure to avoid confusing the results

TABLE 2. Residual and Unirradiated Dosimeter Readings after 12 seconds at different readout temperatures for LiF-Teflon discs.

Readout Hold Temperature °C	2nd Reading %	Unirradiated Dosimeter Rdg. mR Equivalent.
230	5.4	14
250	0.70	15
265	0.48	16
275	0.35	18
290	0.28	45
330 (Dosimeter Melted)	0.22	66

It is apparent from the table that the relatively simple criterion of looking for a minimum in the second readings is not sufficient, as this is at a very high temperature and is accompanied by an increase in the background.

The temperature selected was 270 $\pm$ 5°C as it appears that this gives efficient readout with a relatively low unirradiated dosimeters reading. Also slight changes from the setting did not appear to affect the performance greatly in this region. The 270°C setting was also found to give less than 1% residual and relatively low backgrounds for all other LiF-Teflon dosimeters including thin dosimeters and microrods. The instrument has preset temperatures for standard LiF-Teflon dosimeters and it is this preset readout temperature that is set to 270°C. In manual mode the operator has full control of the readout temperature from 150-350°C.

7. Selection of Pre-heat Temperature

Selection of the optimum pre-heat temperature is the area in which the greatest conflict of requirements has been experienced. This is because the pre-heat is trying to eliminate the low temperature peaks 1, 2, and 3 while leaving untouched peaks 4 and 5. Whether this is even theoretically possible is open to question and in practice it is extremely difficult. In addition there is the further complication of the sensitivity to U-V light which is also affected by the pre-heat temperature. An additional effect which was not anticipated was the (indirect) effect of pre-heat temperature on precision.

The pre-heat time was fixed at 12 seconds as it was felt this was the longest time tolerable operationally.

7.1 Effect of Pre-heat on Main Peak (5) in LiF.

In order to establish the maximum permissible pre-heat temperature a direct experiment was carried out to determine the amount of bleaching of the main peak at different pre-heat temperatures. In order to do this the low temperature peaks has to be eliminated so a number of LiF-Teflon dosimeters were given the standard oven anneal, irradiated to 1000 mR and then any

slight low temperature peaks were removed by treatment in an oven for 15 mins. at 80°C before reading.

The results are shown in Fig. 3 which illustrates the reading obtained in the readout portion of the cycle following pre-heat at different temperatures. A separate counter was used to check the counts obtained in the pre-heat cycle and verify that the total of (preheat + readout) remained constant.

The result obtained showed that the pre-heat started to bleach the main peaks earlier than had been predicted. The dotted curve shows the calculated result for peaks 4 and 5 assuming classical Randoll-Wilkins[12] theory which gives

$$S_R = 100. \exp -(s.t.\exp - (E/kT))$$

where S_R is the % of signal remaining after the pre-heat

E is the trap depth

s is the frequency factor

T is the pre-heat temperature

t is the pre-heat time

assuming[2] $E = 1.25$ eV; $s = 8 \times 10^{11}$ sec^{-1} for peak 5;

$E = 1.19$ eV; $s = 10^{12}$ sec^{-1} for peak 4.

Also assumed in the calculation is a 10°C overshoot for a time of 2 seconds which is in reasonable agreement with that observed. No explanation for the discrepancy in the curve shapes is available at this time.

The practical result of Fig. 3, however, is that to remove less than 10% of the main peaks the pre-heat temperature must be set at less than 150°C.

7.2 Effect of Pre-heat on Low Temperature Peaks.

This is more difficult to isolate and study than the effect on the high temperature peaks discussed in 7.1 as the low temperature peak cannot be studied in the absence of the high temperature peaks. However three methods of evaluation were used.

7.2.1 Glow Curve Analysis

The first and most direct method is the observation of the glow curve as the dosimeter is heated through the pre-heat and subsequent readout cycle. Fig. 4 shows a glow curve, with the temperature-time curve reproduced for comparison, of a LiF-Teflon disc dosimeter previously cycled through the instrument anneal cycle several times and given 100R immediately before readout. One of the difficulties of glow curve analysis with this type of heating curve is apparent from the Figure. Since the maximum temperature in the pre-heat period (caused by overshoot) is after about 4 seconds this is where the maximum light emission occurs, almost irrespective of the actual glow curve shape (Fig. 1) After this maximum the light output falls, but not to zero in LiF

because of the wide distribution of peaks particularly 3 and 4. Folowing the preheat a relatively well shaped peak is obtained.

It is of interest to compare the curve for LiF shown in Fig. 4 with the curve for Lithium Borate shown in Fig. 5. This was taken with the same parameters, but Lithium Borate has two well separated peaks and in this case the pre-heat is able to completely eliminate the low temperature peak without seriously affecting the main peak, as shown by the light output falling to zero at the end of the pre-heat.

7.2.2 Integral Reading Analysis

A more indirect but possibly more useful method is to compare the total integrated reading in the readout portion of the cycle for dosimeters given the same dose but in some of which the low temperature peaks have been eliminated by a pre-anneal at 80°C. The procedure was to cycle a number of LiF-Teflon disc dosimeters through the instrument anneal cycle to ensure they all had the same intrinsic sensitivity due to cooling rate. Half of these were then given an 80°C anneal for 24 hours to eliminate the low temperature traps. They were then all irradiated to 100R and read at different pre-heat temperatures. The counts lost in the pre-heat were monitored in a separate counter as a check. The results are shown in Table 3.

TABLE 3 Counts in Pre-heat and Readout cycle at different pre-heat temperatures for dosimeters with and without prior 80°C anneal.

Pre-heat Temp. °C		90	120	135	145
With 80° Anneal	Reading	106.7	100.4	98.3	88.7
	Pre-heat	4.2	10.7	9.7	15.8
No 80°C Anneal	Reading	126.3	104.2	96.8	80.1
	Pre-heat	27.3	43.0	57.1	72.2

The results suggest that at a pre-heat temperature of 120-135°C the pre-heat is removing all the low temperature peaks and leaving the same proportion of the high temperature peaks independent of the magnitude of the low temperature peaks.

7.2.3 U-V Removal Analysis

In order to test the efficiency of the pre-heat in removal of the intrinsic U-V sensitivity (See section 4) a number of LiF-Teflon disc dosimeters were cycled through the anneal in the instrument several times without irradiation. They were then exposed at 3" from a high intensity laboratory fluorescent light for 15 minutes before reading (this appeared to saturate the effect for this source, no increase in signal was found on increasing the time to 30 min-

utes). Figure 6 shows the net induced signal remaining in the readout cycle due to the U-V exposure (the readings from control dosimeters stored in darkness were subtracted).

The curve demonstrates that a low pre-heat is effective in removing most of the induced effect but that even a very high pre-heat does not eliminate all of the so-called "intrinsic" sensitivity. This does not agree with Mason's conclusion[9] that the intrinsic sensitivity is in a peak at 90°C but on the other hand examination of his curves shows a distinct tail as high as 200-300°C for the peak labelled 90°C.

The practical result is that it is not possible to remove all the U-V sensitivity by a pre-heat but the highest pre-heat temperature gives the best removal.

Since the induced U-V sensitivity after high-level irradiation is in the main dosimetry peak[9] it is obviously impossible to do anything in the pre-heat to affect this. However it should be noted that the anneal cycle will make this effect considerably less marked than that observed after only a readout cycle.

7.2.4 Determination of Pre-heat Temperature

Although the requirements of Sections 7.2.1 - 7.2.3 are somewhat conflicting, there is a range of pre-heat temperatures which satisfy most of the criteria. This range is around 125-140°C. A nominal temperature of 135°C has been chosen as the best compromise. This temperature was used in all subsequent experiments, especially the fading tests which provide another direct proof of the efficiency of the pre-heat cycle.

8. Fading Tests

A direct test of the efficiency of the pre-heat cycle in removing the low temperature peaks is by measuring the fading after irradiation, since a reduction of fading is the reason for removal of these peaks.

The fading was examined directly at room temperature and in a simulated experiment of storage at a high temperature. The procedure was to cycle LiF-Teflon dosimeters through the instrument to anneal them and then irradiate to 100 R and store in darkness for different periods of time before readout. In order to eliminate the effects of readout instrument changes the irradiations were staggered so that all readouts were performed at one session.

The room temperature results showed a fading of 5-10% over 1 week relative to readout 10 minutes after irradiation and the simulated high temperature experiment confirmed this with 10-15% fading after 1 month (simulated) and 30% after 2 years (simulated). This is more than was observed by Mason[9] in a similar experiment with powder using a 140°C preheat. He found no fading (within $\pm$ 3%) over 5 weeks storage at room temperature. This and the results in Table 3 suggest that the fading is rather dependent on the pre-heat temperature used.

9.1 Lifetime Test of LiF-Teflon Disc Dosimeters

Two LiF-Teflon Disc dosimeters were used. For convenience they were only given an accurate irradiation every 5 readout cycles. The dosimeters were removed from the heating element and replaced for every readout cycle. Table 4 shows the readings obtained over 100 such re-use cycles. The full anneal cycle was used and the dosimeters were not cleaned for the duration of the experiment. The dose given was approximately 1700 mR.

TABLE 4. Results of 100 re-use cycles on LiF-Teflon disc dosimeters.

No. of Readout Cycles	5	10	15	20	25	30	35
Reading	1686	1706	1706	1673	1671	1815	1731
No. of Readout Cycles	40	45	50	55	60	65	70
Reading	1585	1741	1672	1656	1670	1615	1641
No. of Readout Cycles	75	80	85	90	95	100	
Reading	1643	1623	1750	1711	1765	1795	

Mean	1693
Standard Deviation	± 2.8%
Mean of 1st 50 cycles	1698
Mean of 2nd 50 cycles	1687
Difference	0.6%

It can be seen that there is no significant change in sensitivity during the experiment. The standard deviation of all the readings is ± 2.8%. The fact that there is no trend in sensitivity is shown by comparing the mean of the first 50 cycles with that of the second 50 cycles, the difference is only 0.6%.

The background from the dosimeters remained constant at between 5-10 mR throughout the experiment.

The results agree with those presented by Wallace[13] who also took LiF-Teflon dosimeters through 100 re-use cycles with no detectable trend in sensitivity after the first few cycles.

9.2 Initial sensitivity Changes following Oven Annealing

As mentioned in Section 2.2 the portion of the standard anneal which determines the subsequent sensitivity is the rate of cooling from the high temperature portion of the anneal. This is considerably slower in most ovens than in the 7300, which means a significant apparent sensitivity change the first time dosimeters are re-used. This is illustrated in Table 5 which shows the sensitivity of several batches of LiF-Teflon dosimeters after different oven annealings and after an anneal cycle in the 7300. Each figure is the mean of 10 dosimeters.

TABLE 5. Sensitivity changes on first anneal in 7300 for different batches of LiF-Teflon Discs.

Production Batch	1st Irradiation	2nd Irradiation (after 7300 Anneal)	% Change
141068	138	175	+ 21
113002	157	190	+ 17
113089	170	193	+ 12
111067	132	191	+ 30
141047	132	179	+ 26
Spread	± 16%	± 5%	

The most striking observation from Table 5 is not the increase in sensitivity of between 12 and 30% which was expected, but the way in which the reproducible anneal cycle in the instrument reduces the difference in sensitivity between different batches. This shows that the spread of ± 16% originally found in the 5 batches was not inherent but was a function of differences in the oven annealing cycle.

In order to provide dosimeters which do not change sensitivity on the first cycle , we have developed an annealing oven which duplicates as well as possible the rapid cooling in the 7300 instrument. This oven has a rotating perforated squirral cage in which the dosimeters are tumbled. This serves the dual purpose of eliminating differences between dosimeters due to positioning in the oven and removes any large thermal mass in contact with the dosimeters. The main feature of the oven is the use of CO_2 cooling to provide very rapid cooling from 300°C. The oven also has a built in programmer to provide complete reproducibility from time to time. The oven cools at a rate of nearly 2°C/second which is sufficiently close to the rate in the instrument to be on the relatively flat portion of the sensitivity versus cooling rate curve.

Dosimeters annealed in this fast cooling oven show less than 5% change in sensitivity after their first anneal cycle in the 7300 instrument.

10. Repeated Low Level Measurements

In order to test a more realistic simulation of low level measurements a single LiF-Teflon disc dosimeter was exposed to a wide variety of doses from 0-100 mR in random order and read with anneal each time. Figure 7 shows the results. The unirradiated dosimeter reading was reduced to 4-8 mR using the background subtraction facility in the 7300 instrument.

11. Possible Use of 80°C Anneal

Even though the pre-heat is relatively efficient in removing both the low temperature peaks and the U-V sensitivity, it tends to introduce an additional component into the variability of groups of readings. Because the signal does not drop to zero at the end of the pre-heat cycle with LiF (Fig.4)

there is some variability in the amount of the various peaks removed by the pre-heat. This depends primarily on the thermal contact of the dosimeter with the heating element. This effect is eliminated if the dosimeters are given an 80°C overnight anneal after readout in the 7300. This procedure does not affect the sensitivity and requires only a very inexpensive oven. It is not a necessary procedure but for those seeking the utmost precision and minimum fading effects it appears to reduce the standard deviation of a number of readings by about 1-2%.

12. Use of Dosimeters other than LiF.

12.1 Lithium Borate (Manganese)

This phosphor is ideally suited for use with the anneal cycle in the 7300 instrument. As shown in Fig. 5 the pre-heat completely eliminates the low temperature peak so troublesome in this phosphor. The anneal is very efficient in removing the signal and also removes any enhanced sensitivity after doses in the superlinear region.

As a definitive test on the pre-heat efficiency the fading of Lithium Borate over a short time scale was measured and compared with the fading with no pre-heat, see Fig. 8.

12.2 Calcium Sulphate (Dysprosium)

The use of Teflon dosimeters containing this phosphor on the 7300 has been reported previously[14,15]. The pre-heat is again effective in reducing the fading and the anneal cycle reproduces the sensitivity very closely from one use to the next.

13. Conclusions

The objective of designing and constructing a TLD reader with a heating cycle that enables the reuse of dosimeters without external oven annealing has been achieved. The four-stage cycle is shown to eliminate previous signal to less than 0.03% residual after 50,000 mR exposure, reproduce sensitivity to better than $\pm$ 3% over 100 re-use cycles, reduce fading to acceptable levels in all phosphors, and reduce the spread in LiF dosimeters caused by variations in oven annealing.

Although the cycle has been specifically evaluated using TLD Lithium Fluoride, the performance with other phosphors generally exceed that with LiF and it is to be hoped that phosphors such as Lithium Borate will find more general acceptance now that the rapid initial fading has been overcome.

This instrument, together with the concept of district classes of "re-usable" and "disposable" dosimeters, can eliminate high temperature oven annealing of thermoluminescence dosimeters and the accompanying problems. In this way it makes thermoluminescence dosimetry a more practical tool for the average user who is more interested in the results than in peculiarities of the technique.

REFERENCES

1. J. R. Cameron, D. Zimmerman, G. Kenny, R. Buch, R. Bland and R. Grant. Health Phys. 10 25 (1964)

2. D. W. Zimmerman, C.R. Rrhyner and J. R. Cameron. Health Physics 12 525 (1966)

3. A. M. Harris and J.H. Jackson. Health Physics 15 457 (1968)

4. B. E. Bjarngard, R.C. McCall and I.A. Berstein. Luminescence Dosimetry Conf. - 650634 (1965)

5. C. R. Wilson, L.A. DeWerd and J. R. Cameron, A.E.C. Report COO-1105-116 (1966)

6. M.J. Marrone and F.H. Attix Health Phys 10 431 (1964)

7. B. K. A. Martensson, C.A. Carlsson and G.A. Carlsson Proc. 2nd Int. Conf. Lum. Dos. Conf.-680920 936 (1968)

8. R. G. Gower et. al. Health Phys. 17 607 (1969)

9. E. W. Mason, N. T. Harrison and G. S. Linsley. Proc. of IRPA Congress Brighton (1970)

10. M. R. Mayhugh, R. W. Christy and N.M. Johnson. J. Appl. Phys. 41, No. 7, 2968 (1970)

11. G. A. M. Webb. J. Sci. Instrum. 44 481 (1967)

12. J. T. Randall and M. H. F. Wilkins. Proc. Rog. Soc. (London) A184 347 (1945)

13. D. Wallace. Proc. of IRPA Congress Brighton (1970)

14. G. A. M. Webb. Proc. Symp. on New Dev. in Phys. and Biol. Radn. Detectors Vienna (1970)

15. G. A. M. Webb, J. E. Dauch and G. Bodin 16th Annual Meeting Health Phys. Society. New York (1971)

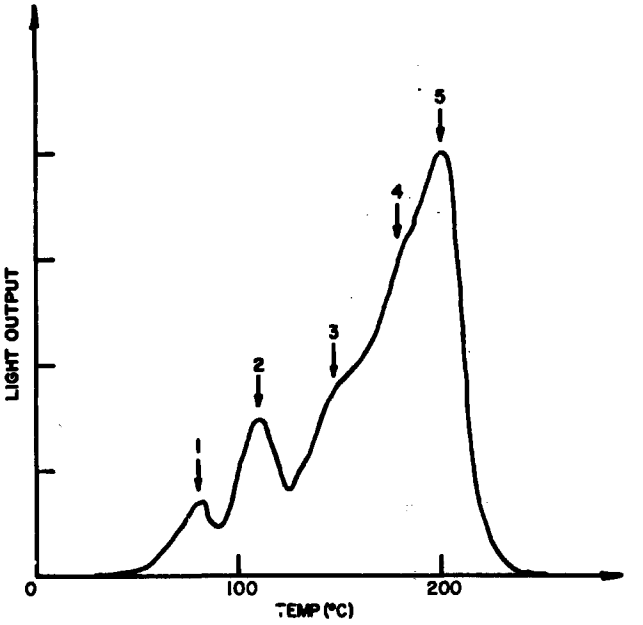

Figure 1. Typical glow curve of LiF after rapid cooling from high temperature (slow linear heating rate). Peaks designated after Cameron[1].

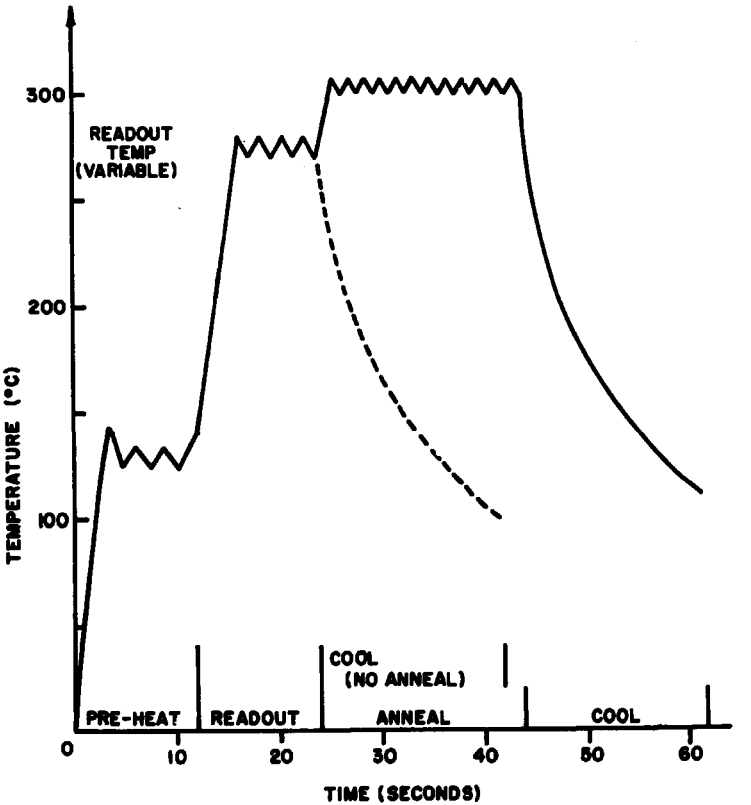

Figure 2. Diagram of Heating Cycle

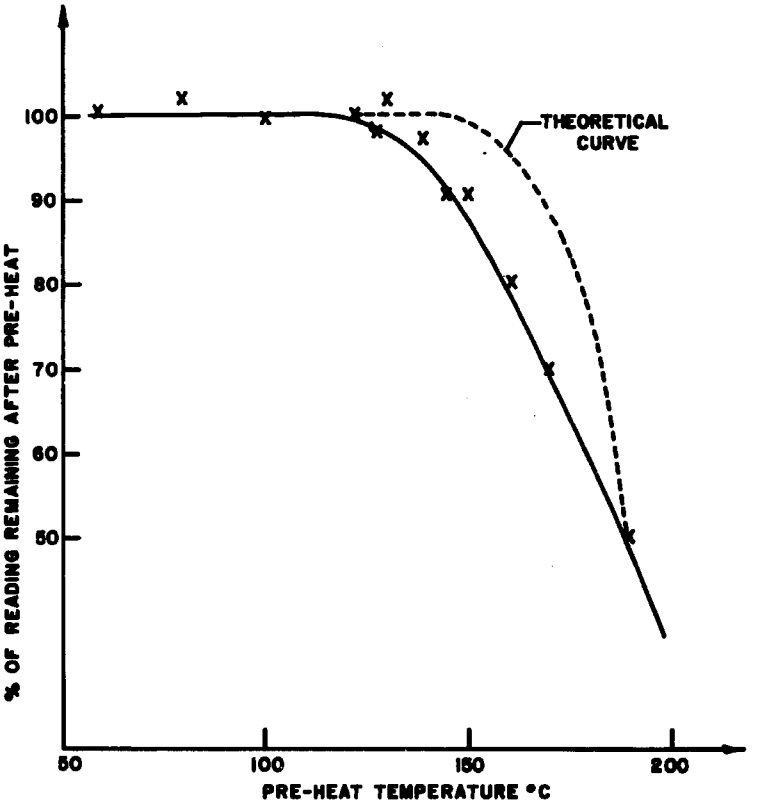

Figure 3. Bleaching of main peak(s) in annealed LiF at different pre-heat temperatures.

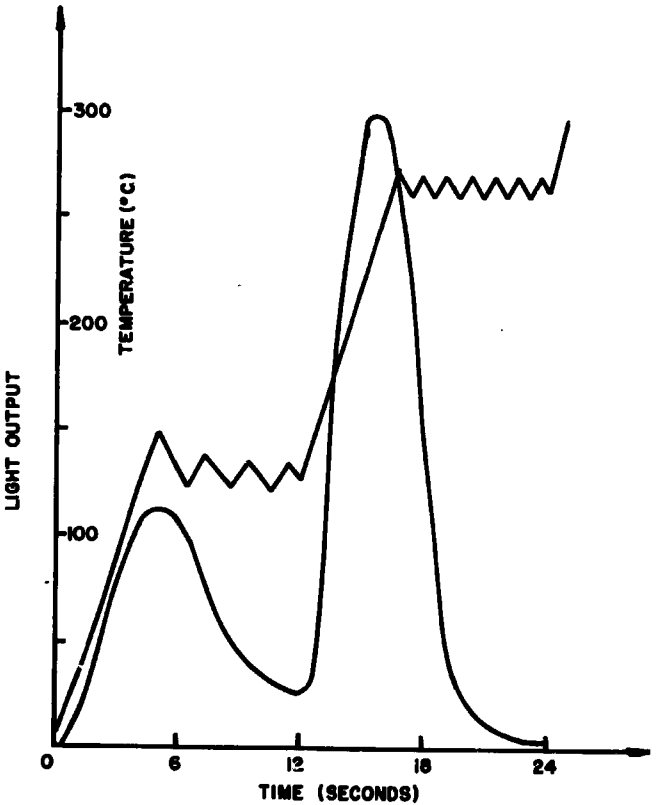

Figure 4. Glow curve of rapid cooled LiF taken on 7300.

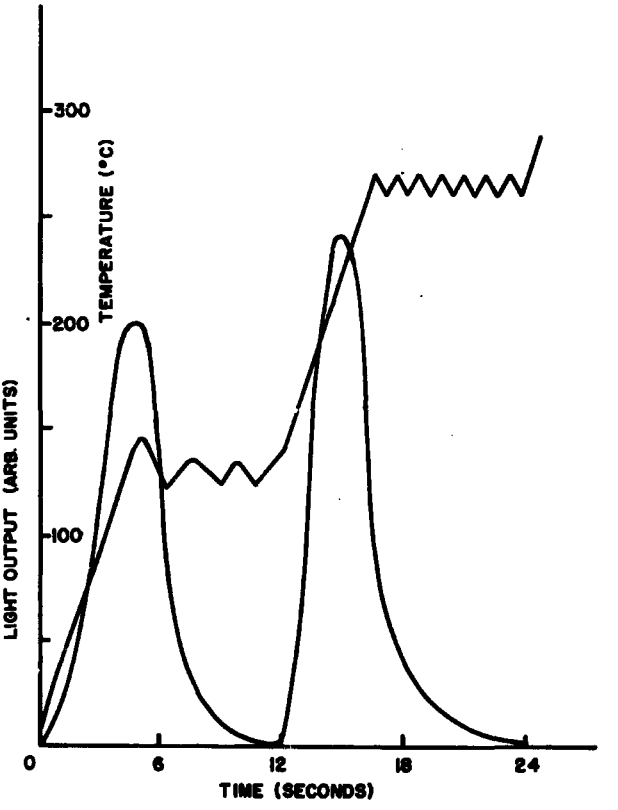

Figure 5. Glow curve of Lithium Borate (Mn) taken on 7300.

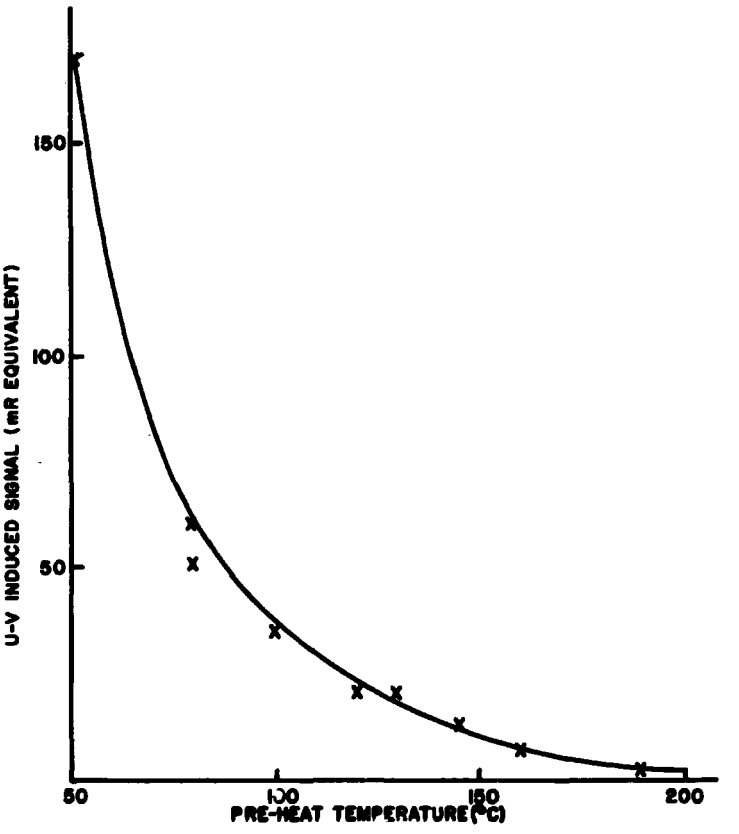

Figure 6. U-V induced reading in unirradiated LiF-Teflon discs after preheat to different temperatures.

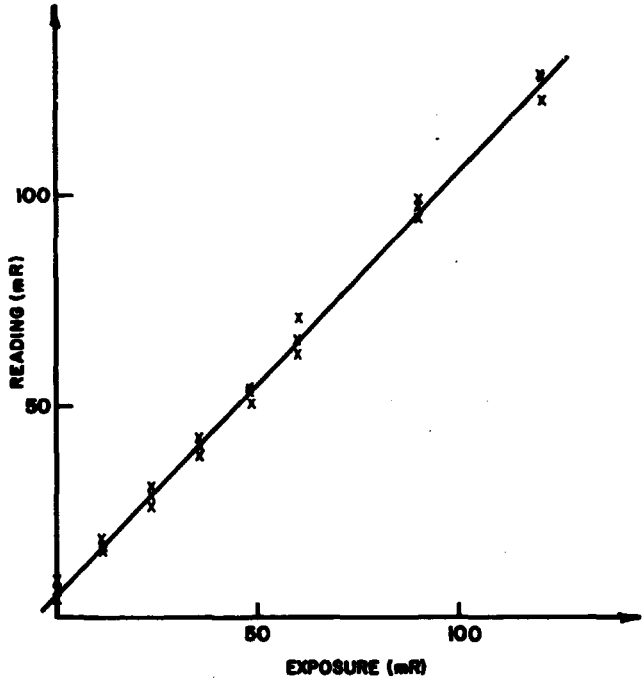

Figure 7. Repeated irradiation and readout of a single LiF-Teflon disc dosimeter.

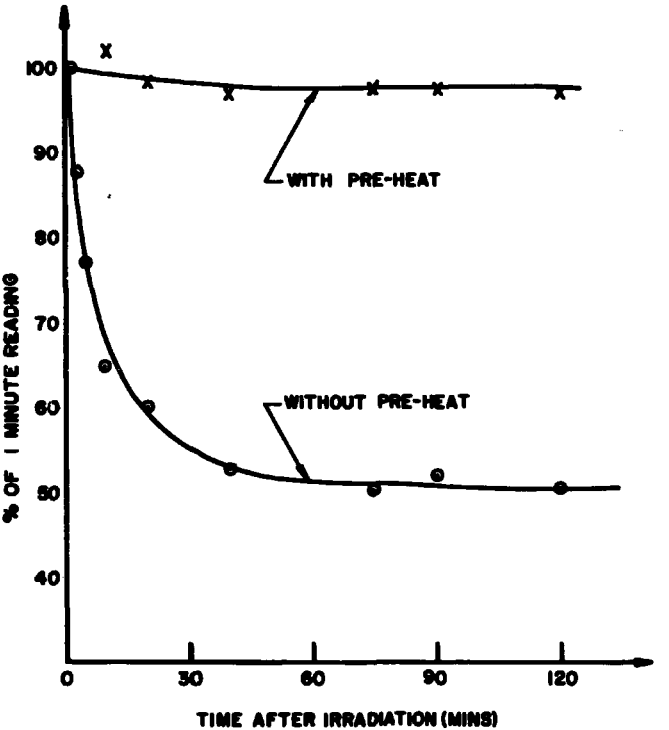

Figure 8. Short-term fading of Lithium Borate (Mn) with and without pre-heat.

Suntharalingam

Reports have been published to the effect that post-irradiation annealing or pre-readout heating could affect the TL intensity of the main glow peak in LiF (TLD-100), probably due to re-trapping by the high-temperature traps of electrons released from the low-temperature traps. Could you please tell us whether you have observed such effects with your LiF-Teflon dosimeters and the pre-readout heat cycle?

Webb

We have not looked in sufficient detail at the glow-curve structure to see this effect. If it is present, it would manifest itself as a reduction in the observed fading.

Attix

I have just a comment in regard to Dr. Suntharalingam's question. The growth of the 200° glow peak observed by Gorbics and Attix when dosed LiF (TLD-100) was annealed at 100°C was erroneously attributed to re-trapping. The effect is observed to be at least as great in undosed phosphors, and therefore must be due to migration and aggregation of traps, as noted by Booth, Johnson, and Attix in Naval Research Laboratory Report 7276.

Significant Changes in TLD Readings Produced by AC Heater Currents

by

J.E. Saunders

Ontario Cancer Treatment and Research Foundation

Hamilton, Ontario, Canada.

Abstract

Variations of up to 9 percent in the light-source readings of a Conrad model 5100B TLD reader were found to be caused by residual magnetic fields in the environment of the photomultiplier tube (PMT). These fields were induced by the final pulse of the preceding AC heater current. Depending on the direction of this pulse, the light-source reading was either increased or decreased. Further investigation revealed that the PMT sensitivity was also directly affected while the heater current was flowing with changes in sensitivity of up to 18 percent between when the current was on and off.

These two effects were investigated in detail for two PMT's, an EMI 6097S and a Centronics VMP 11/44K. The effects depended on the orientation of the PMT, the cathode potential, the magnitude of the heater current, and the magnetic shielding around the PMT.

It has been found that the most satisfactory method of reducing these effects is to increase the distance between the PMT and the heating element to 9 cm with a light-pipe between to maintain the efficiency of the system.

Introduction

TLD readers often use ohmic heating in a metal element to raise the temperature of a TLD phosphor during read-out; the resulting thermoluminescence being measured with a PMT. The magnitude of the heater current (HC) may be as much as 100A, producing considerable local magnetic fields.

The strong influence of magnetic fields on the sensitivity of a PMT is well known and attempts are usually made to reduce this effect in TLD reader designs but there is little data about this reported in the TLD literature. Karzmark, Fowler and White[1] consider the effect of magnetic fields from large DC heater currents upon the PMT but state that if alternating currents are used no significant effects

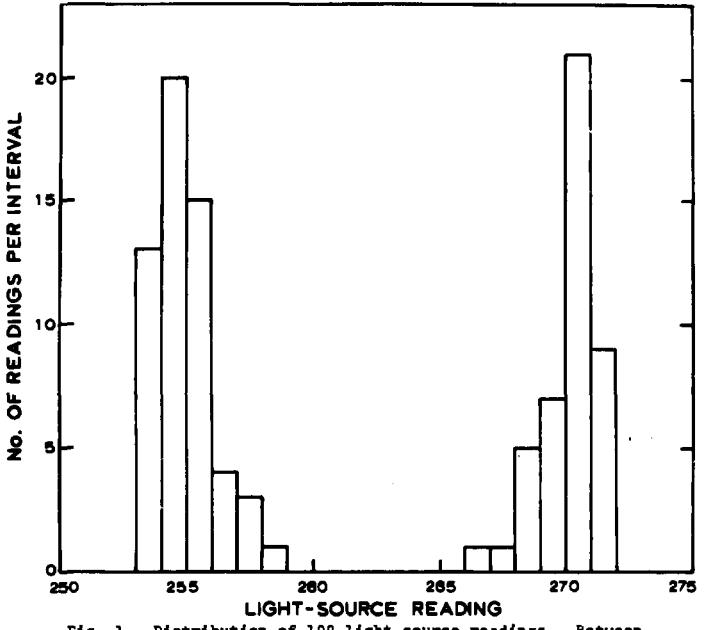

Fig. 1 - Distribution of 100 light-source readings. Between each reading a heater current of 100A AC flowed for about one second. EMI 6097S, 680V.

are to be expected. However, the results presented in this paper show that this is not the case and that magnetic effects may be the source of considerable, yet unsuspected error.

Instrumentation

The results which follow were obtained on a Conrad (Teledyne-Isotopes) model 5100B TLD reader which uses an AC heater current. The PMT in this instrument is an EMI 6097S but measurements have also been made using a Centronics (Twentieth Century Electronics) VMP 11/44K. This latter tube is used in the more recent Conrad reader, model 7100. Both tubes are of the venetian blind dynode type with 2 inch diameter end windows. Magnetic shielding of mu-metal, 0.15 mm thick, is placed around both tubes by Conrad and will be referred to as "normal" shielding in the text. Additional shielding of mu-metal, 0.36 mm thick, was obtained and for measurements made with this around the PMT, in addition to the normal shielding, the term "extra" will be used. The heating element, on which the TLD phosphor is placed, is situated 1.5 cm below the photocathode of the PMT.

Initial Observations

Light-source (LS) readings on the model 5100B were found to vary considerably while reading out a series of dosimeters. Initially, this was attributed to variations in gain of the instrument and corresponding corrections were made to the dosimeter readings. However, it was noticed that the LS readings tended to fall into two groups with few values in between and the reading would only change from one group to the other if there was a heating cycle in between. Fig. 1 shows a frequency distribution of 100 LS readings. Between each reading, a HC of 100A flowed for about one second. These results were obtained on the reader as originally purchased. The two groups of readings are clearly distinguished and differ by about 6 percent. This difference, expressed as a percentage, will be referred to as S.

The value of S depended on the magnitude of the HC used between readings; the greater the current, the greater the value of S. Further investigation showed that the direction of flow of the AC heater current at the moment of switching off determined whether the LS reading would fall into the higher or lower group. This suggested that a permanent magnetic field was being induced by the final pulse of current in the environment of the PMT, affecting its sensitivity for a subsequent LS reading. This was verified when the presence of magnetic poles within the PMT structure itself and the dependence of the polarity of these poles upon the direction of the final HC pulse was detected by a small compass. Also, the change in PMT sensitivity following a heating cycle using a direct current showed a similar correlation with the direction and magnitude of the preceding current.

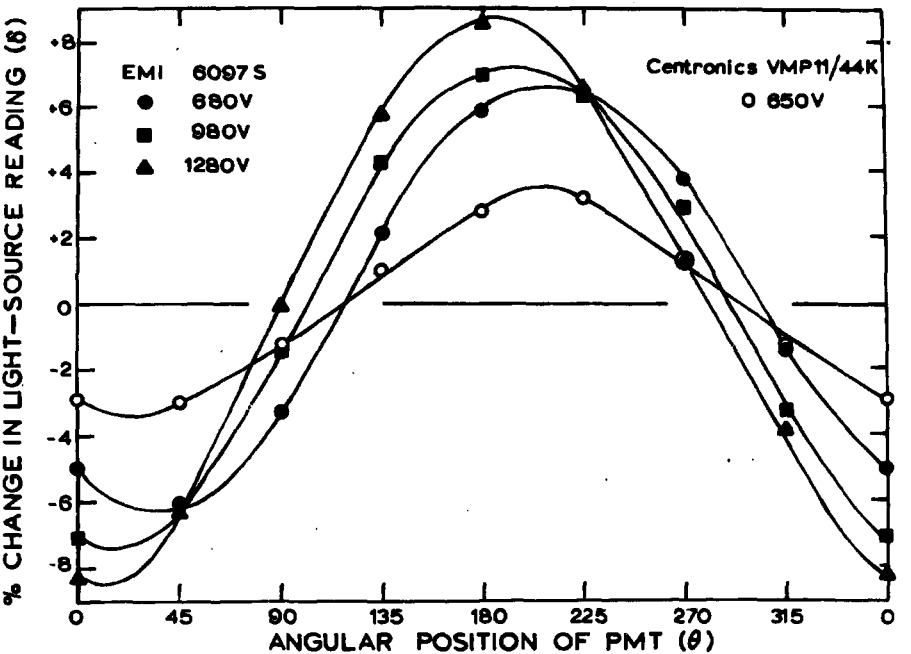

Fig. 2 - Variation of δ with orientation of the PMT about its longitudinal axis for a heater current of 100A AC. Normal mu-metal shielding.

While investigating the cause of these variations in the LS readings, it was also found that the PMT output might be changed by 10 percent or more when the HC was turned on; the output usually being reduced. This change, expressed as a percentage, will be referred to as ϵ.

Determination of δ and ϵ

In order to facilitate the measurement of δ and ϵ as previously defined, the LS was placed on the heating element. This saved repeated handling of the LS which has to be performed in darkness to prevent induced phosphorescence. The HC was only turned on for about 0.5 seconds to minimize heating of the LS and the direction of the HC was determined at the moment of switching off with an oscilloscope. Following this, the anode current of the PMT, as measured on a recorder or digital ammeter, was taken as the LS reading. This procedure was repeated until several LS readings after both positive and negative final HC pulses had been recorded, allowing an estimate of δ to be made. The sign of δ was arbitrarily chosen by subtracting the LS reading produced by negative final pulses of the HC from the reading produced by positive ones.

Finally, the HC was left on for a longer time to obtain an accurate record of the anode current while the HC was flowing. To determine ϵ, the percentage difference between the PMT output with the HC on and with it off, a value for the anode current with no HC was also required. Since the anode current depended on the direction of the final pulse of the preceding HC, the average of the values following final pulses in both directions was used.

Measurements were made at three different cathode potentials for each PMT to cover the range of voltages used in practice. For higher voltages, the LS intensity was reduced by covering it with translucent material so that at no time did the anode current exceed 1.0 microampere. No evidence was found in the course of the measurements to suggest that the effects described in the following sections are dependent upon the intensity of the light received by the PMT.

Variation of δ with PMT Orientation

The data given by Karzmark et al[1] indicate that the effect of a magnetic field upon the PMT will vary as the tube is rotated about its cylindrical axis. Measurements were made every 45 degrees for both the EMI and Centronics tubes using a HC of 100A with the normal mu-metal shielding. The results are shown in fig. 2. The value of δ is plotted against θ, the rotation of the tube. θ is arbitrarily taken as zero for one of the two positions when the venetian blinds of the first dynode are parallel to the direction of the heater current.

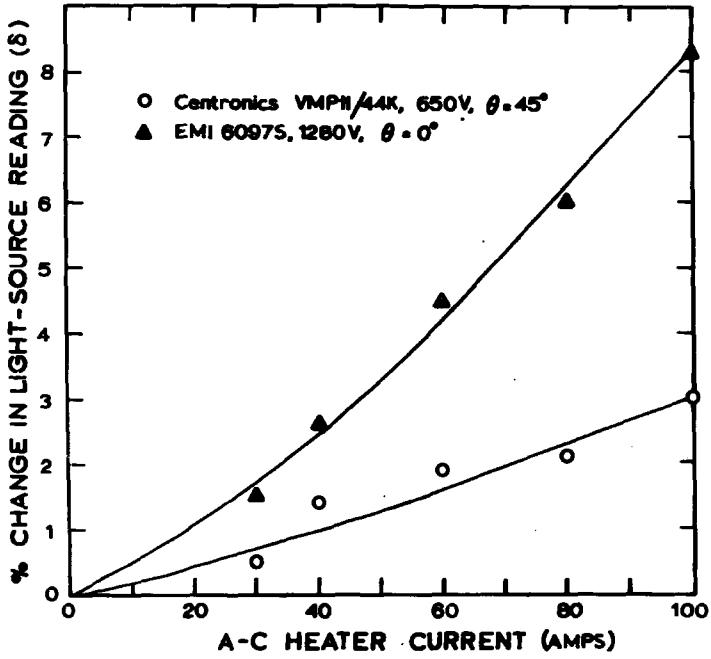

Fig. 3 - Variation of δ with preceding AC heater current. The PMT voltage and orientation give maximum values of δ for each tube.

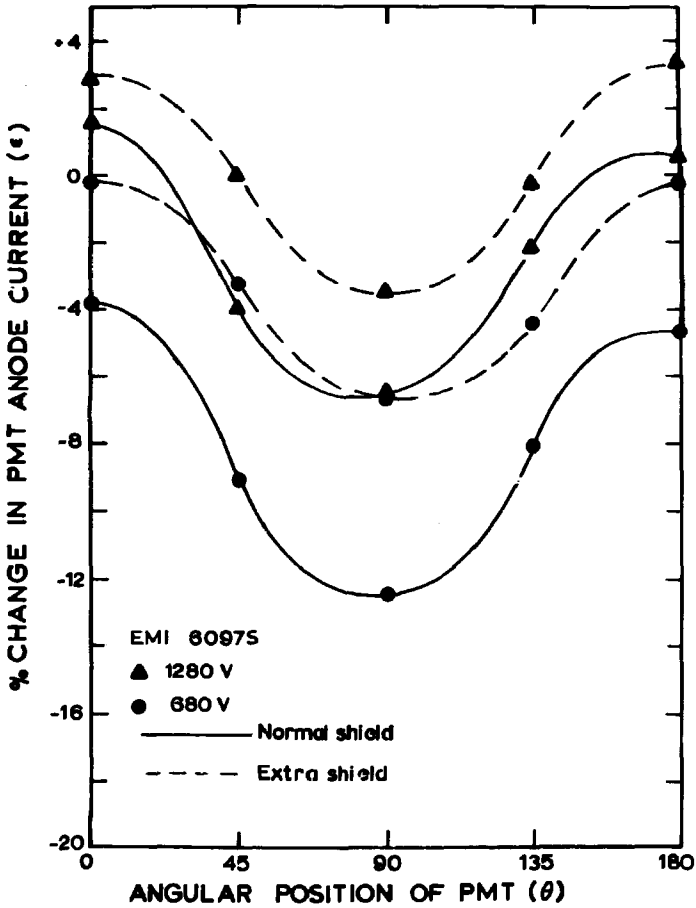

Fig. 4 - Percentage change in PMT output (ε) produced by a heater current of 100A AC versus the orientation of the tube (θ). EMI 6097S.

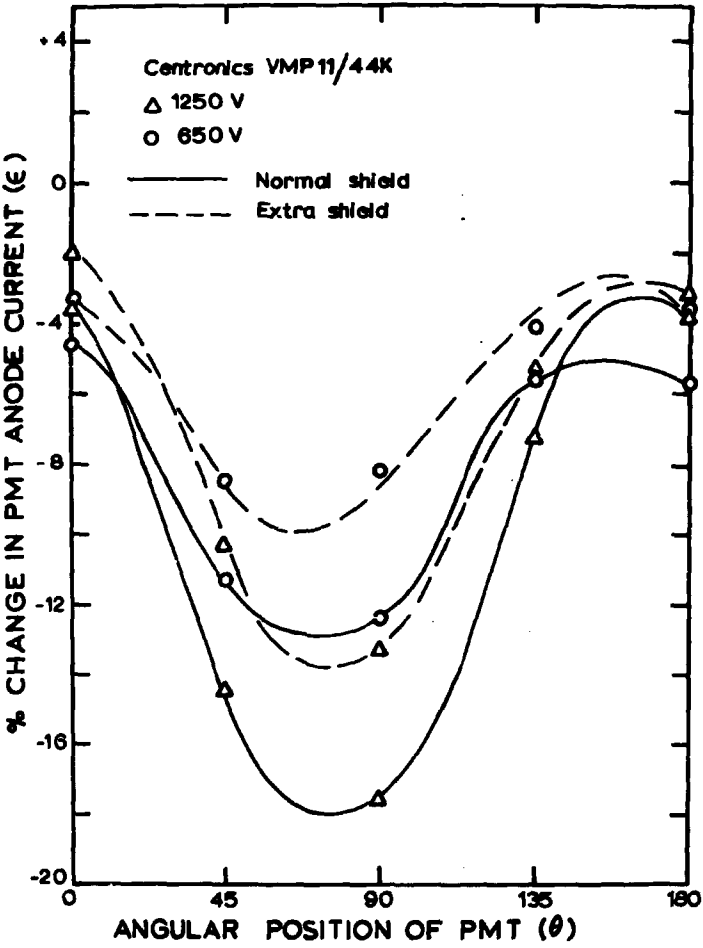

Fig. 5 - Percentage change in PMT output (ε) produced by a heater current of 100A AC versus the orientation of the tube (θ). Centronics VMP 11/44K.

The sinusoidal pattern confirms that the variation in LS readings is caused by a magnetic effect upon the PMT rather than some other component of the reader. The amplitude and phase of the sinusoidal curve for the EMI tube depends on cathode potential over the range of 680V to 1280V, whereas the values for the Centronics tube at 950V and 1250V do not differ from those at 650V by more than one percent absolute. As can be seen from fig. 2, the overall effect is considerably more pronounced for the EMI tube than for the Centronics one.

When the extra shielding of 0.36 mm of mu-metal was added, the value of δ for both tubes never exceeded two percent and was closer to one percent for most values of θ. However, if the extra shielding did not cover about 2.5 cm of the tube at the cathode end, there was very little reduction in the value of δ, suggesting that the region between the cathode and first dynode is the area most sensitive to magnetic fields.

Variation of δ with heater current

Measurements of δ were made for values of the HC up to 100A for both tubes with the normal shielding. The results shown in fig. 3 are for those values of θ and cathode voltage which give maximum values of δ for each tube. The results for other angles and voltages show a similar variation with HC, only with correspondingly smaller values of δ.

Variation of ϵ with PMT orientation

As with δ, it was found that the magnitude of ϵ depended on the orientation of the tube. This dependence is shown in figs. 4 and 5 for the EMI and Centronics tubes respectively for a HC of 100A. The variation over only 180 degrees is given since the pattern is closely repeated from 180 to 360 degrees.

The effect is greatest at approximately 90 degrees for both tubes with a maximum reduction in output of 18 percent for the Centronics tube at 1250V cathode potential. Except for values of θ near to 0 and 180 degrees, the absolute value of ϵ for the Centronics tube is greatest for high cathode voltages. The reverse is true for the EMI tube except that for values of θ near to 0 and 180 degrees and a cathode potential of 1280V, ϵ is positive, i.e. the output of the EMI tube actually increases when the HC is turned on. This is discussed further in the section on DC measurements. In general, the addition of extra shielding reduces the magnitude of ϵ by a few percent for both tubes but, even so, the HC may still change the PMT sensitivity by 10 percent or so.

Measurements were also made at intermediate cathode potentials of 980V for the EMI tube and 950V for the Centronics tube. Values of ϵ halfway between those shown in figs. 4 and 5 were obtained.

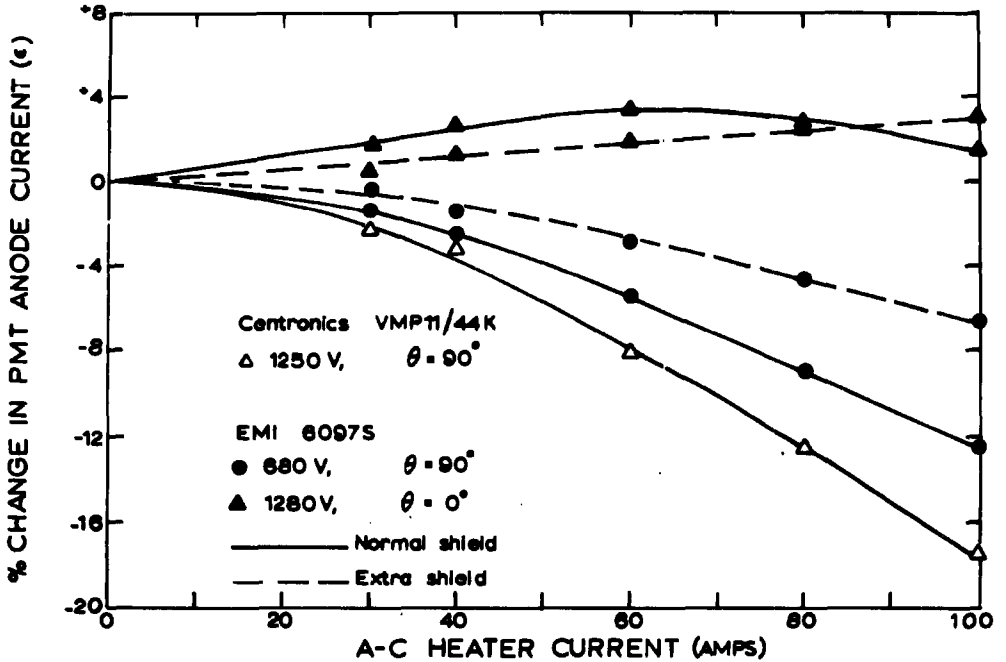

Fig. 6 - Variation of ε with heater current for both PMT's under various conditions.

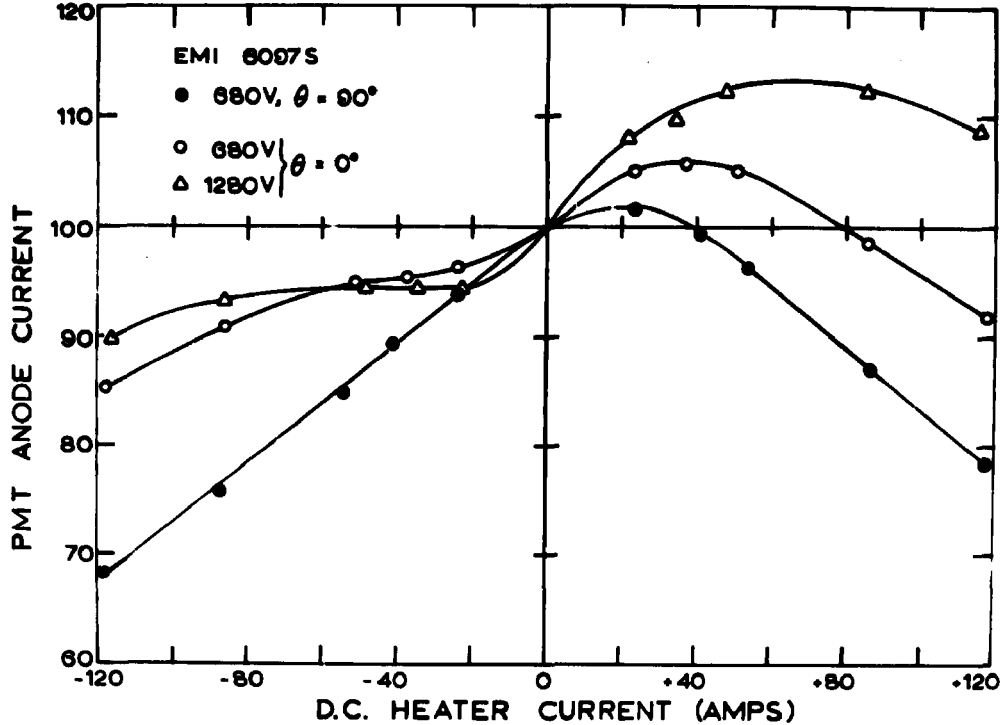

Fig. 7. Dependence of PMT output on DC heater current. Normal mu-metal shielding. EMI 6097S.

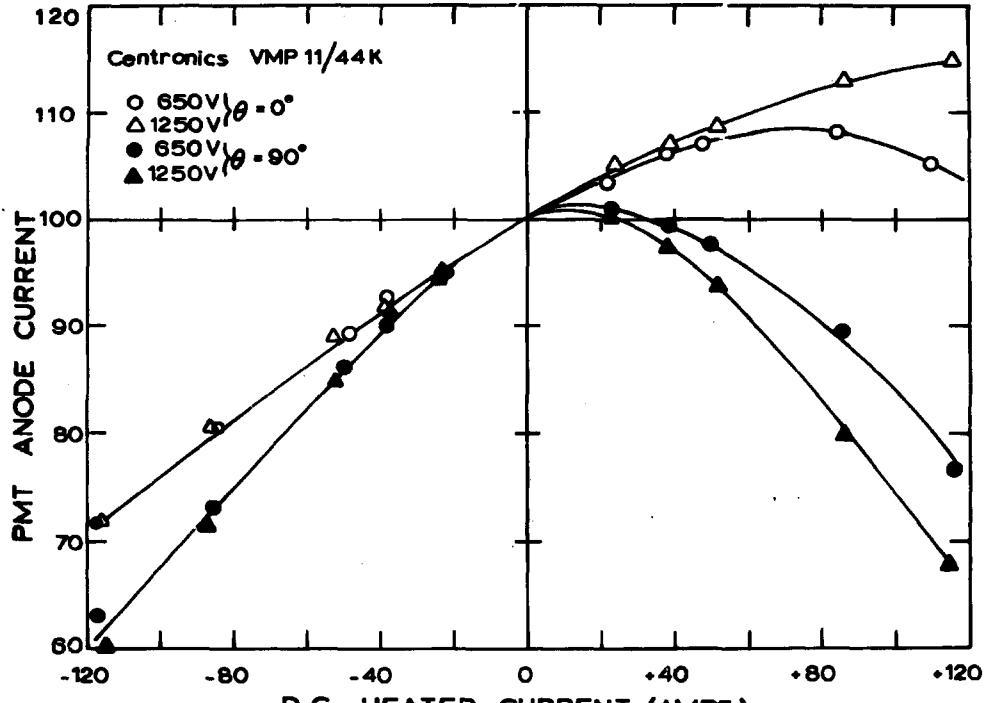

Fig. 8 - Dependence of PMT output on DC heater current. Normal mu-metal shielding. Centronics VMP 11/44K.

Variation of ϵ with heater current

Fig. 6 shows how ϵ varies with the magnitude of the HC at the stated values of cathode voltage and θ. The two lower curves are for those conditions which give nearly maximum values of ϵ for each tube. The effect of adding extra shielding to the EMI tube is shown by the lower dashed line. The variation of ϵ with HC was measured for some other cathode potentials and values of θ and was found to follow a similar pattern except for one situation. This is shown by the uppermost solid curve in fig. 6 for the EMI tube without extra shielding and will be discussed further in the next section.

Measurements with a DC heater current

The effect of small permanent magnetic fields and larger alternating fields upon the PMT's is more clearly understood when the effect of fields from a DC HC is studied. Figs. 7 and 8 show how the output or anode current of the EMI and Centronics tubes depends on the magnitude and direction of a DC HC at various cathode potentials and values of θ. These results are similar to those published by EMI and reproduced by Karzmark et al[1].

For small currents and hence small fields, the output of both PMT's is either increased or decreased depending on the direction of the current. This corresponds to the increase or decrease in LS readings observed after the induction of small magnetic fields by positive or negative final pulses from an AC HC. At a value of 90 degrees for θ, large positive and negative currents both reduce the PMT output giving the large negative values of ϵ which occur at this orientation. However, at zero degrees, large positive currents produce a considerable increase in output and the reduction in output from negative currents is not so great, especially for the EMI tube (Fig. 7). This accounts for the increase in the output of the EMI tube observed at 0 degrees for a cathode potential of 1280V and also for the maximum value of ϵ being produced by an AC HC of about 60A as seen in the uppermost solid curve of fig. 6. The addition of extra shielding, uppermost dashed curve of fig. 6, reduces the magnetic effect of the HC and so the maximum is not reached.

Significance of δ and ϵ

The variation in the LS reading (δ) produced by residual magnetic fields is probably more important in routine TLD dosimetry than the direct effect of the HC upon the PMT output (ϵ). A change in the LS reading would normally be interpreted as a change in sensitivity of the TLD reader resulting in erroneous corrections being applied to dosimeter readings.

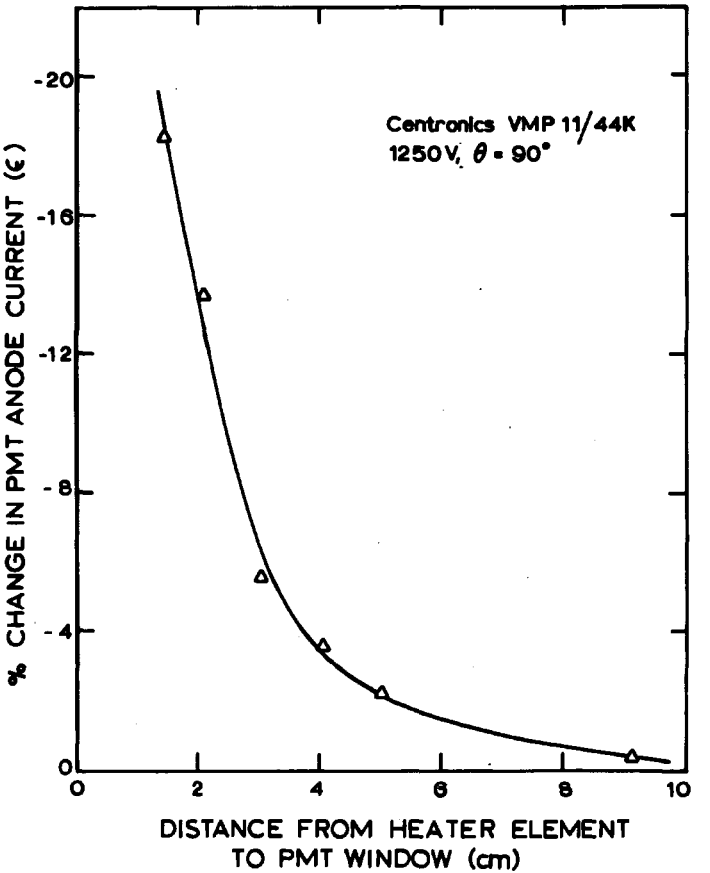

Fig. 9 - Variation of ε with distance of PMT from heater element under worst conditions. Normal mu-metal shielding. 100A AC heater current.

The heating cycle of a TLD reader is normally designed to be very reproducible, therefore, even though the output of the PMT will be affected by the HC during the measurement of thermoluminescence, the value of ϵ should remain constant for all similar heating cycles. Thus, no error would be introduced.

Nevertheless, there are occasions, usually of a research or non-routine nature, when the value of ϵ might not remain constant. Any comparison between TLD readings made with different heater currents would include an error caused by variations in the value of ϵ. Also, any change in the position of the PMT or the material around it could affect the value of ϵ, as is clearly shown by figs. 4 and 5. This would produce a change in sensitivity of the TLD reader while the HC is flowing but not necessarily change the LS reading. Such a change would only be detected by reading out calibrated dosimeters.

Methods of reducing the magnitude of δ and ϵ

The magnitude of both δ and ϵ may obviously be reduced by choosing an appropriate value of θ and by adding extra magnetic shielding. Unfortunately, the values of θ which minimize ϵ tend to produce the largest values of δ and vice-versa, as can be seen by comparison between fig. 2 and figs. 4 and 5. The addition of extra shielding reduces δ to less than two percent for all values of θ which may be acceptable for most work, allowing θ to be chosen to minimize ϵ. The final choice of θ may depend on which source of error is considered to be more important.

It has been found that the most satisfactory way of reducing these effects from the HC upon the PMT is to increase the distance between the tube and the heating element. Fig. 9 shows how the value of ϵ under the worst conditions for the Centronics tube varies with the distance of the photocathode from the heating element. A distance of 9 cm is sufficient to make the influence of the HC insignificant. To overcome the loss in light efficiency, a perspex light-pipe, 8 cm long and 3.8 cm in diameter, has been placed between the element and the photocathode. With this arrangement, the original heat absorbing glass filter which absorbs 15 percent of the thermoluminescence was able to be removed without any increase in background signal or dark current. The resulting system has the same light efficiency as the original one for both lithium fluoride (blue spectrum) and lithium borate (orange spectrum) dosimeters.

Application to other instruments

The results presented in this paper apply strictly to one instrument but similar effects would be expected on similar instruments. Measurements made on another model 5100B reader gave much smaller values of δ, the largest value being two percent, but the value of ϵ showed greater variations with

values from -14 to +14 percent. The PMT is probably the critical component with each one requiring individual investigation.

Acknowledgements

The author gratefully acknowledges the co-operation of the Physics Department of the Ontario Cancer Institute, Princess Margaret Hospital, Toronto for allowing measurements to be made on their TLD reader.

Reference

1. C.J. Karzmark, J.F. Fowler and J.T. White. Luminescence Dosimetry, Proc. Int. Conf. Stanford, 1965, U.S.A.E.C. Report CONF-650637, 278 (1967).

Nink

What is the value of the magnetic field in the geometry of your arrangement?

Saunders

About 10 oersteds without magnetic shielding. The actual value with shielding is unknown.

Schönbacher

We too have noticed, when using the Isotopes 7100 reader unit, a considerable change in the standard light source reading for a series of consecutive measurements. We thought one reason for this could be that there is a groove in the base of the slide inserter which allows it to pass over the thermocouple. When the inserter was in its open position, light could enter along this groove and reach the PM tube. Consequently, the sensitivity of the photocathode of the PM tube changed from time to time. Mechanical modifications were necessary to cure this.

Photon Counting as Applied to Thermoluminescence Dosimetry

by

T. Schlesinger, A. Avni and Y. Feige

Radiation Safety Department
Israel Atomic Energy Commission
Yavne, Israel

and

S.S. Friedland

Department of Physics
Tel-Aviv University
Tel-Aviv, Israel

Abstract

The technique of photon counting have been applied to thermoluminescence dosimetry. A comparison has been made between the sensitivity, accuracy and signal to noise ratio obtained with a system based on this technique and a standard d.c. recording system. We can read at least down to 5 mR with a standard deviation of about 12% over 10 readings as compared to 25 mR with a standard deviation of 50% for the same number of readings. At 25 mR the signal to noise ratio for the new system is 1.3 as compared to 0.15 for the standard system. Refinements of our apparatus and techniques are expected to produce further improvements.

Introduction

In most commercial TLD systems different types of electrometers and voltmeters are used for the measurement of the phototube anode current; which is related to the radiation dose. These instruments are limited in stability and sensitivity by a number of phenomena, e.g.,

a. The strong dependence of the overall gain of the photomultiplier tube on the applied voltage and a number of other parameters such as the surface condition of the dynodes and the history of the tube;

b. The unequal amplification of individual pulses resulting from the statistical nature of the secondary electron emission process;

c. The d.c. drift of the baseline of the phototube dark current produced by changes in the leakage current, the operating voltage, temperature, etc.;

d. Other effects, usually encountered in low level d.c. current measurements, such as the ionization of the residual gases within the photomultiplier tube, etc.

Such instruments require frequent readjustments and recalibrations, moreover, calibrations performed at one dose level are of limited value for measurements of much higher or much lower dose levels.

With the rapid development in the last few years of photon counting techniques, it seemed very desirable to replace the d.c. current measurements in the TLD reader instruments by the newer instrumentation.

The physical principles and advantages of photon counting are adequately described in the recent literature[1,2] and it is sufficient to indicate here the following reported improvements:

a. The minimization of base line drifts by using pulse amplification techniques and suitable pulse discrimination;

b. The detection of lower light levels; actually of single photons;

c. The reduction of the dependence of the operating characteristics of the light measuring system on the applied voltage to the P.M. tube and the physical conditions of the dynodes and the tube surroundings.

In our laboratory a prototype TLD reader utilizing the photon counting technique has been designed and constructed; its capabilities, as compared to conventional commercial readers, has been examined. In particular the sensi-

tivity and accuracy of the system, in the low level dose range of 1-1000 mR, has been studied.

Experimental

1. T.L. Material - The dosimeters used were TLD-100 LiF 1/8" x 1/8" x 0.035" extruded ribbons produced by the Harshaw Chemical Company. This material appears to be the most widely used for Health Physics purposes because of its desirable T,L,D. properties; e.g., linear response over a wide radiation dose range, dose rate and energy independence and tissue equivalence.

2. Read out System - The block diagram of the readout system is presented in Fig. 1. The heating and light collecting unit is described in detail in Fig. 2.

The sample is mounted in a vacuum chamber in close proximity to the photocathode of an EMI low dark current thermoelectrically cooled photomultiplier. A 3 mm thick quartz window is used to separate the vacuum chamber from the phototube housing. The sample holder consists of a heating element-a thin kantal strip, and a stainless steel grid to ensure thermal contact. A constant a.c. current (18 A) is used to heat the sample to a temperature of 280°C within 25 sec, after a preheat to 100°C for 90 sec. The total number of photo electron pulses produced during the temperature variation of the sample from 120°C to 250°C is recorded by an SSR Instrument Co, Model No, 1105 Photon Counter attached to a fast scaler. After the reading the sample is reheated and the nonradiation induced counts (e,g., infrared radiation and all kinds of spurious pulses) are recorded. The net number of counts is related to the radiation dose.

3. Calibration procedures - 20 dosimeters were exposed to different doses of gamma radiation from a 2.6 ci Co^{60} point source at a distance of 2 m. During exposure the dosimeters were inserted into a 6 mm thick perspex holder to allow for electron equilibrium. Before every exposure the dosimeters were cleaned and annealed for 1 hour at 400°C, then allowed to cool slowly (about 100°C/hour) to room temperature. We found that this annealing procedure leads to the best reproducible results.

   After every exposure the dosimeters were divided into two equal groups; one group was read with the photon counting system while the other with a modern commercial TLD reader.

Results

The results of the measurements are presented in Figs. 3-5. Fig. 3 shows the integrated TL as a function of exposure covering the range 1-1000 mR. The upper curve represents the results obtained with the photon counting system. Every point represents the mean number of counts obtained from the reading of 10 dosimeters which had been exposed several times (3-5) to a definite dose. The vertical line at each point indicates the standard deviation of the measu rements. The lower curve represents the results obtained with the commercial instrument. No quantitatively meaningful results could be obtained with this instrument below 20 mR(as will be shown below).

Figure 4 is a plot of the percentage standard deviation of the measure-ments as a function of dose for 10 different dosimeters used at each dose level. The lower curve represents the standard deviation obtained with the photon counting system; a value of about 12% was obtained at 5 mR, about 6% for a dose of 25 mR and about 3% for doses above 100 mR. The lower curve shows the same data for the commercial system. A sharp rise is observed in the percentage deviation for all doses below 200 mR. At 25 mR a value of 50% deviation is observed and rises to a value of 90% for 10 mR.

Figure 5 represents the signal to noise ratio for the measurements at different dose levels with both systems. For 10 mR we obtained a signal to noise ratio of 0,7 as compared to a ratio of 0,05 with the commercial system. For 50 mR a value of 2.6 is obtained with the photon counting system as compared to about 0.2 for the commercial system.

Conclusion

We have demonstrated an improvement by a factor of 5 in sensitivity and a tenfold reduction of the standard deviation in the dose measurements at 25 mR utilizing photon counting techniques. We believe that refinements in our apparatus and techniques will further improve our results.

References

1. G.A. Morton, App. Opt. 7, 1 (1968).

2. E.H. Eberhardt, Appl. Opt. 6, 251 (1967)

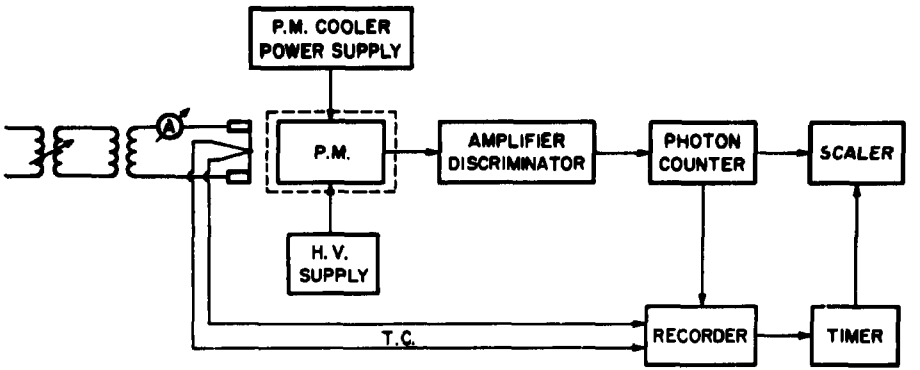

Circuit block diagram

Figure 1 - Block diagram of photon counting system used for thermoluminescence dosimetry. By using pulse amp. and pulse discrimination techniques a good sensitivity is obtained and base line drift is reduced. The P.M. tube is a cooled E.M.I. 9635QB and the amplifier-discriminator and photon counter is an S.S.R. Instrument Co. Model 1105.

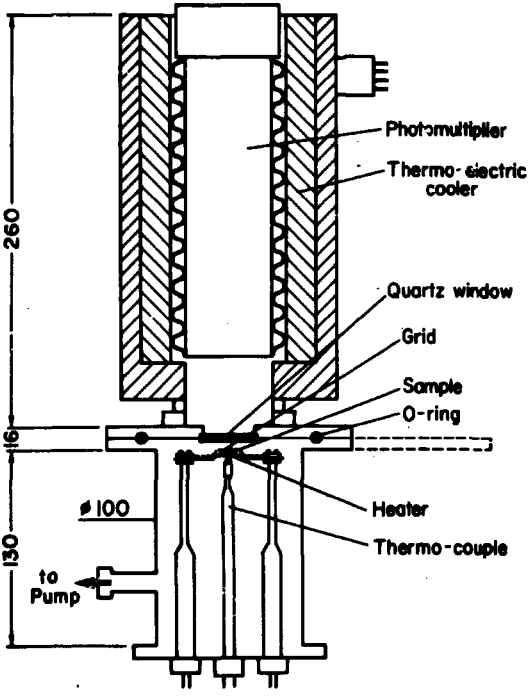

Heating and light collecting unit

Figure 2 - Schematic representation of the heating and the light collecting unit. The P.M. tube is separated from the sample by a 3 mm thick quartz window. The sample is heated in a vacuum chamber.

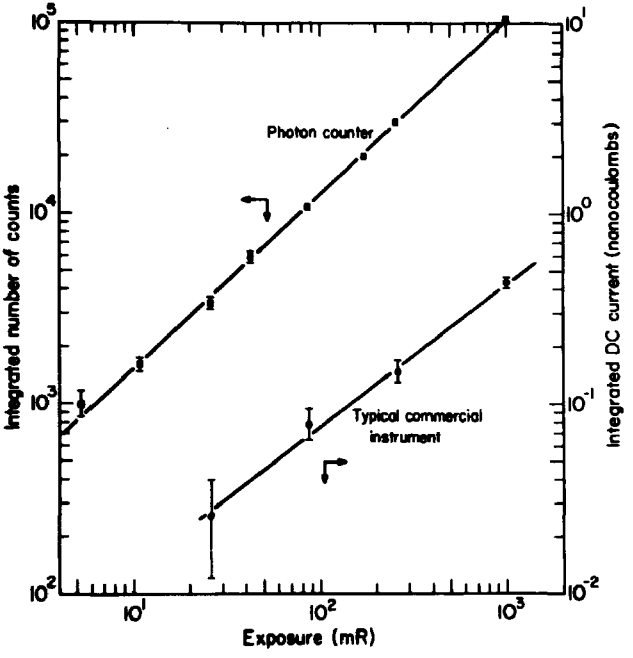

Integrated TL as a function of exposure

Figure 3 - Curves of the output readings of a photon counting system and a commercial system versus dose. The error bar for each point is shown. The upper curve for the photon counting system shows reading down to 5 mR. The lower curve for the commercial system cuts off at 25 mR. The error at 25 mR for the photon counting system is about 6% as compared to about 50% for the commercial system.

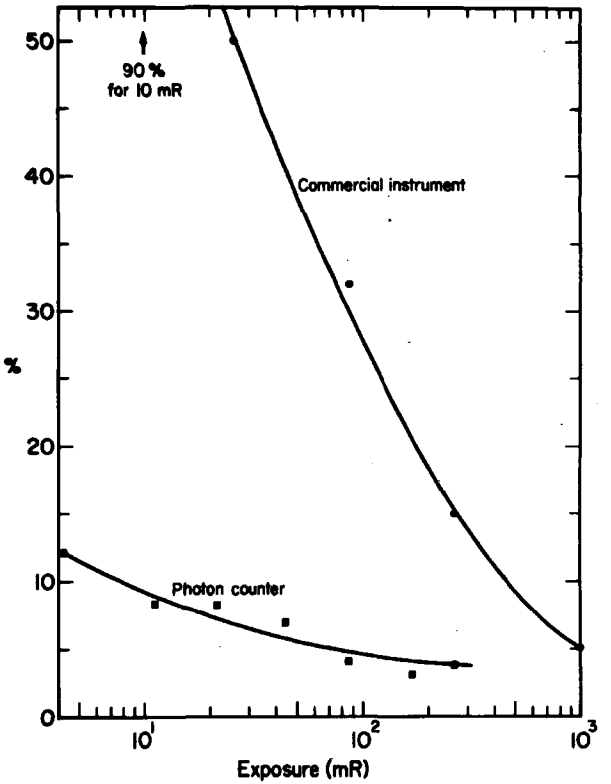

Percentage standard deviation

(20 TLD-100 1/8 x 1/8 x .035" Ribbons)

Figure 4 - Percentage standard deviations for a photon counting system and a commercial system versus exposure dose in mR for a group of 10 dosimeters. The variation in the photon counting system deviation is from 12% at 5mR to 3% at 250 mR. The commercial system shows a sharp rise in the deviation for all doses below 200 mR reaching 90% at 10 mR.

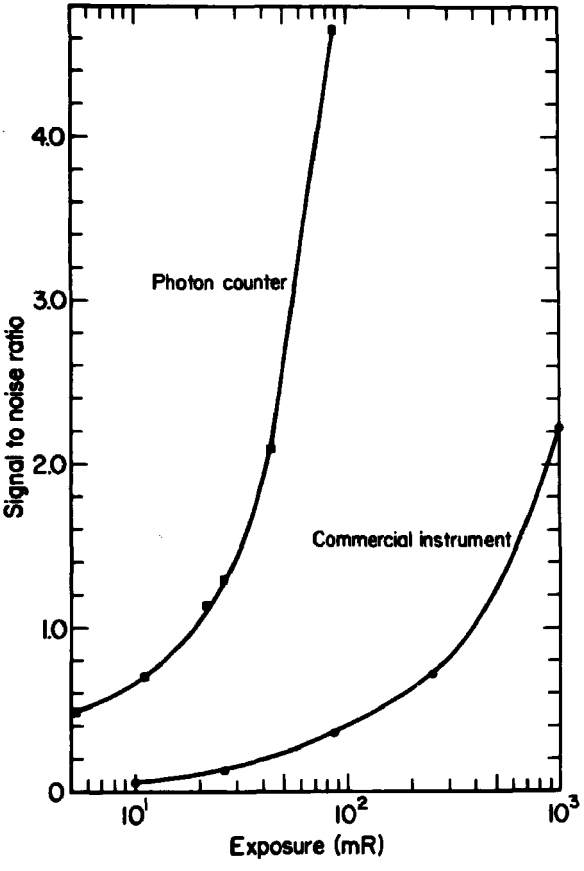

Signal to noise ratio as a function of exposure

Figure 5 - A plot of the signal to noise ratio for a photon counting system and a commercial system as a function of dose in mR. At 80 mR the photon counting system has a S/N of 4.4 as compared to 0.4 for the commercial system. At 10 mR the S/N is 0.7 for the photon counting system as compared to 0.05 for the commercial system.

Aitken

We have been using photon counting in archaeological dating over the past three years, and I fully agree with all the speaker has said about the advantages as far as low light levels are concerned. I would, however, like to point out a drawback for general use. This is the limited dynamic range due to the onset of "pile-up" for high pulse rates. This range is certainly quite wide (a factor of 10^3 to 10^4), but it does make it necessary to have a rough idea of the dose in advance of measurements.

Dosimeter and Reader by Hot Air Jet

by

H. Oonishi, O. Yamamoto, T. Yamashita and S. Hasegawa

Central Research Laboratory
Matsushita Electric Industrial Co., Ltd.
Kadoma, Osaka, Japan

Abstract

A new type of TLD instrument has been developed, in which a dosimeter is heated by hot air injected from a nozzle.

Main characteristics of the instrument are excellent owing to featuring kinetics of heating:

1) dosimeters can be conveniently heated without contacting to heat source;
2) Radiation noise caused by radiations from heated body is minimized, e. g., the pre-dose of rod type dosimeter caused by radiation noise is below 30 μR;
3) the selected part of a dosimeter can be partially heated without heating other parts: holding part, numbering part or other TL element in a composite dosimeter;
4) dosimeter can be heated very quickly, e. g., a rod type dosimeter 2 mm in diameter and 12 mm in length can be heated to 350°C in 4 - 8 seconds.

Introduction

Indirect heating method in TLD reader, in which heating energy is transferred through some indirect medium, as pointed out by Cameron[1], such as light beam, electro-magnetic field or hot gas may have a practical feature that a TL element can be heated without making any contact with the heat source.

Formerly applied direct heating method generally used metal strip or

thin metal plate as heat source which is heated by applying electric current [2]. A dosimeter is in direct contact with heated metal plate and heated by thermal conduction. Practical inconvenience that is offen experienced is imperfect contact which causes large errors in reading.

K. F. Petrock and D. E. Jones[3] have first shown one of indirect heating apparatus using hot nitrogen stream for heating dosimeter. In this apparatus, hot nitrogen gas was steadily sent through a guide pipe and a dosimeter was inserted into a hollow of the pipe and was heated. Owing to its design, however, thermal emission from guide pipe may be appreciable and in addition the apparatus was large.

In this paper, an improved gas type heating apparatus is proposed and constructed. Air was used as the heating medium for simple construction of reader, and hot air jet from a nozzle was applied in each cycle of heating in order to heat only the TL part and to minimize thermal radiation noise from other parts. By such improvement, sensitive and convenient system was obtained.

Construction

Figure 1 shows typical heating apparatus adopting the hot air jet method. Nozzle (4) is the most important and is designed so that the hot air is collectively blown to TL element (5) through it. Pumped air is heated up to about 380°C as it passes through the heat transfer (3). Air filter (1) is installed at the inlet of the pump (2) for dust screening. Figure 2 shows how TL element is heated. Hot air, exhausted from nozzle, flows down hitting TL element and effectively making it emmit luminescence, without heating the other part. The air after heating goes out through exhaust pipe (10). Another constructive feature is that a special 'nest' (7) is set around the element in order to prevent the heat dispersion into surrounding parts.

Various types of dosimeter can be applied to this apparatus of hot air type. Figure 3 shows some examples of dosimeter applicable to this apparatus. Dosimeter (A) in the figure is designed for personnel monitoring: $CaSO_4$: Tm phosphor powder is packed in a glass pipe of 2 mm in diameter which is secured to a holder. When this dosimeter is read, whole body of the dosimeter with the cap removed can be set into the apparatus and the thermoluminescent part is heated by blowing hot air. Dosimeter (B) in the figure is rod type for X-rays and γ-rays: ceramic grains of BeO are packed in a glass pipe of 2 mm in diameter, 12 mm in length. Dosimeter (C) is thin disc 0. 1 mm thick, 10 mm in diameter for β-rays dosimetry in which $CaSO_4$: Tm powder is formed by poly-imid resin. These dosimeters can be set in the apparatus easily and heated quickly as shown in the following section.

Characteristics

Heating:

On detecting a thermoluminescent signal, the higher the heating rate is, the larger the signal-to-noise ratio becomes. In the apparatus of this study the heating ability of a dosimeter was superior. Figure 4 shows glow curves of various types of dosimeter heated by this apparatus. All samples were

heated by a hot air of 390°C in flow rate of 10 lit. /min. Dosimeters used in the examination were $CaSO_4$:Tm encapsulated in a cylindrical glass 2mm in diameter and 12 mm in length (curve A), encapsulated in glass sphere 3mm in diameter (curve B), formed into thin disc by polyimid resin 10 mm in diameter 0. 1 mm in thickness (curve C), and formed into thick disc by fluororesin 10 mm in diameter 1 mm in thickness (curve D). As shown in the figure, dosimeter of thin disc type (curve C) was heated very quickly because its heat capacity was small, whereas the other type of dosimeter was heated moderately. When the temperature of the hot air was raised or the flow rate of the hot air was increased, the heating rate of these dosimeters increased. These relations are similar to the data by Jones in gas-stream type apparatus. However, the extreme change of these condition resulted in another trouble: when flow rate was extremely raised, some type of dosimeter was moved by jet stream; when air temperature was extremely raised, thermal emission from dosimeter appeared. The curves of Figure 4 were observed in a moderate condition.

The efficiency of gas heating, the ratio of the heat energy accepted by a dosimeter to the heat energy of the heated air exhausted by a cycle of reading was measured and it was estimated to be 12 % in the present apparatus and the rod dosimeter.

Thermal Radiation Noise:

When a dosimeter is heated in a heating apparatus, the dosimeter and the other heated parts of the apparatus emit thermal radiation noises. In the apparatus of hot air type, only the thermoluminescent part of a dosimeter is heated and the other part is not heated as highly as to emit a noise. Figure 5 shows a comparison of thermal radiation noise emitted from heating part of two types of apparatus, the hot air type (curve a) and a direct heating type (metal ribbon heater) (curve b) observing glow curves of a rod dosimeter exposed at 1 mR. Appreciable thermal radiation noise is read by the curve b, whereas it is not by the curve a.

The largest inevitable noise in TLD system is the thermal radiation from TL part itself. This apparatus may be designed to the inevitable noise level.

Partial Heating:

Heat can be centered to main part of a dosimeter without heating other part. Figure 6 shows a temperature distribution of a dosimeter for personnel monitoring heated by this apparatus. The temperature was measured by a thermocouple during a cycle of reading, and the maximum temperatures were shown in the figure. Thermoluminescent part could be heated up to 350°C while holding parts were heated to less than 60°C.

Method of partial heating of a dosimeter is important in a practical system, especially in the future system such as composite dosimeter system. An example was shown by this apparatus.

Readout System

A thermoluminescent readout system was constructed using hot air type apparatus. Figure 7 shows picture of a readout instrument in which heating apparatus, optical parts and electronic parts are set together. Block dia-

gram is also shown in Figure 8. The emitted thermoluminescence is detected by a photomultiplier tube, integrated and is shown digitally by dose unit. The feature of this instrument is that various types of dosimeter can be easily applied to it because of its heating apparatus.

This method of heating is also applicable to automatic reader. In a prototype automatic reader a mechanism of automatically sending dosimeters to the heating position was adopted By this instrument. 180 dosimeters per hour could be read semi-automatically.

Gorbics and Attix[4] proposed a composite dosimeter of direct heating type for analysing mixed radiation. However, there were some difficulties in heating composite elements by heat conduction. If an indirect heating apparatus as obtained in this report is applied to a composite dosimeter, a reliable and comparatively simple system will be obtained.

Conclusion

A TLD instrument of hot air type was constructed and examined. Main features of this type are that it can heat dosimeters conveniently and exactly, that a part of a dosimeter can be heated selectively, and that it has superior characteristic in signal-to-noise ratio. Among many types of indirect heating apparatus this type may be the most practical one; it may be advantageous for convenient type reader used for daily monitoring as well as automatic instrument combined with composite dosimeter for authorized dosimetry.

References

1. J. R. Cameron N. Suntharalingam, and G. N. Kenney, Thermoluminescence Dosimetry (Madison:University of Wisconsin Press)(1968).
2. F. Daniels, C. A. Boyd, and D. F. Saunders, Thermoluminescence as a research tool. Science 117, 343 (1953).
3. K. F. Petrock and D. E. Jones, Proceedings of the Second International Conference on Luminescence Dosimetry (ed. by J. A. Auxier), 652-689 (1968).
4. S. G. Gorbics and F. H. Attix, International Journal of Applied Radiation and Isotopes 81-89 (1968).

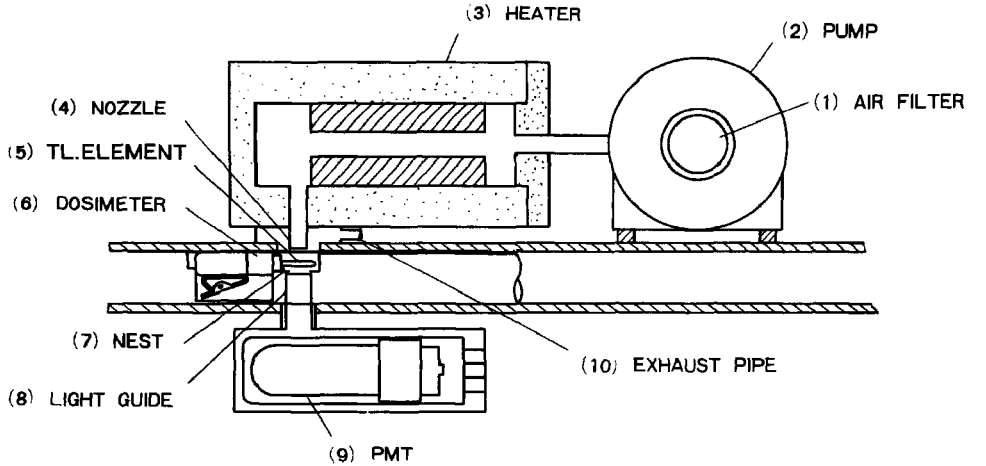

Fig. 1 Construction of the heating apparatus adopting hot air jet method.

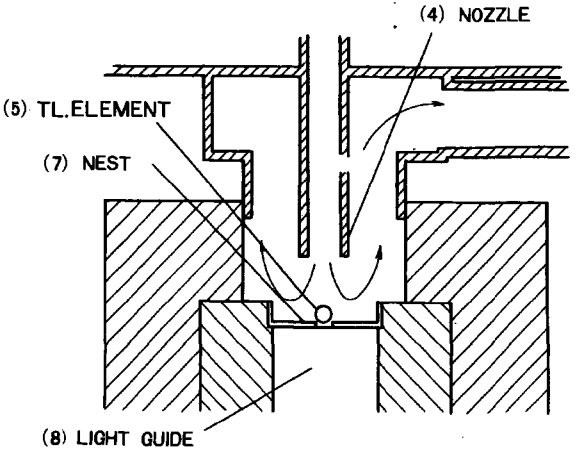

Fig. 2 Heating chamber of the apparatus.

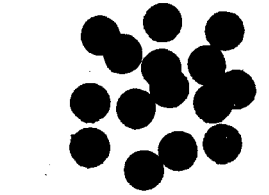

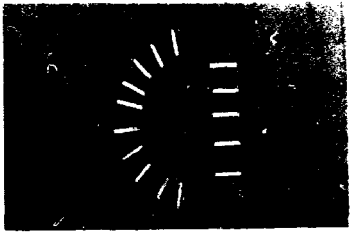

Fig. 3 Example of dosimeters adoptable to the apparatus.

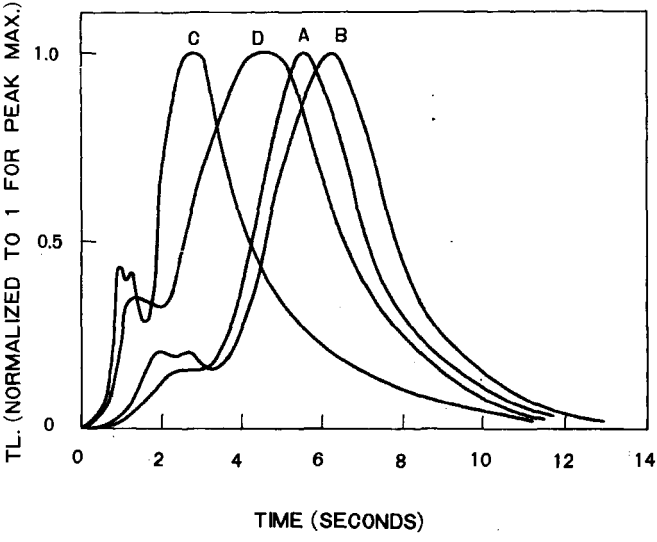

Fig. 4 Glow curves of dosimeters with different shapes:
(A) rod (2 mm x 12 mm) (B) sphere (3 mm)
(C) thin disc (10 mm x 0.1 mm) (D) disc (10 mm x 1 mm)

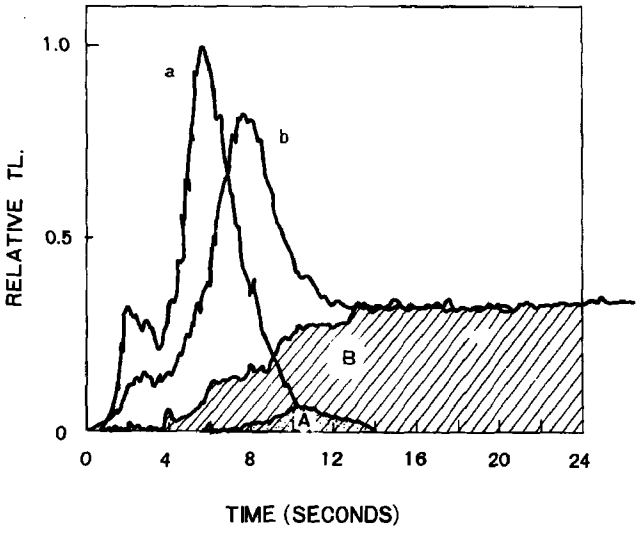

Fig. 5 A comparison of thermal radiation noises emitted from heating parts of two types of apparatus: (a: signal, A: thermal noise) and direct heating type (b: signal, B: thermal noise).

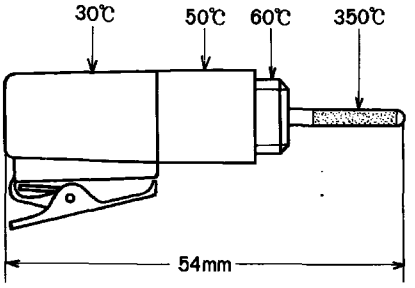

Fig. 6 Temperature distribution of a dosimeter for personnel monitoring (the highest temperature in one cycle of heatings).

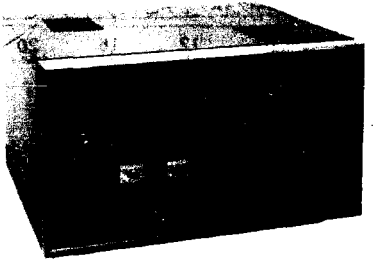

Fig. 7 Picture of the readout instrument.

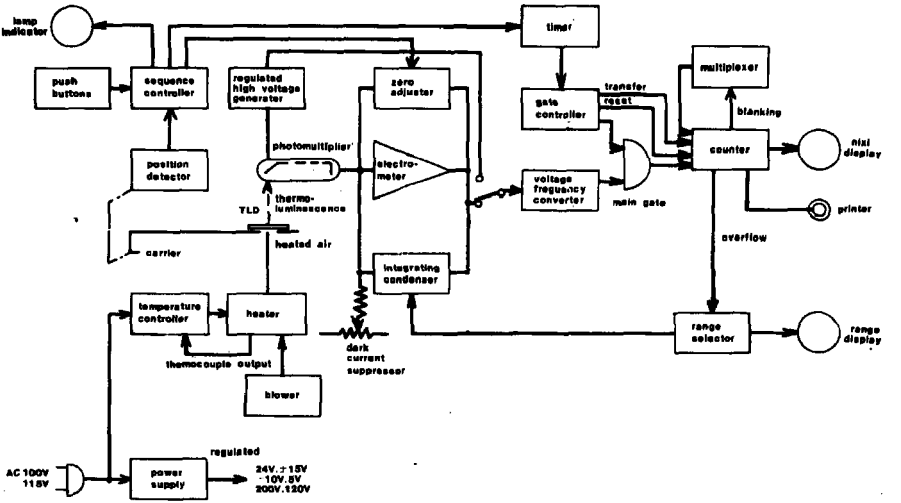

Fig. 8 Block diagram of the readout system.

Becker

I would just like to add that the performance of this instrument is indeed impressive. With the $CaSO_4$:Tm encapsulated in special glass capillaries (no self-dosing), a reproducibility of about 0.1 mR can be obtained in measurements of gamma-ray exposures.

The Emission Spectra of Various Thermoluminescence Phosphors

by

K. Konschak, R. Pulzer and K. Hübner

Technische Universität Dresden, Sektion Physik, Dresden, DDR

Abstract

A measuring equipment for the continuous determination of the emission spectra of thermoluminescence is described. The emission spectra of LiF (Dohnalum 200 Ti), synthetical CaF_2: Mn and an Al_2O_3 ceramic are given. The influence of the absorbed dose on the emission maximum of CaF_2 is shown. The emission spectrum at the photostimulated thermoluminescence was investigated.

Introduction

The investigation of the emission spectra of various TL phosphors was done in order to obtain optimum conditions for photomultiplier and filter in a TL reader.

The spectrum can be measured either pointly or continuously. The measuring expense at the continuous determination is smaller whereas the evaluation is more expensive because of the necessary corrections. The point determination of the emission spectrum requires a high reproducibility of the function. Because we did not obtain this yet the given spectra were measured continuously.

Experimental

The measuring equipment for the continuous determination of the emission spectra consists of 3 function units:

1. TL light production
2. TL light dispersion
3. TL light registration.

The production of the TL light results by indirect heating of the TL phosphor. The phosphors (powder or pellet) were heated in a heating planchet with a diameter of 8 mm and the heating rate is 8 deg/sec.

The 2nd function unit essentially contains the optical part of the device which consists of the beam splitting and the monochromator. Fig. 1 shows the beam splitting which devides the light into 2 components by the aid of a semipermeable mirror. One componentreaches the monochromator and is dispersed there spectrally and with the other component the TL intensity during the measuring time is recorded which is necessary for the correction of the spectrum. The change of the wavelength ensues by the aid of a synchronous motor which is coupled with the wavelength drum of the monochromator. At a revolution frequency of 6 rpm the wavelength range from 360 to 720 nm is measured in 1 minute.

The TL light was detected by a photomultiplier EMI 9524 A. The spectra were recorded with a x-y-recorder which writes immediately the TL intensity as a function of the wavelength.

Results

At the continuously measured spectra one must presume that the spectrum does not change in dependence of temperature.

Visual observations of the emission light of phosphors which were irradiadet with nearly 1 Mrad had shown a color change with increasing temperature. Therefore the spectrum can only given for a few phosphors where this was not observed.

These are LiF (Dohnalum 200 Ti), synthetical CaF_2: Mn and an Al_2O_3 ceramic. At CaF_2 a mixed color is possible, whereas at the ceramic at low temperatures blue light is observed which is not captured at the measurement.

Fig. 2 shows the corrected spectra for the 3 phosphors. These spectra are obtained after results correction for semipermeable mirror, monochromator and photomultiplier response, spectral slit width and TL intensity. The phosphors were irradiadet with

^{60}Co gamma radiation with 20 Krad at a dose rate of $6 \cdot 10^4$ rad/h. The emission maxima are for LiF at 410 nm, CaF_2 at 510 nm and for Al_2O_3 in the red.

In Fig. 3 the influence of the absorbed dose on the emission maximum of CaF_2 is shown. At irradiation with 4 Mrad the emission maximum shifts about 15 nm to lower wavelengthes in comparison to that at 10 krad. This dose dependence should be reduced to structural changes in the lattice structure. These can change both the natural absorption within the crystal and directly influence the activators.

One can repeatedly read off a thermoluminescent dosimeter if the dosimeter after the read out is irradiated with UV radiation (photostimulated TL). It is very interesting to investigate the emission spectrum of the thermoluminescence during the repeated read out. A phosphor irradiated with 1,6 Mrad was normally heated and after this 5 minutes irradiated with a mercury vapor lamp. The glow curve measured after this is in conformity with a primary irradiation with 30 krad. The emission maximum after this UV irradiation agrees with that which is observed with such a gamma dose.

This work was done under contract with VEB RFT Meßelektronik "Otto Schön" Dresden.

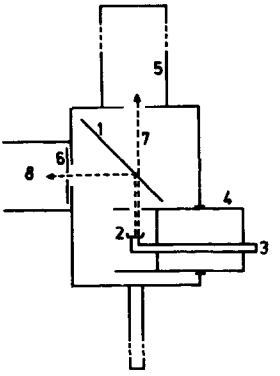

1 semipermeable mirror
2 heating planchet
3 current feeding
4 holder of the heating device
5 photomultiplier (for glow curve)
6 diaphragm
7 light for glow curve
8 light to the monochromator

Fig. 1: Beam splitting

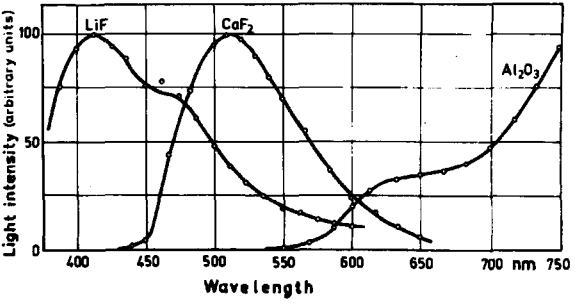

Fig. 2: Emission spectra of LiF, CaF_2 and Al_2O_3

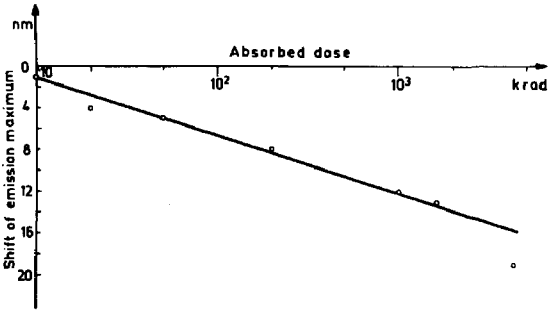

Fig. 3: Shift of the wavelength of the emission maximum as a funotion of the absorbed dose for CaF_2

Schlesinger

Cannot part of the supralinearity in LiF be explained by the change in the emission spectra of the phosphor after a high exposure, since the efficiency of the photocathode is a function of the light wave-length?

Hübner

We have not yet examined this possibility.

Suntharalingam

You may recall that at the last conference in Gatlinburg Peter Bloch from the University of Pennsylvania looked at supralinearity and its correlation with the TL emission at two separate wave-lengths. He indicated the response to be linear at one wave-length and supralinear only for the other component. The data presented here for synthetic CaF_2:Mn show a shift in the emission peak wave-length with increase in dose in the kilorad region even though the material does not show any supralinearity. Hence, I am not too sure whether there is any relation between supralinearity and fine structure of or changes in emission spectra.

Sunta

Any change in spectral quality of TL emission with dose can be very consequential in observed TL response. You have shown a slight shift in the peak wave-length of emission. I have observed a much more drastic change of spectral quality in the case of natural CaF_2 when the exposure is increased beyond 1000 R. Two distinctly new wave-lenghts appeared in the spectrum indicating the creation of new types of centres.

Some Thermoluminescent Properties of Quartz and its Potential as an "Accident" Radiation Dosimeter.

by

David J. McDougall
Mineral Physics Laboratory
Dept. of Geology, Loyola College,
Montreal, Canada

Abstract

Both natural and artificial pressure and thermal effects may be of considerable importance in modifying the thermoluminescence of quartz. Static loading of the order of 1 kilobar may cause increased thermoluminescence in one peak and impact loading of the order of 100 kilobars may decrease the height of the peak and increase the height of another. Cyclical loading can produce large increases in the emission. The maximum radiation sensitivity of the "radiation" peak occurs after annealing at 400°C. Below the 573°C crystallographic transition, high temperature peaks are annealed out but may reappear after annealing above the transition temperature. The variations in peak heights due to pressure and thermal effects are speculatively ascribed to changes in the concentrations of either lattice dislocations or oxygen defects, with metallic impurity ions playing a minor role.

The widespread occurance of quartz in sands, rocks and concrete makes it a potentially useful "accident" radiation dosimeter for approximate measurements provided that certain conditions can be met. Pronounced shock or thermal events concurrently or following the accident would seriously limit its usefulness.

Some Thermoluminescent Properties of Quartz and its Potential as an "Accident" Radiation Dosimeter.

by

David J. McDougall
Mineral Physics Laboratory
Dept. of Geology, Loyola College
Montreal, Canada.

Introduction

Quartz is the second most abundant mineral found in rocks and soils at and near the earths surface. In some sands, gravels, sandstones, conglomerates, quartzites and quartz veins, the composition is nearly pure SiO_2, and quartz is an important constituent of many rocks of sedimentary, igenous and metamorphic origin. It is a common associate of many ore deposits in the form of veins and silicified zones and is present in varying amounts in many soils. In addition, it normally forms a substantial part of concrete aggregates and is frequently a minor constituent in clays used for ceramics. It is usually thermoluminescent and because of its common occurance is a potentially useful material for a wide spectrum of investigations which depend on crystal lattice defect concentrations. A number of recent papers have been concerned with the use of the thermoluminescence of quartz for radiation dosimetry,[1] archaeological dating,[2] geological studies of the sources of sedimentary materials[3] and strain effects in concrete,[4] mine pillers and in the vicinity of underground nuclear explosions.[5,6]

The composition (SiO_2) and the crystal system (hexagonal) appear deceptively simple and may lead to the erroneous conclusion that a simple thermoluminescence response can be expected. Unfortunately, the occurance and distribution of impurity elements is non-uniform; the crystallography is complicated by

twinning, right and left hand forms and several reversible and irreversible phase transitions: it has both pyroelectric and piezoelectric properties; and may be formed throughout large ranges of both temperature and pressure. Several attempts have been made during the last few years to determine the effects of impurity elements on the thermoluminescence of naturally occuring quartz and artificially prepared SiO_2. [7,8,9] Divalent and trivalent iron, germanium, titanium, aluminium, lithium, oxygen and oxygen vacancies have all been suggested to have an effect on the thermoluminescence response. However, it would seem difficult to draw any clear conclusions from the published data because of the variety of procedures and equipment employed, and since, in some cases, contradictory results have been reported. Recent work, some of which is outlined below, suggests that at least some of the contradictory data may have been due to unrecognized pressure and/or thermal effects. Any one of the factors noted above may be reflected in the thermoluminescence response and some caution should be exercised in making comparisons with the thermoluminescence of artificially prepared alkali halides.

Pressure Effects

Recent work in several laboratories has shown that some indication of strain events can be deduced from the thermoluminescence glow curves of a number of rocks and minerals which have been subjected to either static or impact loading. [10,11,12]

Data obtained in the writer's laboratory from naturally and artificially loaded quartz and quartz-bearing rocks indicates that pressure effects may cause very large increases and decreases in thermoluminescence depending on the amount, kind and rate of loading. Some of this work can be summarized as follows:

Quartzites from the vicinity of the Sedan underground nuclear explosion in the western United States, which had been subjected to peak shock loads ranging from about 100 kilobars to in excess of 500 kilobars showed a systematic reduction in the height of the low temperature natural peak with increasing shock. This reduction resembles the decrease due to decreasing the particle size of the samples. However, the higher temperature natural peak of the shocked samples behaves quite differently and shows an irregular and sometimes quite large peak enhancement with increasing impact load [6] (Figure 1). Somewhat similar results have been obtained from limestones in the vicinity of meteorite craters. [10] Thermal activation energy values (in electron volts) obtained by the initial rise method from the artificially excited low temperature "natural" peak increase nearly uniformly with increasing shock, while the same kind of data for the artificially excited "radiation" peak shows an initial rise followed by a sharp decrease [5] (Figure 2). Petrographic and defractometer data obtained from these samples has shown that this decrease coincides with conversion of the quartz to silica glass at shock loads of the order of 500 kilobars. [6]

Slow static loading of the quartzite rock mine pillers of a Canadian uranium mine has resulted in an increase in the natural thermoluminescence of the quartz in cases where the loads approached 1 kilobar. The artificially excited thermoluminescence of both the radiation peak and the natural low temperature peak was found to vary somewhat erratically within a narrow range, but the thermal activation energy of the radiation peak increased

uniformly with load [5] (Figure 2). Concrete cylinders prepared from quartz sand and cement which had been artificially failed in unconfined compression at loads of about 0.7 kilobars also exhibited some apparently non-systematic variations in natural thermoluminescence [4] which appear to be equivalent to the variation in the mine piller quartzites subjected to the same loads.

A sample of granite composed of feldspars, quartz and biotite, which had been artificially failed in unconfined compression at about 1.5 kilobars had somewhat higher radiation and natural thermoluminescent peaks in the crushed portion of the sample than were obtained from essentially underformed samples. A small peak shift to slightly lower temperatures occured in the failed portion of the sample. However, samples which had been repeatedly cycled from zero load to near ultimate strength showed a very large increase in peak height (approximately 5x) a marked decrease in the radiation peak temperature (about 30°C) and flat topped peaks. Both the temperature shift and the flat topped peaks appear to be due to the growth of a new peak in close proximity to the normal peak. (Figure 3) Granite samples which were obtained from the vicinity of two well defined faults in the western United States gave very similar results, with large thermoluminescence values extending out from the faults for roughly 150 meters, lower values within the crush zones of the faults and still lower values at distances in excess of 150 meters of the faults.[3] In these samples, the bulk of the thermoluminescence was obtained from the feldspars with lesser amounts from the quartz. No thermoluminescence would be expected from the biotite.

Thermal Effects

The effects of thermal annealing of crystal lattice defects on the thermoluminescence of several natural and artificial materials has been recently examined in a number of laboratories. [13,14,15,16,17] In a somewhat comparable way to pressure effects, thermal treatment may cause either increases or decreases in thermoluminescence which depend in part on the material and its "history" and in part on the annealing temperature. As one example, the relative rate of decrease in two thermoluminescence peaks with increasing annealing temperature (different rates of annihilation of lattice defects) provides an indication of the temperature of formation of fluorite (CaF_2). [15] In addition, the x-ray excited growth of thermoluminesconce in annealed and unannealed fluorites has been shown to be due to a single stage of growth in the lower temperature peak and two stages of growth in the higher temperature peak [17], which can be interpreted as reflecting two kinds of lattice defects.

Similar experiments have been carried on the thermal annealing of quartz to those done on fluorites. A number of quartz samples were selected which had formed under a large range of temperature conditions (Table I). Portions of these were annealed for two hours at several temperatures between 200°C and 600°C and the thermoluminescence response obtained for x-ray doses up to 1000 rads for both annealed and unannealed samples. Examples of curves for thermoluminescence versus annealing temperature and thermoluminescence versus dose are illustrated in Figures 4 and 5. The following characteristics were observed:

1. In unannealed samples:

a) The low temperature peak (circa 100°C) was never completely drained in the unannealed samples and the order of magnitude of this peak roughly reflects the probable temperature of formation of the sample.

b) A "normal" growth with increasing dose was observed for the low temperature peak.

c) In unirradiated samples, the higher temperature peaks were usually unsaturated and, with one exception (sample 4), did not reach saturation with the doses used.

2. In annealed samples:

a) The maximum sensitivity for the low temperature peak (circa 100°C) was usually obtained after the 400°C annealing treatment. At this annealing temperature the order of magnitude of the peak appears to reflect the probable temperature of formation more accurately than in the unannealed samples. Sample 6 (flint) and sample 7 (chert) which had formed at low temperatures gave anomalous results.

b) In general, the thermoluminescence versus dose curves of the low temperature peak at each annealing temperature appeared to differ only in the sensitivity.

c) Annealing at 400°C eliminated almost all of the higher temperature peaks. However, a somewhat erratic peak at about 200°C continued to be present in samples 4 and 7 up to the 500°C annealing temperature. Annealing at 600°C appeared to produce a

new peak at about 200°C in samples 1, 2 and 4.

d) In contrast to its behaviour in the unannealed samples, the circa 200°C peak saturated at the lowest dose used (166 rads), and sometimes decreased at higher doses after being annealed at 200°C.

Some Dosimetry Experiments with Limestone, Quartz and Concrete

Figure 6 illustrates thermoluminescence versus dose curves for several samples of limestone (A,B,C,F), quartz sand (E) and concrete (D).

The limestone samples A,B and C were obtained respectively at distances of 300, 150 and 1 meter from the contact of a medium sized igneous intrusive and the increase in the thermoluminescence in the direction of the contact is indicative of a natural thermal effect. A strain effect due to faulting is also present as is shown by the low temperature natural peak being substantially higher than the high temperature peak. Limestone sample F has also suffered some thermal effects due to some nearby igneous dikes, but the nearly equal height of the natural peaks indicate an unstrained condition. In all the limestone samples the two natural peaks are essentially saturated for the x-ray doses used (up to approximately 500 rads). For these limestones, thermal decay at room temperature of the radiation peak reduced it to about zero within 24 hours.

The normally unsaturated state of the principle natural quartz peak is shown in the thermoluminescence versus dose curve for sample E, but the completely drained state of the radiation peak appears to be somewhat abnormal. The thermal decay at room temperature for the quartz sample is shown at the

bottom of Figure 6 and appears to have reached equilibrium in about four to six hours, with both the radiation and natural peaks maintaining a higher level than was found for the natural peak in the unirradiated sample.

The concrete sample D was made of non-thermoluminescence portland cement, sample E (quartz sand) and sample F (limestone). The thermoluminescence versus dose curve is a composite of the curves for the two thermoluminescent materials, with the quartz component dominating. However, the decay curve for a 500 rad dose at room temperature was found to more nearly resemble the decay curve for the limestone and the radiation excited effect had virtually dissappeared with 24 hours.

Conclusions

Although still in the preliminary stages, investigations of pressure and thermal effects due to natural and artificial processes on the thermoluminescence of quartz show clearly that both effects may bring about large increases and decreases of emission from some of the peaks. Both kinds of treatment may cause ranges of thermoluminescence which appear to be much larger than variations due to impurity ion content alone.

A static load of about 1 kilobar appears to be required to cause any appreciable increase in the natural thermoluminescence of quartz. Shock loads of 100 kilobars produce marked decreases in the low temperature natural peak, but may cause an increase in a higher temperature natural peak. Cyclical loading of granite suggests that similar treatment of quartz could result in a very high natural and artificially excited response. Within the load ranges examined both static loading and shock tend to make the

quartz a better "insulator" unless there is a change in state. As a generalization, the increases and decreases in thermoluminescence can probably be ascribed respectively to the creation and annihilation of crystal lattice dislocations.

Thermal annealing of many quartz samples at 400°C creates conditions of maximum sensitivity for the radiation peak. (circa 100°C) This sensitization does not appear to coincide with any obvious property of quartz, but it can be speculated that it may be related to either an excess or deficiency of oxygen. The probable relationship of the height of this peak to the temperature of formation of the sample may reflect the kind of impurity ion which can be incorporated in the lattice at a particular temperature. High temperature peaks tend to be removed when the sample is annealed at temperatures around 400°C, but in some instances may reappear when annealed at temperatures above the low quartz-high quartz reversible transition temperature (about 573°C). These high temperature peaks may be equivalent to the peaks resulting from fast rates of loading and hence may result from the formation of crystal lattice dislocations. Other lines of evidence indicate that annealing above the high quartz-high tridymite non-reversible transition temperature (870°C) can also affect the thermoluminescent emission.

Preliminary examination of the dosimetry characteristics of quartz suggest that the stabilization of the radiation excited peaks at a level somewhat above the thermoluminescence of unirradiated samples may make it a useful material to at least determine irradiated or unirradiated conditions following a radiation accident. This would require that a) a comparison

could be made with near by unirradiated material; b) the quartz could be concentrated from other associated materials; c) that there had been no pronounced thermal or shock events concurrently or following the accident. The most convenient procedure would involve core sampling of nearly pure quartz rocks or soils and comparison of thermoluminescence of the surface layer with material from a depth of several centimeters. The usefulness of other quartz bearing materials may depend on the ease with which the quartz can be concentrated. The separation of quartz from many materials such as granite or ceramics, involves hand picking and is not practical if a large number of samples are to be examined in a hurry. On the other hand, quartz can often be fairly readily separated from the limestone and cement used in many concretes by leaching with dilute hydrochloric acid.

Acknowledgements

Financial support for the work described in this paper was provided by the National Research Council of Canada, the Defense Research Board of Canada and Loyola College, Montreal. A blanket acknowledgement is extended to the many individuals who aided the writer by supplying sample materials and data on their geological environments, doing special test procedure in other laboratories and carrying out the thermoluminescence and allied investigations at Loyola College.

References

1. S.J. Fleming and J.Thompson, Health Physics, 18 567. (1970).
2. S.J. Fleming, Archaeometry, 12, 133-145 (1970)
3. J.M. Charlet, Modern Geology, 2, 265-274 (1971)
4. G.Douglas, in Proceedings 13th Symposium on Rock Mechanics, University of Illinois (in press).
5. J.W. Manconi and D.J. McDougall, Amer. Mineralogist, 55, 398-402 (1970).
6. N.M. Short, Journal of Geology, 78, 705-732 (1970)
7. G.W. Arnold, J. Phy. Chem. Solids, 13, 306-320 (1960)
8. W.L. Medlin, J. Chem Phys, 38, 1132-1143 (1963)
9. M. Schlesinger, J. Phys Chem, Solids, 26, 1761-1766 (1965)
10. D.J. McDougall, Meteoritics, 5, (1970).
11. M. Morency, Trans Amer. Geophys. Union, 51, 830-831 (1970)
12. M. Chaye-d'Albissin, Modern Geology, 2, 281-287 (1971)
13. J.R. Cameron, D.W. Zimmerman and C.R. Rhyner, Health Physics, 12,25, (1966)
14. G. Fornaca-Rinaldi, in Thermoluminescence of Geological Materials (Academic Press) 103-110, (1968)
15. D.J. McDougall, Economic Geology, 65, 856-861 (1970)
16. D.J. McDougall, Health Physics, 20, 452-453, (1971)
17. A.K. Menon, Modern Geology, 2, 289-292 (1971)

TABLE V

Description of Quartz Samples

Sample No.	Description	Source	Geological Process and Probable Temp. of Formation
1	Pink, transparent, macrocrystalline	unknown	Pegmatitic-in excess of 600°C
2	Blue, translucent, macrocrystalline	Southern Quebec	High grade metamorphic-500-600°C
3	White, semi-translucent macrocrystalline	Northwestern Quebec	Hypothermal-300-500°C
4	White with sulphides and free gold, translucent, macrocrystalline	Grass Valley Calif.	Mesothermal-200-300°C
5	Purple, transparent macrocrystalline	unknown	Epithermal-50-200°C
6	Flint nodule, dark brown, semi-translucent, cryptocrystalline	unknown	Sedimentary-less than 50°C
7	Chert, light grey, semi-translucent, cryptocrystalline	Southern Ontario	Sedimentary-less than 50°C

Figure Captions

Figure 1—Crushing and impact effects on natural TL of quartzites.

Left: Decrease in particle size causes uniform decrease of natural TL in circa 100°C and circa 200°C peaks (60 mesh = 0.25mm, 100 mesh = 0.149mm, 200 mesh = 0.074mm, 400 mesh = 0.037mm)

Right: Increasing shock (instantaneous loads to in excess of 500 Kb on arbitrary scale of 0 to 6) causes decrease of natural TL of circa 100°C peak and erratic response in circa 200°C peak.

Figure 2—Impact and static load effects on artificially excited TL and thermal activation energy of quartzites.

Left: Increasing shock (instantaneous loads to in excess of 500 Kb on arbitrary scale of 0 to 6) cause decrease of x-ray excited TL of circa 60°C peak (A) and circa 100°C peak (B). Thermal activation energy values increase uniformly for B but rise and then decrease at a load at which quartz is partially or completely converted to a glass (± 300 Kb).

Right: Increasing static loads up to approximately 1 Kb (14 K) cause somewhat irregular responses in x-ray excited peaks A and B. At loads somewhat less than 1 Kb the natural TL of peak B appears to increase in response to increasing load.

Note: TL peak heights in Figures 1 and 2 cannot be directly compared.

Figure 3—Controlled loading effects on x-ray excited TL of granite (50 rad dose).

Left: Cyclical loading from 0 to about 1.5 Kb causes large increases in peak heights, peak temperature shifts and appearance of new peaks.

Center: Static loading to failure at about 1.5 Kb causes noticeable increase in peak heights of portion of sample in which failure occured (curve 2)

Right: Static loading at very low level caused imperfectly prepared sample to crack. Central portion of sample (curve 2) probably represents "normal" TL of the rock.

Note: Little or no difference was found in the heights of the circa 300°C peak(s) in irradiated and unirradiated samples. Standard deviation from the mean of the peak heights from replicate runs on each sample was usually less than 5% and never exceeded 10%.

Figure 4—Effects of annealing temperature on the TL of quartz.

The maximum sensitivity of the circa 100°C peak usually occurs after annealing at 400°C. See Table I for description of samples. Annealing time for each temperature was two hours; x-ray dose for these curves = 1000 rads.

Figure 5—Effects of x-ray dose on TL of annealed quartz.

Pink quartz (sample 1), white quartz (sample 4)

In both quartz samples the circa 100°C peak appears to behave in a normal fashion in response to dose. However

in the pink quartz, the circa 200°C peak saturates at low dose when annealed at 200°C, disappears when annealed at 400°C and reappears when annealed at 600°C. The behavior of the circa 200°C peak in the white quartz shows some similarities but is more erratic.

Figure 6-Effects of x-ray dose on TL of limestones, quartz and concrete.

Top: Samples A,B and C are limestones taken respectively at distances of 300 meters, 150 meters and 1 meter from an igneous contact. Sample D is concrete made from non-thermoluminescent portland cement and Samples E and F. Sample E is quartz sand and Sample F is limestone from a quarry in which there are a number of igneous dikes. The spread between the first and second peaks in the limestone samples is a rough indicator of the amount of strain in the rock. The general increase in TL towards the igneous contact (A,B and C) reflects a natural thermal effect.

Bottom: Room temperature decay curves for x-ray excited TL peaks for quartz sand sample E. Decay time in excess of four days.

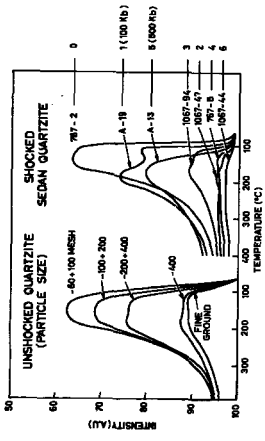

Figure 1.

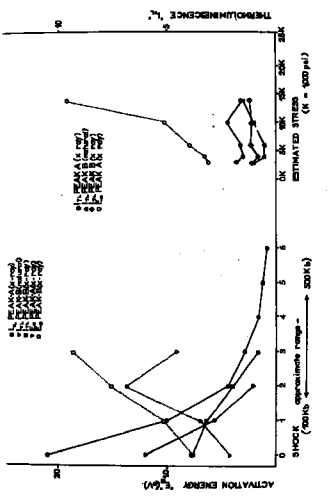

Figure 2

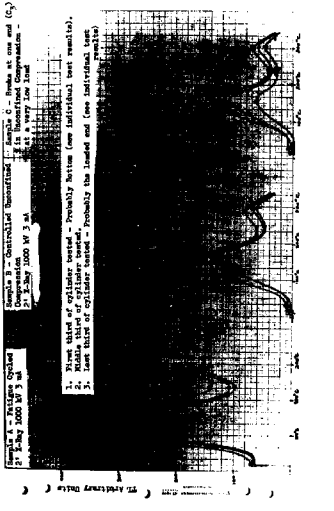

Figure 3

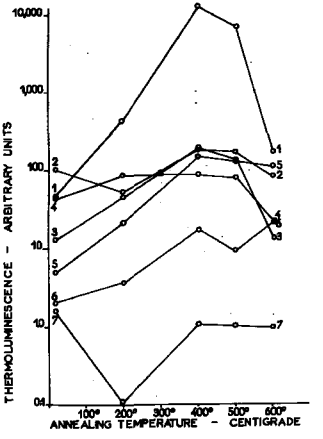

Figure 4

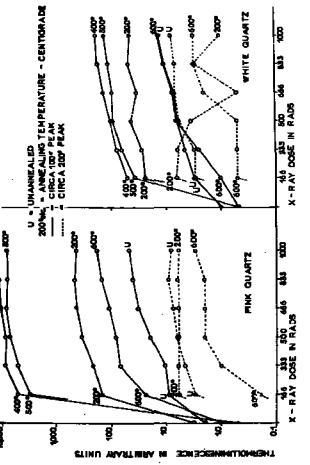

Figure 5

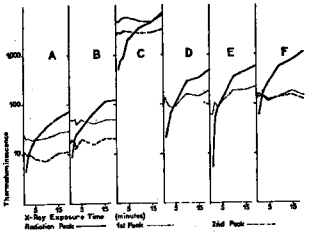

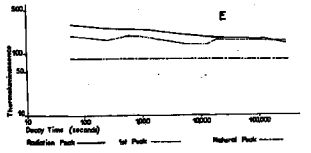

Figure 6

Thermoluminescent Enamels

by

M.Mihailović
Medical Faculty
University of Ljubljana, Yugoslavia

V.Kosi
Chemical Institute "Boris Kidrič"
Ljubljana, Yugoslavia

Abstract

About thirty variaties of TL enamels have been developed and their dosimetric properties investigated. In the following, six variaties of TL enamels and their properties will be presented. Some of them have favourable dosimetric characteristics: They have a simple glow curve. They are linear up to 5.10^4 R Co^{60} γ-ray exposure. They have no fading. The response at 22 KeV_{ef} is fifty persent higher than at 1,25 MeV.

Pre-irradiation annealing experiments at 200°C, 260°C, 320°C and 400°C have been performed. The sensitivity of the borocalumino silicate glass type with lithium content depends appreciably on the temperature of the pre-irradiation annealing. However, the enamels of borocalumino silicate type without lithium but with melt in grains of lithium silicate, are rather independent on the temperature.

The influence of pre-irradiation annealing at 260° and 400°C on fading characteristics has been investigated. The experiments have shown that pre-irradiation annealing has influence on fading.

1. INTRODUCTION

In our earlier work (M.Mihailović[1,2]) TL boroalumino silicate glass has been used as means by which the active CaF_2:Mn was fixed on a silver strip. These, CaF_2:Mn enamel coated dosemeters have many advantages. They are easy to manipulate, they can be reproducibly heated, directly or indirectly, there is no problem of overheating them. They were linear from 5.10^{-2} R to 10^3R Co^{60} γ- radiation, but they had rather unfavourable dependance in the region from approximately 20 KeV to 140 KeV, and they had fading of approximately 30 % in the first three days after irradiation.

In the present investigation we concentrated on the development of TL enamels with better dosimetric properties. We studied boroalumino silicate glass with lithium and without lithium. New TL enamels retained all good properties of earlier enamels, in addition they have following favourable properties: a simple glow curve with one peak only, no fading, a convenient energy dependance.

In the following we shall also report some data on the influence of the pre-irradiation annealing on the fading.

In all experiments peak height of the glow curve was measured. The dosemeters were heated directly by the current which flows throught the silver strip. The heating cycle lasted 30 seconds, the heating rate was 18,0°C/s.

2. THERMOLUMINESCENT ENAMELS

Two types of enamels regarding their chemical composition will be presented. TL enamel of type GL is made from boroalumino silicate glass with lithium as glass forming component. This type will be presented with samples GL 15, GL 3, GL 6. The samples GL 6 and GL 3 have no aluminium oxide, have different alkali and earthalkali metal content. The other type, let us call it type GR is made from boroalumino silicate glass without lithium but with melt in grains of lithium silicate (GR 37) or lithium silicate with B_2O_3 (GR 35, GR 36, GR 38).

All enamels were made from p.a chemicals in a reaction where all components were heated in air at 1100 - 1300°C in a platium crucible. When melted, the enamel was poured on a platinum plate and cooled. After that it was ground, sieved and mass of 80 mg put in a hollow of the silver strip. The enamels of type GL were heated up to 700 - 850°C until they were melted. The enamels of type GR have one component of heigh melting point. It was ground to powder size from 0,2 - 0,5 mm and mixed with an inactive low melting enamel which melts during heating at about 750°C. Most of the dosemeters were baked in argon. The effective atomic numbers of enamels GL 15, GR 35, GR 36, GR 37 are 12.9, 10.3, 11.4, 9.96 respectively.

Glow curves of TL enamels belonging to type GL (GL 15, GL 3, GL 6) are shown in Fig. 1a and those of type GR (GR 35, GR 37, GR 38) in Fig. 1b.

The samples GL 3 and GL 6,as well as,GR 35 and GR 36 *differ only slightly* in composition and their glow curves are quite similar. It is not quite clear why the sample GR 37 (with incorporated lithium silicate grains) has such complicated glow curve. Its sensitivity is, however, appreciably heigher than those of sample GR 35 and GR 36.

So far no attempts have been made to identify the activator in TL enamels.

3. PROPERTIES OF TL ENAMEL DOSEMETERS

TL enamels were used to construct different types of dosemeters. One of the most useful property of the enamel

is that different types of dosemeters can be made easily. The dosemeters can be heated with built in heating coil. For indirect heating, all dosemeters can be made in form of solid pellets of any size, with or without silver tray. The dosemeters with silver tray have very good heating characteristics. The enamel sticks perfectly to the silver, which is very good conductor so that the temperature is uniform over the whole surface.

3.1. Sensitivity, linearity, and supralinearity

Sensitivity, linearity and supralinearity of the response to the gamma-ray dose were also studied.

The sensitivity of the TL enamels with the simple glow curve is usually lower, than those with rather complicated glow curves. Sensitivities to Co^{60} γ-rays of different enamels varies by factor 5, approximately. The linearity has been measured from 0,1 R to 25 R with filtered x-ray source, and from 3o R to 3.10^3 R on Co^{60} γ-ray source. The supralinearity was not observed in this region, except for one enamel.

3.2. Annealing effects

When the dosmeters are exposed to doses higher than 1 R, they have to be annealed. The erasing of remaining dose can be carried out in the reader through its 3o second heating cycle, or it can be annealed in the oven on 36o°C for 5 minutes. The final effect will be the same. An experiment was carried out to determine which procedure is more appropriate. All dosemeters were annealed at 36o°C for 5 minutes, exposed to 6 R x-ray dose and measured. Then the dosemeters were heated through the 3o second heating cycle, exposed to 6 R x-ray dose and measured. The ratio of the peak height measured when the remaining dose was erased in the oven and when erased in the reader is given in Table I. It can be seen that the response of most

dosemeters is higher when erased in the oven than when erased in the reader. The shape of the glow curve remained the same. After this experiment it was decided to adopt the annealing in the oven on 36o°C for 5 minutes.

TABLE I.

The influence of the annealing on the sensitivity of the TL enamels. In the left collomn is the type of the enamel and on the right is the ratio: (Peak height after annealing in oven at 36o°C for 5 minutes)/(Peak height after the annealing in the reader).

GR 35	1,2
GR 37	1,2
GR 38	1,4
GL 15	1,4
GL 3	1,o
GL 6	o,7

Experiments have been made also with pre-irradiation annealing at 2oo°C, 26o°C, 32o°C and 4oo°C in order to determine the influence of the annealing temperature on the sensitivity. The dosemeters were heated to predetermined temperature for one hour, then exposed to 6 R x-ray dose and measured. The TL response for each dosemeter was compared with response after the standard annealing (at 36o°C for 5 minutes).

The results are shown in Fig. 2. Two groups of dosemeters behave differently. The sensitivity of the "glass" enamels of the group GL (GL 6, GL 15, GL 3) changes appreciably with the temperature, the sensitivity being the lowest around 26o°C. On the other hand, the "grain" enamels GR 35 and GR 36 are rather independent on the

temperature of the annealing. Comparing the sensitivities in Table I (5 minutes of annealing) and those in Fig. 2 (1 hour of annealing) one sees that the duration of the annealing has a small influence on the sensitivity.

3.3. Fading

A rather large fading in our old enamel coated dosemeters (30 % in 3 days) was one of the reasons why we continued the investigation of TL enamels. The investigation of the fading of the TL enamels showed that (i) there exists an anomalous fading and (ii) that the pre-irradiation annealing influences the fading.

We adopted the following experimental procedure. The dosemeters were annealed in the oven at 360°C for 5 minutes, exposed to 6 R x-rays, left in dark for 1, 3, 7, 14 days and measured after each time interval. Another group of dosemeters was annealed again at 360°C for 5 min., exposed to Co^{60} γ- rays at different times, left in dark and read out together at the same day. Both procedures provided similar results. The results are shown in Fig. 3 (curves "No annealing").

In order to get the influence of the pre-irradiation annealing on the fading, the dosemeters were annealed for one hour at 260°C, exposed to x-rays and then treated as described earlier. The same was repeated with annealing at 400°C. The results are in Fig. 3 (Curves "260" and "400"). The enamels of the type GR seem to be unaffected by the pre-irradiation annealing. However, the pre-irradiation annealing reduces the rather large anomalious fading in the "glass" enamels of the type GL.

3.4. Nonirradiation - induced thermoluminescence

Nonirradiation-induced TL appears in both GL type and GR type of enamel dosemeters. It can be provoked by shaking and by rubbing. Both peaks are in high temperature range.

Two types of peaks were observed depending on the method of provoking it. Their relative position and the glow curve for 300 mR Co^{60} γ-ray dose for dosemeters GL 15 and GR 37 can be seen in Fig. 4. The shape of their glow curve is rather different from the usual glow curve.

The existence of nonirradiation-induced TL limits the low dose measurements. Low limit for γ-ray doses varies from 0,15 R (GL 15) to 3 R (GR 35).

3.5. Energy dependance

The energy dependance of the dosemeters was measured under the conditions given in Table II.

TABLE II.

Characteristics of radiation beams used to investigate wave lenght dependance

KV_p	Aprox. inherent filtration	Added filtration	Aproximate effective photon energy (KeV)
60	1,5 mm Al	-	22
60	1,5 mm Al	2,5 mm Al	30
100	1,5 mm Al	0,53 mm Pb 2,5 mm Al	70
150	1,5 mm Al	1,5 mm Al 4,0 mm Cu 2,5 mm Al	120
200	1,5 mm Al	0,7 mm Pb 4,0 mm Sn 0,6 mm Cu 2,5 mm Al	170

Energy dependance of dosemeter GL 15 is quite pronounced. Response on 22 KeV_{cr} energy is approximately 5 times higher than the response at 1,25 MeV. The response of dosemeters of the type GL, GL 3 and GL 6 is similar. Dosemeters GR 38, GR 36 are less sensitive in energy region around 22 KeV_{ar}.

The response of GR 36 at 22 KeV_{ar} is approximately twice as high as that at 1,25 MeV.

4. DISCUSSION

We investigated the TL-enamels rather sistematically.

4.1. The results can be summarised by saying that it is possible to make an enamel with good dosimetric properties.

The characteristics of good enamels are demonstrated in the measurement of the dosemetric properties of the dosemeters. Both dosemeters of type GR 35 and GR 36 have the simple glow curve, no fading, satisfactory linearity.

There are two other convenient characteristics of the dosemeters of the type GR 35, GR 36. (i) The dosemeters produced in one series do not differ appreciably in sensitivity. (All other types of dosemeters we produced differ in sensitivity up to 30 %). (ii) The shape of the glow curve is stable under any condition of irradiation. This is not the characteristic of all TL enamels, some of them changed the relative height of the peaks when irradiated at different energies.

The sensitivity to low doses is rather low, for the moment. We hope it can be improved.

4.2. The influence of the pre-irradiation annealing on the fading was noticed in all TL enamels. The measurements showed that the fading can be reduced by choosing the proper pre-irradiation annealing procedure. Further investigations are needed.

REFERENCES

1.) M.Mihailović, V.Kosi, M.V.Mihailović, Z.Milavc:
An Enamel Coated CaF_2:Mn Thermoluminescent Dosemeter and the Reading Instrument,
Phys.Med.Biol., (1967), Vol. 12, No 3, 395-402

2.) M.Mihailović:
Properties of an Enamel-coated CaF_2:Mn Thermoluminescent Dosemeter,
Proceedings of a Symposium, Vienna, October 1966

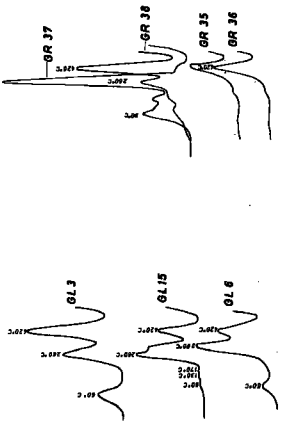

Fig. 1 a - Glow curves of TL enamels of the type GL
Fig. 1 b - Glow curves of TL enamels of the type GR

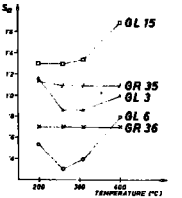

Fig. 2 - The influence of the temperature of the pre-irradiation annealing on the sensitivity of TL enamels. S_a - (Response after annealing at given temperature)/(Response after standard annealing).

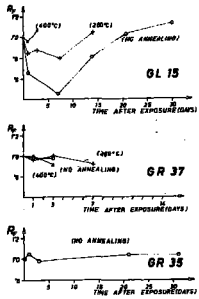

Fig. 3. Effect of the pre-irradiation annealing at 280°C and 400°C on fading. The ratio R_{tr} (Response at various times after exposure)/ (Response immediately after the exposure).

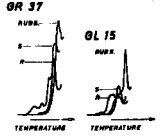

Fig. 4 - Glow curves of nonirradiation-induced TL (S-produced by shaking, Rubb - produced by rubbing with a cloth) and, R - the glow curve after 300 mR γ -ray irradiation

Spurny

When using p.s. chemicals only, have you always used the same or have you received chemicals from different factories?

Mihailovic

So far we have used chemicals from the same factory.

Thermoluminescent Phosphors based on Beryllium Oxide

by

Y. Yasuno and T. Yamashita

Central Research Laboratory
Matsushita Electric Industrial Co., Ltd.
Kadoma, Osaka, Japan

Abstract

Alkaline ions: M^{+1}(Li^{+1}, Na^{+1}, K^{+1}), trivalent ions: M^{+3}(B^{+3}, Al^{+3}), and tetravalent ions: M^{+4}(Si^{+4}, Ge^{+4}) in BeO were found to play a part to thermoluminescent ability of BeO. Controlled ceramics samples artificially doped with such ions were prepared by sintering method. In BeO:M^{+1}, a strong TL showing a main peak at 180°C was observed. Additional doping of M^{+3} besides M^{+1} caused the decrease of the main peak, but it did not disappear, moreover, it dominated in every sample, BeO:M^{+3} or BeO:M^{+4}, even if the intensity was small. At higher exposure level (supralinear region), another peak dominated: 230°C in BeO:M^{+1}(over 100R), 210°C in BeO:M^{+3} (over 40R) and 190°C in BeO:M^{+4}(over 10R). These peaks also appeared by light stimulation on the samples once exposed to high dose and annealed.

Among samples examined, BeO:M^{+1}, in particular BeO:Na, are excellent for TLD: (1) A linear response extending from 2mR to 1000R in BeO:Na, and from 1 mR to 2000R in BeO:Li, (2) Little fading of 180°C peak (initial fading of 5% in the first 1 day and followed fading of 2% in the next 30 days).

Introduction

Typical phosphors, of which the photoelectric absorption is equivalent to that of tissue, are LiF:Mg and:Ti [1] $Li_2B_4O_7$:Mn^{+2} and these phosphors are the most widely used. However, they have some disadvantages: the complicated annealing property of LiF as pointed out by Zimmerman[2] et al. and rather small linear range in $Li_2B_4O_7$:Mn^{+2}, in spite of a lot of trials to improve them.[3], [4]

The third material, which is expected to have both properties of tissue equivalent response and excellent thermoluminescence, is beryllium oxide BeO. Yoshiike[5] et al. investigated commercial BeO ceramics and found that some samples had efficient thermoluminescent properties. Becker[6] et al. made a wider examination on various commercial BeO ceramics in respect to impurities analytically contained and showed some relations between TL properties and TREE properties of BeO. In spite of these investigations, however, what component is effective to TL properties had not yet been clear.

Our trial has been started in the sense of obtaining controlled BeO phosphors containing impurity ions artificially doped and some informations about dopant impurities and TL characteristics were obtained. The preparation method of BeO ceramics containing such dopants and their TL characteristics are described.

Sample preparation and measurement

Purified BeO powder and dopant impurity powder were mixed in a proper ratio. The mixture was extruded into rods, sintered at more than 1800°C and cooled gradually. White ceramic rods of 1. 6 mm in diameter, 10 mm in length were obtained.

Figure 1 shows a microscopic picture of the surface of BeO:Na ceramics thus obtained. Crystal grains of 2-5 μ in size are observed.

Figure 2 shows a picture of X-ray microanalyzing pattern of the same BeO:Na sample observing the distribution of Na atoms in the BeO sample. The glittering dots in the picture correspond to the part containing large amount of Na (Na density of $1\text{-}2\times10^{21}$/cm^3) and the dark area corresponds to the part containing small amount of Na (Na density of about 3×10^{20}/cm^3; i. e. Na/BeO ≦0. 4%). By this observation, distribution of impurity Na in BeO matrix can be learned. Comparing the X-ray microanalysing picture (Fig. 2) with the microscopic picture (Fig. 1), we can know that some circular areas surrounded by white dots in Fig. 2 may correspond to crystal grains in Fig. 1, and that Na atoms occupy selectingly grain boundary of BeO crystals, however, appreciate amount of Na is also contained in the crystal bulk. Such a photographic analysis should give an important information in appreciating TL properties of samples as will be reported in the following sections.

A dosimeter sample was formed by encapsulating a obtained ceramic rod in a glass pipe of 0. 15 mm thick, otherwise, the ceramic sample may be soiled by dusts. Dosimeter samples thus obtained are shown in Fig. 3.

Glow curves were observed using an experimental thermoluminescence analysing instrument. Samples were heated by this instrument from 25°C to 400°C with a heating rate of 8°C/sec.

Thermoluminescence of BeO

Glow curve :

A strong TL was observed in BeO ceramics doped with some impurities, although raw material BeO exhibited little TL. Figure 1 gives the effect of dopant to the TL of BeO.

Beryllium oxide doped with an alkaline ion (BeO:M^{+1}), BeO:Li, BeO:Na or BeO:K, showed strong TL (Fig. 4-(A)). Their glow curves were simple with a peak at 180°C, which is expected to be applicable to a dosimeter. The TL intensity of BeO:M^{+1} increased as the ion content was increased and, then,

reached constant at about 0.4 mol%. The TL intensity of BeO:Li heat controlled was as large as 5 times that of LiF, and BeO:Na and BeO:K, as large as 3 times. (the minimal response of BeO:Li was 1 mR; 30% and that of BeO: Na, 2mR; 20%).

The addition of a small amount of B^{+3} or Al^{+3} besides M^{+1} markedly reduced the main peak at 190°C. *However, the peak did not disappear, but it* dominated in almost all samples even if it was very small. Figure 4-(B) shows glow curve of BeO:Al. The main peak was at 180°C but its intensity was smaller; 1/20 that of BeO:Na. Also, in BeO:Si and BeO:Ga, the 180°C peak dominated but its intensity was 1/10 that of BeO:Na. (Fig. 4-(C)).

Besides the main peak at 180°C, small peaks around 310-350°C and a shoulder at 100°C were observed in some samples. The high temperature peak around 290-350°C was observed, in particular, in BeO:Al, but was also observed in BeO:Si and others. This peak showed a property that when the sample was annealed at 400°C for 1 hour and cooled gradually it reduced extremely. The shoulder at 100°C was observed in some $BeO:M^{+1}$, but was so small as to be recognized only by a careful observation.

Glow curves at high dose level :

The dose responses of the obtained BeO samples, $BeO:M^{+1}$, $BeO:M^{+3}$ and $BeO:M^{+4}$, were linear up to some threshold value of exposure, within which the phosphors may applicable to a dosimeter. Over this threshold value, the response became supralinear, as observed in many other TL phosphors[4),9), 10)]. The glow curves in the supralinear region changed showing another peaks at higher temperature.

Figure 5 shows these changes of glow curves of BeO samples exposed to higher dose. In BeO:Na, as shown in Fig. 5(A), a new peak at 230°C appeared as dose was increased and at 10000R it dominated the glow curve. It is worthwhile to mention that, by carefull observations, the main peak kept its linear relation versus dose even at high dose level.

Similar relations were observed in other samples: in BeO:Al (Fig. 5-(B)), a new peak at 210°C appeared over 40R, in BeO:Ge and in BeO:Si at 190°C over 100R (Fig. 5-(C)).

The threshold dose of supralinearity was varied by dopant ions and their concentrations. In those samples doped with a small amount of M^{+3} or M^{+4}, the threshold dose was very small: it was 1-10R, whereas it was higher in those doped with a large amount of M^{+1}. It was 100R in BeO:Na and 2000R in BeO:Li.

Fading :

Fading properties of the main peak were investigated in detail.

Thermal fading : Figure 6-(A) shows the fading of BeO:Na stored in the dark at room temperature as observed by glow curves. It was seen that the main peak faded considerably rapidly in the first one day with a rate 9%/day and then very slowly with a rate about 3%/month thereafter.

This thermal fading of 180°C peak was accompanied by a small shift of peak temperature as shown in Fig. 6-(B), in which iso-chronomical observation of thermal fading was made. This temperature shift of glow peak means

that the main peak of BeO is composed of composite glow peaks, as pointed by Schulman[2] in case of $Li_2B_4O_7$:Mn.

Light fading : It was observed that fading was accelerated by visible light irradiation. The result of BeO:Na is shown in Fig. 7. The initial fading was 5% in the first 10 minutes, but it reached almost 90% in one day. In contrast to the case of thermal fading, little peak shift was observed.

Rapid fading spontaneously occure : A curious fading was observed in BeO: Li doped with large amount of Li^{+} ion. These BeO:Li, unlike other BeO, exhibited a large peak at 165°C. This peak faded rapidly to half its initial light in several hours in the dark, and, with this decay of the peak, the peak temperature shifted to 180°C. This rapid fading was also observed even in the samples stored at liq. N_2 temperature in the dark. This means that some unstable traps lie in BeO:Li, and that the electrons captured to the trap can be released without any stimulating energy. The initial rapid fading (as large as 5-8%) observed in BeO:Na may be the same phenomenon caused by traps unstable.

TL by spurious stimulation :

Tribo-TL : Beryllium oxide exhibited comparatively large tribo-TL compared with other TL phosphors such as $CaSO_4$. Figure 8 shows the glow curves of BeO:Na powder samples (100μ-300μ in size) suffered to some mechanical treatment without exposing to γ-rays. The glow curve (a) was obtained in the condition that the powder sample was shaken in a small container for fifty cycles (surface stimulation), and glow curve (b), in the condition that the powder sample was pressed by a pressing machine at 20 kg/cm^2 (bulk stimulation). It is characterizing in this figure that when the sample was shaken a broad peak near 230°C appeared, whereas when it was pressed another peak at 180°C, besides the peak near 320°C, appeared.

TL by light stimulation : Schayes[11] reported a light response in CaF_2 once exposed to γ-rays and annealed. A similar phenomenon was observed in BeO. Figure 9 shows glow curves of BeO:Na which were exposed to γ-rays at high dose, annealed at 400°C for 5 minutes and then exposed to light (3000 lux by fluorescent lamp) for an hour. A glow peak was observed at 230°C in this BeO:Na sample. When the exposed dose was less than 50R, the glow peak by light stimulation was undetectable. This phenomenon, however, disappeared by annealing procedure at higher temperature(more than 500°C). The *fact suggests that this light response is due to deeper traps. It is worth*while to mention that the glow peak caused by light stimulation did not appear at 180°C but it appeared only at 230°C.

Other samples such as BeO:Al and BeO:Ge also exhibited light response but their peak temperatures were 210°C and 190°C respectively. It should be noted that the peak temperature of the light stimulation agrees well with that of the supralinear peak in each sample.

Discussion

The glow peaks observed in BeO samples prepared are summerised in Table 1. The most dominant peak observed in many samples was that at 180°C, which was especially strong in $BeO:M^{+1}$. It was also observed in BeO

:M^{+3} or in BeO:M^{+4}, but its intensity was small. The cause of this trap may be some lattice defect usually formed in BeO lattice and M^{+1} may assistantly act to form this.

At higher dose level, a characteric peak of which the temperature is higher than 180°C appeared dominantly : 230°C for BeO:M^{+1}, 210°C for BeO: M^{+3} and 190°C for BeO:M^{+4}. Furthermore, a remarking fact is that each peak appeared also when each sample was heavily exposed, annealed and light-stimulated. The origin of these traps showing higher temperature peaks are characteristic to the valency of the doped ion and these traps may be different centers from that showing the 180°C peak.

Becker[8] observed a TL peak at 180°C and that at 210-230°C in commercial ceramics. Considering that his samples contained $M^{+}(Cu^{+1})$, M^{+3} (Al^{+3}) and $M^{+4}(Si^{+4})$, his results and ours are inconsistant. Tochilin[7] et al. observed in a commercial ceramics that the main peak shifted from 180°C to 230°C in the exposure range of 50-300R. As far as peak shift is concerned, the behavior of Tochilin's BeO is similar to our BeO:Al. It should be noticeable that the peak temperature of 280-350°C observable by surface stimulation in our BeO matches the temperature of TSEE peaks observed by Becker[8] et al.

As appointed by Tochilin[7] and Becker[8] in commercial ceramics, the main peak at 180°C is applicable to dosimetry. The controlled BeO:Na phosphor obtained in this experiment showed the most superior characteristics.

Some complexities of properties observed in samples, for instance, that the peak at 180°C is composed of plurality of peaks near 180°C and that a rapid but small fading is observed, may be caused by irregularity of BeO crystals. As shown in the microscopic picture (Fig. 1), BeO ceramics are composed of many crystal grains and the doped impurity occupies selectingly grain boundary. These irregularity may be further improved by obtaining single crystals.

Conclusion

Controlled BeO ceramics containing impurity ions artificially doped has been investigated as well as their TL properties. It was found that BeO phosphors doped with alkaline ions, BeO:Li, BeO:Na and BeO:K, showed strong TL showing a glow peak at 180°C and the other properties for TLD were also excellent. The TL properties of these three phosphors are similar, but BeO: Na is concluded to be most excellent among them, because K^{+1} in BeO:K emits natural dose and Li^{+1} in BeO:Li is being afraid of instability, whereas BeO: Na has not any noticeable disadvantage. BeO phosphor doped with Na^{+1} might be the most practical phosphor in the future. It is well suited for both personnal monitoring and medical applications.

Acknowledgment

The authors are much indebted to Dr. T. Higashimura of Kyoto University and to Dr. S. Kondo of Osaka University for their many suggestions and discussions during this work.

References

1) J. R. Cameron, N. Suntharalingam, and G. N. Kenney, Thermoluminescence Dosimetry (Madison : University of Wisconsin Press)(1968).
2) J. H. Schulman, R. D. Kirk, and E. J. West, Proc. 1st Int. Conf. Luminescence Dosimetry (ed. by F. H. Attix), 113-117 (1965).
3) D. W. Zimmerman, C. R. Rhyner, and J. R. Cameron, Proc. 1st Int. Conf. Luminescence Dosimetry (ed. by F. H. Attix), 88-102 (1965).
4) C. R. Wilson and J. R. Cameron, Proc. 2nd Int. Conf. Luminescence Dosimetry (ed. by J. A. Auxier), 161-175 (1968).
5) P. Christensen, Proc. 2nd. Int. Conf. Luminescence Dosimetry (ed. by J. A. Auxier), 90-117 (1968).
6) C. A. Jayachandran, M. West, and E. Shuttleworth, Proc. 2nd Int. Conf. Luminescence Dosimetry (ed. by J. A. Auxier), 118-139 (1968).
7) E. Tochilin, N. Goldstein, and W. G. Miller, Health Phys. 16, 1-7(1969).
8) K. Becker, J. S. Cheka, and M. Oberhofer, Health Phys. 15, 381-403 (1970).
9) F. S. W. Hwang, Nature 227, 269-270 (1970).
10) T. Yamashita, N. Nada, H. Onishi, and S. Kitamura, Health Phys. 21, 295-300 (1971).
11) R. Schayes, C. Brooks, I. Koslowitz, and M. Lheureux, Health Phys. 14, 281-283 (1968).

	Main peak at low dose level below 100 R	Superlinear peaks at higher dose level	Shoulders (very weak)	Peaks by Tribo TL
BeO : M^{+}	180°C (strong)	230°C	280 - 310°C 190°C	325°C 185°C
BeO : M^{+3}	180°C	210°C	290 - 310°C	
BeO : M^{+4}	180°C	180°C	290 - 310°C	

Table 1. Peaks of BeO

Fig. 1 Microscopic picture of the surface of BeO : Na ceramics; crystal grains of 2μ - 10μ in size are observed in the picture.

Fig. 2 Distribution of Na atoms in BeO : Na ceramics as studied by X-ray microanalyzing method, the glittering dotts correspond to more than $1\text{-}2 \times 10^{21}/cm^3$ of Na atoms and dark area is $3 \times 10^{20}/cm^3$ (Na/BeO ≈ 0.4 %).

Fig. 3 Dosimeter samples.

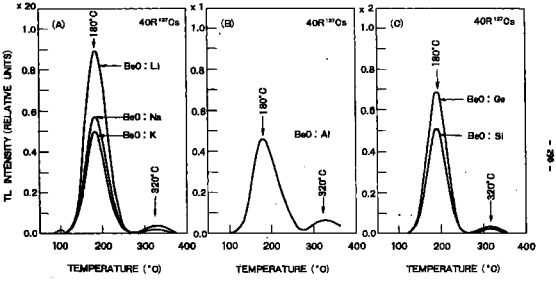

Fig. 4 Thermoluminescent glow curves of BeO ceramics doped with various impurity ions; (A) monovalent ions, (B) trivalent ions and (C) tetravalent ions.

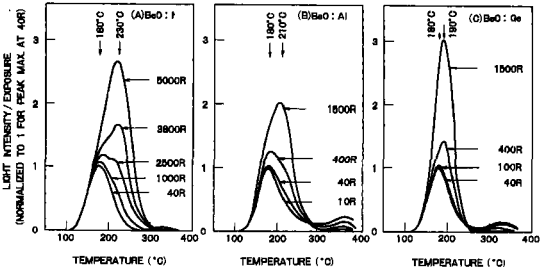

Fig. 5 Changes of glow curves of BeO samples exposed to a dose of supralinear region; (A) BeO : Na, (B) BeO : Al and (C) BeO : Ge

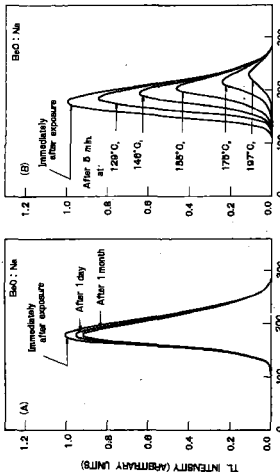

Fig. 6 Thermal fading of BeO : Na as observed by changes of glow curves; (A) stored at room temperature in the dark and (B) stored at higher temperatures for 5 minutes in the dark (non-isothermal fading curves).

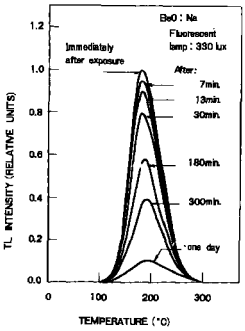

Fig. 7 Light fading of BeO : Na as observed by changes of glow curves; samples were stored under room light of 330 lux (fluorescent lamp).

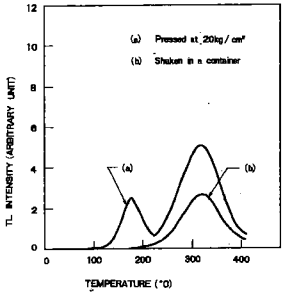

Fig. 8 Tribo-thermoluminescence of BeO : Na as observed by glow curves; curve (a) : shaken in a small container for 50 cycles, curve (b) : pressed by a pressing machine at 20 Kg/cm².

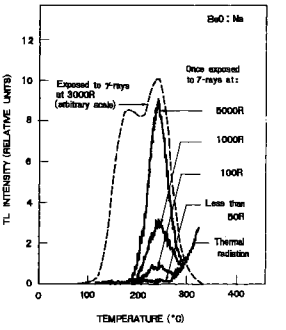

Fig. 9 Light stimulated thermoluminescence of BeO : Na once exposed to high dose and annealed at 400°C, as compared with the glow curve of BeO : Na exposed to γ-ray at 3000 R.

Bigelow

Beryllium oxide luminescence described by Yuokilis, and measured also in our laboratory, appears mainly in the UV-region and for its measurement quartz PM tubes should be used.

Brown

With the beryllium oxide I have been using (reagent grade material from Messers Hopkins and Williams Ltd.) the emission spectrum is very similar to that from LiF, but is a little bluer.

A STUDY OF SILVER, IRON, COBALT AND MOLYBDENUM AS LITHIUM BORATE ACTIVATORS FOR ITS USE IN THERMOLUMINESCENT DOSIMETRY

INSTITUTO DE FISICA, UNAM.

A. Moreno y Rocano*, C. Archundia** and L. Salmeron***

ABSTRACT.-

The behaviour of silver, iron, cobalt and molybdenum as $Li_2B_4O_7$ activators for its use as thermoluminescent dosimetric material has been examined.

The existence of a time persistent fundamental peak at 140°C and 210°C, as well as the rapid disappearance of the 90°C peak indicates silver to be the most reliable.

Discussion is made of 3 techniques for silver activated lithium borate preparation. Selection of the best method in accordance with the spectrum time variation and thermoluminescent response for 0.10, 0.30, 0.40 and 0.50% silver concentration as silver nitrate is presented.

The material under study shows the same spectral responses from 60 KV to 220 KV, 20 mA X-rays and linear thermoluminescent response up to 840 KR exposure from a ^{60}Co gamma source.

*Programa de Capacitación, Comisión Nacional de Energía Nuclear e Instituto de Física de la Universidad Nacional Autónoma de México.

**Programa de Capacitación, CNEN y Laboratorio Nuclear de la UNAM.

***Facultad de Ciencias de la UNAM.

INTRODUCTION.-

Several published reports[1,2,3] have mainly indicated the use of manganese as a lithium borate activator. For that reason, it was interesting to explore the possibility of finding out several other activators with thermoluminescent properties as well as to establish the correlation between the method of material preparation and the spectral and thermoluminescent responses.

EXPERIMENTAL.-

ACTIVATED LITHIUM BORATE PREPARATION AND ACTIVATORS.

All the reagents were obtained from J.T. Baker Chemical Co. of AnalaR grade and were used without further purification.

Three methods for the activated lithium borate preparation were studied which were as follows.

Method I.- Lithium borate was prepared mixing thoroughly in a beaker lithium carbonate (4.34 g) and boric acid (14.55 g). The activator (salt form) was dissolved in the minimal amount of distilled water and added. Gentle mixing allows all carbon dioxide to evolve, proper desecation was obtained in an oven (60°C) and final melting in a platinum crucible was achieved in a furnace at 960°C during 30 min. The melted material was spilled over a laboratory temperature stainless steel plate, ground and

sieved through a brass sieve N°. 40 (350 μ).

Method II.- Difference between method I and II is found in the use of a porcelain crucible instead of the platinum one. The material is melted, ground and sieved in the same way as in method I. Further pressure transformation (9.78×10^7 n/m^2) provided a tablet which was sintered (760°C) and finally ground and sieved in the usual way.

Method III.- Same procedure as in method I, making use of porcelain crucible, without further sintering.

Activators.- As lithium borate activators the following salts AnalaR grade were used without further purification.

a) Fe^{+3} as $FeCl_3.6H_2O$ (Mallinckrodt), 0.457% in weight.

b) Co^{+2} as $CoCl_2.6H_2O$ (Mallinckrodt), 0.362% in weight.

c) Mn^{+6} as MnO_2(Monterrey), 0.146% in weight.

d) Ag^{+1} as $AgNO_3$ (J.T. Baker), 0.10, 0.30, 0.40 and 0.50% in weight.

READ-OUT PROCEDURE.-

The thermoluminescent measurements of the 7.92 ± 0.43 mg activated lithium borate samples were made with a Harshaw thermoluminescent detector, Model 2000 coupled to and X-Y plotter, heating rate set at 250°C/min.

SELECTION OF ACTIVATOR AND RESULTS.-

The different activated lithium borate samples were prepared following method I and irradiated during 5 min with a 40 KV, 20 mA X-ray generator. The glow-curve and its variation with time for lithium borate activated with Fe, Co, Mn, and Ag are shown in figures 1, 2, 3, and 4. From the analysis of these graphs, the best response was due to silver, since the 140°C is more obvious and stable than the 90°C peak. The latter has a relatively short half-life depending on the preparation method whilst the 140°C and 210°C peaks are stable for comparatively long periods of time in relation to exposure and measuring times.

The thermoluminescent decay of identical samples of an initial silver activated lithium borate batch prepared as indicated in method I, irradiated for 5 min with the 40 KV, 20 mA X-ray generator is shown in figure 5. The peak disappears in approximately 2.5 hours, later on, a fairly constant value was obtained for a period of 4 to 5 hours.

Figure 6 shows an activator-free lithium borate glow curve as well as its variation for successive lengths of time after exposure. Rapid decay of the 90°C peak and absence of the 140°C fundamental peak demonstrates the importance of silver as an activator.

The effect of the sintering process can be observed in figure 7, which shows a glow-curve obtained from material prepared by method II and irradiated with 40 KV, 20 mA X-rays.

THERMOLUMINESCENT RESPONSE.-

Samples of silver activated lithium borate with 0.10, 0.30, 0.40 and 0.50% silver prepared with method I technique and exposed to gamma radiation from a ^{60}Co source, gave thermoluminescent responses shown in figures 8,9, 10 and 11. The best response was obtained with the 0.50% silver concentration sample. In these graphs, A curve denotes measurements obtained immediately after exposure, whilst B and C curves denote measurements obtained a certain time after exposure.

The thermoluminescent behaviour for the silver concentration samples ranging from 0,10 to 0,50% are shown in figures 12, 13, 14 and 15, where once more is clearly shown that the 0,50% silver sample gives the best results. A, B and C curves have the same meaning as before. Irradiation was obtained with a 40 KV, 20 mA X-ray generator.

A comparison between 0.10% silver activated lithium borate glow curves obtained by methods I, II and III can be observed in figure 16, where the particular spectrum shape shows clear dependance on the preparation technique

used.

An X-ray crystallographic analysis has shown that materials prepared following methods I and II have crystalline structure and discrete glow curves. Materials prepared with method III technique give an amorphous solid with a nondiscrete thermoluminescent spectrum.

ENERGY RESPONSE.-

The energy response of silver activated lithium borate prepared with method I technique, exposed to different X-ray energies radiation is shown in figure 17. The characteristic 140°C peak as well as the 210-220°C peak can be observed. Absence of the 90°C peak is due to the 2 hours time elapsed between exposure and measuring times.

CONCLUSIONS.-

Silver as silver nitrate has shown to be as good activator for lithium borate as manganese. In order to obtain silver activated lithium borate samples, the best preparation method is here described as method I. Similar information has been mentioned in the literature[4], but we found to be the critical factor the thermal shock produced in melted materials due to the specific nature of the crucible used. The best silver concentration seems to be 0.50% in weight as silver nitrate. In all

cases we obtained very good reproducible results and thermoluminescent responses for X-ray energies ranging from 60 to 280 KV as well as linear thermoluminescent responses up to 840 KR exposure from a ^{60}Co gamma source.

REFERENCES.-

1.- R.D. Kirk, J.H. Schulman, E.J. West and A.C. Nash, "Studies on Thermoluminescent Lithium Borate for Dosimetry", I.A.E.A., Vienna, 1967, SM-78/23.

2.- J.R. Cameron, N. Suntharalingam and G.N. Kennet, "Thermoluminescent Dosimetry", The University of Wisconsin Press, 1968.

3.- J.H. Schulman, "Use of Lithium Borate for Thermoluminescent Dosimetry", A.E.C. Symposium Series 8, April 1967.

4.- C.A. Jayachandran, H. West and E. Shuttleworth, "The Properties of Lithium Borate Powder as a Solid State Dosimeter", Proceedings of the 2nd. International Conference on Luminescence Dosimetry, Gatlinburg Tennessee, Sept. 23-26, 1968.

Gunta

My comment has reference to the question of spectral quality of the TL light emitted by lithium borate samples activated by different dopants. I would imagine that the spectral quality of emission would change with the change of dopant material. This is so because the glow peak temperatures are seen to be independent of dopant impurity, showing that the released charge carriers at different glow peaks are from the lattice centres of the host medium. Impurities will, therefore, play the part of recombination (luminescent) centres. Hence, a change in spectral character of TL emission might be expected.

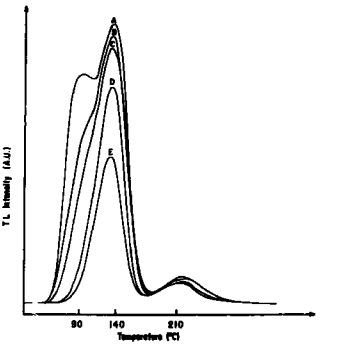

Fig. 1. Glow curves of iron activated lithium borate (0.45% FeCl3. 6 H2O) obtained by method 1, 5 min irradiation with a 40 KV, 20 mA X-ray generator. Irradiation data: 19/8/70, 09.00 h.
Measuring dates: A) 19/8/70, 09.45 h B) 19/8/70, 11.00 h C) 19/8/70, 12.00 h D) 22/8/70, 11.30 h E) 5/8/70, 17.00 h.
Ordinates in all figures, A.U. (Arbitrary Units).

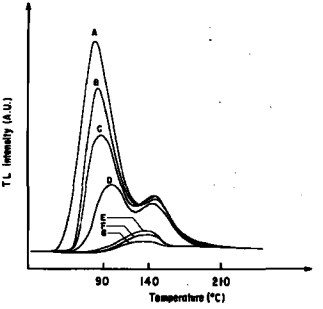

Fig. 2. Glow curves of cobalt activated lithium borate (0.38% CoCl$_2$. 6 H$_2$O) obtained by method I, 5 min irradiation with a 40 kV, 20 mA X-ray generator.
Irradiation date: 18/6/70, 09.30 h.
Measuring dates: A) 18/6/70, 09.30 h; B) 18/6/70, 10.00 h; C) 18/6/70, 10.30 h; D) 18/6/70, 13.00 h; E) 22/6/70 10.00; F) 24/6/70, 10.30 h; G) 5/8/70, 13.30 h.

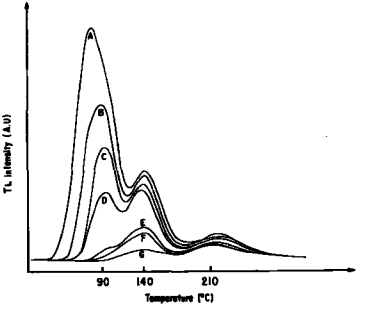

Fig. 3. Glow curves of molybdenum activated lithium borate (0.146% MoO_3) obtained by method I, 5 min irradiation with a 40 KV, 20 mA X-ray generator.
Irradiation date: 18/6/70, 12.30 h.
Measuring dates: A) 18/6/70, 12.30 h; B) 18/6/70, 14.30 h; C) 18/6/70, 18.30 h; D) 19/6/70, 11.30 h; E) 22/6/70, 10.00 h; F) 24/6/70, 10.30 h; G) 5/8/70, 13.30 h.

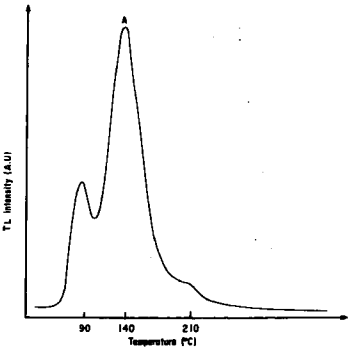

Fig. 4. Glow curves of silver activated lithium borate (0.10% $AgNO_3$) obtained by method 1, 5 min irradiation with a 40 KV, 20 mA X-ray generator.
Irradiation date: 19/6/70, 12.00 h.
Measuring date: A) 19/6/70, 12.00 h.

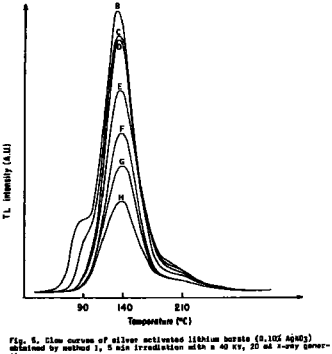

Fig. 5. Glow curves of silver activated lithium borate (0.10% $AgNO_3$) obtained by method 1, 5 min irradiation with a 40 KV, 20 mA X-ray generator.
Irradiation date: 19/6/70, 12.00 h.
Measuring dates: B) 19/6/70, 12.00 h; C) 19/6/70, 29.30 h; D) 19/6/70, 14.30 h; E) 20/6/70, 11.30 h; F) 20/6/70, 13.30 h; G) 6/7/70, 10.30 h; H) 15/7/70, 08.00 h.

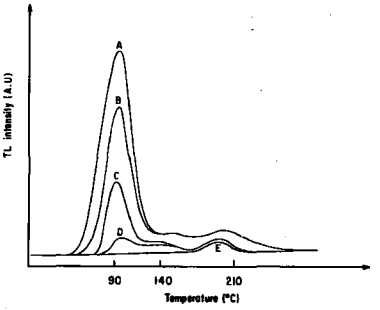

Fig. 6. Glow curves of silver-free lithium borate (0.005% $AgNO_3$) obtained by method II, 5 min irradiation with a 40 KV, 20 mA X-ray generator.
Irradiation date: 21/4/70, 14.30 h.
Measuring dates: A) 21/4/70, 14.30 h; B) 21/4/70, 15.00 h; C) 21/4/70 19.00 h; D) 22/4/70, 09.30 h; E) 23/4/70, 09.30 h.

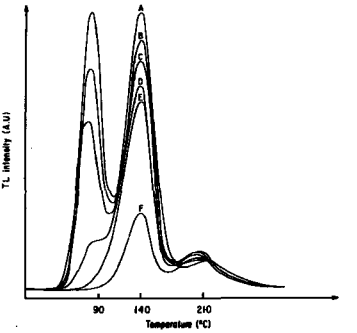

Fig. 7. Glow curves of silver activated lithium borate (0.10% $AgNO_3$) obtained by method II, 5 min irradiation with a 40 KV, 20 mA X-ray generator.
Irradiation date: 29/4/70, 10.00 h.
Measuring dates: A) 29/4/70, 10.05 h; B) 29/4/70, 10.30 h; C) 29/4/70, 11.30 h; D) 29/4/70, 19.00 h; E) 1/5/70, 12.30 h; F) 19/5/70, 14.00 h.

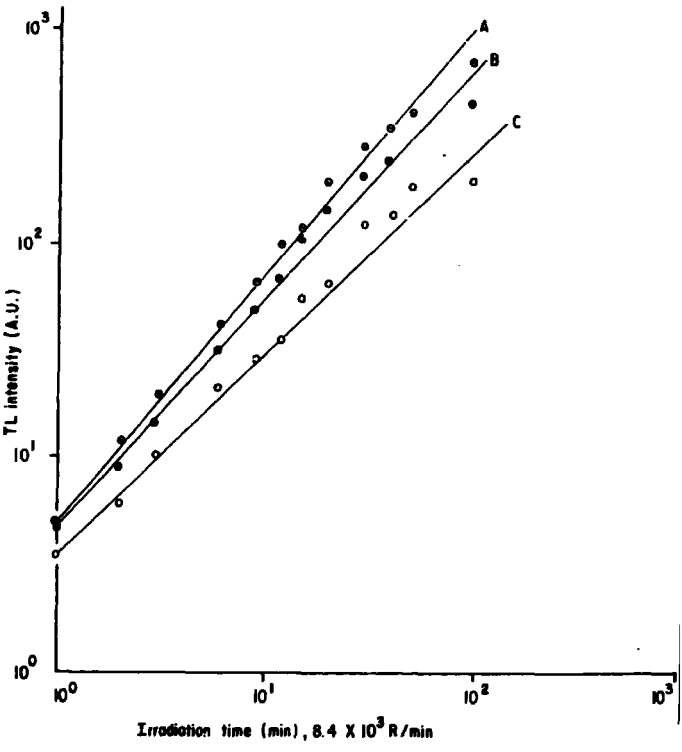

Fig. 8. Thermoluminescent intensity of silver activated lithium borate (0.10% $AgNO_3$) obtained by method 1, irradiated at different times with a 3600 Ci ^{60}Co Gammacell.
Irradiation date: 19/5/70.
Measuring dates: A) 19/5/70, B) 22/5/70, C) 16/6/70.

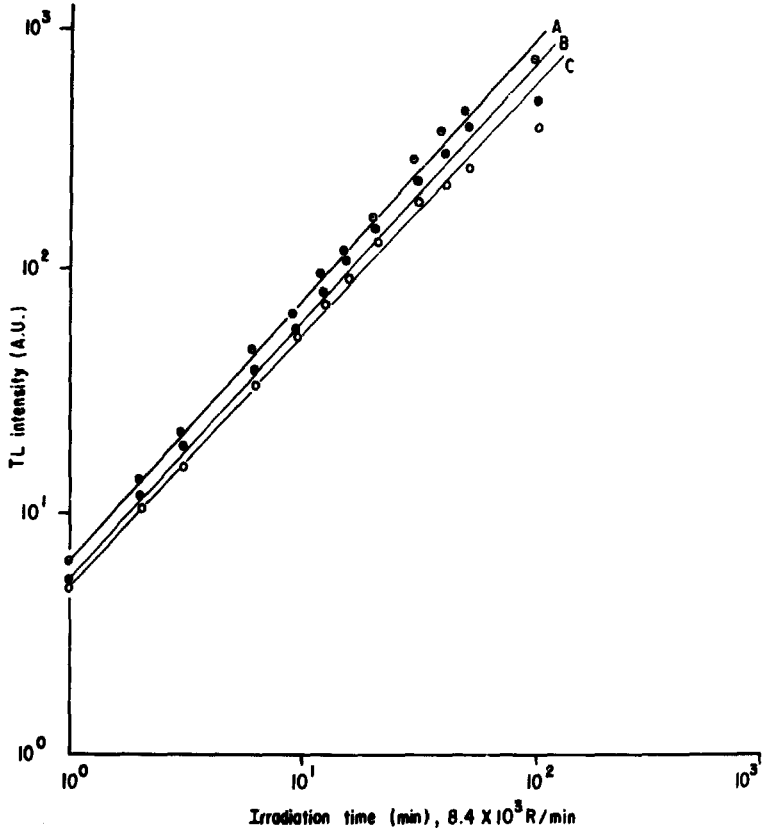

Fig. 9. Thermoluminescent intensity of silver activated lithium borate (0.30% $AgNO_3$) obtained by method I, irradiated at different times with a 3600 Ci ^{60}Co Gammacell.
Irradiation date: 24/6/70
Measuring dates: A) 24/6/70, B) 6/7/70, C) 3/8/70.

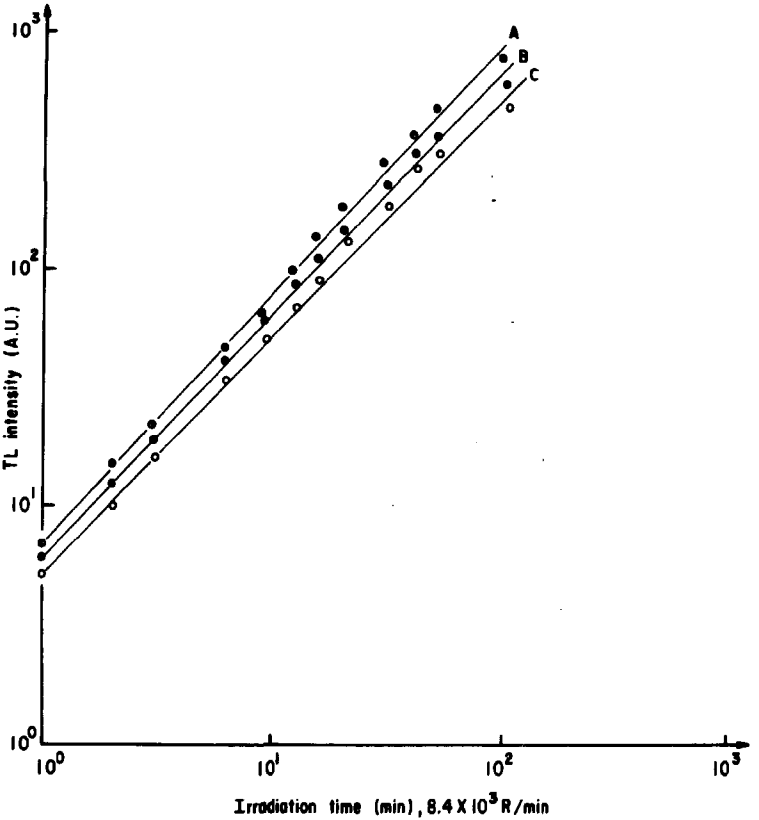

Fig. 10. Thermoluminescent intensity of silver activated lithium borate (0.40% $AgNO_3$) obtained by method I, irradiated at different times with a 3600 Ci ^{60}Co Gammacell.
Irradiation date: 1/7/70.
Measuring dates: A) 1/7/70, B) 13/7/70, C) 4/8/70.

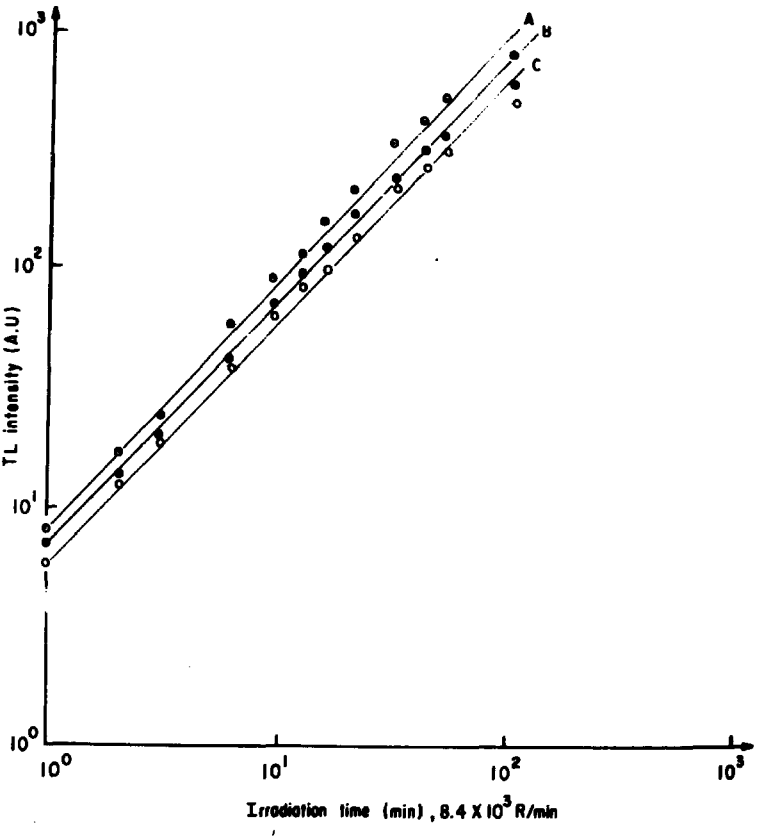

Fig. 11. Thermoluminescent intensity of silver activated lithium boreta (0,50 Ag_2O_3) obtained by method 1, irradiated at different times with a 3600 Ci ^{60}Co Gammacell.
Irradiation date: 2/7/70.
Measuring dates: A) 2/7/70, B) 13/7/70, C) 13/8/70.

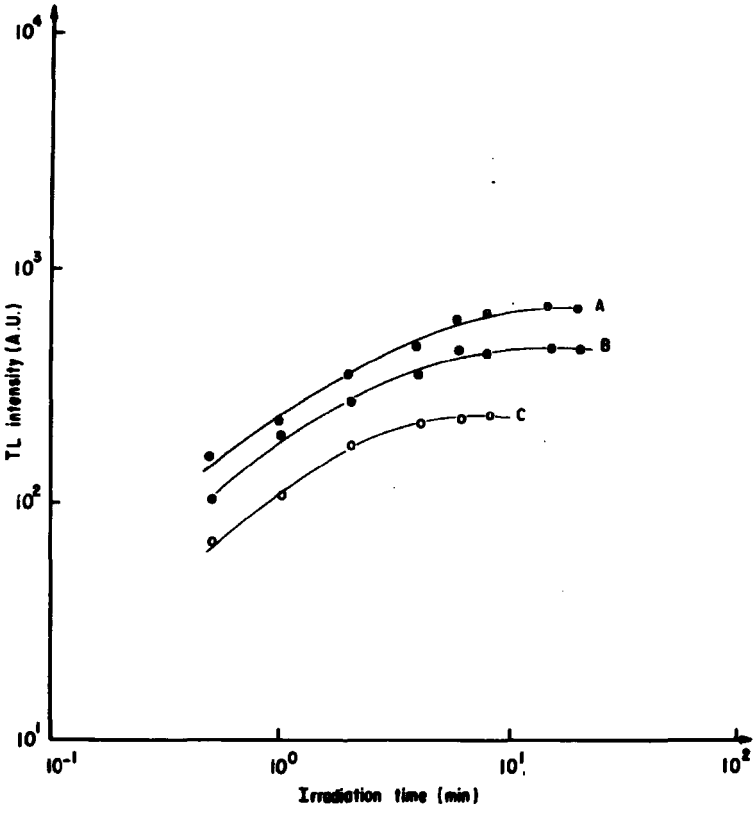

Fig. 12. Thermoluminescent intensity of silver activated lithium borate (0.10% $AgKO_3$) obtained by method I, irradiated at different times with a 40 kV, 20 mA X-ray generator.
Irradiation date: 14/5/70.
Measuring dates: A) 14/5/70, B) 18/5/70, C) 16/6/70.

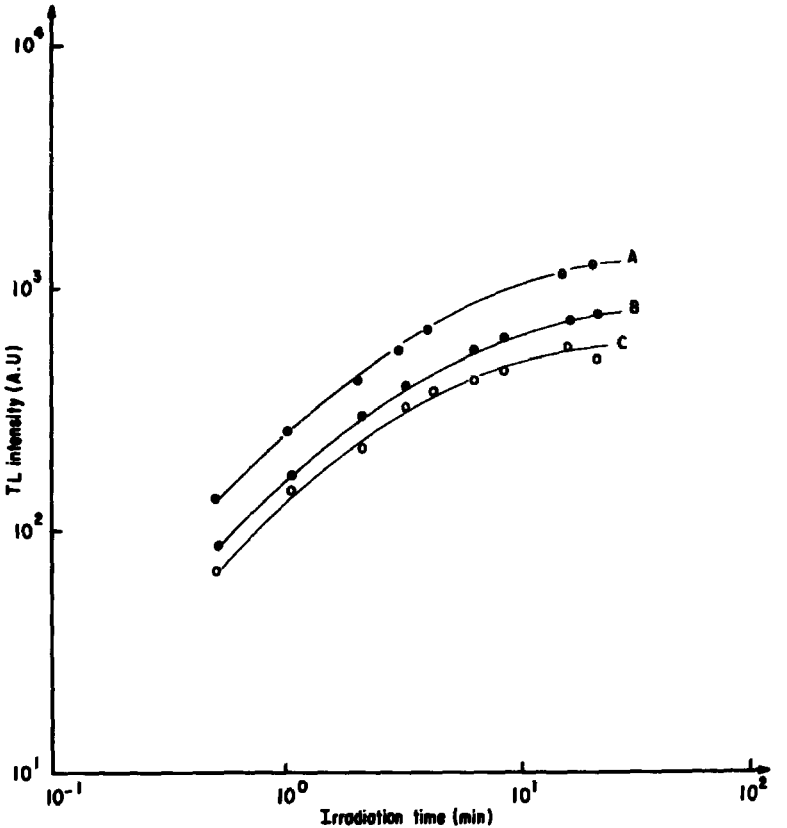

Fig. 13. Thermoluminescent intensity of silver activated lithium borate (0.30% $AgNO_3$) obtained by method I, irradiated at different times with a 40 Kv, 20 mA X-ray generator.
Irradiation date: 23/6/70.
Measuring dates: A) 23/6/70, B) 10/7/70, C) 7/8/70.

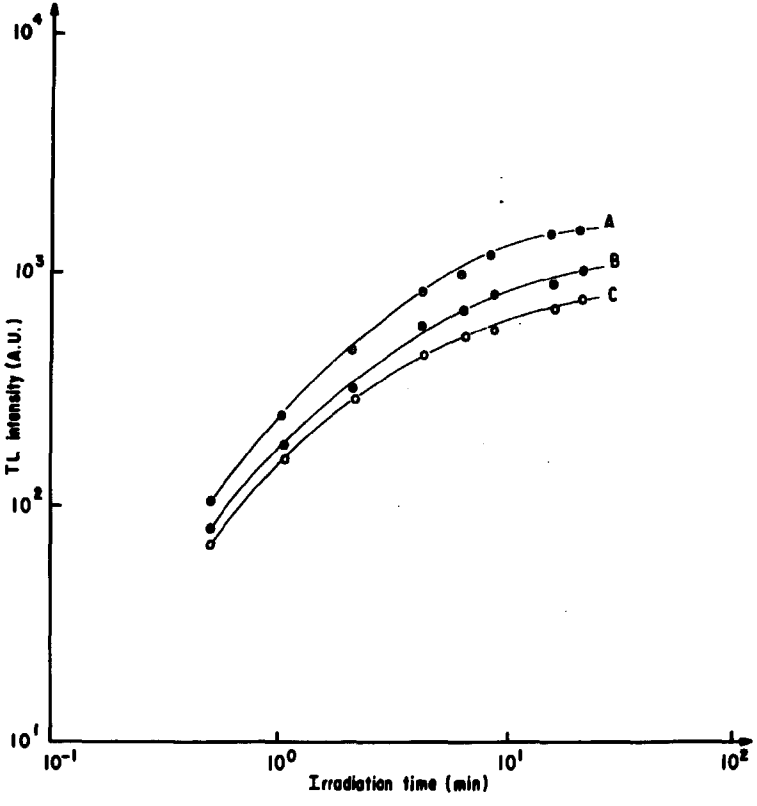

Fig. 14. Thermoluminescent intensity of silver activated lithium borate (0.40% $AgNO_3$) obtained by method I, irradiated at different times with a 40 KV, 20 mA X-ray generator.
Irradiation date: 30/6/70.
Measuring dates: A) 30/6/70, B) 16/7/70, C) 7/8/70.

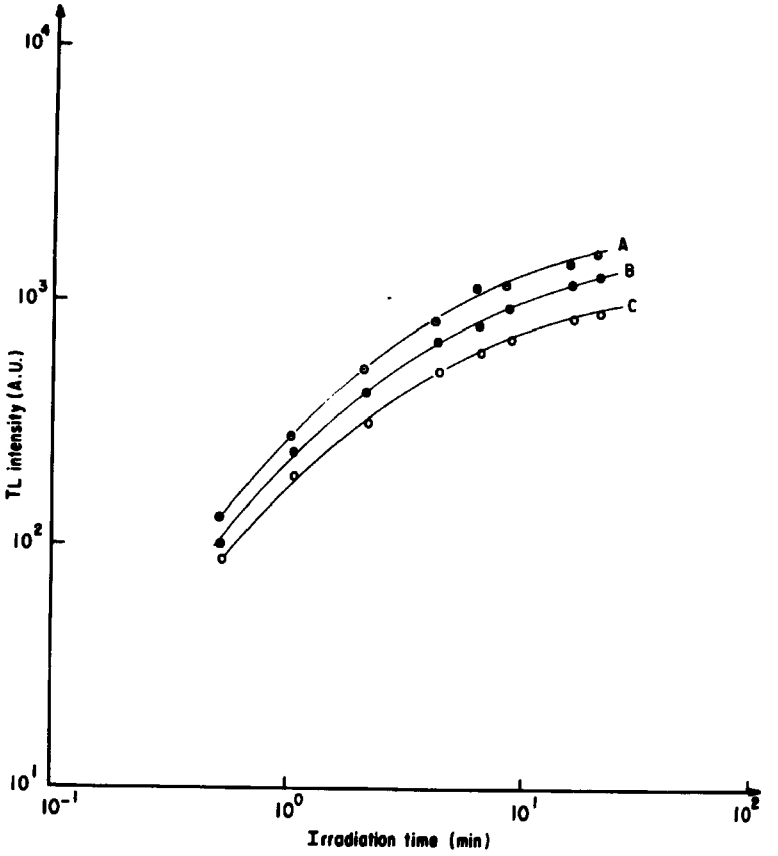

Fig. 15. Thermoluminescent intensity of silver activated lithium borate (0.50% $AgNO_3$) obtained by method I, irradiated at different times with a 40 KV, 20 mA X-ray generator.
Irradiation date: 7/7/70.
Measuring dates: A) 7/7/70, B) 24/7/70, C) 6/8/70.

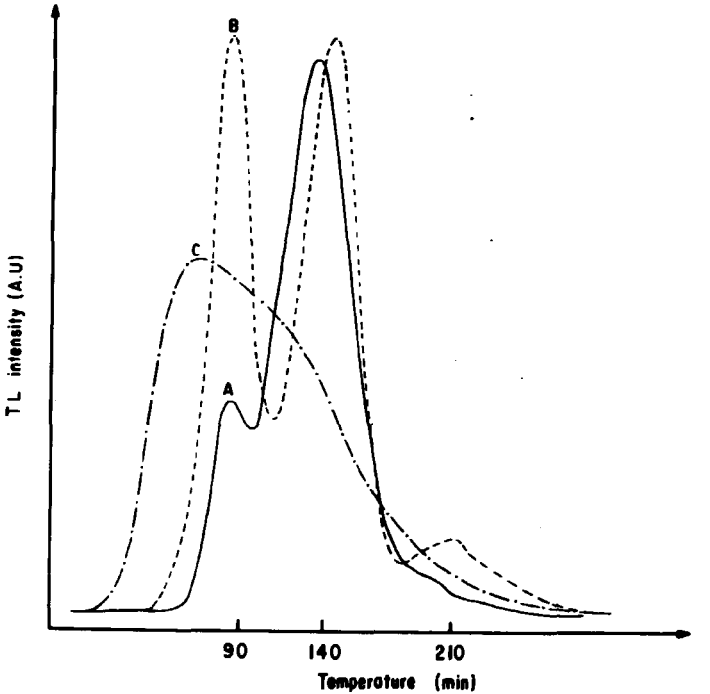

Fig. 16. Glow curves of silver activated lithium borate (0.10% $AgNO_3$) obtained by method I, (A _____), Method II (B - - - -) and method III (C -.-.-.), 5 min irradiation with a 40 kV, 20 mA X-ray generator.

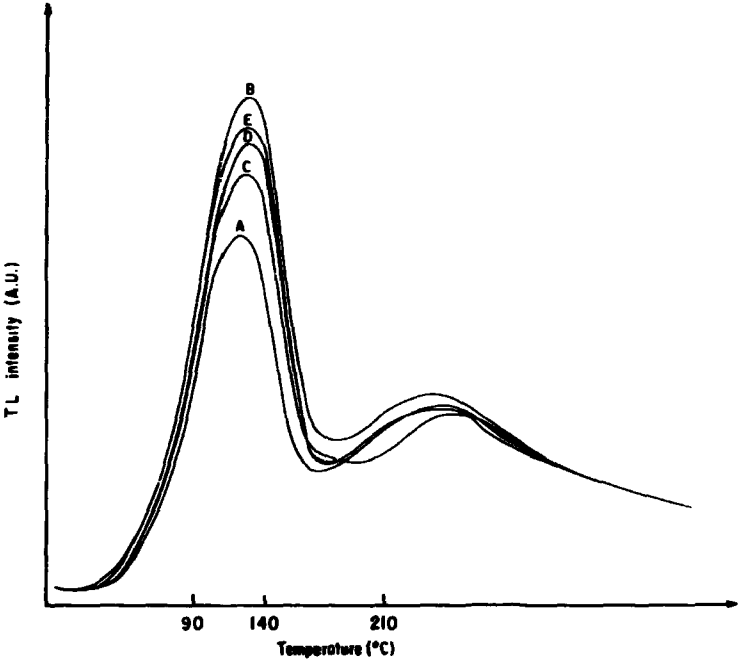

Fig. 17. Glow curves of silver activated lithium borate (0.10% $AgNO_3$) obtained by method I, irradiated at different X-ray energies from The General Hospital X-ray generator.
A) 60 KV, 10 mA, Exposure time: 6 min 40 sec.
B) 80 KV, 10 mA, Exposure time: 5 min.
C) 120 KV, 10 mA, Exposure time: 3 min 20 sec.
D) 140 KV, 10 mA, Exposure time: 2 min 51 sec.
E) 180 KV, 10 mA, Exposure time: 2 min.

Sintered TL Dosimeters

by

T. Niewiadomski, M. Jasińska, E. Ryba

Institute of Nuclear Physics, Cracow, Poland

Abstract

A new method of preparation of the solid form LiF dosimeters is described. It is based on cold compressing and sintering of LiF powder and is simpler than the single crystal growing used previously, allowing batches containing thousands of dosimeters to be produced with a precision better than ± 5% S.D. Some work has been done in investigating the changes of TL properties of a few LiF phosphors during preparation by this new method. Compressing causes a significant loss of TL sensitivity and a change in the glow curve shape of all examined phosphors. The crystal defects responsible for these phenomena are annealed at higher temperatures. The dosimeters become semi-transparent and their mechanical and TL properties are improved when sintered. In this way 4.5 mm dia 0.83 mm thick disks and 1.7 mm dia 4 mm long rods were produced. The properties of sintered dosimeters were compared with other solid form LiF dosimeters of home and foreign production. Sensitivity per rad and per milligram compared with that of TLD-100 powder was found to be: TLD-100 powder - 1, sintered - 0.27, Dolma-Lum LiF-200 Ti /GDR/ powder - 0.9, sintered - 0.5, LiF:Mg,Ti /Institute of Nuclear Physics/ micro-crystalline - 0.9, sintered - 0.57, TLD-100 high sensitivity extruded - 0.44. The lowest detectable dose of sintered disks made of LiF:Mg,Ti is about 1 mrad and that of rods 5 mrads. Single crystal personnel dosimeters have been replaced by sintered disks since March 1971 in our Institute. Some hundreds of these dosimeters are being tested in radiological clinics to check their usefulness.

Introduction

Dosimetric grade LiF is now a widely used phosphor in RTL dosimetry both for radiation protection and medical applications. Handling of the loose powder is very inconvenient and time consuming, especially for routine work. Despite the good quality of commercially available powders their application to low dose measurements is limited, owing to the large crystal surface in contact with atmospheric oxygen. Hence some methods of preparation of solid form dosimeters were elaborated, such as LiF loaded teflon disks /and rods/, developed by Björngard [1] and Krüger [2], or extruded LiF blocks [3]. The teflon disks are used as personnel dosimeters in several establishments [4,5] but the dosimeters containing 100% LiF seem to be more useful for these purposes.

Some methods of production of pure LiF dosimeters have been developed in our laboratory. The single crystal dosimeters, and their use for routine personnel dosimetry, have been described elsewhere [6,7]. This report describes investigations on another kind of solid form dosimeters, undertaken due to some disadvantages of single crystal dosimeters, i.e. relatively high sensitivity differences among them and a time consuming production technology. The sensitivity of these dosimeters varies by about ± 15% S.D., therefore they must be individually calibrated or selected before use.

Sintering and Dosimeter Reproducibility

A number of attempts have shown the possibility of production of the solid form LiF dosimeters in a quite simple way by means of cold compressing and sintering [*]. This method appears to be easier than single crystal growing and allows batches containing thousands of dosimeters to be produced with reproducibility better than ± 5% S.D. It seems also to be less complicated and less expensive than LiF hot extruding [3]. An investigation has been carried out in order to test whether this technology gives good results when different LiF powders are used. Phosphors exhibiting a glow maximum at 200°C, i.e. TLD-100, TLD-700 /USA/, Dohna-Lum LiF 200 and 80 Ti /GDR/, LiF:Mg,Ti /INP/, were used. LiF:Cu,Ag /INP/ with the glow peak at 120°C was also sintered. 32 mg of the powder was dispensed and pressed by means of a tableting machine on disks 4.5 mm dia and 0.83 mm thickness /or rods 1.7 mm dia,

[*] Patent pending

4 mm length/. Some hundreds of the disks were placed on platinum trays and heated in an argon atmosphere. The sintering temperature has a small influence on the TL sensitivity in some limits, but the higher the temperature the better are the mechanical and optical properties of the final product. The dosimeters were visually selected after sintering, because about 5% of them exhibit small dark spots. In this way 9 experimental batches of sintered disks have been produced so far, using one single batch of LiF:Mg,Ti powder weighing 98 g as a starting material.

The reproducibility of the dosimeters was tested taking ten dosimeters from each batch at random and reading them after irradiation to a 0.4 R dose of Co-60 gamma radiation. The results of this test, summarised in Table I, show that the standard deviation of produced dosimeters is about ± 5%, including the errors due to reader instability and irradiation non-reproducibility.

Table I

Mean values and standard deviation of read-outs of representative dosimeters from experimental production

Batch number	Number of dosimeters	Mean response /mV/	Standard deviation /± %/	Mean value of response and S.D.
005	280	12.2	3.0	
006	310	11.6	2.9	
007	250	11.6	2.7	
008	270	12.4	2.6	
009	320	12.4	2.8	11.8 ± 5.5%
010	280	12.3	3.0	
011	270	11.6	2.7	
012	310	11.0	3.2	
013	240	11.2	3.3	

Changes of TL Properties During Production

There are some changes of the TL properties in all investigated phosphors when they are compressed and heated. Magnesium doped phosphors compressed

with a pressure of only 100 atm exhibit a significant glow curve change and a sensitivity decrease by a factor of about 10 - 16. These change are not induced by the powder crushing because phosphors finely crushed in a mortar do not exhibit them. They may be due to some tensions and intrinsic crystal lattice deformations generated by the static pressure. The deformations quench the luminescence and produce some new electron traps, giving glow peaks at temperatures between 230 and 400°C.

The above-mentioned processes for the LiF:Mg,Ti are shown in Figs 1 and 2. Other Mg containing LiF phosphors exhibit similar changes and the differences between them are of little significance.

All these pressure induced changes are thermally unstable. The previous glow curve shape and TL yield is restored when the phosphor is heated to a temperature higher than 200°C even for a short time /see curve 2 in Fig. 1/.

In contrast to the Mg containing phosphors LiF:Cu,Ag do not alter their glow curve shape when compressed. The decrease in the glow maximum by a factor of 3 is the only result of compressing. A further sensitivity decrease follows after sintering, because the high TL yield in this phosphor is obtained by means of the "freezing" of crystal defects attained by sudden cooling.

Although the pressurized and annealed disks exhibit rather good dosimetric properties, they can be used in this form [8] only with special care on account of their low mechanical strength. In addition, their non-radiation induced luminescence is as high as that of the loose powder and which makes low dose measurements difficult. The disks become perfectly tough and semi-transparent and their spurious luminescence decreases significantly when sintered. By sintering the amplitude relations between two stable peaks, i.e. IVth and Vth, are changed to some extent /compare the curves 1 and 3 or 2 and 4 in Fig. 3/ as well as the VIth radiation induced peak appearing at a temperature of about 270°C is decreased /see Fig. 4/.

The TL yield of the sintered dosimeters made from different LiF phosphors, measured per milligram and per rad, compared with that of TLD-100 powder, is tabulated in Table II.

Table II

Relative sensitivity of phosphors and dosimeters
/per mg and rad compared with TLD-100 powder/

Phosphor	TLD-100	Dolma-Lum LiF 200 Ti	Dolma-Lum LiF 80 Ti	LiF:Mg,Ti	LiF:Cu,Ag
powdered	1	0.9	0.65	0.9	8.0
compressed	0.08	0.07	0.07	0.06	2.6
sintered	0.27	0.5	0.4	0.57	0.2
Harshaw h.s. extruded blocks	0.44				
single crystalline blocks				0.35	

Dosimetric Properties

The thermoluminescent LiF phosphors and the solid form dosimeters previously developed in our laboratory were used in personnel dosimetry and radiotherapy routinely. In order to replace these forms by the sintered dosimeters their dosimetric properties were investigated. First of all it was verified that the basic dosimetric properties of LiF:Mg,Ti such as dose response, fading, photon energy dependence, and annealing requirements are not altered by the sintering process. Secondly, the usefulness and properties of the sintered dosimeters were investigated separately for low dose and high dose measurements, because the requirements for TL phosphors are different for these two applications.

For low dose measurements the optimal and least troublesome annealing method for routine use was found, and the lowest detectable dose and the accuracy of measurements were evaluated. The annealing method, well tried during the routine use of the single crystal dosimeters, appeared to be also advantageous for sintered dosimeters. It consists of postirradiation heating at 100°C for 10 minutes. This simple treatment, removing three low temperature peaks, is sufficient because the measured doses are considerably below the limit where increase in sensitivity occurs.

Some glow curve and sensitivity changes occurring after this annealing method compared with a full /preirradiation/ annealing described in the next

paragraph should be noted. These differences may be seen from Fig. 3 where an increase in the IV peak after the postirradiation annealing is evident /curve 1 and 3 compared with 2 and 4/. It may be due to a thermal ejection during annealing of some electrons from the traps responsible for the III peak and their location in traps connected with IV peak enhancing them [*]. Hence, the integrated light output obtained when the phosphor is annealed after irradiation is about 12% higher then that obtained from fully annealed phosphor. This phenomenon occurs for all phosphors investigated, having the main peak at 200°C.

The further enhancement of the IV peak takes place during illumination of the phosphor and dosimeters with fluorescent light, which is described below /see Fig. 7/.

The stability of the dosimeters against the postirradiation annealing was tested, repeating irradiation to a dose of 0.4 rad ten times, annealing, and reading-out a batch of ten dosimeters. The measurement errors between read-outs of the same dosimeter are ± 2% S.D. while those between different dosimeters are ± 4% S.D. A similar experiment with a dose of 100 rads demonstrated that this annealing method does not introduce any sensitivity increase or remarkable errors even at this dose level therefore it was used throughout all the subsequent low dose experiments and also for routine personnel monitoring.

The main difficulty in low dose measurement is a spurious luminescence appearing to some extent in LiF even in the solid form. Fig. 5 shows the spurious luminescence build up for both sintered LiF disks and TLD-100 extruded blocks when they are stored for two months. This luminescence appears at temperatures above 260°C and poses no serious problem because it can be removed either by a properly adjusted maximum dosimeter temperature or/and by use of the nitrogen atmosphere.

Our first reader was an analogue one. It indicated the dose by the voltage measurement across a capacitor loaded with P_M tube anode current. Fig. 6 shows to what extent the reader indications depend upon the heating rate and upon the atmosphere of the heating chamber, when the sintered dosimeters were irradiated to a dose of 10 mrads. Fig. 6 A relates to the heater supplied with constant current. In this heating rate shown by curve 1, only a short

[*] This effect is opposite to the transfer of charge carriers from deeper to shallower traps described by C. Brooks [9].

standstill of instrument indication is evident if an air atmosphere is used /see curve 2/. Its observation requires intense attention and only an experienced employee can read-out the low irradiated dosimeters with good accuracy. The use of a digital voltmeter is very difficult. Hence an improved electronic heater supply has recently been constructed [*] following an idea given by Svenson et al.[10]. The heater temperature, selected previously and controlled by a Fe-constantan thermocouple, is reached in a few seconds and maintained by an electronic device as is shown by curve 1 in Fig. 6 B. In this arrangement a more evident indication standstill occurs and therefore there is a smaller possibility of a wrong read-out. In practice by such heating of the dosimeter one may dispense with the nitrogen flushing and use a digital voltmeter successfully.

The accuracy of the low dose measurements is usually disturbed by the effects of several environmental variables, such as temperature, light, and wearing conditions. The fading of LiF:Mg,Ti response due to the temperature agrees well with the data pulished by several authors for TLD-100. Although the influence of environmental temperature and normal light do not require the introduction of special precautionary measures during dosimeter wearing and assessment, as can be seen from Table III, some changes of the glow peak

Table III

Effect of storage conditions for 4 weeks
/each batch contained 10 dosimeters/

Exposure	Storage conditions	TL-response /mrads/	Standard deviation /± %/
non-irradiated	in darkness	9	10
non-irradiated	in the window	8.5	12
100 mrads single irradiation before storage	in darkness	104 [a]	3
100 mrads single irradiation before storage	in the window	95.5 [b]	2
100 mrads differently administered	in darkness	109	3.5

[*] Designed and made by E. Mnich and W. Wierba.

a - loss of TL signal induced by raised temperature /for a while up to 5°C/ amounted to about 9%,

b - loss of TL signal induced only by sun and daylight amounted to about 4.5%.

Note. The background at the place where all the dosimeters were placed amounted to about 9 mrads per month.

amplitude should be noticed when the dosimeters are illuminated with an intense fluorescent light for several hours. This is shown in Fig. 7 where a distinct decrease in the Vth peak is apparent while the IVth peak increases, whereby the integrated light output remains much the same.

The response of the sintered disks to low doses shown in Table IV demonstrates an increase both in the sensitivity and the measurement errors for doses below 20 mrads. This may be due to a non-radiation induced background.

Table IV

Response of sintered disks to low doses and standard deviation

Dose /mrads/	Response /mV/	Standard Deviation /± %/	Sensitivity increase
5	6.6	9	1.3
10	11.5	8	1.15
100	100	4	1.0
1000	1000	3	1.0

In therapeutic dose measurements and in any other medical applications one has to work with a dose range where a significant supralinearity of response occurs for all LiF 200°C phosphors. It was therefore decided to anneal the sintered dosimeters by the standard method provided for LiF:Mg,Ti, i.e. 1 hour at 400°C followed by 4 hours at 80°C. A continuation of 80°C heating up to 24 hours, recommended for TLD-100 and TLD-700, effects about 20% loss of the stable peaks integrated output in LiF:Mg,Ti without any improvement of the low temperature peaks in comparison with 4 hours annealing. No great sensitivity differences after annealing at temperatures between 350 and 600°C were observed. It was found, however, that the temperature below 390°C did not remove completely the sensitivity enhancement induced by the high dose. For instance, after irradiation to 60 krads and annealing for 1 hr at

370 ± 10°C the sensitivity was still twice as high as without this high dose. The annealing temperature of 400°C stabilized with ± 10°C accuracy seems to be sufficient for the complete removal of all radiation damage due to irradiation up to a dose of 100 krads. It was, however, observed that highly irradiated and annealed dosimeters exhibit decreased sensitivity, as is shown in Table V, without any change of the glow curve shape. Their accuracy is also lower.

Table V

Sensitivity changes due to high dose irradiations */

Predose /krads/	0	1	10	33	63	100
Relative sensitivity	1.0	1.0	0.98	0.92	0.84	0.77

*/ Four sintered disks were irradiated to a dose of 0.1 rad, read-out, irradiated up to the predose, annealed /1 hr at 400°C and 4 hrs at 80°C/, and again irradiated to 0.1 rad.

Neutron response of the sintered dosimeters and their application in routine personnel dosimetry will be published hereafter. Detailed investigations of the usefulness of the sintered dosimeters for radiotherapy dose measurements are being performed in the Institute of Oncology, Cracow and in other establishments.

Conclusions

The experience we have acquired so far shows that the sintered disks have some advantages over both films and pocket ionisation chambers. In comparison with films the sintered dosimeters, like single crystal dosimeters, have a better sensitivity and angular response, allow for a quick read-out, may be re-used, and more exactly determine the dose, especially in the case of a complicated and unknown radiation spectrum. In comparison with pocket chambers, the sintered dosimeters have a lower fading, and make possible the determination not only of the whole body dose but also the skin dose and even point dose. This last possibility, being a consequence of the

small dimensions of the sintered dosimeters is especially valuable in radiotherapy.

Acknowledgements

The authors have pleasure in thanking Mr. W. Korzeniowski for his work in phosphor preparation and dosimeter sintering and Mr. J. Dybeł for making the reader, and of other details during this work.

References

1. B. Djurngard, R.C. McCall, L.A. Bernstein, Proc. Int. Conf. Luminesc. Dosimetry Stanford Univ. Calif. 308 /1965/.

2. E. Krüger, Verfahren zum Herstellen von LiF TL Dosimetern, Patent GDR No 55570.

3. Thermoluminescent Pellets, U.K. Patent No 1,186,899 /1967/.

4. K.E.G. Perry, H.E. Preston, Paper No IRPA/2/P58 on II Int. IRPA Congress, Brighton, U.K., 3-8 May 1970.

5. D.M. Wallace, Paper No IRPA/2/P64 on II Int. IRPA Congress, Brighton, U.K., 3-8 May 1970.

6. M. Jasińska, T. Niewiadomski, E. Ryba, Nukleonika 14, 995, /1969/.

7. T. Niewiadomski, E. Ryba, Radiation Dosimetry, Proc. Int. Summer School on Radiation Protection, Cavtat, 21-30 Sept. 1970, Vol. 2, 308.

8. K.K. Shvarts, Z.A. Grant, T.K. Mashs, M.M. Gruba, Termoluminascentnaja dozimetria, Zinatne, Riga /1968/.

9. C. Brooks, Solid State Dosimetry, Proc. of NATO Summer School, Brussell, /1967/.

10. G.K. Svensson, R.C. McCall, G.L. Babcock, SLAC-PUB-731, II Int. Congress of IRPA, Brighton, U.K. /1970/.

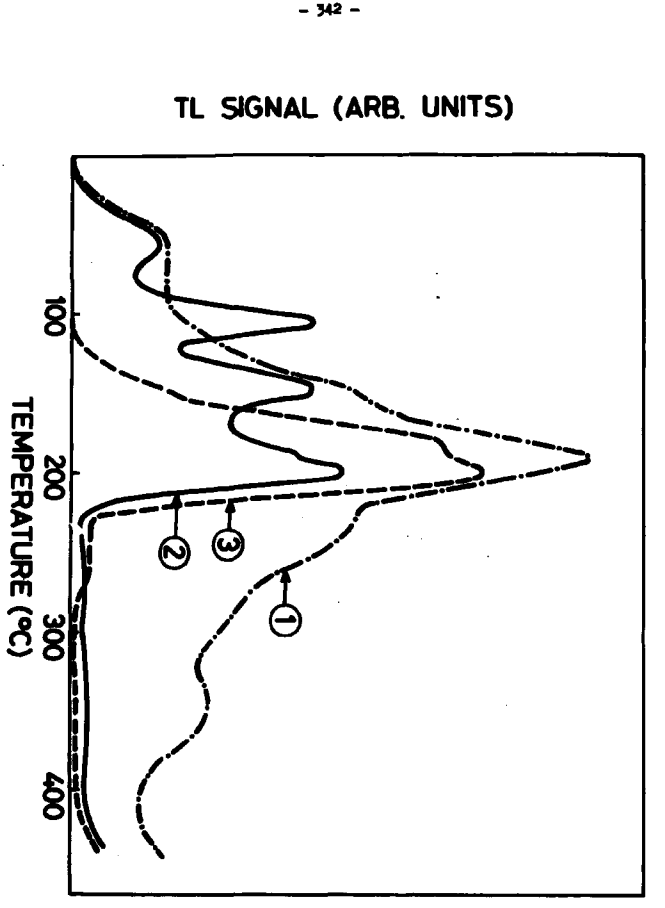

Fig. 1. Variation of LiF:Mg,Ti glow curve with compressing, heating, and sintering.

1 - compressed disk made of the annealed phosphor, D = 480 rads,

2 - compressed disk heated up to 300°C for 30 seconds before irradiation to D = 48 rads,

3 - sintered disk annealed before irradiation to D = 48 rads

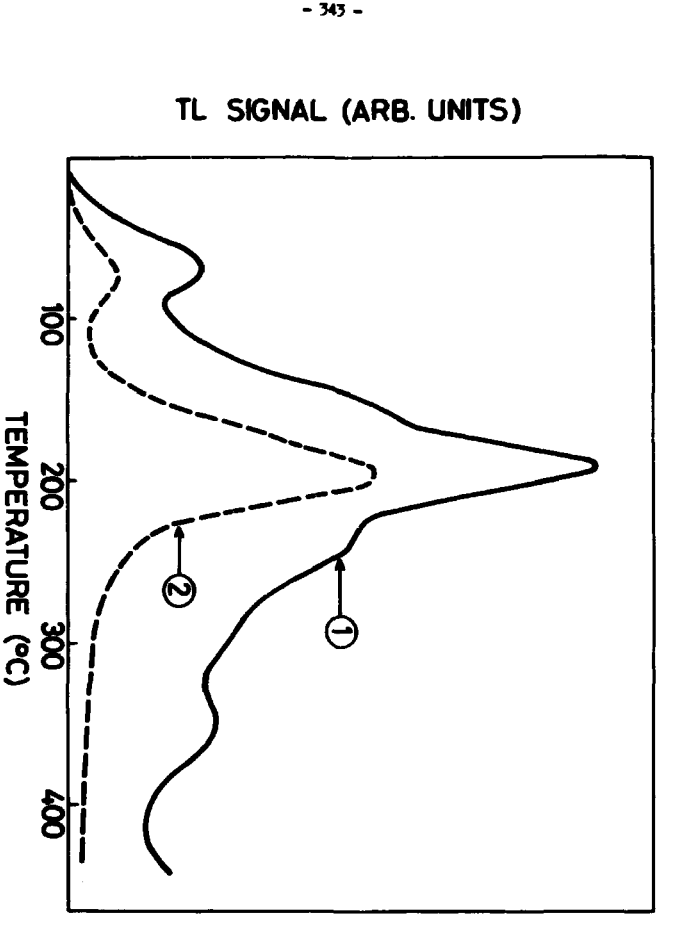

Fig. 2. Comparison of the glow curves of LiF:Mg,Ti powder,

1 - phosphor compressed with 10,000 atm pressure /10 mg of the selected grains undamaged by the pressure/, D = 400 rads,

2 - 10 mg of the powder finely ground in a mortar, D = 48 rads.

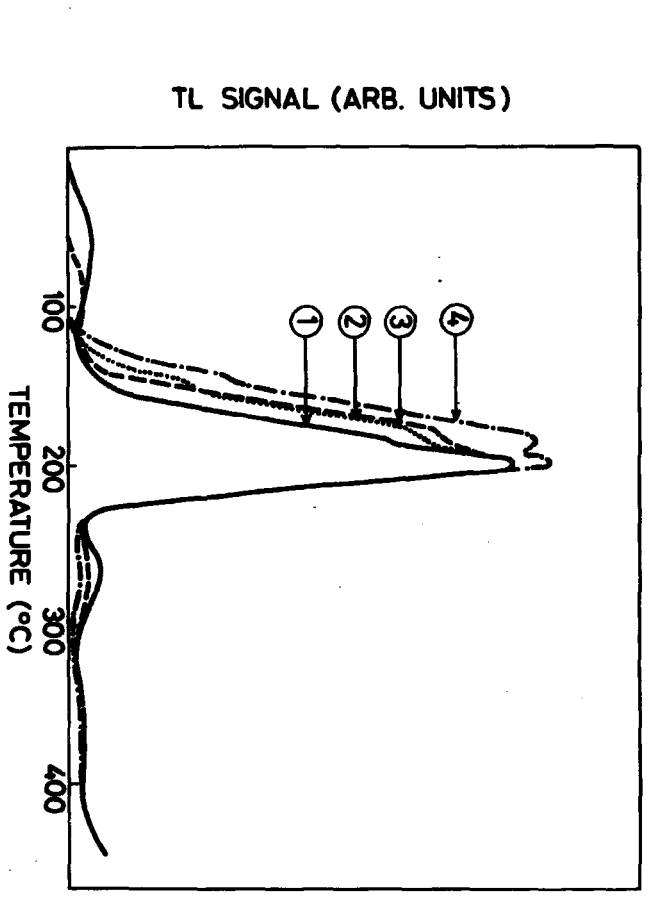

Fig. 3. Glow curves of LiF:Mg,Ti after different annealing procedures,

1 - powder, preirradiation annealing /1 hr at 400°C + 4 hrs at 80°C/,

2 - powder, postirradiation annealing /10 min at 100°C/,

3 - sintered disk annealed as 1,

4 - sintered disk annealed as 2.

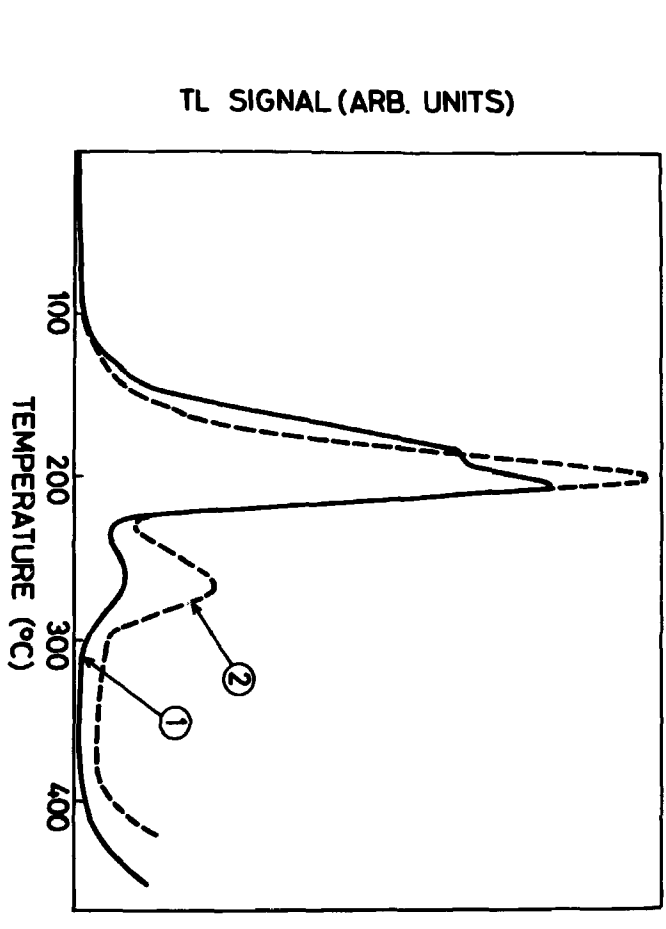

Fig. 4. Influence of the sintering on the VIth peak amplitude in LiF:Mg,Ti
1 - 30 mg of powdered phosphor, D = 48 rads,
2 - sintered disk, D = 48 rads.

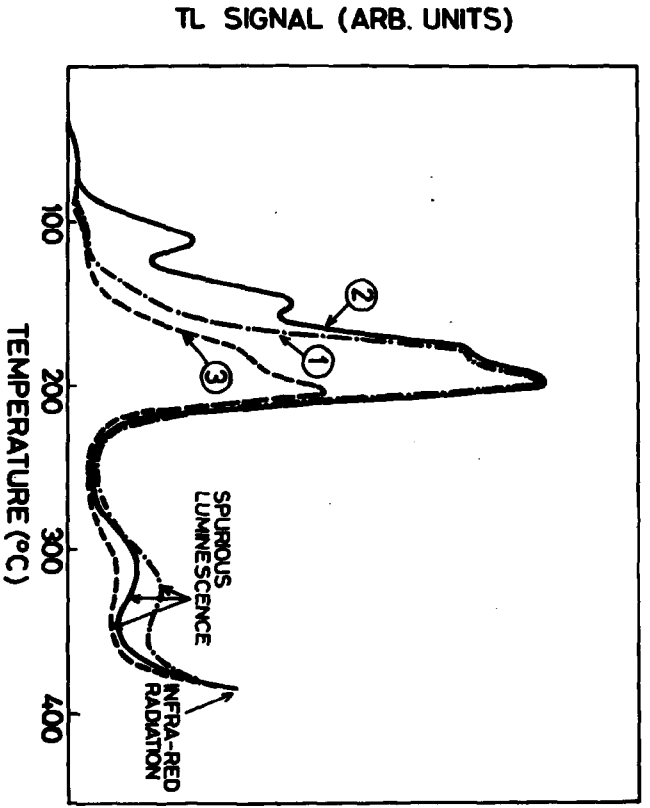

Fig. 5. Spurious luminescence of the sintered LiF:Mg,Ti disk and an extruded TLD-100 high sensitivity block irradiated to 1 rad dose and read-out in an air atmosphere,

1 - LiF:Mg,Ti disk annealed /1 hr at 400°C + 4 hrs at 80°C/, stored 2 months and irradiated,

2 - the same disk irradiated repeatedly,

3 - TLD-100 block annealed as 1, stored 2 months and irradiated.

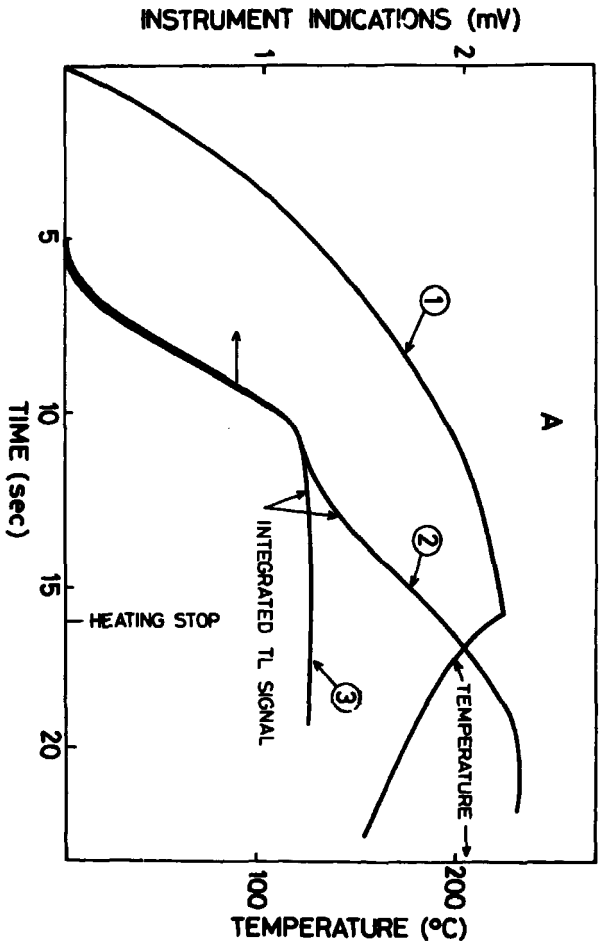

Fig. 6. Analogue instrument indications and thermocouple response versus time recorded during read-out of the 10 mrads dose. Recording was performed under different heating and atmosphere conditions,

1 - thermocouple response,

2 - instrument indication without the nitrogen,

3 - instrument indication with the nitrogen flushed through the heating chamber.

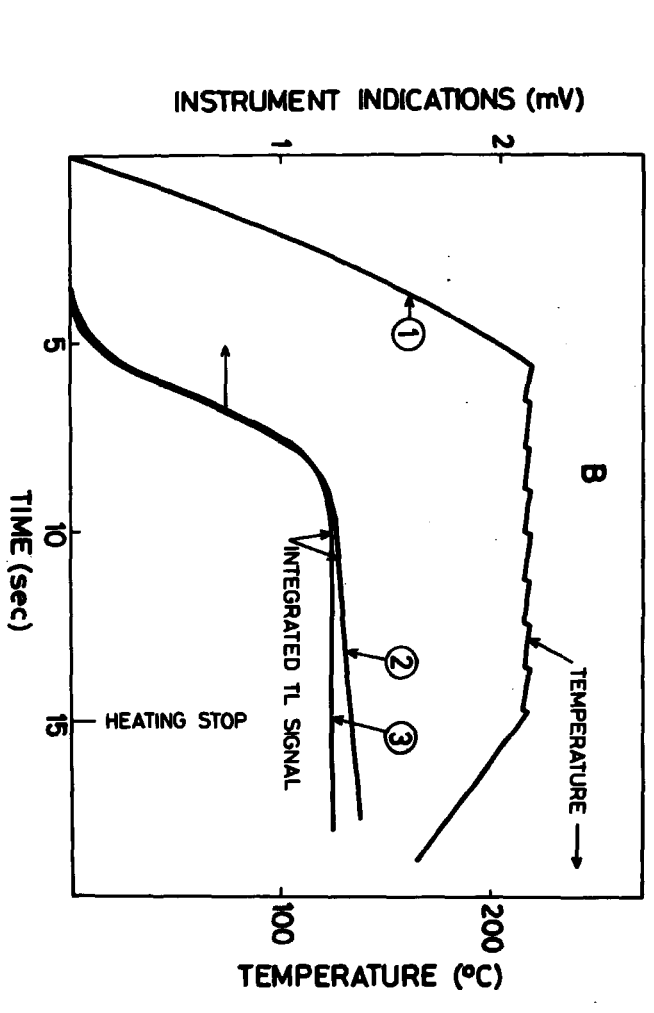
INSTRUMENT INDICATIONS (mV)
1
2
5
10
15
TIME (sec)
HEATING STOP
INTEGRATED TL SIGNAL
TEMPERATURE
B
100
200
TEMPERATURE (°C)

Fig. 6 B.

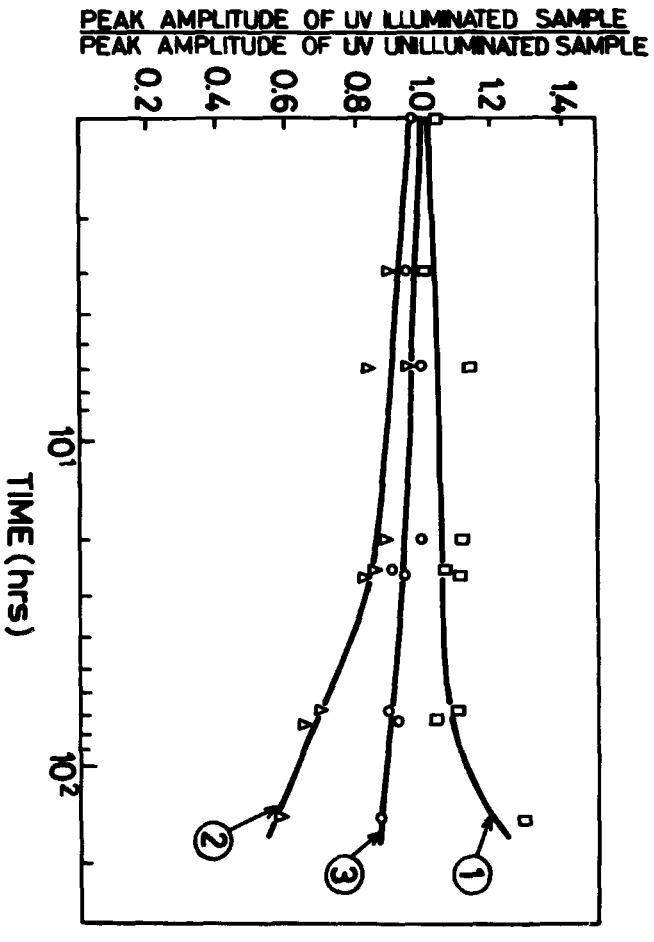

Fig. 7. Influence of a fluorescent light on the stable peaks of the LiF:Mg,Ti. Two 6 watt tubes at a distance of 20 cm /700 lx/ were used,

1 - amplitude of the IVth peak,

2 - amplitude of the Vth peak,

3 - integrated output.

Studies of the Thermoluminescence of Lithium Fluoride Doped With Various Activators

by

M.E.A. Robertson
D.A. Pitman Ltd., Weybridge, U.K.

and

W.B. Gilboy,
Radiation Unit, University of Surrey, Guildford, U.K.

Abstract

'Pure' lithium fluoride with weak TL properties has been doped with various activators and the glow curve structure of each sample examined. Two combinations of activators produced samples with sensitivity comparable to commercially available LiF. The low temperature peaks in these samples were at a higher temperature than the light-sensitive low temperature peak in TLD-700(1) and preirradiation annealing at 80°C for 24 hours did not alter the glow curve structure.

1. Introduction

Lithium fluoride is the thermoluminescent material of choice for many dosimetric applications since it possesses the advantages of a fairly high sensitivity, a wide linear dose range, near tissue equivalence, and it can be obtained with different proportions of the lithium isotope, which enables differentiation between thermal neutrons and other ionising radiations. However, commercially available LiF has two main disadvantages. Firstly, sensitivity is dependent on thermal history. Secondly, the low temperature peaks in the glow curve structure can cause readout errors by fading, retrapping, and sensitivity to ambient light. LiF therefore is still open to improvement.

TLD - 700 (and TLD - 100) is prepared from LiF single crystals and is known to contain Mg, Al and Ti among other impurities.[2] Rossiter et al.[3] has recently prepared similar materials by the addition of Mg and Ti to pure LiF. Jones et al. [4, 5] produced a large number of samples by adding impurities to pure LiF and melting the mixture in a graphite crucible. It was decided to prepare samples by a similar method since the equipment required was readily available, and success would result in a less costly product.

2. Experimental

Preparation of samples was as follows. 'Optran'[7] zone refined LiF was ground to a fine powder. Selected impurities were added, some dry, others in solution. Generally 0.01% by weight of impurity was added. 'Wet' mixes were dried at 90°C for 2 hours. The mixture was placed in a platinum crucible and

heated at 900-950°C for 2 hours in air. The furnace cooling rate was approximately 80°C per hour through the melting point (843°C). The material obtained was ground and sieved and the portions between mesh sizes 80 and 200 were annealed at 400°C for 1 hour and used for glow curve measurements.

Samples were generally dosed to 30 Rads with a cobalt-60 source (dose-rate approximately 1.5 Rads/hr.) and read-out 3 hours after completion of the irradiation. All results given in this paper were obtained from examination of glow curves between 25°C and 300°C, with a linear heating rate of 5°C/sec.

3. Results

Table 1 shows peak temperature and relative peak heights per rad for a selected number of samples. Peak heights per rad are given relative to a value of 100 assigned to the 210°C peak of TLD - 700.

Possible errors in peak temperatures due to limitations in the reproducibility of the sample heating cycle are estimated to be less than 10°C.

Figure 1 shows the glow curve structure of the starting material ('Optran' LiF) in two ways. Curve 1 is the result of a dose of 500 rads at a dose-rate of 20 mrads/hr. i.e. over a period of several months. Low temperature peaks have decayed, and the higher temperature peaks are shown in greater detail. Three peaks are discernible, at 170, 210 and 280°C. Curve 2 was taken after irradiation to 40 rads at 1.5 rads/hr. The main peak is now at 140-150°C, with a small higher temperature peak. Curve 3 shows for comparison the glow curve of TLD - 700. The lowest temperature peak of TLD - 700 visible (125°C) is at least 15°C lower than the lowest temperature peak of the Optran LiF. From Table 1, the 210°C peak in the Optran sample has less than 1% the sensitivity of the 210°C peak in TLD - 700, whereas the low temperature peak is 20% as sensitive. After a remelt, the sensitivity of the Optran sample low temperature peak dropped by a factor of 4.

The addition of MgF_2, $MgCl_2.2H_2O$, MnF_2, and CaF_2 singly as activators produced little measurable thermoluminescence. Li_2TiF_6 (lithium hexafluorotitanate[6]) produced appreciable TL peaks at 150 and 210°C (Figure 2). Li_2TiF_6 + MgF_2 and Li_2TiF_6 + MnF_2 gave less light output than Li_2TiF_6 on its own. With CaF_2 + $CaCl_2$ + Li_2TiF_6 the total light output exceeded the light output of TLD - 700. The peak positions shifted downwards to 135 and 190°C.

Titanium tetrafluoride (TiF_4) produced appreciable thermoluminescence peaking at 150°C and 200°C (Figure 3). Total light output was similar to TLD - 700. Strontium Titanate (Figure 4) was the only other impurity to give two well-defined peaks, at 150 and 210°C. MgF_2 + ZrO_2 gave a fairly good peak at 135°C. Zirconium is the next highest analogue of titanium in the Periodic Table.

Other activators listed in Table 1 produced low sensitivity samples.

The shape of the glow curve and the overall sensitivity of both the TiF_4 and the CaF_2 + $CaCl_2$ + Li_2TiF_6 activated samples did not alter when the above samples were subjected to a pre-irradiation anneal of 80°C for 24 hours.

This is in contrast to TLD - 700, where the low temperature traps are largely removed by the same annealing cycle.

4. Conclusions

The failure of Mg to produce appreciable thermoluminescence in the above samples could be related to sample time above melting point and rate of cooling. Investigations are continuing.

The dependence of LiF TL sensitivity on the presence of Ti is confirmed. Li_2TiF_6, TiF_4, and $SrTiO_4$ all produced appreciable thermoluminescence. The addition of CaF_2 + $CaCl_2$ + Li_2TiF_6 led to a marked enhancement in light output.

The failure of the 80°C anneal to remove the 140-150°C traps in the two most sensitive samples prepared and the difference in temperature between this peak and the 120°C peak in TLD - 700, suggests that the activators causing the 120°C and the 150°C peaks are different.

References

1. Manufactured by the Harshaw Chemical Co.
2. Patent Specification, 1967, No. 1059518, The Patent Office, London.
3. M. J. Rossiter, D. R. Rees-Evans, and S. C. Ellis, J. Phys. D, 1970 Vol. 3. pp. 1816-23.
4. D. E. Jones, J. R. Gaskill, A. K. Burt and S. Block, USAEC Report UCRL - 12151, 1964.
5. D. E. Jones and A. K. Burt, USAEC Report UCRL - 12387, 1965.
6. Manufactured by Alfa Inorganics Inc.
7. Manufactured by B.D.H. Chemicals Ltd.

TABLE 1

Relative Peak Heights and Temperatures - Selected Samples

ACTIVATORS	RELATIVE PEAK HEIGHTS							TOTAL LIGHT OUTPUT
	120°C	135°C	150°C	170°C	190°C	210°C	280°C	
1. Optran			20	< 1		< 1	< 1	20
2. Optran-Remelt			5			< 1		
3. TLD - 700	10					100		110
4. MgF_2	2							
5. $MgF_2 + TiSi_2$	12							
6. $MgF_2 + ZrO_2$		30				< 1		30
7. $MgF_2 + Li_2TiF_6$		15						
8. MnF_2		4				2		
9. $MnF_2 + Li_2TiF_6$		35				10		45
10. CaF_2	< 1					< 1		
11. $CaF_2 + CaCl_2 + Li_2TiF_6$		95			28			123
12. $CaF_2 + CaCl_2 + TiSi_2$		6						
13. Li_2TiF_6			40			18		58
14. TiF_4			60			40		100
15. $DyCl_3$		< 1			< 1			
16. La_2O_3		4			< 1			
17. HoF_3			3		< 1			
18. $SrTiO_4$			15			10		25
19. HfO_2		12			< 1			

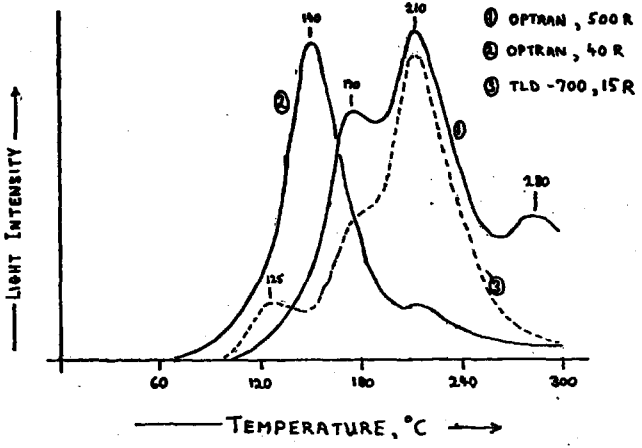

Figure 1. Glow curves of 'Optran' LiF.

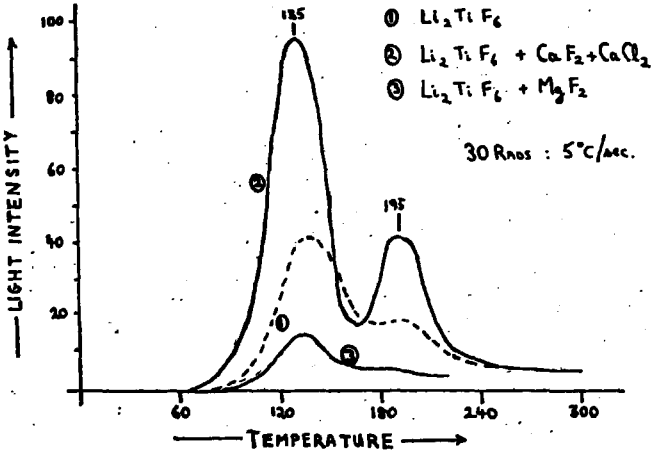

Figure 2. Glow curves of LiF doped with (1) Li_2TiF_6, (2) $Li_2TiF_6 + CaF_2 + CaCl_2$, (3) $Li_2TiF_6 + MgF_2$.

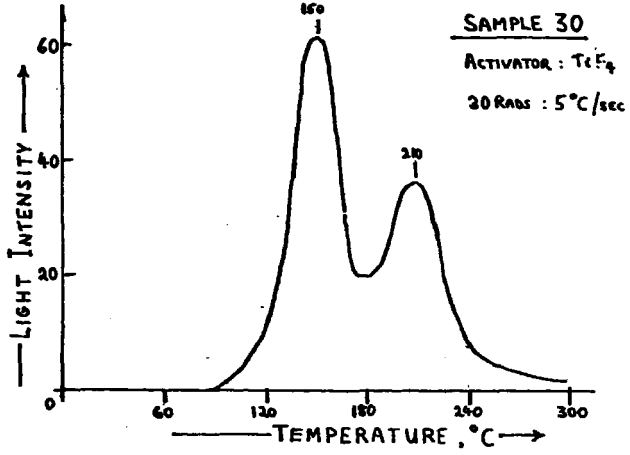

Figure 3. Glow curve of LiF doped with TiF_4.

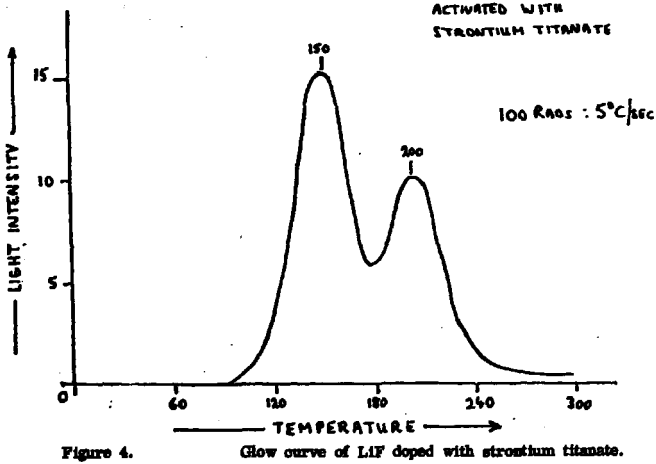

Figure 4. Glow curve of LiF doped with strontium titanate.

Fowler

What does "Optran" consist of?

Robertson

"Optran" is the trade name of zone-refined LiF produced by BDH Chemicals Ltd., Poole, Dorset, UK. A list of maximum impurity levels can be obtained from them. The concentration of titanium is less than 2.7 ppm.

A New TL LiF (NTL-50) Which is Unnecessary of Annealing, Its Properties Especially for Application and the Results of Several Practical Cases

by

Katsumi NABA

Oesterreichische
Studiengesellschsft für Atomenergie
Ges.m.b.H.
Institut für Strahlenschutz
Lenaugasse 10, 1082 Wien, Austria

Abstract

New TL LiF has been developed and named NTL-50, The necess -ary properties for practical application has been studied. The results are as next following

1. There are no change of TL responce during exposure from the temperature -20°C to +40°C
2. Annealing is only necessary to heat 300°C x 3 min without N_2 flow until 1,000 R previous exposure. For over 1,000 R previous exposure, annealing should be done at 300°C x 1 hr with N_2 gas flow.
3. Under 1 R measurement: N_2 flow is necessary
   Over 1 R measurement: without N_2 flow
4. Spurious luminescence can be eliminated by 110°C x 5 min pre-heating.

and several application have been done about next following

1. Measurement of contamination : Quick and convenient measure

-ment about surface,water and air H-3 contamination
 a. Surface contamination after fire accident
 b. Surface contamination under external γ rays
 c. Surface contamination in waste disposal site
2. Development of new finger ring (Doppel Ring) and its applica -tion for Gloved Box working.
3. Separate ß and γ measurement from mixed radiation by TLD and Fluoroglass dosimetry.

Introduction

Thinking about the recent development of TLD studies, the most important problem is how to make the measurement correct -ly and conveniently. The new TL LiF which is made from new starting materials has been developed and named NTL-50. The basic properties and some application have been studied and reported. The basic properties are summarized as next following

1. Linearity of TL vs dosis and measurable range several mR ~ 10,000 R
2. Energy dependence for low energy photon at 25 Kev :1.25 for powder,1.50 for Silicon resin Disk
3. Emission spectra of TL : 300 mμ ~ 500 mμ
4. Polar responce
5. repeated usability : Over 100 times

Considering about practical application, the next following properties are important

1. Spurious luminescence
2. Fading at several temperature
3. Variation of responce during exposure at environmental temperature
4. Change of sensitivity as a function of previous exposure
5. Responce of thermal radiation from TL LiF in air and N_2 gas
6. Effect of pre-irradiation annealing on the responce of LiF
7. Annealing or elimination of previous exposure history

Acording to the above mentioned properties of NTL-50, the standard measuring procedure have been decided and several practical application were carried out about following case.

1. Measurement of surface contamination
2. Measurement of H-3 in air by Disk
3. Measurement of finger dosis for Gloved Box working using a newly developed finger ring
4. ß and γ dosis measurement seperatly from mixed ß,γ rays by TLD and Fluoroglass dosimetry

I. Some properties of NTL-50,LiF which are necessary for practical application

TL materials and measurement apparatus are as next following

(1) NTL-50, LiF powder. Disk: Silicon resin adhesive
D = 12 mm, thickness = 64 mg/cm^2
(Nemoto Tokushu Kagaku Co., Tokyo)

(2) Aloka TLR 101 Digital Reader prototype
This apparatus can be integrated light yield digitaly from 150°C to 250°C by temperature regulation. It does not use time regulation. (Japan Radiation and Medical Electronics Co.,Tokyo)

1. Spurious luminescence

Spurious luminescence on the 1st peak is easily caused by exposure to visible light,friction and other stress beside radiation. The quenching of spurious luminescence in the dark room was studied. After saturation with visible light, the samples were placed in a dark room at room temperature. The results are shown in Fig 1 . Keeping the samples for 30 min ~ 14 hrs in a dark room, the 1st peak was observed to decrease, but did not disappear completely even after 14 hrs. Judging from these results, the capture electron trap associated with these pheno -mena seems to be a shallow trap. Therefore the spurious lumine -scence may be trapped off by heating at 110°C for 5 min or 150° C x 30 sec. The fading of spurious luminescence seems to be very important for the accucuracy of measurement.

2. Fading with temperature after irradiation

Fading at different temperature after exposure was investigated for NTL-50. The results are shown in Fig 2. Under 40°C, no significant fading was observed after 15 days, but over 60°C, the fading increased and reached about 37 % at 100°C after 15 days. From these results, even if the TL material is used on or

in the human body, no change upon the NTL-50 responce may be expected.

3. Responce change at different temperature during irradiation

This experiment were conducted for a temperature range from -40°C to 100°C with the irradiation of NTL-50 by Co-60 γ rays. The results are shown in Fig 3. No significance change in the responce was observed from -20°C to 40°C. Disk which is combined with Silicon resin adhesive shows some decrease of TL responce under -20°C, but for other higher temperature, such variation are same as powder.

4. Change of sensitivity as a function of previous exposure for TL LiF

After irradiation of several level γ rays used Cs-137 source, the change of TL sensitivity were measured and shown in Fig 4 . There are no change of sensitivity under 1,000 R exposure. For over 1,000 R to 5 x 10^5 R exposure, the increse of sensiti -vity are observed. For over 5 x 10^5 R exposure, the decrease are observed. Therefore over 1,000 R previous exposure, an annealing should be done at 300°C x 1hr with N_2 gas flow.

5. Responce of thermal radiation from TL LiF in air or N_2 gas during heating

These comparison are summarized in Fig 5 . From this results, N_2 gas flow are necessary for the measurement of mR level.

6. Effect of pre-irradiation annealing on the responce of TL LiF

After irradiation of several level dosis from 100 R to 5x10^5R, several kinds of annealing were carried out (1) no annealing -- -- 300°C x 3 min (2) 300°C x 30 min (3) 300°C x 1 hr and these change of sensitivity were compared. These results are shown in Fig 6 . From this results, for under 1,000 R previous exposure, the annealing only necessary 300°C x 3 min without N_2 flow. From 1,000 R to 10,000 R previous exposure, these annealing should be done under N_2 flow, 300°C x 1 hr.

7. Effect of room light on TL LiF

Some authors have reported about light effect upon TL material. For the measurement of low dosis, this problem is very important. Direct sunlight upon TL material caused a strong effect not only 1st, 2nd peak but also main peak, therefore black paper or thin Aluminum are always used. The room lamp also make effect upon TL material, but this effect is not so severe as sunlight. The effect of room light were experimented under brightness of 500 LX Fluorescence light. The results are shown in Fig 7. From this results, it is clearly recognized that the saturation of light effect is completed after exposure of 60 sec. From this phenomena, saturation will be occured only about restricted shallow traps. This effect is easily eliminated by pre-heating method of 110°C x 5 min or 150°C x 30 sec.

8. Annealing (elimination of previous history)

Thinking about the annealing procedure of TL material, nowa-days this problem is very important for the practical applica-tion. A long hours annealing under N_2 gas flow is not convenient for practical application. From the results of Fig 6, this procedure about NTL-50 is only necessary to heat at 300°C x 3 min until 1,000 R previous exposure dosis. Under the level of 1R previous dosis, there are only 0.3 % light yield remain after 300°C x 3 min heating, but for over 1,000 R previous exposure, the annealing of 300°C x 1 hr are necessary. This improvement about the annealing will make the practical application easier. But thinking about the repeated use and change of sensitivity, this heating temperature does not always exceed over 300°C and duration of heating does not exceed over 5 min without gas flow.

II Abstract of measuring procedure

The next measuring procedure have been decided using Aloka TLR-101 digital reader. The standard calibration of this apparatus is done by a newly developed standard radioactive self-luminous material. A project lamp are used as heating source. The measuring procedure are summarized as next following.

1. Heat treatment of NTL-50 before irradiation
300°Cx3 min heating without gas flow(Until 1,000 R previous dosis)

2. Pre-heating before measurement

110°C x 5 min or 150°C x 30 sec heating without N_2 gas flow.

3. Necessity of gas flow during measurement

(1) under 1 R measurement : N_2 gas flow is necessary

(2) Over 1 R measurement : without N_2 gas flow

4. Range of measuring temperature

150°C ~ 250°C, after finishing of measurement at 250°C, heating are moreover continued about several seconds.

III Practical application

1. Measurement of surface contamination

Basic studies about surface radioactive contamination have been done and reported. These results which were obtained by Disk are summarized as next following

Sr-Y-90 ----- 10^{-3} μCi/cm^2 ----- 6 mR/hr ± 30 %

Co-60 ----- " " ----- 1 mR/hr ± 30 %

Using this result, the next following application have been done.

(1) Measurement of surface contamination under γ rays in Chemical Laboratory where R.I is used

Under the background of γ rate exposure, the surface contamination were measured at the level of 10^{-4} μCi/cm^2.

(2) Measurement of surface contamination at Chemical Laboratory where radioactive fire accident was occured

From ceiling and walls, γ contamination were measured at the level of 10^{-5} ~ 10^{-4} μCi/cm^2.

(3) Measurement of surface contamination in waste disposal site by TL Disk

At first, personal dosimetry were carried out using TLD powder. The results are shown in Tab 1. From this results, 183 mR/week exposure was observed, therefore the measurement of surface contamination were completely done. These results are shown in Tab 2. The contamination over 10^{-2} μCi/cm^2 has been measured from the surface of container in which contains radioactive waste liquid. Over 10^{-3} μCi/cm^2 were measured from floor and surface of the other containers. The rest of containers and the table were contaminated at the level of 10^{-5} ~ 10^{-4} μCi/cm^2.

The most parts of floors were under the level of 10^{-5} μCi/cm^2.

2. Measurement of water contamination

Basic studies about the measurement of water contamination were carried out and reported. Comparing TLD method with other conventional method example for G.M or Scintilation detector of water proof, TLD method is not convenient, therefore such appli-cation has not yet done.

3. Measurement of H-3 air contamination

Using a Standard H-3 water (Packard, Standard of Liquid Scint-illation Spectrometer), the H-3 air contamination has been made in cylindrical polyethylene container (volume:930 ml). The radio-active concentration in air is 3 x 10^{-6} μCi/cc. The other one container was used as control experiment. These container were covered with Aluminum foil not to occured light effect upon TL material. After putting Disk in two containers for 3 days, both group of Disk were dried by the next method. (1) After moistened of disks with absolute alcohol, humidity in disk will be evapora-ted together with alcohol. (2) Heating of disks were carried out in electric furnace at 110°C x 5 min.

Above all mentioned procedures should be done under protection of light . These results are summarized as next following

H-3, μCi/cc air	H-3 exposure(1)	Control(2)	(1)-(2)
3 x 10^{-6}	36 mR ± 3 %(5 samples)	11 mR ± 5 %	8 mR/day

4. Responce of TL LiF at several distance from Pm-147

At the distance from 2 cm to 15 cm, the measurement were made by Disk. The results are shown in Fig 8. Such measurement will be easily done by TL Disk.

5. Application for finger ring

For Gloved Box workers, the measurement of finger dosis have been done with newly developed finger ring, this ring is named "Doppel Ring". A pair of polyethylene or other tissue equivalent resin ring were coupled and between a pair of ring, TL powder is packed. The thickness of upper and side wall of containning part is restricted 20 mg/cm^2. In Fig 9 show the results of

practical application for Gloved Box workers. All workers of Gloved Box willingly use this Doppel Ring for radiation control.

6. Seperate measurement of mixed ß and γ rays using TLD and Fluoroglass dosimetry

(1) Source and exposure

Sr-Y-90	10 mCi in Penicilline bottle.	at 10 cm, 30 min
Co-60	8 mCi	at 1 m, 22 hrs

Glass: Toshiba Fluoroglass FD-P8-3, Reader: Toshiba FGD-6

The suitable type of Fluoroglass for ß rays measurement is T9-3 glass and BB-1 holder, but considering about ß sensitivity of FD-P8-3 Fluoroglass, its property of negligible low sensiti-vity seems to be suitable only γ rays measurement from ß,γ mixed radiations. The results are shown in Tab 3. The estimation value is only ß radiation + γ radiation. Comparing about the value of ß + γ (measurement) with TLD and Fluoroglass, this difference is meaned only ß radiation dosis. This method will be one of the convenient method for the separate measurement from ß,γ mixed radiation.

IV Future problem

1. Improvement of TL LiF

Concernning the annealing of NTL-50, this procedure is suitable for practical application, but thinking about the necessity of N_2 gas flow under 1 R measurement, this procedure are yet troubl-esome. Further work will be necessary for the development of such TL material.

2. Application fields

The most suitable fields of TL LiF is medical application. Considering from the measuring method of surface ß contamination, this method will be easily applied to the measurement of skin dosis. Other application fields are the measurement of radiation distribution in human body when Co-60 or ß rays were irradiated upon Cancer organ example for Uterine Cancer and Cancer of Digestive Organs.

Acknowledgement

The writer gratefully acknowledges helpful discussion with Dr. Ch.Tritremmel during this work.

References

1. K.Naba, Y.Nishiwaki et al, IRPA II Congress. 25 - 26 (1970)
2. K.Naba, A.Hefner and Ch.Tritremmel, International Synposium on Rapid Methods for Measurement of Radioactivity in the Environment. Munchen (1971)
3. T.F.Johns, et al, IAEA-SM-143/9. (1970)

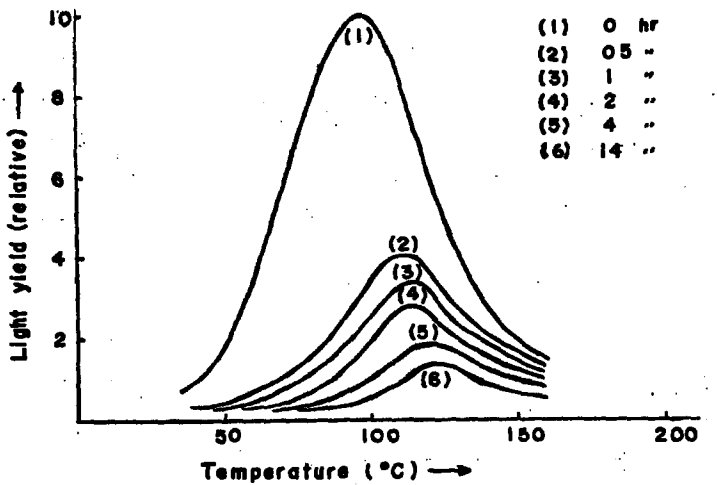

Fig.1 Fading of the Spurious Thermoluminescence (caused by visible light) in dark room

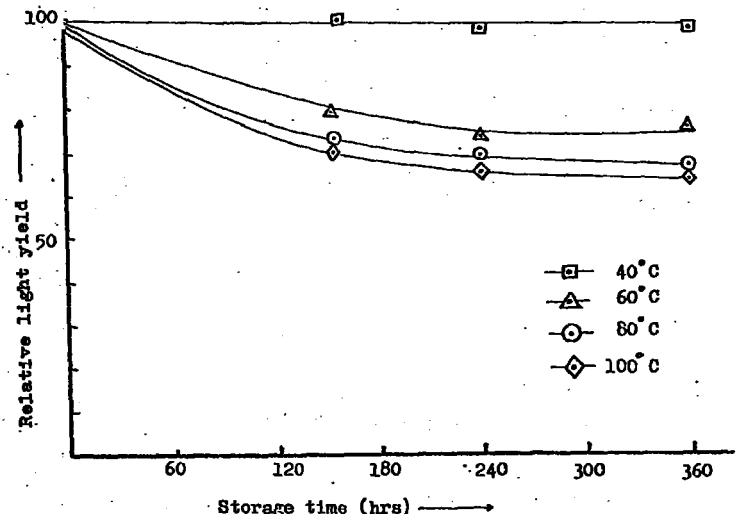

Fig. Fading of Thermoluminescence (NTL-50, LiF) at several Temperature

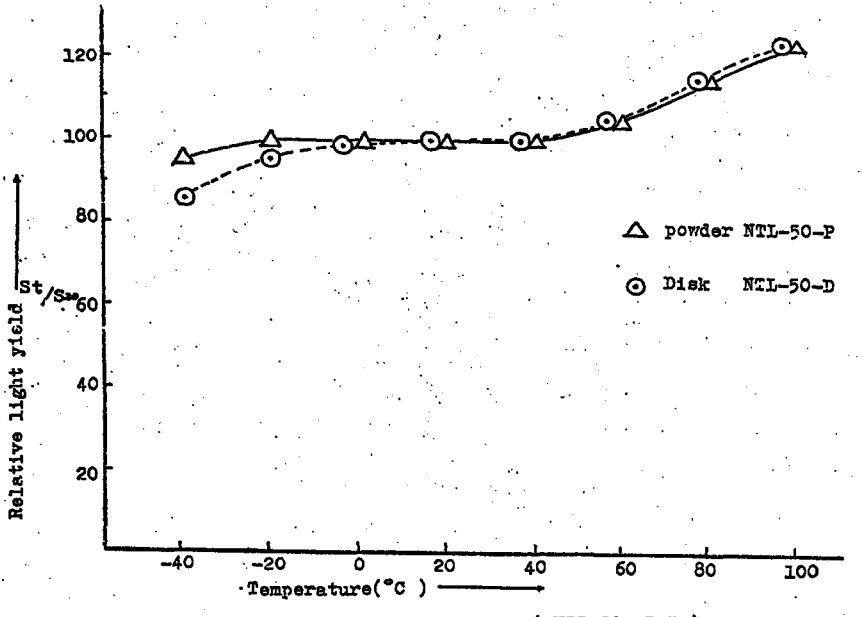

Fig 3 Variation ofresponce when TL (NTL-50, LiF) were irradiated (Co-60 γ rays) at several temperature

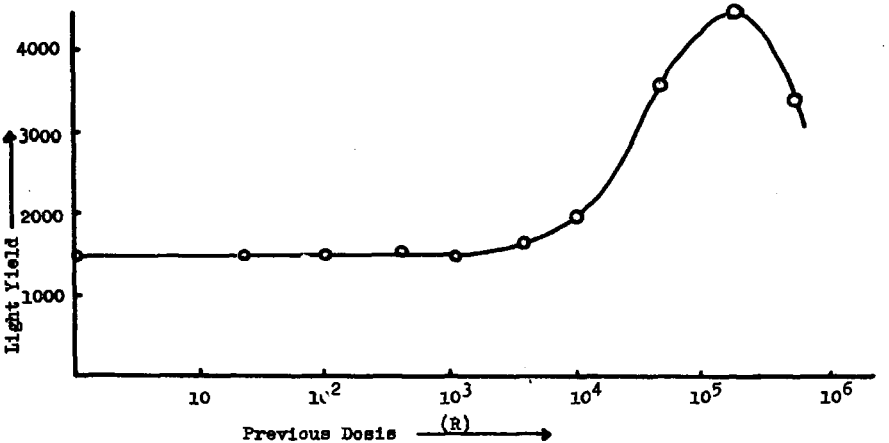

Fig4. Change of Sensitivity as a Function of Previous Exposure for T.L. LiF (NTL-50 Powder)

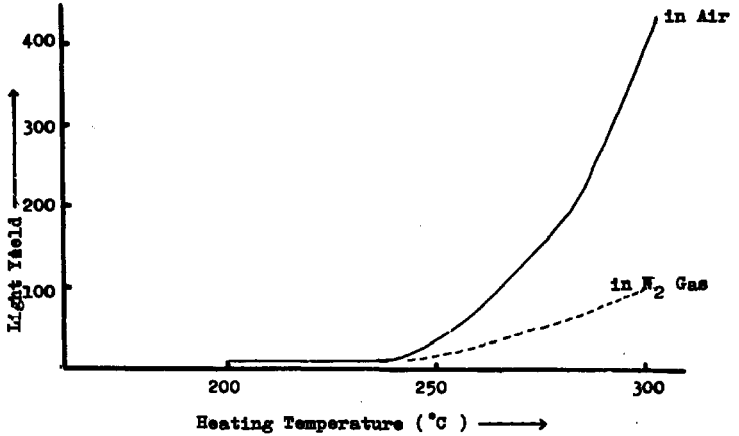

Fig 5. Responce of Thermal Radiation from T.L. LiF (NTL-50 Powder) in Air & N_2 Gas

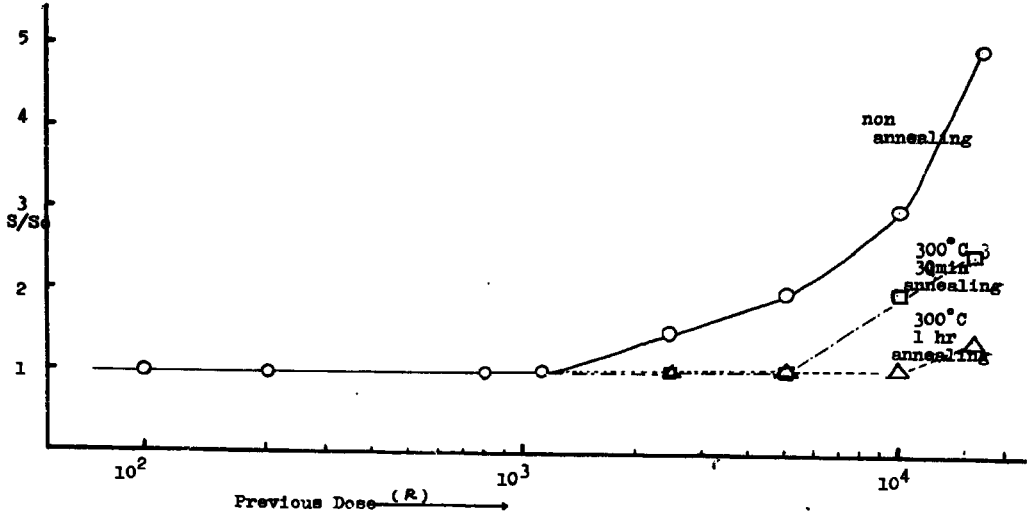

Fig 6. Effect of Pre-irradiation Annealing on the Responce of T.L. LiF (NTL-50 Powder)

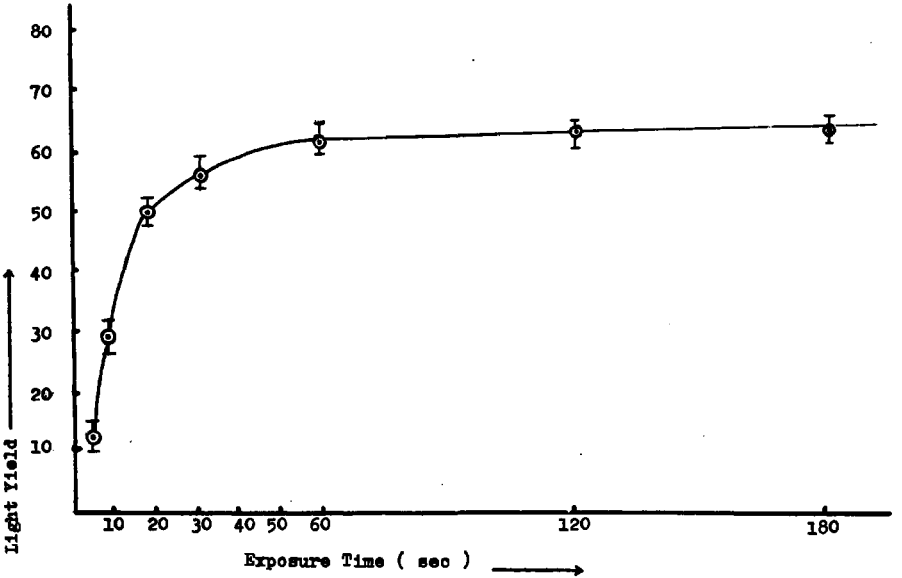

Fig 7 Effect of Light (500 lux) in Room on T.L. LiF (NTL-50 Powder)

Tab 1 Results of Personal Dosimetry about persons who were working in Waste Disposal Site by TLD (NTL-50 Powder)

Name	mR/week	Standard Deviation	No. of T.L. sample
J.S	53	3 %	3
H.K	6	8 %	"
A.L	13	0	"
P.A	12	9 %	"
A.B	11	13 %	"
K.N	1	-	"
S.H	188	2 %	"
K.S	12	4 %	"

Table Measurement of Surface Contamination in Waste Disposal Site by TLD (NTL-50, LiF. Disk type)

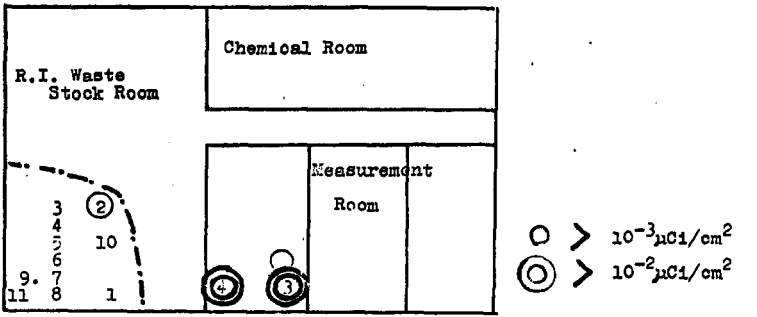

No. of Sample	object	mR upper / mR lower	exposure hrs	Ratio (β,γ)	exposure radiation dosis	surface radiation dosis	level of surface contamination
1	floor in stock room	5557 / 5921	117	0.16 γ	5464 mR/117 hrs	3.9 mR/hr	γ: 3.9×10^{-3} μCi/cm^2
				0.36 β	5353 " "	4.8 "	β: 8.0×10^{-4} "
2	surface of container in stock room	35 / 39	117	0.16 γ	34 mR/117 hrs	0.03 mR/hr	γ: 3.0×10^{-5} "
				0.36 β	31 " "	0.05 "	β: 10^{-5} "

Table Measurement of Surface Contamination in Waste Disposal Site by TLD (NTL-50,LiF. Disk type)

No of Sample	object	mR upper / mR lower	exposure hrs	ratio (β,γ)	external radiation dosis	surface radiation dosis	level of surface contamination
3	filter of container	1934 / 7307	88	γ:0.16	987 mR/88 hrs	71 mR/hr	γ:7.1x 10^{-2} μCi/cm^2
4	surface of container	1776 / 4548	"	γ:0.16	527 " "	45 "	γ:4.1x 10^{-2} "
5	surface of container in stock room	29 / 52	"	γ:0.16	25 " "	0.32 "	γ:3.2x 10^{-4} "
				β:0.36	15 " "	0.42 "	β:7.0x 10^{-5} "
6	"	153 / 167	117	γ:0.16	150 mR/117 hrs	0.21 "	γ:2.1x 10^{-4} "
				β:0.36	145 " "	0.34 "	β:6.0x 10^{-5} "
7	"	195 / 197	"	-	195 " "	---	---
8	"	566 / 595	"	γ:0.16	560 " "	0.21 "	γ:2.1x 10^{-4} "
				β:0.36	550 " "	0.33 "	β:6.0x 10^{-5} "
9	"	315 / 318	"	-	315 " "	---	---
10	table in stock room	152 / 153	"	-	152 " "	---	---
11	surface of container in stock room	81 / 110	"	γ:0.16	76 " "	0.21 "	γ:2.1x 10^{-4}
				β:0.36	62 " "	0.39 "	β:6.5x 10^{-5}

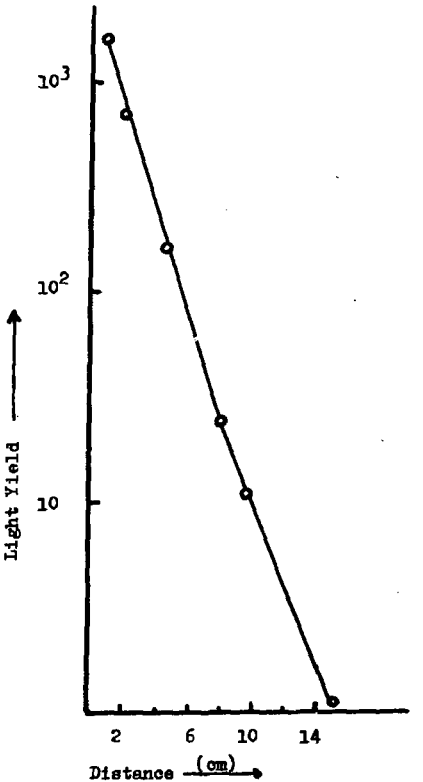

Figs. Responce of T.L. LiF(NTL-50) at Several Distance from Pm-147

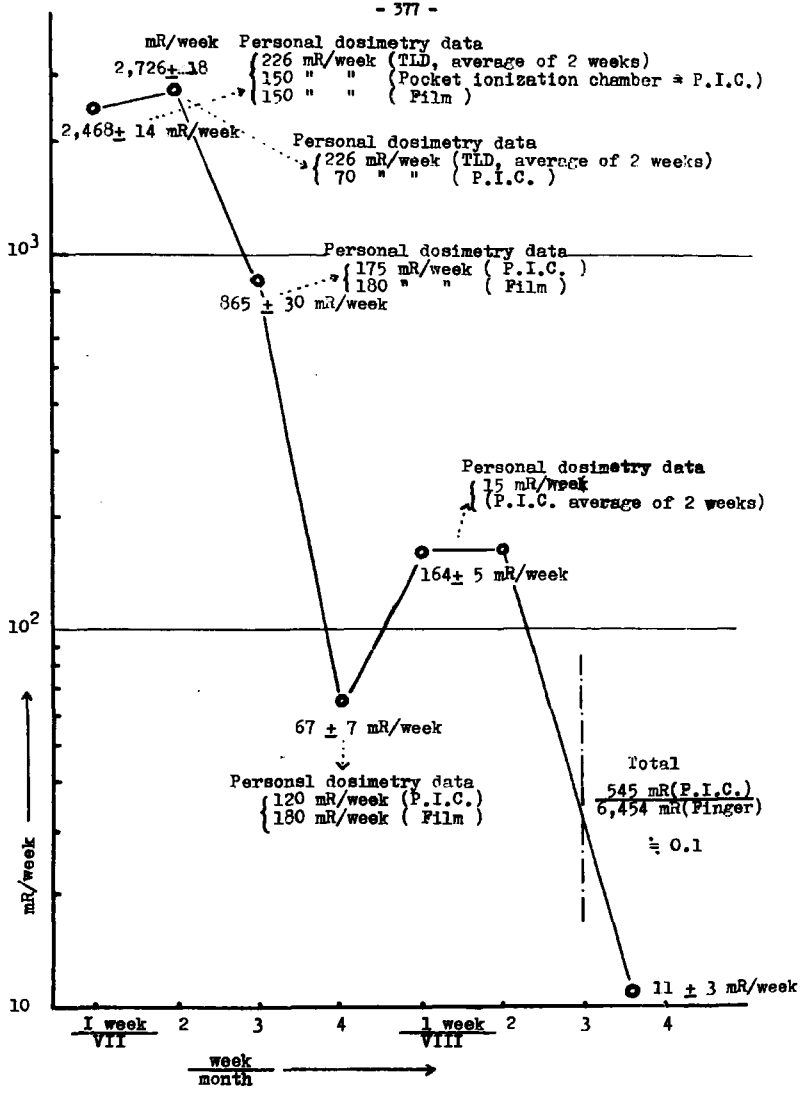

Fig.7. Measurement of Finger Radiation Exposure during Glove Box Working by new TLD Finger Ring (Doppel Ring, NTL-50 Powder)

Tab3. Seperate Measurement of Mixed ß and γ radiation using TLD and Fluoro Glass Dosimetry

1. Radiation source and exposure condition

Sr-90	10 mCi in Peniciline bottle.	at 10 cm, 30 min.
Co-60	80 mCi (estimated)	at 1 m, 22 hrs.

2. Kind of dosimeter

(a) TLD: LiF:Mg, NTL-50 Disk type, Reader —— Aloka TLR 101

(b) Glass: Toshiba Fluoroglass FD-P3-3, Reader——Toshiba FGD-6

Results

	TLD (Disk)	Fluoroglass
only ß radiation	354 ± 4 mR	22 ± 5 mR
only γ radiation	195 ± 1 mR	199 ± 15 mR
ß + γ (estimation)	549 mR	221 mR
ß + γ (measurement)	549 ± 37 mR	211 ± 15 mR

Mason

I noted with interest the light-induced peak which occurs in NTL-50 LiF at about 100°C in the glow curve. A similar peak is known to be induced in TLD-700 LiF by UV light. Do you have any explanation for the origin of this peak?

Naba

I have made direct sunlight exposure of NTL-50 disks (Si resin) without light-protective material. I observed that a large effect occurred not only for the 1st and 2nd peak, but also for the main peak. Therefore, after direct exposure of NTL-50 to sunlight or UV-light, measurement in the mR level is impossible, and a light-protective cover is necessary. I think that the UV-induced peak at 100°C is caused by a shift from other high-temperature peaks.

THERMOLUMINESCENT RESPONSE OF NATURAL BRAZILIAN* FLUORITE TO ^{137}Cs GAMMA-RAYS

by

S. Watanabe and E. Okuno

Instituto de Energia Atômica and Instituto de Física
University of São Paulo, São Paulo, Brazil

Abstract

Thermoluminescent response of natural Brazilian fluorite to ^{137}Cs gamma-rays has been studied, having in mind both the understanding of the supralinearity phenomenon and the utilization of this fluorite in radiation dosimetry.

Virgin fluorite was pre-annealed at 580ºC for ten minutes followed by 400ºC for two hours and then irradiated to different exposures between 25 and 1.2 MR. The response of glow peak II (pan temperature 180ºC) is linear up to 3 kR, beyond which it becomes supralinear and finally saturates at about 300 kR. Under these conditions, the response of glow peak III (pan temperature 290ºC) is not supralinear, and saturation is reached sooner, at about 100 kR.

The correlation between supralinear response and sensitization has also been studied. Samples irradiated to different exposures, as above, were individually annealed after irradiation for 15 minutes at 400ºC and then exposed to 100 R. Peak III exhibited sensitized response above 3 kR previous exposure, whereas peak II demonstrated only slight sensitization, and then only near 100 kR previous exposure. Thus, sensitization is anti-correlated with supralinear response for these two peaks.

Peak II was found to be sensitized, however, when the post-irradiation anneal was at 175ºC instead of 400ºC, and thus eliminated only peaks I and II, not I, II and III. Also, supralinear response can be obtained from peak III when the virgin phosphor is annealed at 600ºC for times longer than 10 minutes.

These results are qualitatively explained by the model postulating competing traps, although this model must be applied in a slightly altered form. Other existing models do not seem appropriate.

Based in part upon portions of a thesis submitted by E. Okuno to the Institute of Physics, University of São Paulo, in partial fulfillment of the requirement for the Ph.D. degree.

Introduction

The common thermoluminescent dosimeters exhibit linear response to low exposures, while at high exposure they demonstrate saturation effects where all traps are filled and response can not increase. In the intermediate region, say 500 to 1,000 R, these materials often exhibit supralinear response, that is, their emission per Roentgen of exposure begins to increase. Several phenomenological models have been proposed to explain this effect, but choosing between the models is usually difficult.

Supralinearity has been found experimentally for LiF:Mg[1], $Li_2B_4O_7$:Mn[2], and some other material[3], while CaF_2:Mn responds linearly from 0.1 to 3 x 10^5R. Schayes et al.[4] found that peaks II, III, IV, and V occurring at 175, 260, 385 and 525ºC in the glow curve of Belgian natural calcium fluoride present nonlinearity above 10 kR.

We have studied Brazilian natural calcium fluoride, intending its application in dosimetry. The results indicate that its TL response as a function of exposure or absorbed dose is most likely caused by competing traps.

Thermoluminescence vs. Exposure

The fluorite used in this work was collected near Criciuma, Santa Catarina State, Brazil, and was distinguished from other samples by its green color. Before use, the fluorite was crushed, powdered and sieved through 80 onto 200 mesh Tyler screens.

Irradiation was at room temperature using ^{137}Cs gamma-rays to expose samples contained in cylindrical polyethylene capsules. Unless otherwise noted, irradiation was preceded by annealing 10 minutes at 580ºC and then 2 hours at 400ºC, both followed by quick cooling (less than 3 minutes) to room temperature. This treatment largely eliminates TL induced during geological storage (we will call this natural TL), particularly that corresponding to peaks I through V.

Most TL measurements were taken on the CON-RAD model 5100 reader which uses constant current in the planchet.

Results

a) Response to Gamma-Rays

Figure 1 shows typical glow curves and heating cycles for these experiments. The shape of the glow curve is largely insensitive to different pre-irradiation annealings, or cooling rates, although some heat treatment must be given to eliminate the natural TL.

Since peaks II and III are the important ones for dosimetry we concentrated on these peaks. Their heights as functions of exposure are shown in Fig. 2 where we plot TL/R against exposure, since this form is most easily read. For peak II we see that response is initially linear to about 3 kR, then supralinear to about 100 kR, and finally saturates beyond this value. Glow peak III is different; it responds linearly to about 200 R, then less than linearly to saturate at about 100 kR.

Supralinear response in peak III can be obtained, however, if the pre-annealing is varied from the normal one. Figure 3 demonstrates the effect of pre-annealing for 10, 30, and 60 minutes at 600ºC in the place of the normal 10 minutes at 580ºC. After 10 minutes at 600ºC the response is much as Fig.2. Annealing for 30 minutes reduces the overall sensitivity, but the peak now demonstrates a slight supralinearity, as shown in the middle curve of the

figure. Annealing for 60 minutes further reduces the sensitivity and increases the supralinearity, as seen in the bottom curve. Peak II on the other hand remains supralinear, but displays a decreasing sensitivity similar to that of peak III.

b) Sensitization

Some TL phosphors irradiated to exposures able to cause supralinearity present an increased sensitivity to low exposures, once the high exposure TL is erased thermally. Such an increase in sensitivity is called sensitization.[5] In dosimetry LiF:Mg a direct correlation was found between supralinearity and sensitization.

Our samples exhibited a sensitization effect shown in Fig. 4. The samples were given the exposure shown on the ordinate, then annealed 15 minutes at 400°C to empty traps corresponding to peaks II and III. Before final read out they were irradiated to 100 R test exposure. The top curve shows that peak III is sensitized by previous exposures larger than about 3 kR. The sensitivity corresponding to 10^6 R previous exposure is close to 2.25 times larger than that corresponding to a previous exposure less than 1 kR. On the other hand peak II does not display a clear sensitization, except a small increase near 10^6 R, as shown by the bottom curve of Fig. 4. Comparison with Fig. 2 shows that the supralinear peak is not sensitized, and vice versa. It is also interesting to note that peak II begins to show its increased sensitivity only when peak III has begun to saturate.

To test the idea that peak III might be a competing trap we measured the sensitivity of peak II with peak III filled, and compared with the case when peak III is empty. Figures 5, 6, and 7 show the results.

In each case the sample was given a previous exposure, as indicated in the figures. A portion of each sample was then given one of two treatments: 1) Annealing at 300°C for 30 minutes to empty II and III traps filled by the previous exposure, 2) Annealing at 175°C for 15 minutes to only empty II traps. The samples were then given a 1,000 R test exposure, and read to determine the effect of III filling on II's sensitivity. The three figures demonstrate clearly that filling III traps causes sensitization of peak II. The dot-dashed curve in each figure is the same as the solid one, except peak II has been eliminated by annealing 20 minutes at 145°C. This dot-dashed curve shows that changes in peak II's apparent height aren't due to overlap with peak III.

The measurements in this experiment were taken on the Harshaw reader with slow, externally controlled heating to resolve the peaks as well as possible. This better resolution indicates that the so called peak II may consist of two superimposed peaks.

Displacements of Peak Position

Peak position in the glow curve may change due to high exposure or post-annealing treatment. Figure 8 shows such a displacement of peak III to lower temperature (up to about 10°C) as the exposure increases beyond about 3 kR, while no such effect is observed for peak II. There seems to be some correlation between this effect and supralinearity. A different kind of displacement of peak III was found for sensitized material, while again peak II did not move. In this last case peak III first moved to higher temperature from about 3 kR up to about 15 kR, and then displaced to lower temperature above 15 kR.

In many instances the peak position shifts as the time of post-annealing increases. This effect will be discussed elsewhere[6].

Model Calculation

Cameron, Zimmermann, and Bland[1] proposed a mathematical model in which it was assumed that the radiation creates additional traps, giving rise to supralinearity. The principal argument against the model was the fact that the "created" traps appeared physically identical to the original traps. This seemed like an improbable coincidence. The competing traps model[7] already mentionned was next proposed.

The traps creation model predicts a TL proportional to

$$L(R) = \{N_o\beta(e^{\alpha R}-e^{\beta R}) + N_F(\alpha(1-e^{-\beta R}) - \beta(1-e^{-\alpha R}))\} / (\alpha-\beta) \qquad (1)$$

where L(R) is the number of filled traps at exposure R, N_o is the initial number of traps, N_F is the maximum number of traps, α is the probability constant for the creation of traps, and β is the probability constant for the filling of traps.

The competing traps model predicts a TL proportional to

$$L(R) = N_F (1 - e^{-\gamma R}) - N_{oc} (1-e^{-\delta R}) \qquad (2)$$

where N_F is the maximum of traps to be filled, N_{oc} is the maximum number of competing traps, γ is the probability constant of creating an electron which is captured, and δ is the probability constant of filling a competing trap.

Numerical calculations were carried out to find parameters that fit the observed curves of Fig.2. For peak III without supralinearity $\alpha = 0$ and $\delta = 0$, and both models give the same expression for L(R). The best fit is obtained for

$$N_o = N_F = 1.1 \text{ in the arbitrary units}$$

$$\beta = \gamma = 2.7 \times 10^{-5}\ R^{-1}$$

For peak II we have

$$5N_o = N_F$$

$$\alpha = 0.5 \times 10^{-4}\ R^{-1}$$

$$\beta = 1.1 \times 10^{-5}\ R^{-1}$$

in the model of traps creation, and

$$N_F = 8.5 \text{ in the arbitray units}$$

$$N_{oc} = 0.13\ N_F$$

$$\delta = 2.7 \times 10^{-5}\ R^{-1}$$

$$\gamma = 5.8 \times 10^{-6}\ R^{-1}$$

in the competing traps model.

The theoretical curves are also represented in Fig. 2. The behavior of peak III can thus be fully predicted by both models, while for peak II the model of creation of traps provides a good fit, but the other one does not. This is due probably to the fact that we assumed only peak III traps as competing traps. The effect of deeper traps can not be quantitatively considered at this point since data on TL vs. R are lacking.

We also calculated the sensitization factor S/S_o for peak II where S_o is the TL reading of a non-sensitized sample after an arbitrarily chosen test exposure, and S is the TL reading of a sensitized one for the same test exposure. In Fig.9 calculated values of the sensitization factor are plotted as a function of previous exposure. Since in the traps creation model the sets of solutions (α, β, N) and (β, α, $N\ \beta/\alpha$) are equally good ones as far as TL vs. R is concerned, S/S_o were evaluated for these two sets. The first set gives the dashed curve, and the second set, the solid curve. Although neither of them predict the measured values, the second set is favored over the first set. The dashed curve in Fig. 10 is the predicted S/S_o-curve from the competing traps model, which does not fit the experimental curve either, but it is as close as the solid curve to the measured values, in Fig.9.

Both models predict, however, no sensitization effect for peak III although experimentally a considerable S/S_o value was found.

Conclusions

We interpret the above results to favor the model of competing traps[7], although the model must be made more general to explain the data. Basically, the normal competing traps model postulate competitive traps of large cross section which trap charge carriers at relatively low exposures, then saturate, giving other centers a better chance to capture carriers; whence supralinearity is induced. Sensitization could then occur if the intervening treatment erases the low temperature TL, but does not empty the competing traps. We explain the above experiments as follows:

1. Deep competing traps cause supralinearity in peak III, if they are sufficiently emptied prior to irradiation. Ten minutes at 600°C does not sufficiently empty them, while 60 minutes does.

2. The Fig. 3 seems to show a non-influence of peak VI or deeper traps on peak II, since the shape of the TL vs. exposure curve of peak II was not changed by emptying peak VI although TL reading decreased due to longer annealing at 600°C.

3. Since peak III is only supralinear under special conditions (deep traps relatively empty), peak II traps and the deep traps must divide the available carriers during irradiation. Peak III is sensitized, therefore, when the deep traps are full, and this division does not take the carriers away from III traps.

4. Comparing Fig.2 and Fig.4 we see that, while peak II that is supralinear is not sensitised (for exposures less tahn 500 kR), peak III has an opposite behavior. This result contrasts the behavior of TL peaks in TLD-100. This result combined with the one shown in Fig.3 indicates that peak III competes with peak VI since, both peak III's sensitization and supralinearity occur when peak VI is filled and no supralinearity takes place for empty (or almost empty) peak VI. On the other hand figures 5, 6 and 7 show a sensitization

of peak II when III is full and no sensitization when III is empty, indicating a competition of these two peaks.

To see whether the interim heat treatment influences or not the sensitization of fluorite, experiments are in progress wherein the interim annealing temperatures are varied from 300, 400 to 500°C, for times varying between 0 and 120 minutes for each temperature. The preliminary result indicates that there is no marked interim annealing effect, meaning that the behavior of peaks II and III is not essentially due to such a treatment, except for a decrease in sensitivity of both peaks for higher temperature as well as longer heating.

5. The displacement of the position of peak III in Fig.8 seems to be correlated with the way the TL response behaves when the fluorite is irradiated to high exposure. If a continuous distribution[6] of peak III traps (in trap depth) is assumed, Fig.8 indicates that high exposure predominantly detroyes the deeper traps.

6. It should be noted that glow curves obtained with a very low heating rate (Figs.5, 6, and 7) show a new peak between I and II not observed with faster heating rates.

7. Fitting peak III curve in Fig.2 requires adjustment of one parameter, namely, β in Eq.(1) and γ in Eq.(2). To fit peak II curve we have to note, however, that in creation of traps model the parameters α, β and N_F/N_F must be adjusted independently of β-value found for peak III. Now in the case of the competing model, assuming that the supralinearity of peak II, is due to peak III, γ-value found for peak III must be used, therefore only two parameters δ and N_F/N_{DC} are left free to be varied. Thus, although the creation of traps model appears to give a better fit, we cannot be sure that this model is favored mainly because of the results shown in Figs.5, 6, and 7.

In short, Figs.3, 5, 6, and 7 favor the competing traps model, but, numerical results in Fig.2 favor the creation of traps model.

Acknowledgement

We are indebted to Dr. Michael R. Mayhugh for valuable discussions, to Department of Biology of the University of São Paulo and Hospital A.C.Camargo for making available their Cs-137 and Co-60 sources, respectively, for irradiation of materials used in this work.

REFERENCES

1. J.R. Cameron, D.W. Zimmerman, and R.W. Bland, Luminescence Dosimetry, AEC Symp. Ser. vol.8, CONF-650637, p.47 (1967).

2. J.H. Schulman, R.D.Kirk, and E.J. West, Luminescence Dosimetry, AEC Symp. Ser. Vol.8, CONF-650637, p.113 (1967).

3. Y. Yamashita, N.Nada, H.Onishi, and S.Kitamura, Proc.of Second Inter.Conf. on Luminescence Dosimetry, USAEC-CONF-680920, p.4 (1968).

4. R.Schayes, C.Brooke, I.Kozlowitz, and M.Lheureux, Luminescence Dosimetry , AEC Symp. Ser.vol.8, CONF-650637, p.138 (1967).

5. J.R. Cameron, L.DeWerd, J.Wagner, C.Wilson, K.Doppke, and D.W. Zimmerman , Solid State and Chemical Rad.Dosimetry in Medicine and Biology, IAEA, Vienna, p.77 (1967).

6. S.Watanabe and S.P.Morato, paper numer 7, Session II in this Conference.

7. J.R.Cameron, N.Suntharalingam, C.R.Wilson, and S.Watanabe, Proc. of Second Intern. Conference on Luminescence Dosimetry, USAEC-CONF-680920, p.322 (1968).

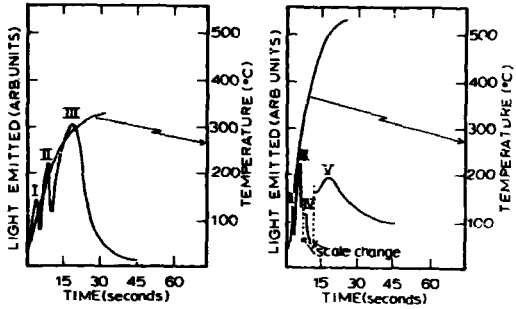

Fig.1. Typical glow curves of fluorite for the two different heating cycles after a 100 R (left) and 10 kR (right) exposure to Cs-137.

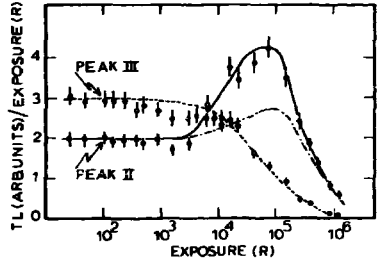

Fig.2. TL/R as a function of exposure for peaks II(black circles) and III (open circles). The dashed line is the best fit obtained using either the traps creation or the competing traps model for peak III. The solid and the dot-dashed lines are the best fits obtained using the traps creation and the competing traps model for peak II, respectively. The competing traps model was applied in a restricted form.

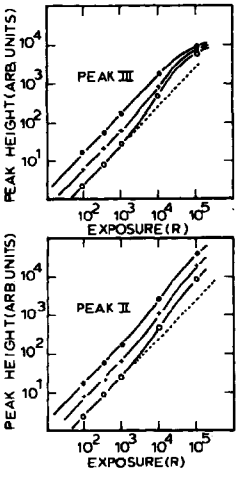

Fig.3. Peak height as a function of exposure for samples pre-annealed at 600°C for 10 minutes (black circles), 30 minutes (crosses) and 60 minutes (open circles). The dashed line represents linear response.

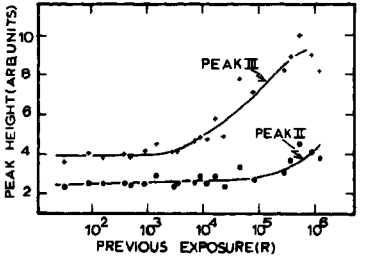

Fig.4. Peak height induced by a 100 R test exposure as a function of previous exposure. Black circles correspond to peak II and crosses to peak III.

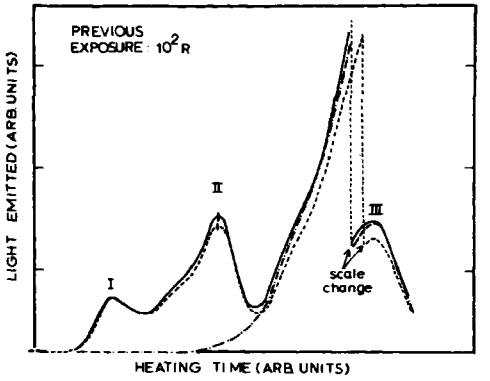

Fig.5. Glow curves of samples irradiated to 1,000 R test exposure. These samples were given 100 R previous exposure. Solid line: the TL without emptying peak III traps, i.e., with 15 min anneal at 175°C. Dashed line: the TL for emptied III traps, i.e., 30 min at 300°C anneal. Dot-dashed line: Isolation of peak III with 20 min at 145°C anneal after 1,000 R test exposure, but with 15 min at 175°C anneal, before 1,000 R exposure.

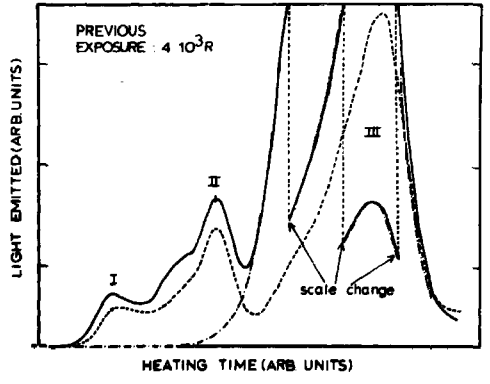

Fig.6. Same as in Fig. 5 except for a 4 kR previous exposure.

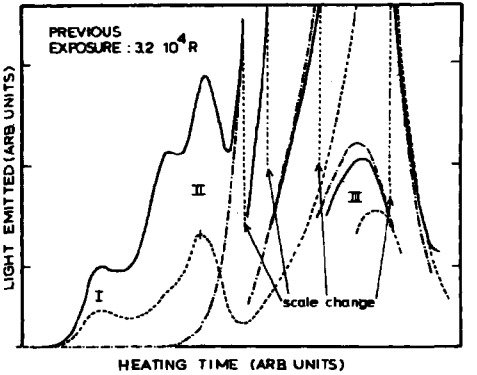

Fig.7. Same as in Fig. 5 except for a 32 kR previous exposure.

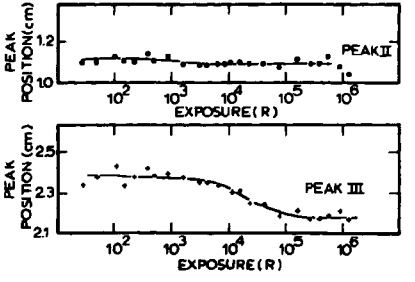

Fig.8. Position as a function of exposure for peaks II and III.

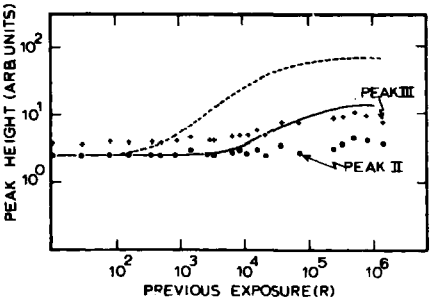

Fig.9. Sensitization factor as a function of previous exposure. Theoretical curves were obtained using traps creation model for peak II. The dashed curve corresponds to $\alpha = 0.5 \times 10^{-4} R^{-1}$ and the solid one to $\alpha = 1.1 \times 10^{-5} R^{-1}$.

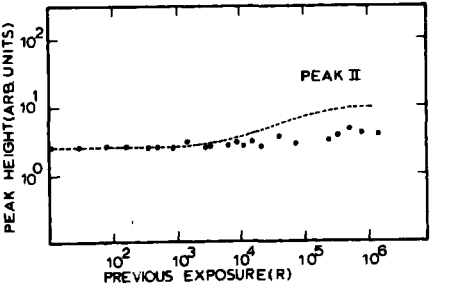

Fig.10. Sensitization factor as a function of previous exposure. The theoretical curve was obtained using the competing traps model.

Thermoluminescence of Natural CaF_2 and its Applications

By

C.M. Sunta
Health Physics Division
Bhabha Atomic Research Centre
Bombay-85, India

Abstract

Thermoluminescence glow curves are recorded from room temperature to 550°C for a number of natural CaF_2 samples. Light-green-transparent crystalline specimens are found to possess maximum sensitivity to γ ray exposure and are most suitable for the dosimetry of ionising radiations as well as ultraviolet rays.

The spectrum of the thermoluminescent light consists of a number of sharp lines spread in a wide spectral range from ultraviolet to infrared. Almost all of the emission lines can be attributed to one or other of the rare earth impurities. It is proposed that the thermoluminescence mechanism in CaF_2 involves the release of holes from lattice centres and their recombination at the rare earth impurity sites.

A model of photostimulated thermoluminescence is presented.

1. Introduction

Natural CaF_2 (fluorite) is one of the most sensitive thermoluminescent materials useful in radiation dosimetry. Significant amount of dosimetric work[1-5] has been done earlier using this substance. The phenomenon of emission is however, still not fully understood.

2. Glow Curves

The procedure for recording the glow curves is given in brief in another paper[6] of this conference. Glow curves of eighteen different samples are given in Fig.1 arranged according to the colour of the samples. Activation energies of some of the well separated peaks are determined using the method of initial rise. The procedure adopted is described in detail elsewhere[7]. Results are given in Table-1. Kinetics of glow peaks was found to be of second order (Table-2) using the method

Table-1

Activation Energy E, of Glow Peaks

Peak Temp.°C	E ev	Peak Temp.°C	E ev
75	1.24 ± 0.01	350	2.10 ± 0.02
150	1.34 ± 0.02	440	1.83 ± 0.05
250	1.68 ± 0.02	500	2.04 ± 0.02
300	1.96 ± 0.02		

Table-2

Determination of order of kinetics

T_g °K	E ev	τ	δ	ω	$\Delta = \frac{2kT_g}{E}$	δ/ω	$\frac{1+\Delta}{e}$
423	1.34	17.5	15.7	33.2	0.0540	0.4698	0.3678
623	2.10	23.5	18.8	42.3	0.0516	0.4444	0.3869
773	2.04	38	33.8	71.8	0.0652	0.4708	0.3919

Since $\frac{\delta}{\omega} > \frac{1+\Delta}{e}$ in all the three cases calculated, kinetics is of second order.

of Halperin et al[8]. The parameters used in determining kinetics are given in Fig.2.

3. Spectra of Glow Peaks

The spectral quality of emission was found to be same for all the specimens as well as their individual glow peaks[7,9]. The sharp line nature of the TL spectra shows that emission may be associated with rare earth ions, since these are known to be the common impurities in natural CaF_2 samples[10]. Comparison of the TL spectra of the rare earth doped CaF_2 samples prepared in the laboratory with those of the natural samples confirmed this. Fig.3 shows that the major part of the TL spectrum of the natural CaF_2 samples corresponds to Ce, Tb, Dy, Er and Sm impurities. These impurities therefore form luminescence centres in CaF_2.

It has been clearly shown by earlier workers[11,12] that rare earth impurity ions in CaF_2 lattice which are usually in trivalent state are reduced to divalent on irradiation and that these are reoxidised to trivalent state on heating.

$$RE^{3+} \underset{\text{HEAT}}{\overset{\text{IRRADIATE}}{\rightleftharpoons}} RE^{2+}$$

It therefore, means that rare earth impurity ions function as electron trap type luminescent centres. Since glow peak temperatures are independent[7,12] of individual impurity ions, the TL mechanism should involve the release of holes from lattice centres and their recombination at rare earth impurity sites. A schematic representation of different types of hole centres is given in Fig.4.

Spectral character of thermoluminescence is found to change with the amount of radiation dose. This is of importance in dosimetric application. Fig.5 shows the spectrum of glow peak appearing around 250°C after different exposures. The change in spectral character indicates the creation of new types of centres with increased exposure. It has been argued[7] that the spectra shown in Fig.5 are due to emission from Ce impurity ions in CaF_2 lattice. The bands at 317 and 338 nm are attributed to Ce^{3+} ions in cubic sites and the broad band at 375 nm is attributed to Ce^{3+} ions in O^{2-} compensated sites. The cubic emission is observed with strong intensity after high exposure.

4. Photostimulated Thermoluminescence (PSTL)

It has been shown earlier[1,13] that if an irradiated natural CaF_2 sample is partially annealed to leave some of the glow peaks unbleached, the thermoluminescence of residual (unbleached) peaks can be transferred to other peaks by ultraviolet irradiation. This kind of transfer is seen from higher temperature peaks to those of lower temperature and vice-versa[13]. Fig.6 shows the PSTL glow curve

from liquid nitrogen temperature to 550°C. Fig.7 shows linear relation between the residual peak (500°C) intensity and the intensity of one of the PSTL peaks. An important similarity between the parent residual peak of 500°C and the PSTL peaks is that their spectral quality is same (Fig.8), showing that the luminescent centre is common for both types of peaks. It has been found[7] that the centre concerned is a Ce^{3+} ion locally compensated by O^{2-}. A model is presented in Fig.9 to explain the phenomenon of PSTL.

An interesting observation related with PSTL in CaF_2 is that the intensity of glow peaks increases with increase in the temperature of the sample during light exposure. Fig.10 shows plot of the actual observations. This phenomenon can be explained by assuming an excited state of the parent trap very close to the free state and that the trap population after optical excitation follows Boltzmann's law of thermal distribution of energies. Using the latter assumption the energy gap between the first excited state and the free state turns out to be 0.32 ev (Fig.11). The excited state energy above the ground state of the trap is 3.38 ev, since at this photon energy the monochromatic excitation curve of PSTL glow peaks shows a sharp maximum[7,13].

An important fact about the PSTL of natural CaF_2 is the regeneration of glow peaks by UV exposure in the entire temperature range from 77°K upwards when the residual peak of 500°C is present in the sample. This shows that the nature of the charge carrier liberated at individual glow peaks should be same. Since it has been established earlier[12] that in the case of glow peaks below room temperature the liberated charge carrier is a hole, it implies that for high temperature glow peaks also this should be of hole type.

5. Application in γ, X and UV Dosimetry

Looking to the host of natural CaF_2 varieties that are available, it is important that a proper judgement should be made to select the most suitable one for use in dosimetry. Our experience shows that light-green-transparent crystalline samples have maximum sensitivity and are best suited for dosimetry of ionising radiations. Same type of samples are found to be useful also in UV dosimetry. UV dosimetry is based on the transfer of charge carriers from the deepest trap (corresponding to the glow peak of 500°C) to that of the dosimetry peak (250°C). Since the 500°C glow peak (deepest trap) is observed to be strongest in light-green-transparent crystals, these samples are naturally suitable for UV dosimetry. Fig.12 shows the calibration curve for UV exposure obtained by exposing a 400°C treated light-green natural sample to different doses of UV rays. It is worth noting that the reduction in residual peak (500°C) intensity is negligibly small after each UV exposure. This enables the sample to be reused a number of times without resensitisation to buildup the 500°C glow peak.

The author is thankful to Dr.A.K.Ganguly for his keen interest and many stimulating discussions.

References

1. Schayes,R., Brooke,C., Koslowitz,I. and Lheureux,M., "Luminescence Dosimetry" Attix, F.H. (Ed.) (USAEC, Division of Technical Information, CONF - 650637, 1967) P.158.

2. Sunta,C.M., Nambi,K.S.V., Kathuria,S.P., Basu,A.S. and David,M., Radiation Dosimetry of Population in Monazite Bearing Areas using Thermoluminescent Dosimeters BARC/519 (1971).

3. Sunta,C.M., Nambi,K.S.V., Kathuria,S.P., Basu,A.S. and David,M., Personnel Monitoring using TLD at Manavalakkurichy BARC/I-12(1969)

4. Gopal-Ayengar, A.R., Sundaram,K., Mistry,K.B., Sunta,C.M., Nambi,K.S.V., Kathuria,S.P., Basu,A.S. and David,M., Fourth U.N.Int. Conf. Peaceful Uses of Atomic Energy, Geneva(1971)

5. Nambi,K.S.V., and Sunta, C.M., Indian J.Pure & Appl. Phys. 6, 294 (1968).

6. Sunta,C.M., Bapat,V.N. and Kathuria,S.P., Paper in this Conference.

7. Sunta,C.M. Ph.D.Thesis, Agra University.

8. Halperin,A. and Braner,A.A., Phys. Rev. 117, 408 (1960).

9. Sunta,C.M., J.Phys. C, Solid State Phys. 3, 1978 (1970).

10. Przibram,K., "Irradiation Colours and Luminescence" (Pergamon Press, London 1956).

11. Arkhangelskaya,V.A., Opt.Spectry. 18, 46 (1965).

12. Merz,J.L. and Pershan,P.S., Phys.Rev. 162, 217 (1967).

13. Sunta,C.M. Phys.Stat. Sol. 37, K 81 (1970).

14. Hayes,W. and Twidell,J.W., Proc.Phys. Soc. 79, 1295 (1962).

15. Hall,T.P.P., Leggeat,A., and Twidell,J.W., J.Phys. C, Solid St.Phys. 2, 1590 (1969), 3, 2352 (1970).

16. Sierro,J., Phys. Rev. 138, A 648 (1965).

17. Weber,M.T., and Rierig,R.W., Phys.Rev.134,1492 (1964).

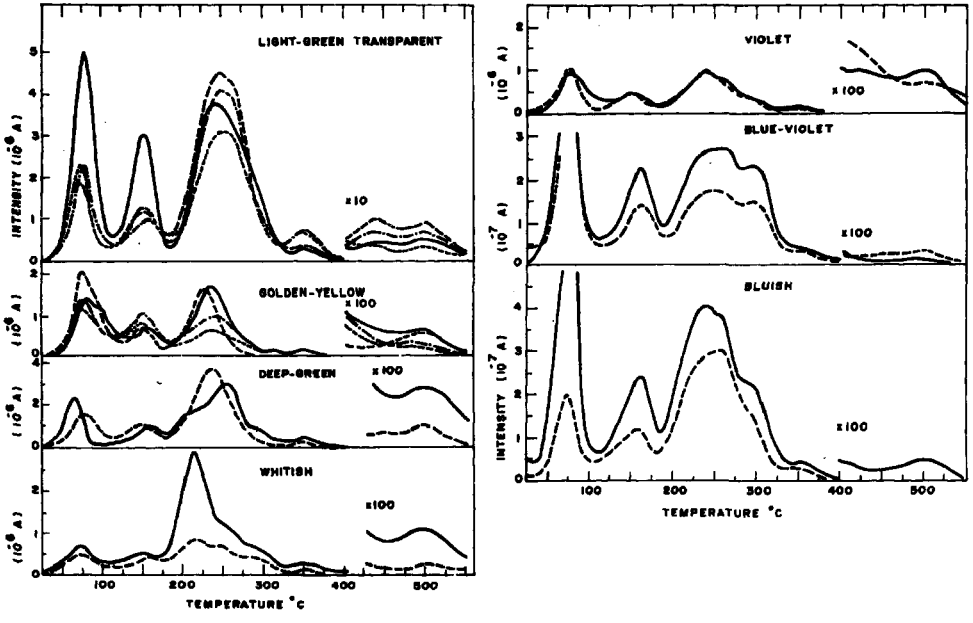

Fig.1 - TL glow curves of different fluorite samples

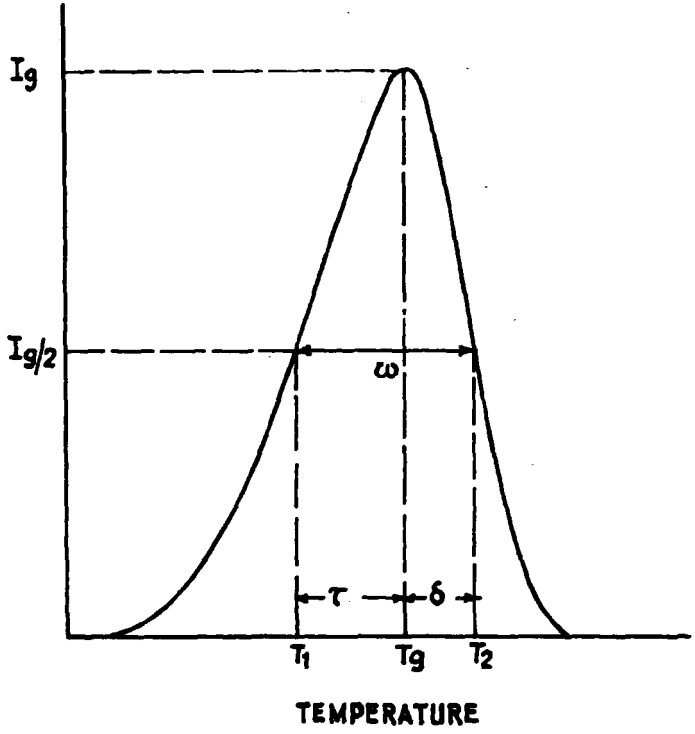

Fig.2 - Shape of a typical glow peak showing different parameters.

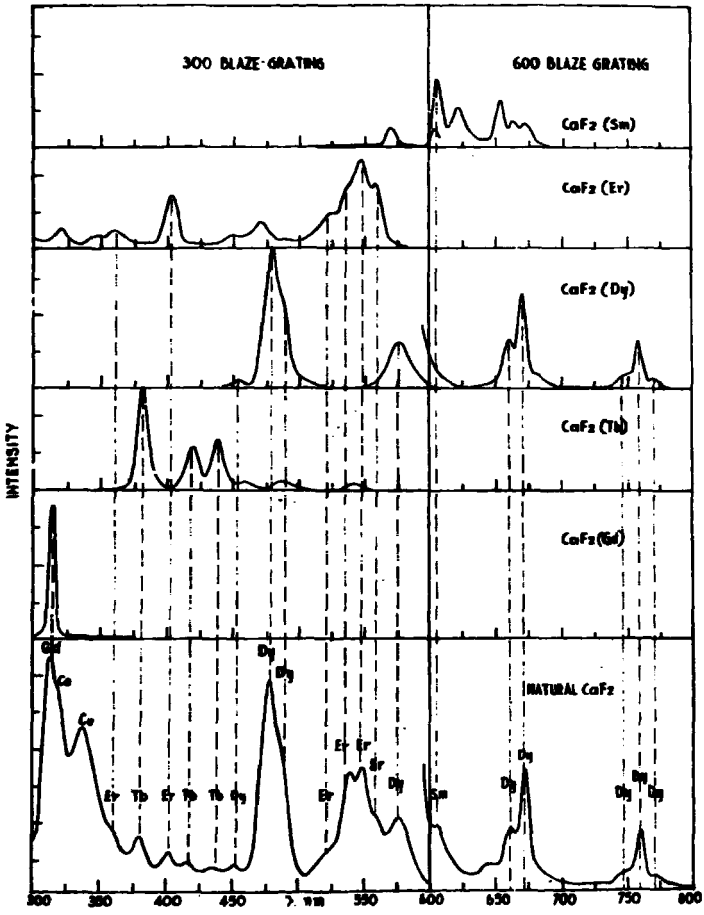

Fig.3 - Comparison of TL spectrum of natural CaF_2 with the spectra of rare earth doped CaF_2 samples.

STRUCTURE OF THE TRAP	NAME & DESCRIPTION, MAX. TEMP OF STABILITY	REFERENCE
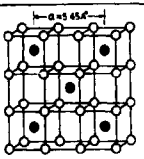	THE CALCIUM FLUORIDE LATTICE. IONIC RADII ARE NOT DRAWN TO SCALE	
	Vk CENTRE, F_2^- MOLECULAR ION ALIGNED ALONG <100> DIRECTION, 138°K.	14
	MODIFICATION OF Vk CENTRE,(100) F_2^- MOLECULAR ION ADJACENT TO SUBSTITUTIONAL Na^+ ION, STABLE AT ROOM TEMPERATURE	15
	MODIFICATION OF Vk CENTRE, TRAPPED HOLE AT THE SITE OF AN INTERSTITIAL F^- ION FORMING A F_2^- MOLECULAR ION ALONG <111> DIRECTION. STABLE AT ROOM TEMPERATURE.	15
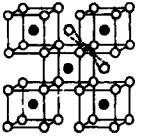	MODIFICATION OF Vk CENTRE, TRAPPED HOLE AT A PAIR OF NEAREST NEIGHBOUR INTERSTITIAL F^- IONS ALONG <110> DIRECTION. IT IS AN AGGREGATE DEFECT COMPLEX WITH THE TRIVALENT CATION IMPURITIES LIKE Y^{3+} AND Lu^{3+} SUBSTITUTED FOR Ca^{2+}. QUITE STABLE ABOVE ROOM TEMPERATURE.	15
	Vp CENTRE, F_2^- MOLECULAR ION WITH BENT BOND ADJACENT TO Ca^{2+} VACANCY, 330°K.	16
	SUBSTITUTIONAL O^{2-} ION ADJACENT TO A TRIVALENT RARE EARTH SUBSTITUTIONAL IMPURITY. TRAPPED HOLE WILL CHANGE IT TO O^-	17

● Ca^{2+} ○ F^- ⊕ M_2^{3+} ● Y^{3+} OR RE^{3+} ● O^{2-} □ Ca^{2+} VACANCY

Fig. 4 Schematic representation of different types of hole centres. Sharing of trapped hole is shown by O::O. Lattice distortions are not shown.

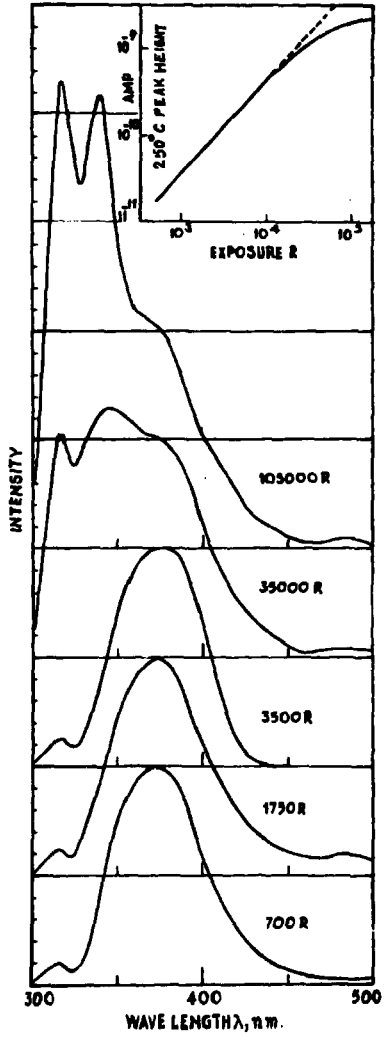

Fig.5 - Dose dependence of the TL spectrum.

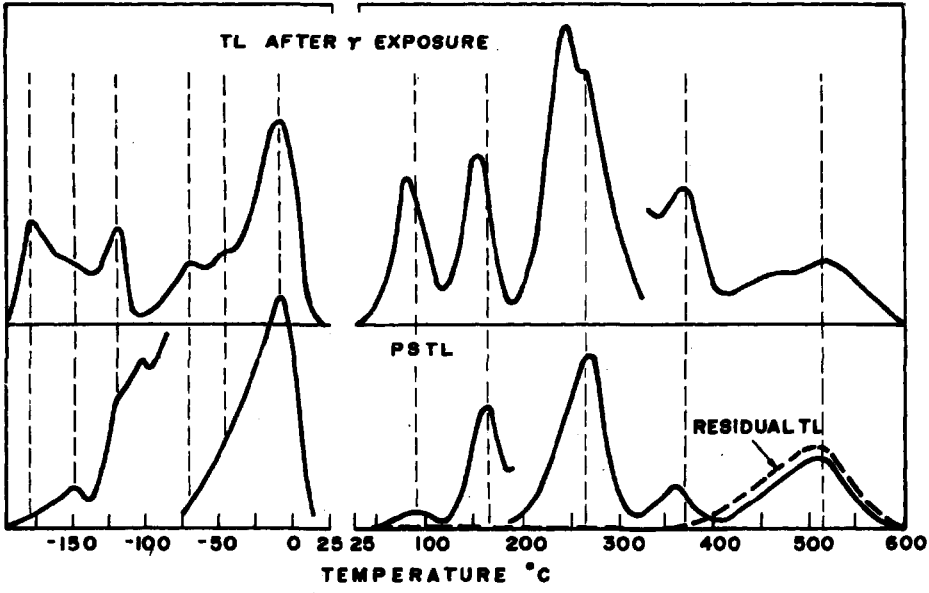

Fig.6 - (A) Glow curve produced after γ exposure

(B) PSTL glow curve produced by 365 nm light exposure when the glow peak of 500°C is present in the sample.

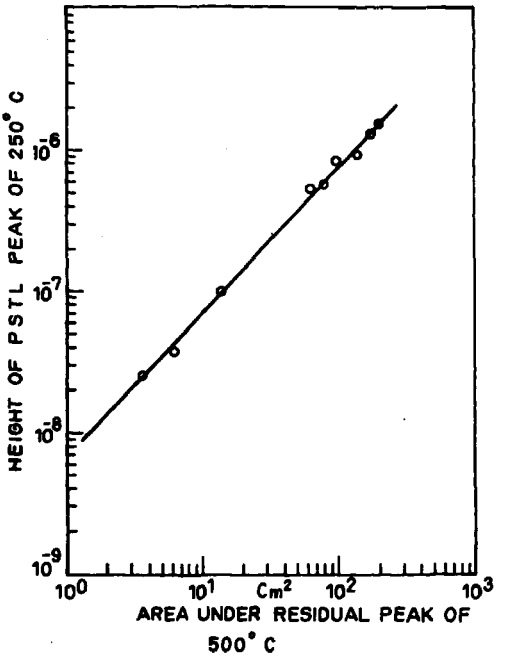

Fig.7 - UV sensitivity as a function of residual TL in 500°C glow peak.

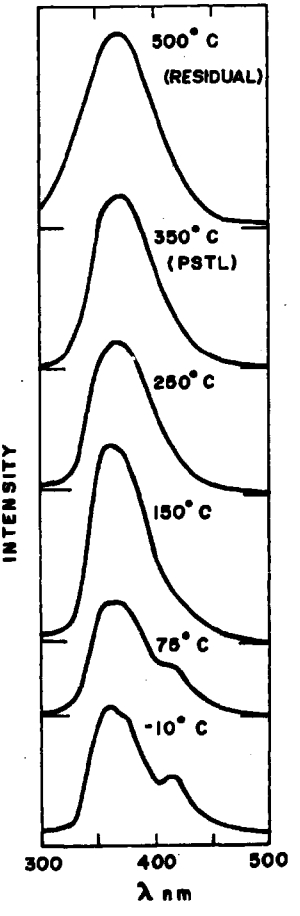

Fig.6 - Spectra of PSTL peaks and their comparison with the spectrum of residual peak..

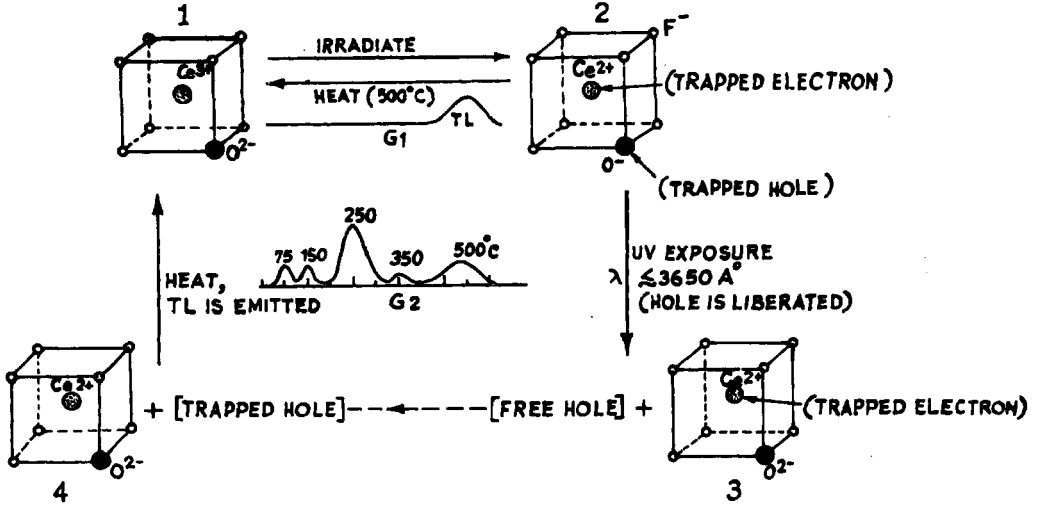

Fig.9 - Model of PSTL in natural CaF_2. An aggregate centre consisting of Ce^{3+} locally compensated by O^{2-} is assumed for the glow peak of 500°C. On γ exposure Ce^{3+} becomes Ce^{2+} (electron trapped) and O^{2-} becomes O^- (hole trapped). Light exposure (365 nm) liberates the holes, which are retrapped in other empty hole trap locations resulting in PSTL.

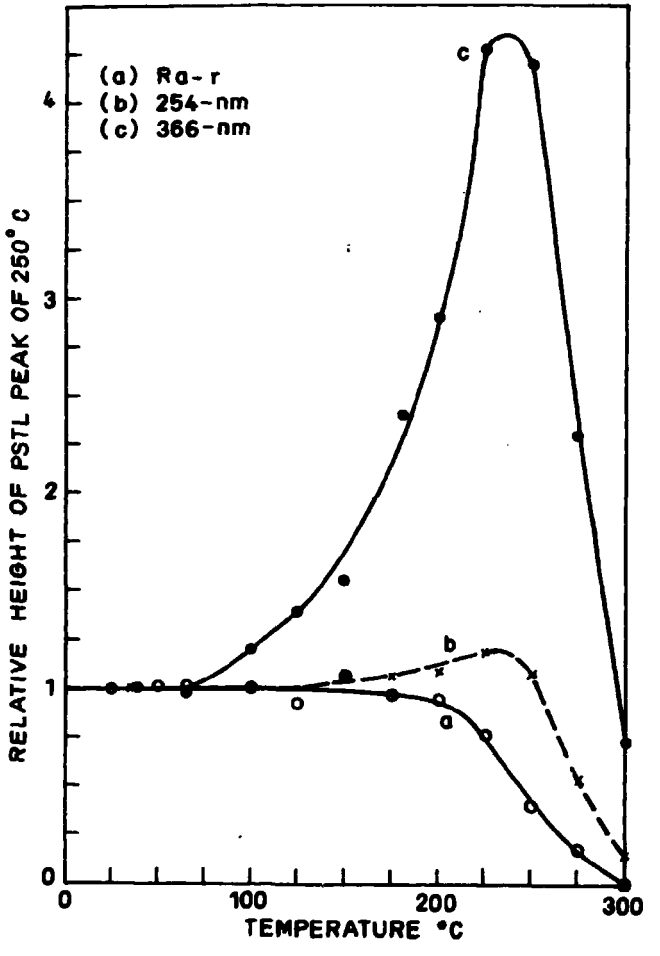

Fig.10 - Temperature dependence of PSTL.

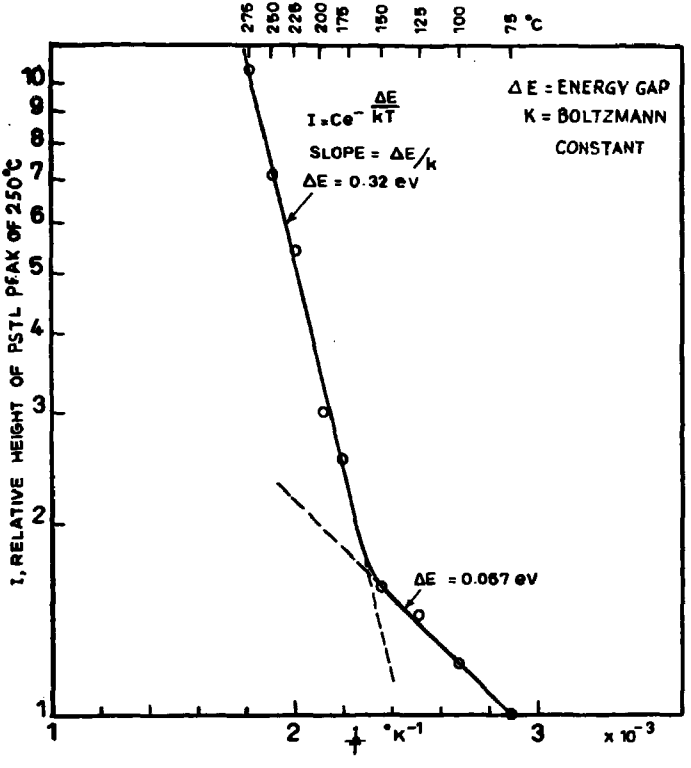

Fig.11 - I vs. $\frac{1}{T}$ for PSTL peak of 250°C.

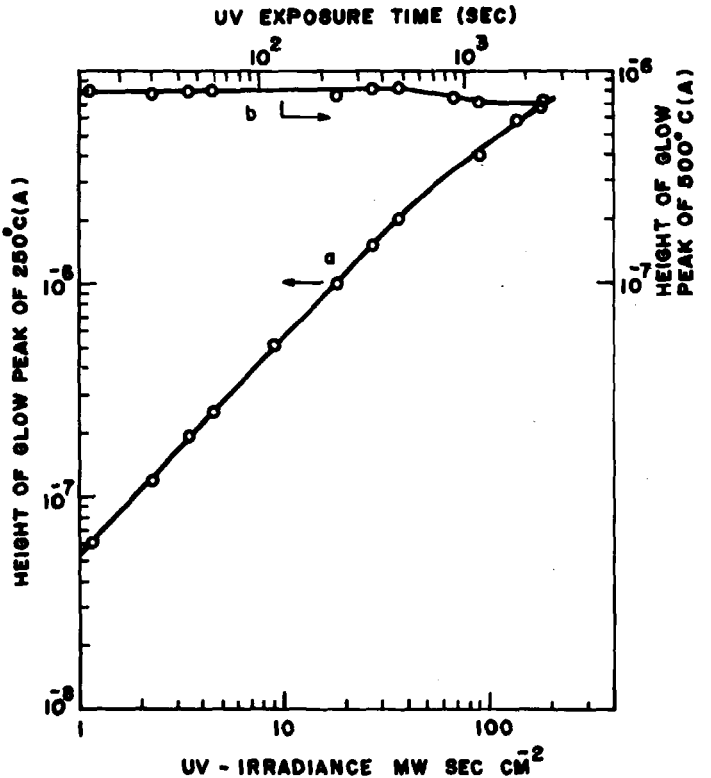

Fig.12 - (a) Calibration curve for UV exposure.
(b) Intensity of residual peak of 500°C after each UV exposure.

Fleming

You suggested that one TL peak may be attributed to a rare earth - oxygen complex; yet previous literature (e.g. Merz and Pershan) suggests that the oxygen ion destroys TL sensitivity. Do you have any evidence for your attribution?

Sunta

The TL peak which I have attributed to a cerium-oxygen aggregate defect is indeed a very weak one and appears at 500°C. If oxygen is incorporated, TL at low-temperature peaks might be quenched. Merz and Pershan did their TL measurements between liquid-nitrogen temperature and room temperature. My argument for the $(Ce^{3+}-O^{2-})$ complex as the cause of the glow peak at 500°C is mainly the following: The emission spectrum of this peak appears to be that of oxygenated $CaF_2(Ce^{3+})$. Other arguments are given in ref. No. 7 (unpublished).

Webb

In the UV transfer you mentioned, is the response spectrally dependent or broad-band?

Sunta

The response is very much dependent on spectral energy. This has already been published (ref. No. 13).

Schlesinger

Referring to the difference between electron and hole traps, we made some experiments to distinguish between these two types of traps by measuring the electrical conductivity of the sample simultaneously with the recording of the TL curve. Electrons escaping from the traps during the thermal activation are rising to the conduction band and therefore cause a conduction peak. The effective mass of the holes is much greater, and the conduction peak caused by holes escaping from traps is therefore much smaller.

IMPROVEMENT OF SENSITIVITY AND LINEARITY OF RADIOTHERMOLUMINESCENT LITHIUM FLUORIDE

G. Portal , F. BERMAN, Ph. BLANCHARD and R. PRIGENT
Département de Protection
COMMISSARIAT A L'ENERGIE ATOMIQUE
FONTENAY AUX ROSES 92 - FRANCE

Abstract

A pre-irradiation thermal annealing on dosimeter standard grade lithium fluoride (TLD-LIF) is necessary to eliminate shallow traps which are relatively unstable, reducing the measurement accuracy.

The authors have studied the origin of these traps and have found out that it was possible to delay their formation by Na incorporation, during the preparation process. So the importance of these low energy traps can be lowered to a minimum and it is possible to eliminate them at the reading stage with a simple device.

They present also a new type of sensitised lithium fluoride which is 3 to 4 times more sensitive than the current product and linear from 1 mrad to 10^4 rads.

Sintered dosimeters, designed for personnel monitoring prepared from this new product, present a high sensitivity and a very low spurious triboluminescence signal, and can be read without nitrogen.

Introduction

The phenomenon of radiothermoluminescence, which has long been known and has for some twenty years been applied to dosimetry of ionising radiation, is now finding expanding applications in the fields of radioprotection, radiotherapy and radiobiology.

Numerous radiothermoluminescent (RTL) materials have already been studied and users select those which are best suited to the problem in hand.

Lithium fluoride is one of the most important of the commonly-used materials. It does, however, exhibit certain shortcomings which restrict its use.

Lithium fluoride is a virtually "tissue equivalent" material and is particularly appreciated in the field of radioprotection. Its use is however somewhat complicated by the fact that it must be regenerated after each measurement. Additionally, its sensitivity is distinctly inferior to that of certain materials such as dysprosium-activated calcium sulphate[1] and it is not at its best in measuring low absorbed doses.

Again, radiobiologists and radiotherapists are looking for RTL material which exhibits a linear response up to several thousand rads. This is not the case for LiF which exhibits a region of supralinearity above 200 or 300 rads. In the range of irradiation with which these specialists are concerned, work is difficult and precision is affected.

We have investigated the origin of the shortcomings and attempted to minimise them by developing a new type of RTL lithium fluoride with improved characteristics.

I - Merits and demerits of the commonely available material

Lithium fluoride, like beryllium oxide and lithium borate, is a member of the group of RTL materials which exhibit electromagnetic radiation absorption characteristics which are very close to those of tissue*. Hence, it is quite suitable for measurement of absorbed doses, even in the case of low energy electromagnetic radiation (10 to 60 keV). This is not true of other materials such as calcium fluoride which, at 25 keV, has a hypersensitivity factor which is about 10 times as great. Thus, lithium fluoride is particularly attractive for measurement of tissue absorbed doses.

Although lower than that of calcium fluoride and calcium sulphate, its sensitivity is 5 to 10 times as great as that of others "tissue equivalent" materials such as beryllium oxide and lithium borate. Additionally, in contrast to beryllium oxide and lithium borate, which emit in the long wavelength region, lithium fluoride exhibits an emission spectrum with a maximum at 400 nm. Hence, by using an optical filter, its characreristic emission can easily be separated from that originating from the heating system, which is advantageous for measurement of small doses.

In view of all these qualities, lithium fluoride is currently one of the most widely used RTL materials. It does however exhibit certain disadvantages.

* Commonly known as "tissue equivalent materials".

Instability of traps

The shallow traps which are emptied at low temperature (peaks I, II and III, Fig.1b) are not stable enough for precise measurements. Hence, they have to be eliminated and this can be effected by means of a suitable thermal treatment. This involves heating at 400°C for one hour, followed by slow cooling and 24 hours at 80°C. These treatments modify their distribution ; the thermoluminescence curve for the untreated material (Fig. 1b) is changed and becomes similar to the one shown on Fig. 1a. It will be seen that the low temperature peaks have disappeared.

This improvement is not, however, final since the distribution of the traps is further modified when the material is heated in the reading device ; the thermoluminescence spectrum again exhibits low temperature peaks (Fig. 1b). Hence, the material connot be re-used without being further heat-treated.

Utilisation of lithium fluoride is thus not as straightforward as would appear at first sight.

Linearity defect

The quantity of light emitted by lithium fluoride is not a linear function of the absorbed dose.

Three regions can be distinguished, viz :

(i) a linear region from 0 to 200 rads
(ii) a supralinear region from 200 to 10^5 rads
(iii) a saturation region above 10^5 rads.

Thus, in order to measure doses above 200 rads, a calibration curve has to be plotted. This complicates the reading process and affects the precision of results to a significant extent.

This defect is of particular relevance to measurements carried out by radiobiologists and radiotherapists since it falls within their range of utilisation.

Sensitivity

We have seen that lithium fluoride is the most sensitive of the tissue equivalent dosimetric materials. However, it can only be used in the low dose region (approximately 10 mrads) if a very sophisticated apparatus is used, comprising :

(i) a low noise or cooled photomultiplier
(ii) a very efficient nitrogen sweep disigned to minimise the effect of triboluminescence
(iii) high-performance amplification.

This type of equipment is relatively expensive and

delicate. If lithium fluoride exhibited greater sensitivity, it would be possible either to measure lower doses or use a simpler reading device.

II - Instability of lithium fluoride traps

Constitution of traps

It is now well established that the existence of dosimetric traps is associated with the presence of traces of magnesium. Pure lithium fluoride gives a material which is not radiothermoluminescent.

The most recent investigations [2,3,4] indicate that this involves hole traps consisting of alkali ion $\square^{+}$ vacancies which are necessarily created in the crystal to balance out the local excess of positive charges due to the presence of divalent magnesium ions, Mg^{2+}.

According to Claffy[2], peak I is associated with the presence of vacancies separated from divalent Mg^{2+} ions. According to Grant and Cameron[5], and Harris and Jackson[6], peaks II and III seem to arise from the combination of 2 by 2 complexes. Stoebe et al.[7] consider that peaks IV and V airse form , by 3 combinations, whereas Claffy[2] considers that these complexes (or dipoles) are combined in clusters.

Regeneration

Thus, the most stable traps must correspond to the densest group of dipoles ; in order to obtain a thermoluminescent material without unstable peaks, it is therefore necessary to promote the formation of clusters of complexes. This is achieved by treatment at 400°C (Fig.2). This accelerates formation of dipoles and the subsequent slow cooling promotes grouping [2,8] ; heating at 80°C eliminates any remaining shallow trap but does not affect deep traps since this temperature is note sufficient to dissociate the clusters.

Reading

When the thermoluminescent material is heated in the reading device, however, it is raised to 250 or 300°C. This temperature level dissociates the clusters and disperses the complexes ; these have no time to recombine because of the sharp rate of cooling and this amounts to a quench which immobilises the complexes and promotes formation of shallow traps. Hence the product must again be regenerated.

III - Lithium fluoride suitable for re-use without regeneration

Stability of PTL material

We have produced a lithium fluoride (PTL) which, when heated, behaves rather differently form the normally-available lithium fluoride described above. The treatment temperature is no longer the same (cf. Fig.3). Best results are obtained at 490°C. Additionally, cooling must be effected very rapidly, in about 10 seconds. It is as though, at this temperature, the dipoles tended to cluster together, with rapid cooling promoting immobilisation.

In contrast to common dosimetric materials, we find that on reading the heating time is not long enough to dissociate the clusters ; the RTL spectrum is little affected by repeated use of the same sample (Fig.4)

This appears to be due to the fact that the energy of dissociation of the clusters is distinctly higher in the case of this new material. In order to investigate the phenomenon, we carried out the following experiment :

A conventional lithium fluoride (TLD 700) and a PTL sample were heat treated at 210°C, prior to being used, for periods of 2 seconds to 24 minutes. This treatment was designed to simulate the thermal cycles responsible for the modifications exhibited by the spectrum of the thermoluminescent material during the period of heating in the reading device. This temperature was chosen since experience showed that it gave a fairly good representation of the average effect of a heating cycle in the reading device when there was a sharp rise in temperature up to approximately 230°C.

Following the heat treatment, the samples were cooled fairly rapidly and then irradiated.

The curves in Fig. 5 show the heights of peaks V and II, for both types of lithium fluoride, with respect to treatment time.

It can be seen that the distribution of the TLD 700 peaks is profoundly modified within seconds ; thus within 10 seconds, which corresponds to the heating cycle time for most reading devices on the market, peaks II and V exhibit substantially the same amplitude.

In contrast to this , it is surprising to note that PTL resists distinctly better. Despite the instantaneous appearance of peak II, this only reaches the amplitude of peak V after about 15 minutes treatment. This shows that the energy of dissociation of the PTL clusters is distinctly higher than that of conventional lithium fluorides.

Preparation of PTL

We originally prepared various materials (PTL 66 and PTL 69)[9,10] exhibiting these characteristics following a rather complex series of heat treatments carried ou at the crystal growing stage.

More recently [11,12] we discovered a new production process which enables quite comparable results to be obtained more rapidly and have produced a new material PTL 71* containing 10 000 ppm of sodium. The presence of this impurity lowers the melting point of the lithium fluoride and enables the crystals to grow at the optimum temperature for the formation of very stable dosimetry traps.

Elimination of the effect of unstable traps

First, it will be seen that the PTL does not present 5 types of trap like the commonly available material. Three main peaks appear on the thermoluminescence curve in Fig.6. It seems that the levels III and IV, although present, are so slight as not to be noticed ; they appear on ly after 15 minutes treatment at 200°C in the experiment described above.

This has the fundamental advantage of enabling tne unstable traps I and II to be separated from the stable traps corresponding to level V. This separation can be effected at the actual time of reading by using a pre-erasure stage** which [13] enables shallow peaks to be eliminated before the start of the reading (Fig.7).

While the same technique can be used with conventional materials, the presence of the intermediate energy peak III entails inaccuracy of measurement unless allowance is made for the time the irradiated sample is stored prior to the reading.

Limitations of the method

In point of fact, as can be seen from Fig.5, there is a gradual change in the various thermoluminescence peaks ; peaks I and II tend to grow at the expense of peak 5. This effect is accelerated if the heating cycle temperature of the reading device is increased or if the measurements are carried out at very brief intervals.

---

* Currently marketed in the form ol natural lithium (PTL 710), or enriched (PTL 717) to 99.95% isotope 7, by CEC,4-8 Place des Etats-Unis, 92-MONTROUGE.

** A reading device using this principle is produced by SAPHYMO Srat, 51 rue de l'Amiral Mouchez, 75-PARIS 15ème.

Under normal conditions of utilisation for radioprotection, lithium fluoride looses less than 5% of its initial sensitivity after being re-used some fifty times.

IV - Supralinearity of lithium fluoride

Origin of supralinearity

There is as yet no well-established explanation of the increase in the sensitivity of lithium fluoride after irradiation.

After proposing a number of hypotheses [14,15], Cameron[16] assumes the existence of a limited number of electron traps which act as "poison" traps since they do not contribute to the light emission process.

When all these traps are filled, only those electron traps which are involved in the PTL effect are still available hence the luminescence efficiency is increased.

Claffy et al. [17] explain this phenomenon by the formation of F centres which act as luminescence centres. The electron-hole pairs created by ionisation are trapped along the secondary electron paths. As long as the density of these traks is not very great, only electrons and holes from one and the same track can recombine on heating ; when, however, it increases, the secondary electron traks are very close and the F-centre electrons created along a trak can also recombine with the holes captured along another trak ; this interlocking, as it were, of trajectories increases the probability of radiative recombination and hence the luminescent efficiency.

Increase in sensitivity of lithium fluoride

Thus, a more sensitive RTL material can be obtained by simple irradiation. Additionally, it can be pre-irradiated in such a way that the effective range takes in the point of inflexion I (Fig.8) where the effects of increase in sensitivity and saturation of traps by irradiation balance each other out. At this point, the increase in sensitivity of the material is at a maximum and, due to this compensation effect, it exhibits a linear reponse over a wide range. Hence, the PTL 71 yields the response represented as a dotted line on Fig.8.

This presupposes, however, that we are in a position to empty the irradiated dosimetric traps of the RTL material. Zimmerman and Cameron [18] obtained this result by heat treatment at 280°C for 60 minutes of lithium fluoride which had been pre-irradiated to 10^4 rads. This temperature is not high enough to de-activate the F centres although it is sufficient to empty the hole traps. Franck and Edelmann[19] treated a lithium fluoride of their own production at 310°C for one hour.

However, these treatments do not enable the traps to be totally evacuated ; some predose persists ; Franck estimates this to be 0.5 - 1.5 rads. Hence, while more sensitive, lithium fluoride treated in this manner cannot be used to measure low doses. This phenomenon had already been observed by. Kirk and Schulman[20] with manganese-activated lithium borate.

It is not to be ruled out that this effect may arise from deeperlying traps, particularly peak VI with a maximum corresponding to 280°C, which becomes preponderant at strong irradiation levels. If these traps are not themselves vacant they may well, over a period of time, lose part of the trapped holes to the advantage of the dosimetry peak by a transfer effect.

We have submitted PTL 71 to similar treatments. The results obtained are given on Fig. 9, which shows :

a) the remaining value of peak VI

b) the radiometric sensitivity of peak V with respect to treatment temperature.

It will be seen that traps VI are only emptied as from 360°C whereas, under our experimental conditions, sensitivity was scarcely altered, the additional F centres not having been destroyed.

In this way, we succeded in totally eliminating the predosage of lithium fluoride, which enables it to be used for measurement of the lowest levels of irradiation. The sensitivity of this new material (PTL 72)* is three to four times as great as that of PTL 710/717 ; its final value will be determined by the industrial preparation process.

V - Performance of detectors using PTL 720/727

This new material exhibits a response which is a linear function of the absorbed dose over a very wide range (1 mrad to 10^4 rads); hence, it is a "universal" dosimeter which can be used for both radioprotection and for radiobiology and radiotherapy.

It retains the quality of PTL 710/717 ; it can, inter alia, be re-used without regeneration, which considerably simplifies the measuring process and enables it to be employed for more routine applications.

---

* This material is shortly to be marketed by CEC under the desination PTL 720, based on natural lithium, or PTL 727 based on lithium enriched in isotope 7 (99.95%).

PTL 720 is very sensitive to thermal neutrons and has to be replaced by PTL 727 for measurement of gamma and beta radiation in the presence of neutrons. The latter material is prepared from lithium enriched to 99.95% of lithium 7, which gives it a sensitivity equivalent to 0.6 Rem (Co-60)for a fluence of 2.08×10^9 thermal neutrons per sq. cm**.

The sensitivity of these two new fluorides is three times as great as that of any of the lithium fluorides hitherto available on the market ; hence it is possible either to obtain improved characteristics for measurement of low doses or - which is certainly at least as important - to use less sophisticated and hence less expensive reading apparatus.

These materials are used to produce sintered pellets 7 mm in dia. and 8/10 mm thick. By virtue of their high sensitivity, their RTL emission is distinctly superior to that of stray phenomena such as triboluminescence. Hence, the measurements can be carried out without using a nitrogen sweep ; stray luminescence is less than 10 mrads. This being so, the construction of a genuinely portable reader can be envisaged.

** The irradiation experiments were carried out with the Stirca graphite pile at the Cadarache Nuclear Studies Centre by M. BRICKA and J. CERCY, to whom our thanks are due.

R E F E R E N C E S

(1) T.YAMASHITA, N.NADA, H.ONISHI, S.KITAMURA - Health Physic 21 - 295-300 (1971)

(2) E.W.CLAFFY, Luminescence Dosimetry, A.E.C. Symposium, Série 8 (1967) 74

(3) C.C.KLICK, E.W.CLAFFY, S.G.GORBICS, F.H.ATTIX, J.H.SCHULMAN, J.G.ALLARD - Journal of applied physics, 38, 10 (1967) 3867. R.M.GRANT, J.r, Ph.D.Thesis, University of Wisconsin, 1965.

(4) R.W.CHRISTY, N.M.JOHNSON, R.R.WILBARG, Journal of applied physics, 38 5 (1967) 2099

(5) R.M. GRANT, Jr.CAMERON, Journal of applied physics 37 10 (1966) 3791

(6) A.M.HARRIS, J.H.JACKSON, Brit.J.applied physics serie 2, vol.2 (1969) 1667

(7) T.G.STOEB, G.M.GUILMET, J.K.LEE - Radiation Effects - 1970 - Vol.4. - Page 189-193

(8) D.W.ZIMMERMAN, C.R.RHYNER, J.R.CAMERON, Health Physics, 5 12 (1966) 525

(9) G.PORTAL, H.FRANCOIS, Ph.BLANCHARD, Premier Congrès Européen de l'Association Internationale de radioprotection - Menton 9-11 octobre 1969

(10) G.PORTAL, F.BERMANN, Ph.BLANCHARD, Colloque AIEA, Vienne - 23-27 Nov. 1970 - SM 143/55

(11) G. PORTAL, Brevet n° EN 7103757 - 4.2.71

(12) G.PORTAL, 2ème Congress europeen de la société de radiologie n°396 - Amsterdam 14-18 juin 1971

(13) R.CHENAULT, E.PORROT, G.PORTAL, R.PRIGENT, Brevet n° 148588 du 18.4.68

(14) J.R.CAMERON, D.W.ZIMMERMAN, R.W.BLAND, AEC, Proceedings Intern. Conf. on luminescence dosimetry June 21-23 1965 - STANFORD - California

(15) J.R.CAMERON, L.DEWERD, J.WAGNER, G.WILSON, K.DOPPKE, D.ZIMMERMAN, Solid State and Chemical Radiation Dosimetry in Medecine and biology. Symposium Vienna 3-7 octob.1966

(16) J.R.CAMERON, N.SUNTHARALINGAM, C.R.WILSON, S.WATANABE, Second international conference on luminescence dosimetry, Gatlingurg Tennessee, Sept. 23-26 1968

(17) E.W.CLAFFY, C.C.KLICK, F.H.ATTIX, Second international conference on luminescence dosimetry Gatlinburg - Tennessee- Sept. 23-26 1968

(18) D.W.ZIMMERMAN, J.R.CAMERON - 1964 Progress Report USAEC - Contrat AT (11-1) 1105

(19) M.FRANK, B.U.EDELMANN, Kernenergie n°7 - 228-231 1966

(20) R.D.KIRK, J.H.SCHULMAN, E.H.WEST, A.E.NASH - Proccedings of Solid State and chemical radiation dosimetry in medecine and biologie AIEA, Vienne 3-7 octobre 1966.

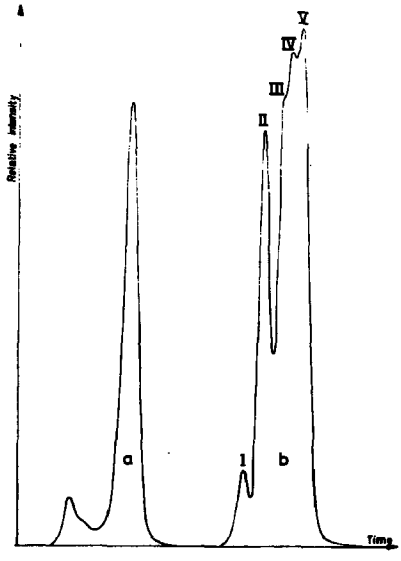

FIG 1 Thermoluminescence spectrum of TLD 700
a) annealed
b) unannealed

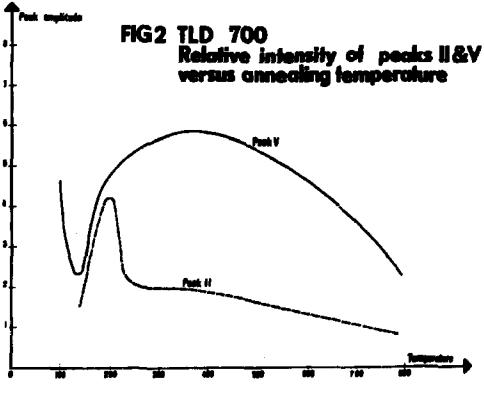

FIG 2 TLD 700
Relative intensity of peaks II & V versus annealing temperature

FIG 3 PTL
Relative intensity of peaks II & V versus annealing temperature

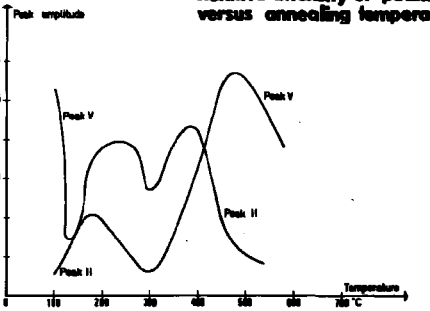

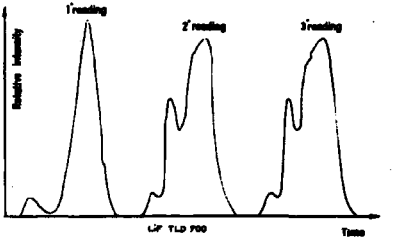

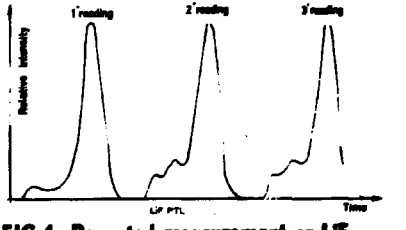

FIG 4 Repeated measurement on LiF

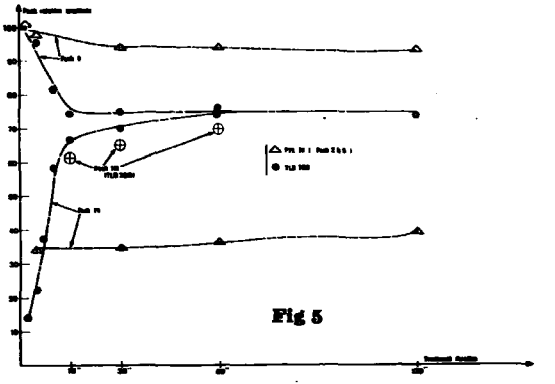

Fig 5

Effect of a 200°C treatment on peaksII-5 V relative amplitude for PTL & TLD 700

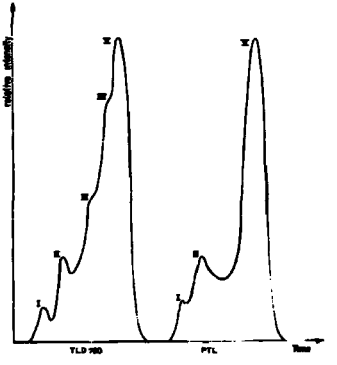

Fig 6 Comparison of TLD 700 and PTL spectrum

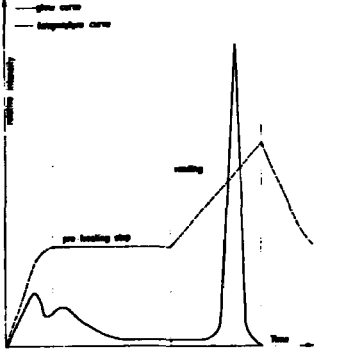

Fig 7 Pre-heating in the reader

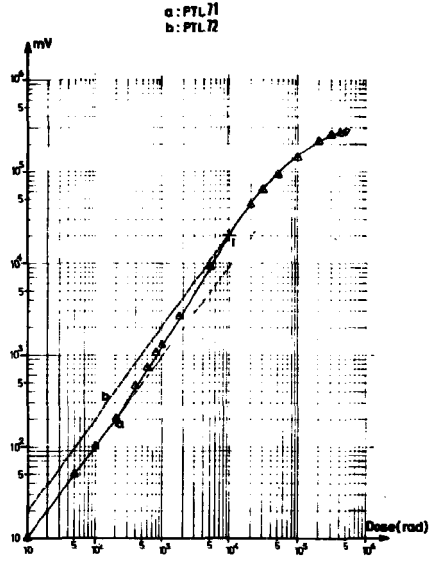

FIG 8: LIF Linearity

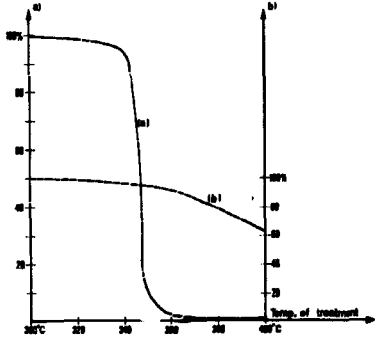

a) Relative intensity of peak VI remaining after treatment
b) Sensitivity of peak V after treatment

FIG 9

Suntharalingam

Could you please tell us what dopants were used in the preparation of your new PTL lithium fluoride?

Portal

This lithium fluoride contains 200 ppm of Mg and 10 000 ppm of sodium.

Suntharalingam

The new material you have described also shows supralinearity and increase in sensitivity. Hence after measurement of large doses the dosimeter will have to be annealed. Also, since your reader has a pre-readout heat cycle, no low-temperature annealing, or regeneration, as you call it, is necessary. This is true for the widely used LiF (TLD-100) or (TLD-700) too. Hence, I do not see any specific advantage of this new material.

Portal

Yes, the new material described shows supralinearity and must be regenerated after large-dose measurement. But in the case of personnel dosimetry irradiation to large doses is fortunately not very frequent. On the other hand, the sensitized material does not show supralinearity before 10^4 rads. As for the case of LiF (TLD-100) or (TLD-700), as I mentioned in my lecture, it presents an unstable intermediate-energy peak which is very difficult to eliminate, and so the accuracy of the measurement is slightly altered.

Suntharalingam

What is the precision of your measurements at low doses?

Portal

The precision of our measurements on a French C.E.C. sintered disc with a SAPHYMO-SRAT reader is about $\pm$ 1%. This is true for laboratory measurements; we have no experience in routine measurements.

Julius

Could you tell something about the mechanical properties of the sintered discs PTL 72?

Portal

They present the same mechanical resistance as other commercialized sintered dosimeters.

Puite

Have you studied the effect of fading due to UV light and room light?

Portal

Yes, the results are the same as those for normal lithium fluoride. For dosimeters exposed for five months in open air in the south of France we observed a fading of about 60%; for dosimeters placed near an UV lamp we observed, after fifteen days, a 30% fading.

Further Studies on the Dosimetric Use of BeO as a Thermoluminescent Material

by

G. Scarpa, G. Benincasa and L. Geravolo

Comitato Nazionale per l'Energia Nucleare, Laboratorio di Dosimetria e Standardizzazione, C.S.N. Casaccia, C.P. 2400, 00100 Roma (Italy)

Abstract

The study was carried out on commercial ceramic beryllium oxide disks with an impurity content of 0.5% and an effective atomic number of 7.1. The proposed annealing procedure (5 minutes at 600 °C) was selected on the grounds of best reproducibility of readouts. The glow curve shows two main peaks, the second one saturating quickly for exposures higher than 1000 R. The temperature of the first peak varies between 220 and 240 °C depending on dose level; its area is linear with dose till about 100 R, then supralinear.

The reproducibility of peak area from exposure to exposure of a given sample varies between 0.7 and 2.4% in the range from 0.5 up to 100,000 R; slightly worse results have been obtained using the peak-height method and in the low-dose region.

The dependence of response on photon energy is not very marked; the maximum value being 1.25 (^{60}Co = 1.00) at about 100 KeV, i.e. even lower than that of LiF.

The fading in darkness is rather slow, attaining a value of about 8% in 2 months. During the third and fourth week an apparent slight recovery takes place.

The response to u.v. light of irradiated BeO, after read-out, was also investigated; using this method a reassessment, ofthethefprevious radiation dose is feasible, even if not very accurate.

Introduction

The present study is an extension of previous experimental work carried out by one of us (G.S.)[4,5] on the TL properties of 3 commercial grades of sintered ceramic beryllium oxide, manufactured by a British firm.

The rather promising results obtained in that first stage encouraged us to go on with experiments, in order to get a more detailed picture of the dosimetric characteristics of this thermoluminescent substance.

Materials and methods

The beryllium oxide used in the present investigation is manufactured in the U.S.A. and is commercially available as Thermalox 995, with a total content of impurities of 0.5%, i.e. the same as for the British material. The calculated effective atomic number is 7.1, to be compared with 7.4 for water and soft tissue.

All measurements were carried out on 0.25 in. diameter, 0.03 in. thickness disks (average weight: about 70 mg).

The reading equipment used was the Harshaw TL analyser model 2000, equipped with an RCA 8042, S11 PM-tube and a "window" digital integrator enabling the integration to be carried out between two selected temperatures. The heating rate

was adjusted at about 10 °C/sec for most of the readouts. The temperatures of the peaks were measured after a careful calibration of the built-in temperature meter by means of fusibles of known melting point.

Some comparative readouts were also taken using a home-made reader equipped with a u.v.-sensitive photomultiplier (EMI 6256 S), with no infrared filter: a two-fold increase of the TL signal was thus achieved, due to the spectral emission of BeO.

Experimental measurements and discussion

a) Annealing. One of the first problems investigated was the annealing procedure to be used on BeO in order to eliminate the effects of the previous exposure. The experiment was carried out by using a constant annealing time (5 minutes) and different temperatures ranging from 400 to 700 °C. The BeO samples had been irradiated to 100 R.

The results are shown in fig. 1, in which the peak area and its standard deviation are plotted against the annealing temperature. Each point of the graph is based upon 100 measurements (10 readouts on each of 10 disks).

It can be seen that the best reproducibility (lowest S.D.) is achieved at around 600 °C, whereas the absolute value of TL output is practically constant between 500 and 700 °C.

The whole experiment was then repeated at 1 R level, with practically the same results.

b) Glow curve. Fig. 2 shows the shape of the glow curve of Thermalox 995 at various dose levels, from 25 mR up to 100,000 R. At 25 and 100 mR only one peak can be separated from the high background, even if the reading is carried out in a nitrogen atmosphere. The effect of the inert gas flowing is illustrated in the first two insertions of fig. 2 and consists

in a marked decrease of background (probably due to elimination of spurious TL emission of the sample) above 200 °C.

Starting from 1 R level a second peak becomes evident at higher temperature, about 350 °C.

The temperature of the first peak is marked on each glow curve and it shows a distinct increase with exposure; the highest value is reached between 1,000 and 10,000 R and it then drops down to about the starting level.

As we go up with the dose the second peak gets relatively lower and lower, till it disappears in the high-dose region. The ratio of the heights of the two peaks is indicated beside each glow curve. This behaviour is exactly the reverse of what happens in LiF and is probably due to an early saturation of available deeper traps.

Fig. 3 is a plot of the absolute height of the second peak as a function of exposure level and shows very clearly this saturation effect after a nearly linear rise.

c) Dose response. The relationship between TL response of BeO and exposure is illustrated in fig. 4, where both area and height are plotted against exposure. ^{60}Co gamma rays were used.

It is apparent that, after a linear region extending up to about 100 R, both curves become supralinear and, above 10,000 R, tend to saturate. These results are based upon a very large number of measurements and agree substantially with the first results published by Tochilin, Goldstein and Miller[7] and by Scarpa[4,5]. In the very low exposure region a slight sublinearity seems to be present; this is shown more clearly in fig. 5.

Fig. 6 is a plot of the linearity index versus exposure and better illustrates the behaviour described above. The top value reached by this index is 1.2 at 1000 R.

d) Reproducibility. In order to assess the reproducibility (or precision) of dose measurements attainable using sintered

BeO, a large set of repeated readouts was carried out at each dose level on several Thermalox disks. The results are summarized in fig. 7, where the percent standard deviation is plotted versus exposure.

It can be seen that, at least in this respect, the method of integrating the signal within the peak is generally better than that of measuring the peak height. An exception to this rule is only found in the low-dose region; below 0.5 R, in fact, the figures of %S.D. undergo a quite distinct increase for both methods, but more markedly for the peak area technique. From 0.5 up to 100,000 R the %S.D. varies between 0.7 and 2.4% for the area method, between 1.7 and 7.3% for the height method.

e) Energy response. The energy dependence of the response of Thermalox 995 to X and gamma radiation was investigated by exposing 12 disks to 100 R of ^{60}Co radiation and of well filtered X rays generated by two commercial units. The spectral distribution of the two lower energy radiations was analysed using a Ge(Li) spectrometer, to assess peak position and width. Tab. 1 summarizes the main characteristics of the X-ray beams used.

Tab. 1 - Main characteristics of X-ray beams used in the experiment on energy dependence.

high voltage (KV)	current (mA)	added filter	effective energy (KeV)	F.W.H.M. (KeV)	H.I.
40	5	1 Al	18.4 *	13	-
80	5	0.3 Cu	34 *	31	-
180	15	1 Cu + 0.5 Al	91	-	0.96
280	10	3 Cu + 1 Al	148	-	0.97
400	10	2 Pb + 1 Sn + 0.6 Cu + 1 Al	222	-	0.98

* modal energy as measured with a Ge(Li) spectrometer

The results of the experiment, normalised to unity for 1.25 MeV of ^{60}Co gamma rays, are shown in fig. 8. It can be seen that the curve of peak areas is somewhat better than that of peak heights, starting with values around unity and showing a broad peak of 1.25 at about 100 KeV. The position of this response curve is intermediate between the one published by Tochilin et al.[7] and the one reported by Scarpa[4,5] on British BeO of nuclear grade, the first being higher and the second lower than the present curve.

The top value of 1.25 seems even lower than those reported for Lithium Fluoride.

Also shown in fig. 8 is how the first-to-second peak height ratio is strongly influenced by the photon energy. The highest value of 13 is reached at about 100 KeV, while the ratio falls to about 7 at 1.25 MeV.

f) Fading in the dark. As far as the fading characteristics of Thermalox 995 are concerned fig. 9 illustrates the results of two experimental sets, in which a number of BeO disks were stored in the dark at room temperature, for a maximum period of 2 months. In order to minimize the effect of a possible reader drift, the samples were exposed to radiation at different times and all read out during a single session.

After an initial fall of 5 to 6% during the first two weeks, both plots show a sort of slight "recovery" reaching a maximum at the end of the first month, after which a slow decay starts again. This behaviour is somewhat similar to some early results obtained by Fowler et al.[1] on LiF, which were not confirmed by later experiments[6].

The total decay in 2 months was of the order of 8%.

g) Response to u.v. light. In the last few years some studies have been carried out on the feasibility of getting a second readout out of an irradiated and read sample of TL

material. Among the contributions recently published in the dosimetric literature we would mention the one by Mason[2] on LiF. This author gets the second readout by exposing the phosphor, after the normal readout, to u.v. light. The interpretation given by the same author is based upon the release of charge carriers from hypothetical high-temperature traps and subsequent retrapping of these carriers in the dosimetric trapping centres.

The intrinsic response to u.v. of unirradiated BeO is very little, corresponding to less than 100 mR of gamma radiation.

As far as irradiated BeO is concerned, fig. 10 shows that the exposure time to u.v. light giving the highest second readout is around 15 minutes, when a 16 W lamp and a 10 cm distance are used. The subsequent gradual decrease of the curve is probably due to the prominence of u.v.-induced decay over u.v.-induced build-up.

The pattern of this response to u.v. after gamma exposures ranging from 1 up to 100,000 R is illustrated in fig. 11. It can be seen that, on the whole, the second readout (after u.v.) is much more linear than the first one; the ratio of second to first readout is around 25% at low doses and falls down to 2.5% at very high doses.

When repeated u.v. exposures and readouts are carried out on an irradiated sample, a quick drop of the TL signal from readout to readout is observed (fig. 12), so that the sixth reading gives only the 14% of the original value. This fall is probably the result of a depletion of high temperature traps.

All the above results show that the u.v. response of BeO is not basically different from that reported for LiF. The only difference lies in the TL yield, which appears to be far higher for BeO, at least in the low and medium dose regions. This could be important in the reassessment of low radiation

doses.

The precision of such reassessment is still being studied in our laboratory; the first results seem to indicate a standard deviation from exposure to exposure of about 10%, but more experimental work is in progress in our laboratory to see if this figure can be substantially reduced by using a more sophisticated technique.

Even with this reserve, the proposed method of re-estimating a radiation dose using the TL response induced by u.v. light seems to be useful, at least in some fields of radiation dosimetry as, e.g., in radiation protection measurements.

I wish to express my gratitude to Prof. E. Casnati and Dr. G. Rienzo for their experimental assistance and most helpful comment and criticism during the writing of this paper. I also wish to thank Mr. A. Marchetti for carrying out the dosimetry and all the irradiations of the samples.

References

1. J.F. Fowler, E. Shuttleworth, V. Svarcer, J.T. White, C.J. Karzmark, Nature 207, 997-998 (1965).
2. E.W. Mason, Phys. Med. Biol. 16, 303-310 (1970).
3. C.R. Rhyner, W.G. Miller, Health Phys. 18, 681-684 (1970).
4. G. Scarpa, Phys. Med. Biol. 15, 667-672 (1970).
5. G. Scarpa, Second Int. Congress of I.R.P.A., Brighton (1970)
6. Suntharalingam, J.R. Cameron, E. Shuttleworth, M. West, J.F. Fowler, Phys. Med. Biol. 13, 97-104 (1968).
7. E. Tochilin, N. Goldstein, W.G. Miller, Health Phys. 16, 1-7 (1969).

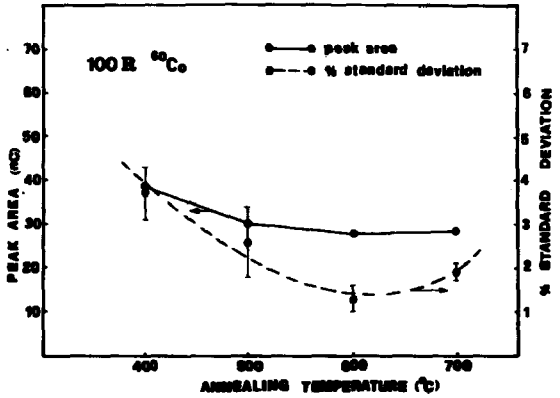

Fig. 1 - Peak area and its standard deviation versus annealing temperature. Exposure: 100 R.

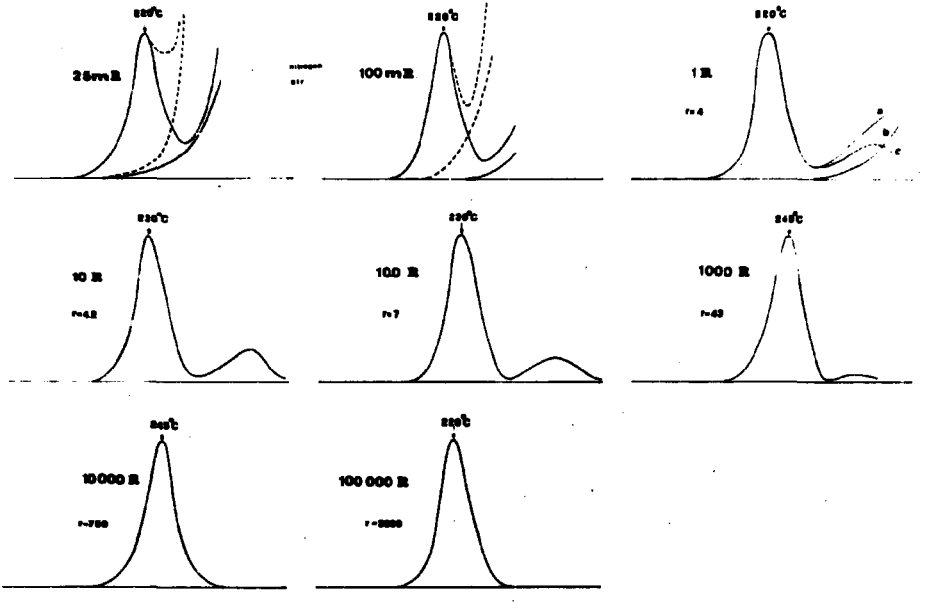

Fig. 2 - Shape of the glow curve of Thermalox 995 at various dose levels. Temperature of first peak and ratio between first and second peak are also indicated.

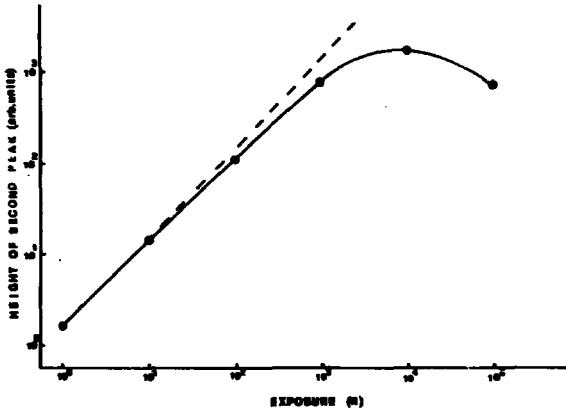

Fig. 3 - Abosulte height of the second peak versus exposure level. The dashed curve shows linearity.

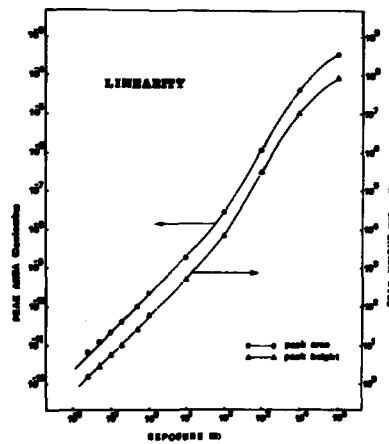

Fig. 4 - Peak area and peak height versus exposure level, for ^{60}Co gamma radiation.

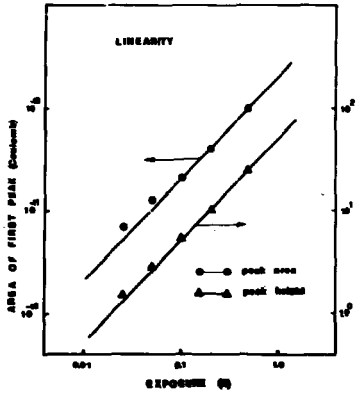

Fig. 5 - Detail of fig. 4 in the low dose region.

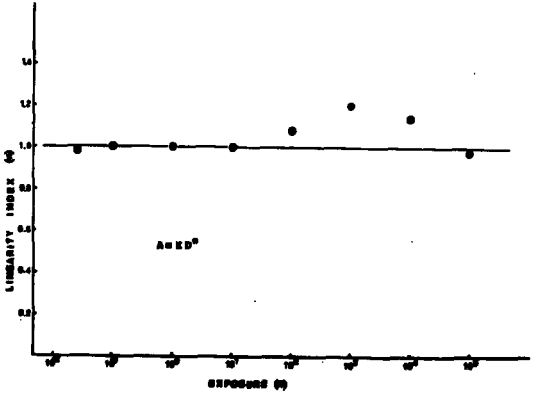

Fig. 6 - Linearity index versus exposure.

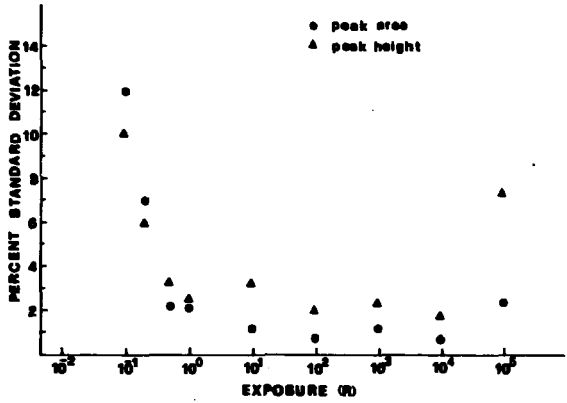

Fig. 7 - Percent standard deviation of repeated readouts versus exposure.

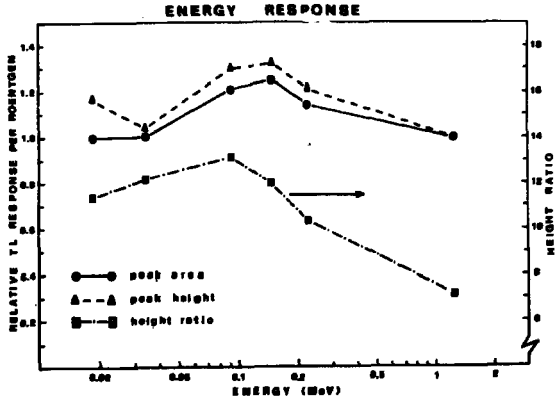

Fig. 8 - Energy dependence of response of Thermalox 995 to X and gamma radiation, normalized to unity for 1.25 MeV of ^{60}Co gamma rays. Also shown is the ratio between the heights of the first and the second peak.

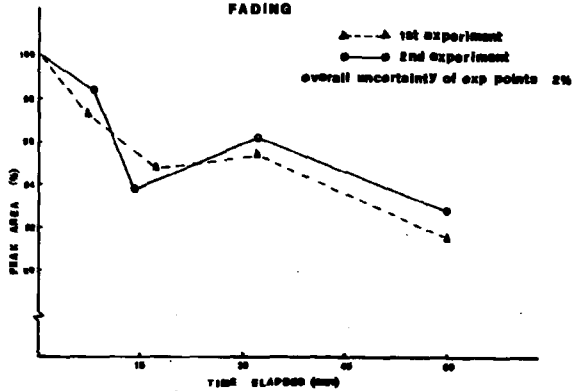

Fig. 9 - TL response of Thermalox 995 versus storage time in the dark.

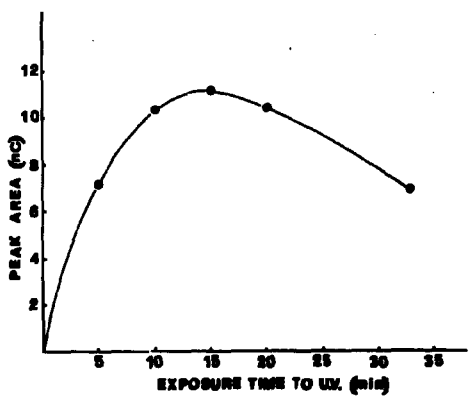

Fig. 10 - Induced response of BeO to u.v. light versus exposure time.

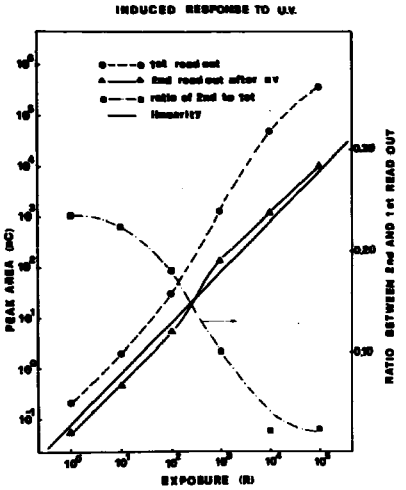

Fig. 11 - Response of BeO to u.v. light versus gamma exposures ranging from 1 up to 100,000 R. The ratio between the second and the first readout is also indicated.

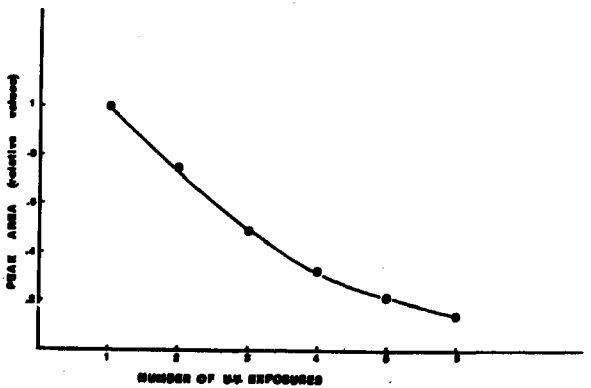

Fig. 12 - Behaviour of the TL signal after repeated exposures to u.v. and readouts.

Jones

Can you explain the energy dependence of the peak height to peak area ratio?

Scarpa

No, but I should like to emphasize that each experimental point of the curves I have shown is the mean value of twelve independant measurements, so I think that the described behaviour is real and not caused by experimental errors.

Fowler

Your results on beryllium oxide, taken with the results reported yesterday by Yasuno and Yamashita, suggest that BeO is one of the potentially most useful TLD materials in the tissue-equivalent range. Please, can you comment, however, on the toxicity hazard from handling BeO?

Scarpa

I am afraid it would take a rather long time to deal with this question thoroughly. It is well known that the main hazard of BeO lies in inhalation of finely powdered material. The threshold tolerance concentration of BeO powder in the air of factories manufacturing this substance is generally considered to be 2 microgrammes per cubic metre. Now calculating with 50 cubic metres - the mean volume of an ordinary laboratory room - the above-stated limit would correspond to the release of 0.1 mg of BeO. According to our experience with more than 2500 readouts, the weight loss observed in each single sample over long series of annealings and readouts did not exceed this order of magnitude. So the powder production should be quite negligible in ordinary use; harmful effect from the use of ceramic BeO would therefore be highly unlikely.

Becker

The rather complex question of beryllium toxicity can, I believe, be summarized as follows: Highly dispersed ("unfired") BeO powder can, if inhaled, induce a dangerous reaction in some persons who are allergic to it. No such reaction occurs after the BeO has been sintered ("fired") at high temperatures

as is the case with BeO ceramics, which have even been implanted into animals with no harmful results (under the same conditions, implantation of LiF was lethal). Ceramic BeO is an extremely hard, high-melting (~2400°C), and chemically resistant material and can be considered completely harmless under normal handling conditions.